2019

Unbiased global proteomic profiling of patient-derived meningiomas of all grades to identify molecular signatures of differentially expressed proteins and phosphoproteins.

Dunn, Jemma Suzanne

http://hdl.handle.net/10026.1/14675

http://dx.doi.org/10.24382/1257
University of Plymouth

UNIVERSITY OF PLYMOUTH

UNBIASED GLOBAL PROTEOMIC PROFILING OF PATIENT-DERIVED MENINGIOMAS OF ALL GRADES TO IDENTIFY MOLECULAR SIGNATURES OF DIFFERENTIALLY EXPRESSED PROTEINS AND PHOSPHOPROTEINS

by

JEMMA SUZANNE DUNN

A thesis submitted to the University of Plymouth

in partial fulfilment for the degree of

DOCTOR OF PHILOSOPHY

School of Medicine and Dentistry

September 2018

Acknowledgements

Firstly, I would like to thank my Director of Studies Dr. Sara Ferluga for your unconditional support and guidance throughout my PhD. You shared your scientific expertise and knowledge and trained me to be a scientist, a goal I did not believe I would ever achieve. You taught me to have confidence in my work and inspired me to continue when I lost my way. I aspire to be half the scientist you are and will forever be grateful for your help during the last four years.

I would like to acknowledge Dr. Edwin Lasonder for the willingness you have shown to always find time to explain my endless queries surrounding the field of proteomics. As a supervisor, you guided me through unfamiliar analyses and your knowledge has been and continues to be invaluable.

Lastly, of my supervisory team, I would like to thank Prof. Oliver Hanemann for giving me the opportunity to undertake a PhD and become part of his research group. I do not believe either of us knew exactly what this project would entail and I appreciate your motivation to keep pushing me to get the most from it.

There are several academics outside of my supervisory team I would also like to extend my thanks to for their assistance with my project. For your dedication and endless patience in analysing my samples in the mass spectrometer I would like to thank Dr. Vikram Sharma. Your positive attitude and patience with me when things were not always going to plan did not go unnoticed. To Dr. Claire Adams I would like to thank you for your commitment to genotyping the samples in this project as well as your continued support in sourcing samples and ensuring ethical approval was always met. My thanks also go to Dr. Matthias Futschik for generating the Volcano plots for this project and more generally, taking the time to assist in resolving and explaining my many bioinformatics queries in the final stages of my PhD. Finally, I would like to acknowledge Dr. David

Hilton whom I am extremely grateful to for not only sourcing the majority of the samples used in this project, but for all the help and support you provided for what became a slightly larger than anticipated IHC endeavour. I am truly grateful to have had the chance to work with you and for the time you sacrificed on my project, as well as being appreciative of the advice you have given and the listening and moaning you have endured as a friend.

I have been extremely lucky to have had the never-ending support of my family throughout my PhD. I would truly not have been able to continue my studies without the help of my parents and I cannot thank you both enough. To my brother, you have made me the proudest auntie in the world three times over and I feel incredibly lucky to be a part of all your lives. Their beautiful little faces kept me going when I wanted to give up and I hope one day to be even half the parent you have become.

To my dearest friend Jon, known forever as 'London Jon' for the duration of this PhD, our friendship has somehow survived many obstacles over the years and yet again, you have done nothing but support me throughout this latest choice of mine. I am forever grateful to have you in my life and am not sure what I would do without you.

To James, I cannot possibly repay the undeniable friendship and IT support you have so calmly provided in my many, many, many times of need during my studies. I hope I provide a sufficient amount of stories surrounding the comedy that is my life to make it marginally worthwhile.

Finally, I would like to thank not only my research group as a whole, but also many of my fellow students and previous housemates whom I am privileged to now call my friends. Jon, Jade, Kayleigh, Emma, Joe, I cannot put into words how much you all mean to me; you are true friends. I am in awe of each of you and your intelligence, and cannot thank you enough for the unquestionable support and laughs we have shared, long may it

continue. To Rob, you were my partner in crime for some time during this PhD and guided me when I wanted to give up, I will forever be grateful to you for making me laugh an unquantifiable amount. We joke, but I truly admire your scientific abilities and have complete faith that you will inspire many in the following years, I hope one day we really do work together again. To Tracey, I admire your perseverance in life and am so thankful that during our numerous hours of running together you taught me to not only push my physical abilities but also my mental ability to complete my PhD. I would also like to thank Sarah, Foram, Ollie, Chris and Rick for keeping me sane, dealing with my daily stupidity and being all round great friends. Lastly, my thanks go to Liyam and Bora for keeping me on the straight and narrow in the final stages of this project. We really did become a family, you both drive me mad like family can, but you have hearts of gold and without your continuous hugs and supportive talks I would have been lost, I hope I make the same impact in your lives as you have in mine.

AUTHOR'S DECLARATION

At no time during the registration for the degree of Doctor of Philosophy has the author been registered for any other University award without prior agreement of the Doctoral College Quality Sub-Committee.

Work submitted for this research degree at the University of Plymouth has not formed part of any other degree either at the University of Plymouth or at another establishment.

This study was financed with the aid of a studentship form the Brain Tumour Research.

Publications (or public presentation of creative research outputs):

Collord G, Tarpey P, Kurbatova N *et al.* (2018) An integrated genomic analysis of anaplastic meningioma identifies prognostic molecular signatures. Sci Rep. 2018 Sep 10;8(1):13537. DOI: 10.1038/s41598-018-31659-0. PEARL (OA): http://hdl.handle.net/10026.1/12383. See appendix for full publication.

Dunn J, Ferluga S, Sharma V *et al*. (2018) Proteomic analysis discovers the differential expression of novel proteins and phosphoproteins in meningioma including NEK9, HK2 and SET and deregulation of RNA metabolism. EBioMedicine. 2018 Dec 26;40:77. DOI: 10.1016/j.ebiom.2018.12.048. PEARL (OA): http://hdl.handle.net/10026.1/13181. See appendix for full publication.

Presentations at conferences:

EACR 25th Biennial Congress. Amsterdam, Netherlands. June 30 - July 3, 2017. Poster presentation.

BNOS Conference 2017. Edinburgh, UK. June 21-23, 2017. Poster presentation.

British-Irish Meningioma Society 2nd Symposium. London, UK. May 13, 2017. Oral presentation.

Glioma Club 2016 - BNOS Junior Forum. London, UK. October 28, 2016. Oral presentation.

117th British Neuropathological Society Meeting. London, UK. March 3, 2016. Oral presentation.

78th Harden Conference: Protein Kinases in Health and Disease. Winchester, UK. September 15-18, 2015. Poster presentation.

Word count of main body of thesis: 61104

Signed

Date

Jemma Suzanne Dunn

Unbiased global proteomic profiling of patient-derived meningiomas of all grades to identify molecular signatures of differentially expressed proteins and phosphoproteins

Abstract

Meningioma is the most frequent primary intracranial tumour. Surgical resection remains the main therapeutic option as pharmacological intervention is still hampered by the poor knowledge of the molecular signature of these tumours. In order to elucidate the proteomic profiling of meningiomas and identify proteins involved in their pathogenesis, we completed a comparative mass spectrometry analysis of meningioma tissue of all WHO grades, analysing global proteins, phosphoproteins and phosphopeptides. We performed differential expression analyses and functional annotation studies to identify commonly upregulated proteins and phosphoproteins in all grades of meningioma compared to meningeal tissue as well as grade-specific candidates relevant for tumour progression. Top candidates were validated by Western blotting and immunohistochemistry in an independent sample set, confirming for example significant overexpression of proteins including EGFR, STAT2 and EPS8L2 across all grades, as well as the aberrant activation of the PI3K/AKT/mTOR pathway. Further, we validated upregulation in all grades of the total and activated phosphorylated form of the NIMA-related kinase, NEK9, involved in mitotic progression and of the transmembrane protein CKAP4. Novel proteins identified in meningioma and validated as commonly overexpressed in all grades were the nuclear proto-oncogene SET and the splicing factor SF2/ASF, while another newly identified protein that was specific for high-grade meningiomas was the glycolytic enzyme hexokinase-2, involved in cellular metabolism.

In summary, we generated a proteomic thesaurus of meningiomas in order to decipher aberrantly expressed proteins and activated pathways; this body of knowledge will eventually lead to the identification of relevant biomarkers and possible novel therapeutic targets.

Table of Contents

Table of Figures

Table of Tables

Abbreviations

2D-GE	Two-dimensional gel electrophoresis
ABC	Ammonium bicarbonate
ACAD9	Acyl-CoA dehydrogenase family member 9, mitochondrial
ACN	Acetonitrile
ACSS3	Acyl-CoA synthetase short-chain family member 3, mitochondrial
ARID1A	AT-rich interactive domain-containing protein 1A
AKT1	RAC-alpha serine/threonine-protein kinase
AKT2	RAC-beta serine/threonine-protein kinase
AKT3	RAC-gamma serine/threonine-protein kinase
ALDH1A1	Retinal dehydrogenase 1
ALDH5A1	Succinate-semialdehyde dehydrogenase, mitochondrial
ALPL	Alkaline phosphatase, tissue-nonspecific isozyme
ANP32E	Acidic leucine-rich nuclear phosphoprotein 32 family member E
ARF	Tumor suppressor ARF
ATOX1	Copper transport protein ATOX1
ATR	Serine/threonine-protein kinase ATR
BAP1	Ubiquitin carboxyl-terminal hydrolase BAP1
BCA	Bicinchoninic acid
BIN1	Myc box-dependent-interacting protein 1
BM1	Ben-Men-1
BUB3	Mitotic checkpoint protein BUB3
CAST	Calpastatin
CDH11	Cadherin-11
CDH13	Cadherin-13
CDH2	Cadherin-2
CDKN2A	Cyclin-dependent kinase inhibitor 2A
CDKN2B	Cyclin-dependent kinase 4 inhibitor B
CDKN2C	Cyclin-dependent kinase 4 inhibitor C
CHEK1	Serine/threonine-protein kinase Chk1
CHEK2	Serine/threonine-protein kinase Chk2
CKAP4	Cytoskeleton-associated protein 4
c-KIT	Mast/stem cell growth factor receptor Kit
CNS	Central nervous system
CPPED1	Serine/threonine-protein phosphatase CPPED1
CREB1	Cyclic AMP-responsive element-binding protein 1
CSF	Cerebrospinal fluid
DAB	3,3'-diaminobenzidine
DAVID	The database for annotation, visualization and integrated discovery
DDX10	Probable ATP-dependent RNA helicase DDX10
DDX17	Probable ATP-dependent RNA helicase DDX17

DDX19B	ATP-dependent RNA helicase DDX19B
DDX24	ATP-dependent RNA helicase DDX24
DDX39A	ATP-dependent RNA helicase DDX39A
DDX42	ATP-dependent RNA helicase DDX42
DDX5	Probable ATP-dependent RNA helicase DDX5
DDX6	Probable ATP-dependent RNA helicase DDX6
DKK1	Dickkopf-1
DKK3	Dickkopf-related protein 3
DMEM	Dulbecco's modified eagle's media
DMSO	Dimethyl sulfoxide
DOCK	Dedicator of cytokinesis
DTT	DL-Dithiothreitol
ECL	Enhanced chemiluminescence
EDTA	Ethylenediaminetetraacetic acid
EFNB2	Ephrin-B2
EGFR	Epidermal growth factor receptor
EIF2	Eukaryotic initiation factor 2
EMA	European Medicines Agency
EMT	Epithelial-to-mesenchymal transition
EPB41	Protein 4.1
EPH	Erythropoietin-producing hepatocellular
EPS8	EGF receptor kinase substrate 8
EPS8L1	Epidermal growth factor receptor kinase substrate 8-like protein 1
EPS8L2	Epidermal growth factor receptor kinase substrate 8-like protein 2
EPS8L3	Epidermal growth factor receptor kinase substrate 8-like protein 3
ERK	Extracellular signal–regulated kinase
ERM	Ezrin, radixin, moesin
FAK	Focal adhesion kinase
FBS	Foetal bovine serum
FC	Fold change
FDA	US Food and Drug Administration
FDR	False discovery rate
FERM	Four-point-one, exrin, radixin, moesin
FFPE	Formalin fixed paraffin embedded
FRET	Fluorescence resonant energy transfer
GADD45A	Growth arrest and DNA damage-inducible protein GADD45 alpha
GAPDH	Glyceraldehyde-3-phosphate dehydrogenase
GBM	Glioblastoma multiforme
GEF	Guanine nucleotide exchange factor
GO	Gene Ontology
GPCR	G-protein coupled receptor
GSK3β	Glycogen synthase kinase 3β

GTR	Gross total resection
HEPACAM	Hepatocyte cell adhesion molecule
HK1	Hexokinase-1
HK2	Hexokinase-2
HMC	Human meningeal cells
HPF	High-power fields
HRP	Horseradish peroxidise
HSPE1	10 kDa heat shock protein, mitochondrial
IDH3A	Isocitrate dehydrogenase [NAD] subunit alpha, mitochondrial
IDH3B	Isocitrate dehydrogenase [NAD] subunit beta, mitochondrial
IHC	Immunohistochemistry
IMAC	Immobilised metal affinity chromatography
INHAT	Inhibitor of acetyltransferases
IPA	Ingenuity Pathway Analysis
KASP	Kompetitive allele specific PCR genotyping system
KLF4	Krupple-like factor 4
KT21	KT21-MG1
LC-MS/MS	Liquid chromatography tandem mass spectrometry
LEPR	Leptin receptor
LFC	Log_2 fold change
LFQ	Label-free quantification
MAPK	Mitogen-activated protein kinase
MAPK2	Mitogen-Activated Protein Kinase 2
MCM	Minichromosome maintenance
MEG3	Maternally expressed 3
MEK	Mitogen-activated protein kinase kinase 1
miRNA	MicroRNA
MLPA	Multiplex Ligation-dependent Probe Amplification
MOAC	Metal oxide affinity chromatography
MRC2	C-type mannose receptor 2
MRE11	Double-strand break repair protein MRE11
MS	Mass spectrometry
mTOR	Mammalian target of rapamycin
mTORC1	mTOR complex 1
mTORC2	mTOR complex 2
MUC4	Mucin-4
MX1	Interferon-induced GTP-binding protein Mx1
NAD	Nicotinamide adenine dinucleotide
NADH	Nicotinamide adenine dinucleotide (NAD) + hydrogen (H)
NCBP1	Nuclear cap-binding protein subunit 1
NDRG2	Protein NDRG2
NEK6	Serine/threonine-protein kinase Nek6

NEK7	Serine/threonine-protein kinase Nek7
NEK9	Serine/threonine-protein kinase Nek9
NF2	Neurofibromatosis 2
NFAT	Nuclear factor of activated T cells
NFKB1	Nuclear factor NF-kappa-B p105 subunit
NGS	Next-generation sequencing
NH_4OH	Ammonium hydroxide
NMT	Normal meningeal tissue
NSUN2	tRNA (cytosine(34)-C(5))-methyltransferase
PAK2	P21 (RAC1) activated kinase 2
PBS	Phosphate-buffered saline
PBST	Phosphate-buffered saline tween
PCR	Polymerase chain reaction
PD-1	Programmed death receptor 1
PDGF	Platelet-derived growth factor
PDGFR-α	Platelet-derived growth factor receptor-α
PDGFR-β	Platelet-derived growth factor receptor-β
PDK1	3-phosphoinositide-dependent protein kinase 1
PD-L1	Programmed-death ligand 1
PDLIM2	PDZ and LIM domain protein 2
PFS	Progression-free survival
PI3K	Phosphoinositide 3-kinase
PIK3CA	Phosphatidylinositol-4,5-bisphosphate 3-kinase catalytic subunit alpha
PIK3R1	Phosphatidylinositol 3-kinase regulatory subunit alpha
PIP_2	Phosphatidylinositol (4, 5)-bisphosphate
PIP_3	Phosphatidylinositol (3, 4, 5)-trisphosphate
POLR2A	DNA-directed RNA polymerase II subunit RPB1
PP2A	Protein phosphatase 2A
PPP3CA	Serine/threonine-protein phosphatase 2B catalytic subunit alpha isoform
PPP3CB	Serine/threonine-protein phosphatase 2B catalytic subunit beta isoform
PPP3R1	Calcineurin subunit B type 1
PRAS40	Proline-rich AKT substrate of 40 kDa
PRC2	Polycomb repressive complex 2
PRKAR1A	Protein kinase, CAMP-dependent, regulatory, type I, alpha
PRKCG	Protein kinase C gamma type
PRKDC	DNA-dependent protein kinase catalytic subunit
PTEN	Phosphatase and tensin homologue deleted on chromosome 10
PTM	Post-translational modification
PTPN7	Tyrosine-protein phosphatase non-receptor type 7
PTTG1	Securin
PTX3	Pentraxin-related protein PTX3

PVDF	Polyvinylidene difluoride membrane
PXN	Paxillin
RAD54L	DNA repair and recombination protein RAD54-like
RB	Retinoblastoma-associated protein
RIPA	Radioimmunoprecipitation assay
RT	Room temperature
RTK	Receptor tyrosine kinase
S100-A10	Protein S100-A10
SDS-PAGE	Sodium dodecyl sulphate polyacrylamide gel electrophoresis
SERPINE1	Plasminogen activator inhibitor 1
SERPINE2	Glia-derived nexin
SET	Protein SET
SF2/ASF	Serine/arginine-rich splicing factor 1
SF3B2	Splicing factor 3B subunit 2
SF3B5	Splicing factor 3B subunit 5
SFRP3	Secreted frizzled-related protein 3
SFRT	Stereotactic fractionated radiotherapy
SHH	Sonic hedgehog
SMARCB1	SWI/SNF-related matrix-associated actin-dependent regulator of chromatin subfamily B member 1
SMARCE1	SWI/SNF-related matrix-associated actin-dependent regulator of chromatin subfamily E member 1
SMO	Smoothened, frizzled family receptor
SNP	Single nucleotide polymorphism
snRNP	Small nuclear ribonucleoprotein
SNRPD3	Small nuclear ribonucleoprotein Sm D3
SNRPE	Small nuclear ribonucleoprotein E
SNRPF	Small nuclear ribonucleoprotein F
SON	Protein SON
SPT16	FACT complex subunit SPT16
SRC	Proto-oncogene tyrosine-protein kinase Src
SRSF3	Serine/arginine-rich splicing factor 3
SRSF7	Serine/arginine-rich splicing factor 7
SRS	Stereotactic radiosurgery
SSH1	Protein phosphatase Slingshot homolog 1
SSRP1	FACT complex subunit SSRP1
STAGE	Stop and go extraction
STAT1	Signal transducer and activator of transcription 1-alpha/beta
STAT2	Signal transducer and activator of transcription 2
STRING	Search Tool for the Retrieval of Interacting Genes/Proteins
SUCLG2	Succinate--CoA ligase [GDP-forming] subunit beta, mitochondrial
SUFU	Suppressor of fused homolog
SUPT16H	FACT complex subunit SPT16

SWI/SNF	Switch/Sucrose nonfermentable
SVIL	Supervillin
TBST	Tris buffered saline-Tween-20
TERT	Telomerase reverse transcriptase
TFA	Trifluoroacetic acid
TIMP3	Tissue inhibitor of metalloproteinase 3
TiO_2	Titanium dioxide
TOP1	DNA topoisomerase 1
TOP2B	DNA topoisomerase 2-beta
TP73	Tumor protein 73
TRAF7	Tumor necrosis factor receptor-associated factor 7
TRIP6	Thyroid receptor-interacting protein 6
VEGF	Vascular endothelial growth factor
VEGFR	Vascular endothelial growth factor receptor
WB	Western blot
WHO	World Health Organization
XRCC5	X-ray repair cross-complementing protein 5
YAP	Yes-associated protein
ZrO_2	Zirconium dioxide

1 Introduction

1.1 Background to the study

Meningiomas are tumours of the meninges, the thin layer of tissue covering the brain and spinal cord. They are the most frequent intracranial tumour with an estimated incidence of 7.86 cases per 100,000 people per year and limited therapeutic options (Preusser, Brastianos & Mawrin, 2018). While the majority of meningiomas can be surgically resected or treated with radiotherapy, complicating factors including inaccessible tumour location, incomplete resection and aggressive histological features lead to disease progression or tumour recurrence with associated patient morbidity and mortality. Recent studies have provided advances in the characterisation of the molecular background of meningioma; for example, next-generation sequencing (NGS) technologies were used to identify recurrent driver mutations, relating these to tumour histology and location, and transcriptomic analyses were utilised to describe differential expression of genes between different meningioma subtypes so identifying potential prognostic markers. Moreover, by extensive DNA methylation analyses the epigenetic alterations of meningioma have revealed the potential to subclassify these tumours based on their molecular background (Sahm *et al.*, 2017). Yet, despite this increased body of knowledge, targeted therapies are still far from becoming a treatment option for patients.

This study used an unbiased proteomic screening approach by studying frozen meningioma specimens encompassing all grades and comparing the results to healthy normal human meninges to identify aberrantly expressed proteins. In addition to generating global proteome data, we also screened for phosphoproteins and phosphopeptides, allowing the detection of altered protein activity and associated dysregulated signalling pathways within these tumours. Subsequent analyses and validation of these datasets enabled us to suggest a panel of candidate proteins and

phosphoproteins with the potential to become biomarkers or therapeutic targets of meningioma. In the following introduction, current meningioma literature will be discussed along with molecular targeted therapies and potential biomarkers for patients as well as the technologies being utilised to uncover these.

1.2 Meningioma site of origin and histopathological classification

Meningiomas are the most common primary intracranial tumour, originating from the meningeal coverings of the brain and spinal cord (Whittle *et al.*, 2004). The meninges are a layer of protective tissues composed of three membranes: the dura mater, the thickest of the membranes situated closest to the skull and vertebrae; the arachnoid mater, the middle layer of the meninges with a web-like morphology; and the pia mater, the thinnest and innermost layer lining the brain and spinal cord. Meningiomas originate from arachnoidal cap cells situated in the arachnoid villi of the arachnoid mater (Fig. 1.1) (Marosi *et al.*, 2008). Arachnoidal cap cells are a subset of arachnoid cells, which are present at the apex of the villi and function in the resorption of cerebrospinal fluid (CSF) (Marosi *et al.*, 2008). Meningiomas may arise from any arachnoidal cap cell, with the majority occurring in the cranial meninges; most commonly found at the convexity, parasagittal and sphenoid regions; and less frequently at the cerebellopontine angle, optic-nerve sheath and the choroid plexus; the remaining form in the spinal meninges and very rarely at ectopic sites such as the ear, mandible, foot and lung (<1%) (Hallinan, Hegde & Lim, 2013; Whittle *et al.*, 2004).

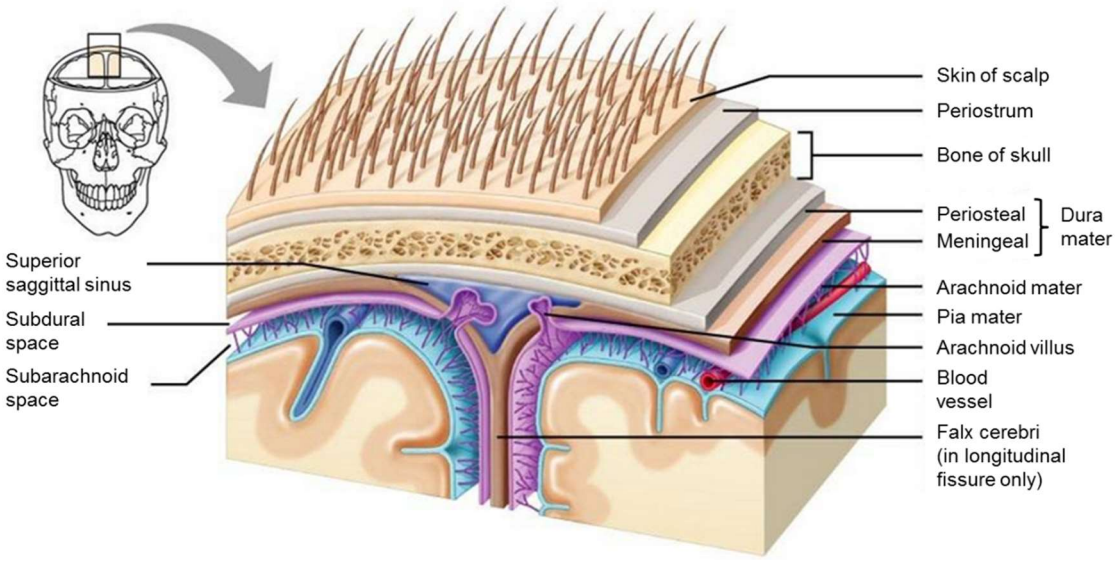

Figure 1.1 Schematic representation of the meninges. The meninges consist of three layers: the dura mater, arachnoid mater and pia mater. Meningioma are thought to arise from arachnoidal cap cells located in the arachnoid villi. Image adapted from (Lifeinharmony, 2018).

Histological grading of meningiomas is based on the World Health Organization (WHO) classification system, which encompasses three grades covering 15 histological meningioma subtypes (Fig. 1.2) (Louis, 2016). The majority of meningiomas, around 80%, are slow-growing WHO grade I tumours generally benign in nature with few mitotic figures (Riemenschneider, Perry & Reifenberger, 2006; Whittle *et al.*, 2004). WHO grade I classification includes nine histological subtypes, of which the most commonly diagnosed are meningothelial, fibrous and transitional (Riemenschneider, Perry & Reifenberger, 2006). WHO grade II, also known as atypical meningiomas, account for approximately 18% of all meningiomas and are defined by a particular set of criteria alongside two distinct histological meningioma variants, clear-cell and chordoid (Commins, Atkinson & Burnett, 2007; Riemenschneider, Perry & Reifenberger, 2006; Whittle *et al.*, 2004). These more aggressive meningiomas generally present with a mitotic rate of 4-19 mitoses per 10 high-power fields (HPF) (Perry *et al.*, 1997) and may

display further histological features including increased cellularity, high nuclear-to-cytoplasmic ratio, prominent nucleoli, a sheet-like growth pattern, foci of necrosis and brain invasion (Louis, 2016; Riemenschneider, Perry & Reifenberger, 2006; Whittle *et al.*, 2004). Lastly, WHO grade III represent 1-3% of all meningioma cases and are largely referred to as anaplastic (malignant) in histology. They may exhibit obvious malignant cytology (similar to a carcinoma or sarcoma) or a high mitotic index of 20 or more mitoses per 10 HPF (Louis, 2016). Similarly to grade II, the WHO grade III classification includes a further two rare subtypes of meningioma, rhabdoid and papillary, which demonstrate specific individual histological patterns in addition to malignant tendencies (Louis, 2016; Whittle *et al.*, 2004). Rhabdoid meningioma are comprised predominantly of rhabdoid cells resulting in large tumour cells with irregularly placed nuclei and abundant eosinophilic cytoplasm; whereas papillary meningioma are characterised by a perivascular pseudopapillary pattern in which the tumour cells appear to cling to blood vessels (Louis, 2016).

Interestingly, there is a tendency for particular histopathological meningioma subtypes to originate from a specific intracranial site. Among grade I meningiomas, the meningothelial subtype is often located at the skull base and spine while fibroblastic meningiomas are more commonly found at the convexity of the brain. Grade II and III meningiomas are situated mainly at the convexity or with a parasagittal location and less frequently at the skull base (Ketter *et al.*, 2008; Kros *et al.*, 2001; Lee *et al.*, 2006; Mawrin, Chung & Preusser, 2015).

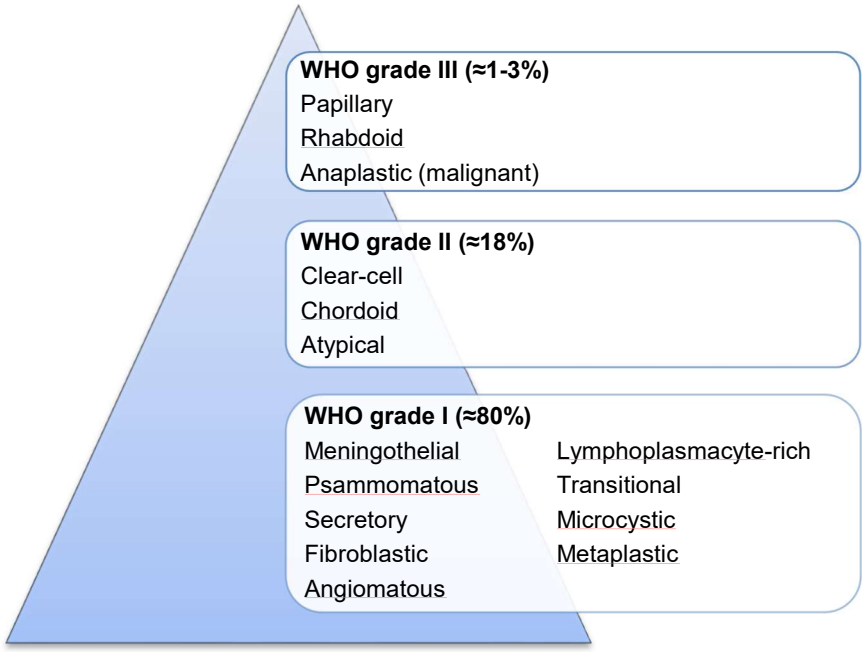

Figure 1.2 Histological variants of WHO grade classification of meningiomas. WHO grade I classification comprises of nine histological subtypes that are slow growing, benign tumours accounting for the majority of meningiomas (80%) (Riemenschneider, Perry & Reifenberger, 2006; Whittle *et al.*, 2004). Approximately 20% of meningiomas are classified as WHO grade II or III. These high-grade classifications are generally more aggressive in nature with malignant tendencies and each consists of three histological subtypes (Commins, Atkinson & Burnett, 2007; Louis, 2016).

1.3 Clinical presentation

Many meningiomas are asymptomatic and are discovered incidentally through investigations of unrelated medical symptoms (Whittle *et al.*, 2004). These tumours present a predicament for therapeutic intervention since little is known about their natural history and growth patterns (Chamoun, Krisht & Couldwell, 2011). Surgical resection is dependent upon consideration of several factors, predominantly the risk of surgical complications including mortality and permanent morbidity, alongside the age and medical condition of the patient (Chamoun, Krisht & Couldwell, 2011; Kuratsu, Kochi & Ushio, 2000). Generally, the suggested treatment strategy is to closely monitor

incidental meningiomas by clinical and radiological follow-ups for changes in tumour growth and neurological symptoms before performing surgical resection (Chamoun, Krisht & Couldwell, 2011; Kuratsu, Kochi & Ushio, 2000).

Symptomatic meningiomas present with a wide variety of clinical signs related to their location, size, compression of adjacent neurological structures, invasion of adjacent brain tissue, and obstruction of CSF pathways and venous drainage (Whittle *et al.*, 2004). Frequent symptoms include seizures, raised intracranial pressure, headaches and focal neurological deficits such as personality changes, impaired vision, anosmia and aphasia (Fathi & Roelcke, 2013; Whittle *et al.*, 2004).

1.4 Meningioma incidence and risk factors

Meningiomas are estimated to constitute 36% of all brain tumours, preferentially affecting women, with an annual incidence of 10.5 per 100,000 females and 4.8 per 100,000 males, and a female-to-male ratio of 2:1 and 9:1 for intracranial and spinal meningiomas, respectively (Louis, 2016; Riemenschneider, Perry & Reifenberger, 2006). The risk of meningiomas increases with age and incidence is highest in the elderly, commonly occurring in the sixth and seventh decade of life with a median age of 65 years (Louis, 2016; Marosi *et al.*, 2008). In adolescents and young adults 15-39 years of age, meningiomas account for approximately 16% of all primary brain and central nervous system (CNS) tumours, and are the second most frequent behind tumours of the pituitary (Ostrom *et al.*, 2015). Meningiomas in childhood are generally rare, representing 0.4-4.1% of paediatric-age tumours and 1.5-1.8% of all intracranial meningiomas (Tufan *et al.*, 2005), with a reported male predominance in contrast to adult meningiomas (Erdincler *et al.*, 1998; Germano *et al.*, 1994).

Established risk factors of meningiomas include deletion or germline mutations of the tumour suppressor gene *Neurofibromatosis 2* (*NF2, merlin, neurofibromin 2*).

Aberrations of *NF2* predispose individuals to the autosomal dominantly inherited disorder neurofibromatosis type 2 (NF2), characterised by the occurrence of several tumours of the CNS, including meningioma (Marosi *et al.*, 2008; Perry, Gutmann & Reifenberger, 2004). Genetic alterations of *NF2* in meningioma will be discussed in more detail later in this chapter. Aside *NF2* abnormalities, the only other well recognised risk factor is exposure to ionizing radiation that has been proven as a causative environmental risk factor of meningioma development (Longstreth *et al.*, 1993; Sadetzki *et al.*, 2002; Salvati *et al.*, 1997).

Meningioma in adulthood are associated with a female predominance hypothesised to reflect hormonal changes that may predispose women to meningioma development more commonly in adulthood (Black, 1993). Yet, the potential role of hormone receptors in meningioma pathogenesis remains controversial and requires further investigation (Claus *et al.*, 2011; Wiemels, Wrensch & Claus, 2010). Diseases proposed to be associated with a significantly increased risk for developing meningioma include pre-existing diabetes mellitus in males and females (40-69 years) and arterial hypertension in female patients aged 60-69 years (Schneider *et al.*, 2005). Studies investigating head injury in relation to meningioma development have yet to be confirmed as a contributing risk factor, although some studies suggest head trauma more than 10 years prior to be associated with an increased risk of meningioma (Phillips *et al.*, 2002; Wiemels, Wrensch & Claus, 2010), whilst mobile phone use has been deemed unrelated to meningioma incidence (Benson *et al.*, 2013).

1.5 Current therapies

1.5.1 Surgical excision

Surgical excision is the standard primary treatment for symptomatic meningiomas and is often required to alleviate neurological symptoms (Alexiou *et al.*, 2010). The decision to

operate is influenced by the surgical accessibility of the tumour, severity of symptoms, the natural history of the tumour and the medical history of the patient (Marosi *et al.*, 2008).

Gross total resection (GTR) of tumour, including surrounding dural attachment and infiltrated bone can often be curative (Marosi *et al.*, 2008). However, successful total tumour resection cannot be achieved in over 50% of newly diagnosed meningiomas (Fathi & Roelcke, 2013). Many meningiomas surround vital neural or vascular structures, or are en plaque and are thus only partially resectable (Whittle *et al.*, 2004). Surgical resection is also limited by anatomical location which may render a tumour inoperable; whilst in patients with higher grade meningioma, surgical excision has minimal impact on tumour management with increased recurrence rates (Norden, Drappatz & Wen, 2007). Effective therapeutic options for these patients are currently still lacking.

Significant postoperative morbidity has been reported following the attempted excision of meningioma including cranial neuropathies and vascular injury, culminating in a reduced quality of patient life due to permanent disabilities and neurological deficits (Lang, Neil-Dwyer & Garfield, 1999; Whittle *et al.*, 2004). Consequently, an approach of subtotal resection to minimise operative morbidity followed by observation and radiation therapy of residual tumour is sometimes preferred to GTR (Whittle *et al.*, 2004).

1.5.2 Radiotherapies

Radiotherapies can be offered as primary or adjuvant treatment for meningiomas and include conventional radiotherapy, stereotactic radiosurgery (SRS) and stereotactic fractionated radiotherapy (SFRT). The use of radiation therapies as primary treatment is suggested for meningiomas that are surgically inaccessible or may be encasing vital structures (Apra, Peyre & Kalamarides, 2018). SRS and SFRT allow for a focussed and

accurate delivery of radiation to the tumour thus limiting damage to surrounding healthy tissue (Alexiou *et al.*, 2010).

Adjuvant radiotherapy of partially resected benign cerebral meningiomas has been shown to significantly reduce tumour progression but not affect overall survival (Soyuer *et al.*, 2004). Radiotherapy is generally less utilised in grade I tumours and it is still debated as to whether adjuvant radiotherapy applied following excision of benign meningioma could be beneficial (Mawrin, Chung & Preusser, 2015).

In comparison with a grade I predicted five year recurrence rate following GTR of 3%, grade II and grade III meningioma rates are much higher at 38% and 78%, respectively (Marosi *et al.*, 2008). Adjuvant radiotherapy is therefore generally recommended at the area of resection and is considered a beneficial treatment strategy for aggressive grade II and III lesions (Mawrin, Chung & Preusser, 2015). Yet, its role in the management of grade II meningiomas is still uncertain with improvements in overall survival and progression-free survival (PFS) seen following partial resection, but not following GTR (Graffeo *et al.*, 2017; Park *et al.*, 2013).

Irrespective of meningioma grade, radiotherapy is associated with risk of complications including alopecia, double vision, seizures, headache, oedema, radio-necrosis, neurologic deficits, cranial nerve palsy, delayed hydrocephalus and radiation-induced meningioma (Fathi & Roelcke, 2013; Yamanaka, Hayano & Kanayama, 2017).

1.5.3 Chemotherapies

To date, traditional chemotherapies have not been effective in the treatment of meningioma and are only considered for those patients experiencing tumour recurrence or progression, subsequent to exhaustion of surgery and radiotherapy options, or for those with surgically inaccessible tumours and in rare cases of metastatic meningioma (Mawrin,

Chung & Preusser, 2015; Wen *et al.*, 2010). The administration of chemotherapies following pretreatment with surgery and radiation therapy has often resulted in uncontrolled case studies producing unreliable outcome data (Fathi & Roelcke, 2013). Further, the molecular pathogenesis of recurrent and progressive meningiomas is not sufficiently defined to enable an effective chemotherapeutic routine to be developed (Miller *et al.*, 2014).

The majority of classical chemotherapies such as dacarbazine, doxorubicin, ifosfamide, temozolomide and irinotecan have produced disappointing results without significant PFS (Apra, Peyre & Kalamarides, 2018; Chamberlain, Tsao-Wei & Groshen, 2004; Chamberlain, Tsao-Wei & Groshen, 2006). In addition, multidrug chemotherapy trials are scarce and appear unpromising. Treatment of patients with malignant meningiomas using an adjuvant combination of cyclophosphamide, doxorubicin and vincristine was found only to produce modest efficacy (Chamberlain, 1996). Currently, the only chemotherapeutic in use is the oral ribonucleotide reductase inhibitor, hydroxyurea, shown to induce apoptosis of cultured meningioma cells (Schrell *et al.*, 1997; Sherman & Raizer, 2012). However, its efficacy is controversial, often failing to reduce tumour size and patients experiencing tumour progression post-treatment (Chamberlain & Johnston, 2011; Loven *et al.*, 2004). Furthermore, patients often receive concurrent radiotherapy during administration of hydroxyurea making it difficult to confirm true therapeutic response (Moazzam, Wagle & Zada, 2013).

1.6 Genetic alterations in meningioma

1.6.1 *NF2* mutations

The tumour suppressor gene *NF2* was the first gene to be identified in the genetic aetiology of meningioma (Rouleau *et al.*, 1993; Trofatter *et al.*, 1993). *NF2* is located on chromosome 22q12 and encodes the protein NF2 (also known as Merlin/Schwannomin)

(Trofatter *et al.*, 1993). NF2 is a member of the 4.1, ezrin, radixin, moesin (FERM) gene family with strong structural similarity to the proteins ezrin, radixin and moesin (ERM proteins) (Gusella *et al.*, 1999). It is a cytoskeletal protein linking the plasma membrane to the actin cytoskeleton (Trofatter *et al.*, 1993) and works as a tumour suppressor by regulating contact-dependent inhibition of cellular proliferation through various pathways including the EGFR (epidermal growth factor receptor), Hippo, PI3K/AKT/mTOR (phosphoinositide 3-kinase (PI3K)–AKT–mammalian target of rapamycin (mTOR)), Notch and SHH (sonic hedgehog) signalling pathways (Curto *et al.*, 2007; Maitra *et al.*, 2006; Rong *et al.*, 2004b; Zhao *et al.*, 2007).

The molecular mechanisms underlying the regulation of NF2 activity have been related to its phosphorylation status, in particular the phosphorylation of serine 518 (S518) (Rong *et al.*, 2004a). Phosphorylation of NF2 on S518 by the kinase PAK2 (P21 (RAC1) activated kinase 2) was found to prevent the N-terminus interacting with the C-terminus resulting in an 'open' inactive form (Rong *et al.*, 2004a). In contrast, a more recent study by Sher *et al*. (2012) concluded that when phosphorylated on S518 NF2 forms a more, but not fully, 'closed' state with reduced ability to conduct its growth suppressor function (Sher *et al.*, 2012). Although conflicting, both studies state that phosphorylation on S518 results in reduced function of NF2.

Germline *NF2* mutations cause the autosomal dominantly inherited disorder NF2, which is the most firmly established genetic syndrome predisposing individuals to meningioma development (Perry, Gutmann & Reifenberger, 2004). It is characterised by the development of multiple tumours of the CNS including bilateral vestibular schwannomas, meningiomas and ependymomas (Petrilli & Fernandez-Valle, 2016). Intracranial meningiomas are the second most common tumour of NF2 patients and around 50-75% of patients will develop the tumour during their lifetime, often with

multiple occurrences (Evans *et al.*, 1992; Smith *et al.*, 2011). Further, *NF2* is the most frequently genetically altered gene in meningiomas, with somatic mutations identified in approximately 60% of sporadic and in the majority of NF2-associated meningiomas (Perry, Gutmann & Reifenberger, 2004; Riemenschneider, Perry & Reifenberger, 2006; Ruttledge *et al.*, 1994).

Inactivation of the *NF2* gene is found across all meningioma grades. Commonly, inactivation is associated with recurrent monosomy of chromosome 22 or loss of heterozygosity (LOH) of chromosome 22q. This is accompanied by mutations in the remaining *NF2* allele and loss of tumour suppressor function, thus following the Knudson's two-hit hypothesis (Knudson, 1971; Riemenschneider, Perry & Reifenberger, 2006). *NF2* mutations typically consist of protein-truncating nonsense or frameshift mutations associated with a more severe NF2 phenotype, whilst less frequent missense and splice site mutations are accompanied with a milder phenotype (Brastianos *et al.*, 2013; Ruttledge *et al.*, 1996). Aside from mutational inactivation, aberrant hypermethylation of the *NF2* gene has also been identified in sporadic meningiomas as an epigenetic mechanism of *NF2* inactivation (Lomas *et al.*, 2005). Mutations of the *NF2* gene are found in meningiomas of all WHO grades and are therefore considered to be an early event in tumour development (Whittle *et al.*, 2004).

1.6.2 Non-*NF2* germline mutations

Multiple meningiomas occur in fewer than 10% of meningioma patients and may be caused by germline mutations of *NF2*. However, in non-NF2 patients diagnosed with multiple meningiomas, predisposing germline mutations of genes other than *NF2* were until recently, unknown. Studies have now identified germline mutations in several genes to be implicated in meningioma pathogenesis. These include *SMARCB1* (*SWI/SNF-related matrix-associated actin-dependent regulator of chromatin subfamily B member*

1) and *SMARCE1* (*SWI/SNF-related matrix-associated actin-dependent regulator of chromatin subfamily E member 1*), two subunit genes of the Switch/Sucrose nonfermentable (SWI/SNF) chromatin-remodelling complex; the SHH signalling pathway gene *SUFU* (*suppressor of fused homolog*) and most recently the ubiquitin carboxy-terminal hydrolase gene *BAP1* (*ubiquitin carboxyl-terminal hydrolase BAP1*) (Aavikko *et al.*, 2012; Bacci *et al.*, 2010; Christiaans *et al.*, 2011; Shankar *et al.*, 2017; Smith *et al.*, 2017; Smith *et al.*, 2013; Smith *et al.*, 2014).

Several studies have investigated the contribution of germline *SMARCB1* mutations in the development of multiple meningioma with conflicting outcomes. One study reported a germline *SMARCB1* mutation in meningiomas derived from a family diagnosed with schwannomatosis (Bacci *et al.*, 2010); whilst another failed to detect *SMARCB1* germline mutations in patients with multiple meningiomas (Hadfield *et al.*, 2010). A later study of familial multiple meningiomas confirmed presence of a *SMARCB1* germline missense mutation detrimental to protein function (Christiaans *et al.*, 2011). The authors concluded *SMARCB1* germline mutations to be more likely associated with familial cases of multiple meningioma similar to their identification in familial schwannomatosis (Bacci *et al.*, 2010; Christiaans *et al.*, 2011).

Heterozygous loss-of-function *SMARCE1* germline mutations were initially detected in individuals with familial multiple spinal meningiomas absent of *NF2* mutations but have since also been found in cranial meningiomas (Smith *et al.*, 2013; Smith *et al.*, 2014). SMARCE1 is known to have many roles including as a pro-apoptotic factor and thus its loss may result in apoptotic dysregulation (Smith *et al.*, 2013). Interestingly, *SMARCE1* germline mutations predispose to meningioma of clear-cell histology appearing to influence histological subtype rather than tumour location (Smith *et al.*, 2017; Smith *et al.*, 2014). Indeed, loss of SMARCE1 expression has recently been shown

to be a highly specific diagnostic biomarker for clear-cell meningioma (Tauziede-Espariat *et al.*, 2018).

Similarly to *SMARCB1* and *SMARCE1*, germline mutations of the tumour suppressor gene *SUFU* were identified in a case of familial multiple meningioma (Aavikko *et al.*, 2012). Functional analyses showed the mutation to reduce the negative regulation of the SHH pathway by *SUFU* causing a predisposition to meningioma development (Aavikko *et al.*, 2012).

Most recently, germline mutations of the tumour suppressor gene *BAP1* which codes for the ubiquitin carboxy-terminal hydrolase, BAP1, have been reported in the grade III rhabdoid meningioma histological subtype (Shankar *et al.*, 2017). BAP1 loss has been linked to ubiquitin deregulation and reduced time to tumour recurrence suggesting germline *BAP1* mutations predispose to this aggressive histological subtype (Shankar *et al.*, 2017).

1.6.3 Non-*NF2* somatic mutations

The genetic background of the approximate 40% sporadically occurring meningiomas absent of *NF2* mutations has been investigated by several genomic studies. Two defining studies by Clark *et al*. (2013) and Brastianos *et al*. (2013) described recurrent oncogenic somatic mutations in subsets of meningiomas devoid of *NF2* alterations, referred to as non-*NF2* mutant meningiomas (Brastianos *et al.*, 2013; Clark *et al.*, 2013).

In a genomic analysis of 300 meningiomas, Clark *et al*. (2013) identified mutations in *TRAF7* (*tumor necrosis factor receptor-associated factor 7*), *KLF4* (*Kruppel-like factor 4*), *AKT1* (*RAC-alpha serine/threonine-protein kinase*), and *SMO* (*Smoothened, frizzled family receptor*) that were mutually exclusive of *NF2* mutations (Clark *et al.*, 2013).

TRAF7 is an E3 ubiquitin ligase with the ability to induce apoptosis and has been found to harbour mutations in nearly 25% of meningiomas (Clark *et al.*, 2013). Over 90% of *TRAF7* mutations in meningioma were mapped to its WD40 domains through which it binds various molecules to affect signalling pathways such as NF-κB (Clark *et al.*, 2013). Clark *et al*. (2013) also discovered *TRAF7* mutations often co-occurred with the recurrent K409Q mutation in the transcription factor KLF4, most commonly recognised as one of four factors that together induce reprogramming of differentiated somatic cells back to a pluripotent stem cell state (Clark *et al.*, 2013; Takahashi *et al.*, 2007). The residue K409 is located in the DNA binding domain of KLF4 and when mutated may prevent differentiation and drive embryonic genetic programmes resulting in tumour formation (Clark *et al.*, 2013). Interestingly, the co-occurrence of $KLF4^{K409Q}$ and *TRAF7* mutations has consistently been identified in secretory meningioma suggesting this mutational combination may predispose to this histological variant (Reuss *et al.*, 2013).

Subsequent to conducting a genomic analysis of 65 meningioma, Brastianos *et al*. (2013) also observed recurrent *AKT1* and *SMO* mutations in non-*NF2* mutants as did Clark *et al*. (2013) (Brastianos *et al.*, 2013; Clark *et al.*, 2013). Similarly to $KLF4^{K409Q}$, the $AKT1^{E17K}$ mutation was observed to co-occur with *TRAF7* mutations, yet was mutually exclusive of $KLF4^{K409Q}$ (Brastianos *et al.*, 2013; Clark *et al.*, 2013). This oncogenic $AKT1^{E17K}$ mutation causes constitutive activation of AKT1 and downstream stimulation of the PI3K/AKT/mTOR pathway (Carpten *et al.*, 2007). Additional genomic studies have found $AKT1^{E17K}$ to predominantly associate with grade I meningioma of meningothelial and transitional histology, originating most frequently from the anterior or median middle fossa of the skull base as well as the olfactory groove (Boetto *et al.*, 2017; Sahm *et al.*, 2013; Yuzawa, Nishihara & Tanaka, 2016).

Mutations of *SMO*, a member of the SHH signalling pathway, have been found in around 5% of non-*NF2* mutants (Brastianos *et al.*, 2013; Clark *et al.*, 2013). Two recurrent mutations have been described; L412F, previously described in desmoplastic medulloblastoma (Jones *et al.*, 2012), and the oncogenic somatic missense mutation W535L, reported to activate SHH signalling in basal cell carcinoma (Reifenberger *et al.*, 1998). *SMO* mutations have been observed to associate with meningothelial histology and localise to the anterior medial skull base and olfactory groove (Boetto *et al.*, 2017; Brastianos *et al.*, 2013; Clark *et al.*, 2013).

Following these key studies, comprehensive genomic analyses have identified additional mutations of genes mainly in grade I meningiomas including *PIK3CA* (*phosphatidylinositol-4,5-bisphosphate 3-kinase catalytic subunit alpha*), *PIK3R1* (*phosphatidylinositol 3-kinase regulatory subunit alpha*) and *AKT3* (*RAC-gamma serine/threonine-protein kinase*) (Abedalthagafi *et al.*, 2016; Clark *et al.*, 2013; Clark *et al.*, 2016). These mutations are mutually exclusive of *NF2* mutations and have been associated with activation of PI3K/AKT/mTOR signalling (Abedalthagafi *et al.*, 2016; Clark *et al.*, 2013; Clark *et al.*, 2016). Other genes found to possess somatic driver mutations mutually exclusive of *NF2* mutations in benign grade I meningiomas include *POLR2A* (*DNA-directed RNA polymerase II subunit RPB1*), *PRKAR1A* (*protein kinase, cAMP-dependent, regulatory, type I, alpha*) as well as previously unidentified mutations of *SUFU* (Clark *et al.*, 2016).

The overlap between the most frequently observed recurrent mutations identified in meningiomas described above are depicted in Figure 1.3.

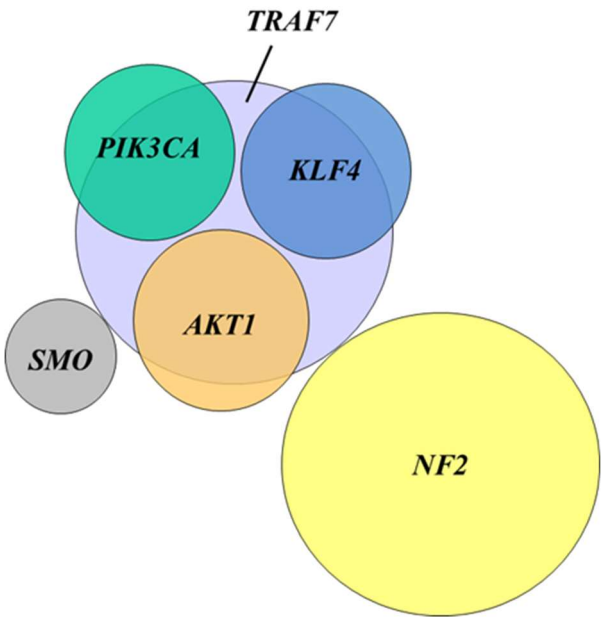

Figure 1.3 Schematic representation of the overlap between recurrent mutations identified in meningioma. Image adapted from Abedalthagafi *et al*. (2016) (Abedalthagafi *et al.*, 2016).

Non-*NF2* somatic mutations discussed so far were predominantly discovered in grade I meningioma and have greatly increased our knowledge of the genetic landscape of these benign tumours. In contrast, fewer non-*NF2* somatic mutations have been discovered in meningioma undergoing malignant progression. The recurrent mutation most frequently associated with malignant progression lies in the promoter of the *TERT* (*telomerase reverse transcriptase*) gene (Goutagny *et al.*, 2014; Harmanci *et al.*, 2017; Sahm *et al.*, 2016). This mutation is associated with increased expression of the protein encoded by *TERT*, a ribonucleoprotein enzyme essential for chromosome telomere replication, and leads to the proliferation of cancer cells (Sahm *et al.*, 2016). *TERT* promoter mutations have thus been suggested to act as a progressive prognostic marker of high-grade meningioma (Harmanci *et al.*, 2017). Interestingly, a recent analysis of anaplastic meningioma did not observe any mutations of the *TERT* promoter but did reveal the presence of somatic driver mutations in the SWI/SNF chromatic regulatory complex, most frequently in the SWI/SNF component *ARID1A* (*AT-rich interactive domain-containing protein 1A*) (Collord *et al.*, 2018). This complex is known to act as a tumour

suppressor by antagonising the oncogenic chromatin modifying protein PRC2 (polycomb repressive complex 2) (Collord *et al.*, 2018). The study identified mutations of SWI/SNF complex genes in 16% of the anaplastic meningiomas analysed, concluding this finding to hold prognostic and therapeutic value (Collord *et al.*, 2018).

Taken together, the genetic studies discussed here have been pivotal in elucidating the mutational profile of meningioma. Moreover, by determining mutations associated with histological variants and anatomical location the possibility of harnessing these genetic alterations as future biomarkers increases, however their mechanistic involvement with meningioma development has yet to be established (Smith, 2015).

1.6.4 Chromosomal copy-number alterations

Karyotypic aberrations increase considerably in frequency and complexity toward the higher meningioma grades (Riemenschneider, Perry & Reifenberger, 2006). Cytogenetic changes observed in grade II and III include chromosomal losses of 1p, 6q, 9p, 10, 14q and 18q, and chromosomal gains at 1q, 9q, 12q, 15q, 17q and 20q (Riemenschneider, Perry & Reifenberger, 2006). Of these, only chromosome 9p loss has shown clear association with candidate driver genes of tumourigenesis identified as the tumour suppressor cell cycle regulator genes *CDKN2A* (*cyclin-dependent kinase inhibitor 2A*), *ARF* (*tumor suppressor ARF*), and *CDKN2B* (*cyclin-dependent kinase 4 inhibitor B*) (Bostrom *et al.*, 2001). Association of the remaining copy-number variants with driver genes is still largely unclear. Although several potential genes have been screened; such as *TP73* (*tumor protein 73*), *CDKN2C* (*cyclin-dependent kinase 4 inhibitor C*), *RAD54L* (*DNA repair and recombination protein RAD54-like*), *EPB41* (*protein 4.1*), *GADD45A* (*growth arrest and DNA damage-inducible protein GADD45 alpha*), and *ALPL* (*alkaline phosphatase, tissue-nonspecific isozyme*) on chromosome 1p; and *NDRG2* (*protein NDRG2*) and *MEG3* (*maternally expressed 3*) on chromosome 14q; evidence for their

mutation and a role in meningioma pathogenesis has not been conclusive (Bi *et al.*, 2017; Riemenschneider, Perry & Reifenberger, 2006).

1.7 Molecular targets in meningioma

The conventional cancer treatments of surgery, radiotherapy and chemotherapy are not effective for all cancers and are associated with risk of side effects. As discussed in the previous subsections (1.5.1 – 1.5.3), chemotherapies have shown minimal therapeutic efficacy in meningioma, whilst surgery and radiotherapy are associated with complications including postoperative morbidity and radiation neurotoxicity. Therefore, the development of effective pharmaceutical therapeutics is desperately required to treat these tumours.

Targeted therapy has gained extensive recognition in the field of cancer therapeutics and much translational medical research is now based around defining the molecular profile of a particular cancer. By elucidating the altered molecular mechanisms and signalling pathways involved in tumour development and survival, tumour-specific features can be identified. By exploiting these features, targeted therapies aim to selectively affect only cancer cells or the surrounding tumour microenvironment for a targeted therapeutic delivery, reducing toxicity to off-target healthy cells (Padma, 2015).

1.7.1 Preclinical studies

Growth factor receptors have been implicated in meningioma pathogenesis and studies have shown some promise in targeting their overexpression and associated downstream signalling pathways (Wen *et al.*, 2010).

Meningiomas of all grades have been found to coexpress the PDGF (platelet-derived growth factor) ligands AA and BB and the PDGF receptor-β (PDGFR-β) (Maxwell *et al.*, 1990; Wang *et al.*, 1990; Yang & Xu, 2001), with studies demonstrating a correlation of

PDGFR-β activation with increased cell division and membrane expression of PDGFR-β in over 80% of meningioma analysed (Black *et al.*, 1994; Hilton *et al.*, 2016; Nagashima *et al.*, 2001). These findings have warranted the investigation of PDGFR inhibitors in meningioma. Pfister *et al*. (2012) evaluated the PDGFR-β inhibitors sunitinib and tandutinib as well as gambogic acid in primary meningioma cells and concluded all three agents were effective at inhibiting cell migration (Pfister *et al.*, 2012). More recently, upon treatment of the malignant meningioma cell line IOMM-Lee with the multi-tyrosine kinase inhibitors sorafenib and regorafenib, cell proliferation was reduced by the downregulation and inhibition of PDGFR (Tuchen *et al.*, 2017). These preclinical studies would suggest PDGFR-β to be an attractive therapeutic target in meningioma.

Growth factor stimulation of receptors such as PDGFR and EGFR is commonly transduced through the activation of kinase cascades including the MAPK (mitogen-activated protein kinase) and the PI3K/AKT/mTOR pathways, both known to be key regulators of cell proliferation (Wen *et al.*, 2010).

Constitutive activation of MAPK has been identified in meningioma cells and upon stimulation with PDGF-BB ligand, cell proliferation was observed to increase in part via MAPK activation (Johnson *et al.*, 2001). Treatment of meningioma cells with the MEK (mitogen-activated protein kinase kinase 1) inhibitor PD098059 decreased MAPK phosphorylation and inhibited cell growth (Johnson *et al.*, 2001). Preclinical studies have also investigated the effects of inhibiting members of the PI3K/AKT/mTOR pathway shown to be active in grade I meningiomas, including by stimulation with PDGF-BB ligand (Johnson *et al.*, 2002). Treatment with the PI3K inhibitor wortmannin was found to produce a reduction in phosphorylation of downstream signalling components in meningioma cells following stimulation with PDGF-BB ligand (Johnson *et al.*, 2002). Preclinical combinatorial treatments have also been applied to the PI3K/AKT/mTOR

pathway including the mTOR inhibitor everolimus combined with octreotide, an agonist of the sst2 somatostatin receptor known to have elevated expression in meningioma (Graillon *et al.*, 2015). Here, treatment produced an additive inhibition of meningioma cell proliferation but only in some cases, whilst in another study, the use of everolimus alone exhibited significant reduction of proliferation and survival in benign and malignant meningioma cell lines (Graillon *et al.*, 2015; Pachow *et al.*, 2013).

Drug treatments targeting growth factors and components of associated signalling pathways have thus demonstrated some potential as therapeutic targets in meningioma; however other targets and signalling pathways have also shown therapeutic potential.

The programmed cell death protein 1 pathway (PD-1/PD-L1) has shown promise as a novel therapeutic target in meningioma. This pathway modulates T cell activity resulting in their reduced activity and proliferation (Gelerstein *et al.*, 2017). High-grade meningiomas have been described to express the PD-L1 ligand (programmed-death ligand 1), indicating suppression of tumour infiltrating regulatory T cells that harbour the complementary PD-1 (programmed death receptor 1) receptor (Du *et al.*, 2015). Administration of the anti-PD-1 antibody nivolumab in a single patient with sphenoid wing meningioma exhibited a significant reduction in tumour size following a six month treatment (Gelerstein *et al.*, 2017). Consequently, a phase II trial evaluating the effectiveness of another anti-PD-1 antibody, pembrolizumab is now recruiting meningioma patients (NCT03279692).

Another treatment that may hold therapeutic efficacy in meningioma is the pan-histone deacetylase inhibitor, AR-42. Studies have shown inhibition of *NF2*-deficient meningioma cell proliferation and substantial tumour regression *in vivo* following six months treatment with AR-42 (Burns *et al.*, 2013; Bush *et al.*, 2011). These investigations suggest AR-42 may hold therapeutic efficacy for patients with *NF2*-deficient

meningioma. Indeed, a clinical trial assessing AR-42 in the treatment of vestibular schwannoma and meningioma is currently recruiting (NCT02282917).

More recently, Angus *et al*. (2018) confirmed the expression and activation of several kinases including EPH (erythropoietin-producing hepatocellular) RTKs (receptor tyrosine kinases), c-KIT (mast/stem cell growth factor receptor Kit), and SRC (proto-oncogene tyrosine-protein kinase Src) family kinase members in *NF2*-deficient meningioma (Angus *et al.*, 2018). The authors revealed that co-targeting of the mTORC1/2 (mTOR complex 1/2) pathway with the dual mTORC1/2 inhibitor AZD2014 in combination with the multi-kinase inhibitor dasatinib, led to a synergistic suppression of primary *NF2*-deficient meningioma cell growth (Angus *et al.*, 2018).

1.7.2 Clinical trials

The development and application of effective targeted molecular therapies in meningioma has encountered mixed successes in clinical trials (Chamberlain, 2012; Wen *et al.*, 2010). Of these, many have focussed on the inhibition of hormone and growth factor receptors as well as growth factor ligands and their downstream signalling pathway components.

The role of hormone receptors in the development of meningioma has long been disputed yet this has not discouraged interest in the possibility of hormonal targeting therapies. Presence of the oestrogen receptor and progesterone receptor has been described in approximately 10% and 70% of meningiomas, respectively (Chamberlain, 2012; Wen *et al.*, 2010). However, the application of anti-hormonal treatments has proved largely disappointing. A phase II study of the anti-oestrogen agent tamoxifen in patients with refractory meningioma did not yield significant anti-tumour activity; whilst a phase III study of the anti-progesterone agent mifepristone in patients with unresectable meningioma found no significant difference in overall survival between placebo assigned and treated patients (Goodwin *et al.*, 1993; Ji *et al.*, 2015).

The increased expression of PDGF ligands and PDGFR-β as well as the preclinical studies discussed above have led to clinical trials targeting PDGFR-β in meningioma. The multi-tyrosine kinase inhibitor imatinib mesylate (Gleevec®) has been used in clinical trials for the inhibition of PDGFR-α and β. In a phase II trial of 23 patients with recurrent meningioma imatinib treatment was well tolerated and achieved therapeutic plasma levels, although the drug was found to have no significant activity (Wen *et al.*, 2009). Another phase II trial of 21 patients with progressive or recurrent meningioma used imatinib in combination with the chemotherapeutic agent hydroxyurea (Reardon *et al.*, 2012). Whilst treatment was well tolerated it demonstrated only modest anti-tumour activity, producing a poorer PFS among high-grade patients than those with grade I tumours (Reardon *et al.*, 2012). The multi-tyrosine kinase inhibitor sunitinib has also been evaluated in a phase II trial of recurrent or progressive high-grade meningioma as a single-agent therapy against both PDGFR and VEGFR (vascular endothelial growth factor receptor) (Kaley *et al.*, 2015). Here, sunitinib demonstrated some therapeutic efficacy with 15 patients (42%) meeting the primary endpoint of PFS at six months but treatment was associated with significant toxicity (Kaley *et al.*, 2015). The poor efficacy of imatinib and toxicity of sunitinib reported in these trials suggests that unlike the promising preclinical studies targeting PDGFR-β discussed above, these inhibitors would not be suitable targeted therapies of PDGFR in meningioma.

Studies have also investigated targeting growth factor ligands themselves. Former studies have reported both VEGF (vascular endothelial growth factor) and VEGFR to be expressed in meningioma as well as VEGF expression increasing with grade (Hilton *et al.*, 2016; Lamszus *et al.*, 2000; Pistolesi *et al.*, 2004). It thus follows that trials in meningioma have been conducted using the monoclonal antibody bevacizumab, which binds VEGF isoforms and inhibits angiogenesis.

Trials of bevacizumab treatment have demonstrated inconsistent efficacy in meningioma. Lou *et al*. (2012) reviewed 14 patients with recurrent meningioma and concluded single-agent bevacizumab or combination treatment with chemotherapy was associated with a six-month PFS of 86% and anti-tumour activity (Lou *et al.*, 2012). In contrast, Nunes *et al*. (2013) described only 29% of NF2-associated meningiomas to show a radiographic response of 20% reduction in tumour volume whilst receiving bevacizumab (Nunes *et al.*, 2013). More recently, Shih *et al*. (2016) administered bevacizumab in combination with the mTOR inhibitor everolimus to 17 patients with recurrent meningioma in a phase II trial (Shih *et al.*, 2016). However, patient toxicity and a median PFS analogous to earlier trials of single-agent bevacizumab treatment indicated this combinatorial approach failed to produce an additive response (Lou *et al.*, 2012; Nayak *et al.*, 2012; Shih *et al.*, 2016).

Similar to PDGFR and VEGFR, EGFR has been found overexpressed in meningioma (Carroll *et al.*, 1997; Hilton *et al.*, 2016; Wernicke *et al.*, 2010) and its activation by the ligands EGF and transforming growth factor-α (TGF- α) has been shown to stimulate proliferation of meningioma cells *in vitro* (Johnson *et al.*, 1994; Weisman, Raguet & Kelly, 1987). Thus, small molecule EGFR inhibitors have entered clinical trials. In a phase II trial the EGFR inhibitors gefitinib or erlotinib were administered to 25 patients with recurrent meningiomas (Norden *et al.*, 2010). Treatments were generally well tolerated but produced no objective imaging responses and a six-month PFS of only 25% and 29% for grade I and high-grade tumours respectively. The study concluded neither inhibitor exhibited a significant response (Norden *et al.*, 2010).

The identification of recurrent genetic alterations in meningioma has increased substantially in recent years as previously discussed in Section 1.6. However, the potential to harness these mutations for therapeutic benefit has been limited by the lack

of knowledge surrounding their mechanistic role in meningioma pathogenesis, as well as the small number of therapeutic options against this catalogue of identified genetic alterations. A phase II trial to evaluate the use of either a SMO or FAK (focal adhesion kinase) inhibitor based on the *AKT1*, *SMO* and *NF2* mutational status of patients with progressive meningioma was set up in 2015, but has since been suspended (NCT02523014).

Further to this, Weller *et al*. (2017) documented the treatment of a patient diagnosed with metastatic meningioma harbouring the recurrent AKT^{E17K} mutation using the AKT inhibitor AZD5363 (Weller *et al.*, 2017). Treatment was generally well tolerated and the patient exhibited disease stabilisation with minor reduction in tumour volumes; responses not seen with earlier treatments (Weller *et al.*, 2017). This report suggests an AKT inhibitor in patients harbouring the $AKT1^{E17K}$ mutation may hold therapeutic promise, whilst more generally; standardised molecular screening of patient tumours could facilitate the future application of appropriate targeted treatments.

An overview of the molecular targets and associated pathways discussed in this section is shown in Figure 1.4.

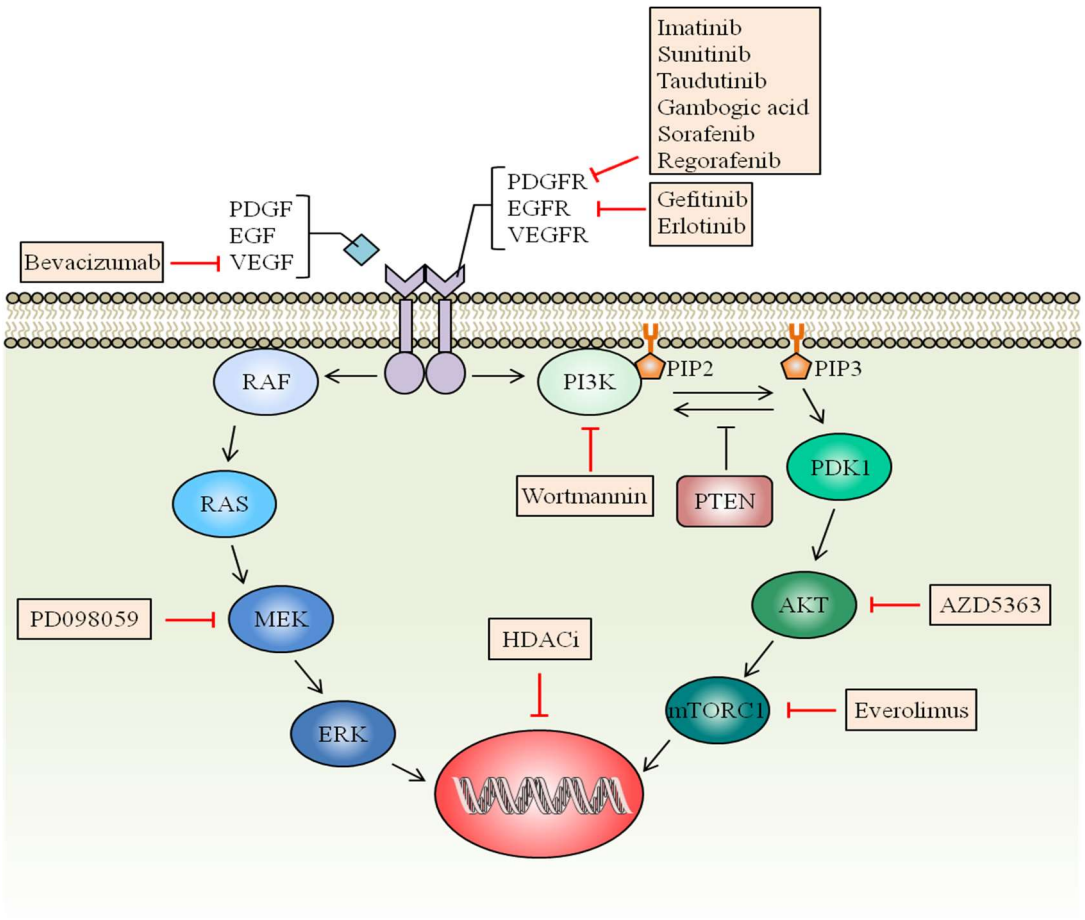

Figure 1.4 Overview of a selection of molecular targets and associated signalling pathways in meningioma. This figure summarises a selection of therapeutics and their associated molecular targets that have been evaluated in meningioma for their efficacy as potential targeted treatments. Two oncogenic pathways; the phosphoinositide 3-kinase (PI3K)–AKT–mammalian target of rapamycin complex (mTORC) (PI3K/AKT/mTOR) pathway and the MAPK (mitogen-activated protein kinase) pathway, often associated with many of the targets and activated in meningioma are also shown. PDGFR, platelet-derived growth factor receptor; EGFR, epidermal growth factor receptor; VEGFR, vascular endothelial growth factor receptor; PI3K, phosphoinositide 3-kinase; PTEN, phosphatase and tensin homologue deleted on chromosome 10; mTORC1, mammalian target of rapamycin complex 1; HDACi, histone deacetylase inhibitors; PDK1, 3-phosphoinositide-dependent protein kinase 1; ERK, extracellular signal–regulated kinase; MEK, mitogen-activated protein kinase kinase 1; PIP_2, phosphatidylinositol (4, 5)-bisphosphate; PIP_3, phosphatidylinositol (3, 4, 5)-trisphosphate. Adapted from Norden *et al*. (2007) (Norden, Drappatz & Wen, 2007).

Taken together, the preclinical and clinical studies discussed here illustrate that there is still a lack of established molecular targets with proven therapeutic efficacy in meningioma. The progress of defining molecular targets in meningiomas has been challenging due to several limiting factors. Studies have often been restricted by the lack of preclinical animal models that reflect the sporadic development and genetic background of meningioma in which to test potential targeted therapies (Norden, Drappatz & Wen, 2007). The progress of targeted molecular drug development for meningioma has, for a long time, been fairly stagnant due to limited knowledge surrounding their molecular pathogenesis and the relatively low number of patients requiring alternative treatments aside conventional regimes (Norden, Drappatz & Wen, 2007). Consequently, pharmaceutical companies have been reluctant to invest heavily into the development and verification of targeted therapies in these tumours (Norden, Drappatz & Wen, 2007).

Clinical trials have to date largely concentrated on targeting growth factors and their receptors in meningioma, yet none have shown responses to rival the current treatment regime for these tumours. Studies have revealed the activation of multiple growth factor signalling pathways in meningioma providing a possible explanation for the poor efficacy of single-agent treatments (Hilton *et al.*, 2016). Future therapies will likely require the combinatorial targeting of molecules and associated signalling pathways following an improved understanding of meningioma pathogenesis. Indeed, the scientific field of 'omics' is unravelling the molecular landscape of meningioma by producing large, unbiased datasets enabling the identification of novel targets that can be exploited for therapy. The move towards omics-based approaches in characterising meningioma molecular profiles is discussed in the following Section 1.8.

1.8 'Omics' studies in meningiomas

1.8.1 The 'omics' era

In the last two decades, the emergence of the field of 'omics' sciences has greatly enhanced our ability to investigate the molecular systems of a biological sample. The suffix 'omic', is derived from the Greek word for 'body', and has been used in a biological context to specify a body of knowledge surrounding a particular class of biological molecule (Epstein & Lin, 2017). The repertoire of omics based studies is ever-growing and includes the detection of genes (genomics), mRNA (transcriptomics), proteins (proteomics), metabolites (metabolomics) and epigenetic modifications (epigenomics), yet this is not an exhaustive list (Epstein & Lin, 2017). Omic approaches have led to the development of high-throughput techniques, allowing the targeted or unbiased global screening of molecules in a biological sample. They permit the simultaneous identification and quantification of multiple molecules across many samples producing large databases of information. Following bioinformatic analyses, these databases enable the complex interactions of a biological system to be elucidated upon. Ultimately, omics studies lead not only to a better understanding of normal state physiological processes but also in defining the molecular signatures of disease.

High-throughput biological profiling of disease, including cancer, facilitates the generation of novel molecular biomarkers, as well as molecular targets for therapy (Geurts van Kessel, 2010). Further, the rise of systems biology, combining the integration of multi-omics datasets with bioinformatics to achieve a more complete overview of a biological system, has produced a shift towards 'personalised medicine' (Hood, Balling & Auffray, 2012). Personalised medicine represents a discipline that is predictive, personalised, preventive and participatory, and has hence been termed 'P4 medicine' (Hood & Friend, 2011). This concept represents a shift from a conventional reactive

medical approach to disease, toward a proactive approach focussed on the wellness of an individual. It allows for the prediction of disease development by comparison of patient biological datasets with those of the population, using the patient's own healthy measurements as a control, thus taking into account individual variability to provide personalised tailored healthcare (Hood, Balling & Auffray, 2012; Hood & Friend, 2011). The preventative aspect of P4 medicine is becoming increasingly pertinent in optimising the health of an individual as the abundance of information surrounding alterations of molecular composition and signalling in a disease state rises. Omics-derived data will be available to guide the implementation of patient-specific therapies to prevent disease development or progression (Hood & Friend, 2011). Lastly, fundamental to future translation of omics datasets into a healthcare setting will be patient participation in the acquisition and availability of personalised electronic datasets alongside the education of medical professionals to interpret this data (Hood & Friend, 2011; Tebani *et al.*, 2016).

In the following sections, the use of omics-based techniques in meningioma as well as a summary of significant findings in the field will be discussed.

1.8.2 Overview of omics applications in meningioma

Omics studies have been applied to meningioma to unravel the molecular landscape of this disease. This subsection will discuss some of the key findings in the meningioma omics field in recent years.

1.8.2.1 Genomics

Genetic alterations of meningioma have now been relatively well characterised using cytogenetic techniques and NGS-based methods. Many of these were previously described in detail in Section 1.6. Genomic studies have identified chromosomal aberrations, most frequently the recurrent monosomy of chromosome 22 observed

throughout all grades, whilst high-grade meningiomas are associated with additional copy number variations of both gains and losses (Riemenschneider, Perry & Reifenberger, 2006). Genomic analyses have also confirmed genes possessing germline mutations (*NF2*, *SMARCB1*, *SMARCE1*, *SUFU* and *BAP1*) (Aavikko *et al.*, 2012; Bacci *et al.*, 2010; Christiaans *et al.*, 2011; Hadfield *et al.*, 2010; Perry, Gutmann & Reifenberger, 2004; Shankar *et al.*, 2017) and genes containing recurrent somatic mutations (*NF2*, *TRAF7*, *KLF4*, *AKT1*, *SMO*, *PIK3CA*, *PIK3R1*, *AKT3*, *POLR2A*, *PRKAR1A*, *SUFU*, *TERT*, *SMARCB1* and *BAP1*) contributing to meningioma pathogenesis (Abedalthagafi *et al.*, 2016; Brastianos *et al.*, 2013; Clark *et al.*, 2013; Clark *et al.*, 2016; Reuss *et al.*, 2013; Shankar *et al.*, 2017). Furthermore, genomic alterations have been found to coincide with particular histological subtypes and tumour locations (Boetto *et al.*, 2017; Brastianos *et al.*, 2013; Clark *et al.*, 2013; Reuss *et al.*, 2013).

1.8.2.2 Epigenomics

Despite great advancements in genomic studies, around 20% of meningiomas have not yet been found to harbour known oncogenic driver mutations (Bi *et al.*, 2016). In those meningiomas absent of known mutations and potentially those with already defined mutations, epigenetic modifications may play a fundamental role in tumourigenesis and progression. Epigenetic mechanisms are defined as heritable changes that influence patterns of gene expression without affecting the DNA sequence and include DNA methylation, microRNAs (miRNAs), histone modifications and chromatin remodelling (Sandoval & Esteller, 2012). The reprogramming and deregulation of epigenetic modifications is now widely recognised as a hallmark of cancer and has led to numerous epigenomic investigations to establish the contribution of this field in cancer (Sandoval & Esteller, 2012).

In meningioma, epigenetic studies have identified alterations in DNA methylation of specific tumour suppressor genes and correlated these findings with specific WHO grades. One well known tumour suppressor gene demonstrating an altered DNA methylation profile in meningiomas is *TIMP3* (*tissue inhibitor of metalloproteinase 3*), encoding a protein that inhibits the activity of matrix metalloproteinases and thus can aid in reducing the invasive and metastatic potential of tumour cells (Barski *et al.*, 2010). Hypermethylation of the *TIMP3* promoter and its associated transcriptional downregulation has been frequently found among grade III meningiomas and suggested as a marker of malignancy (Barski *et al.*, 2010). Other studies have even revealed comethylation of genes as potential prognostic markers, such as the hypermethylation of HOXA genes within the homeobox gene family that have been reported to be associated with high-grade meningiomas (Di Vinci *et al.*, 2012).

Most recently, Sahm *et al.* (2017) performed DNA methylation profiling of meningiomas and described a stratification approach based on distinct methylation profiles of these tumours independent of WHO grading (Sahm *et al.*, 2017). In the study, a comprehensive analysis of approximately 500 meningioma samples was performed, integrating DNA methylation profiling, copy-number aberrations, recurrent mutations and histology to define six distinct methylation classes of meningioma (Sahm *et al.*, 2017). This methylation-based classification appears to provide a more accurate prediction of tumour progression, recurrence and prognosis associated with each class than the current WHO classification that relies solely on histology to predict clinical outcome (Sahm *et al.*, 2017).

In addition to aberrant DNA methylation patterns, the differential expression of miRNAs and their regulation of the cancer transcriptome have become increasingly recognised in meningioma pathogenesis. Studies generating miRNA expression profiles

in meningioma have revealed the altered expression of miRNAs with individual WHO grades, tumour progression and recurrence. MiRNAs have even been shown to act as multifunctional miRNA tumour suppressors (Saydam *et al.*, 2009). In benign meningioma the downregulation of miR-200a, a miRNA that targets β-catenin mRNA, was found to correlate with an upregulation of β-catenin expression at both the mRNA and protein levels in meningioma, leading to activation of the β-catenin/Wnt signalling pathway frequently implicated in cancer development (Saydam *et al.*, 2009). Further, miR-200a targets the mRNAs of the transcriptional repressors ZEB1 and SIP1 that function to downregulate expression of the adhesion protein E-cadherin; and thus in absence of miR-200a, E-cadherin levels are reduced, promoting the epithelial-to-mesenchymal transition (EMT) and tumour growth (Saydam *et al.*, 2009). Hence, the identification of dysregulated miRNA expression in meningioma, like many other cancers, can provide insights into potential biomarkers and therapeutic targets.

In contrast to the identification of altered DNA methylation and miRNA expression in meningioma, changes in the pattern of histone modifications including acetylation, methylation, phosphorylation, sumoylation, and ubiquitination have not yet been comprehensively described. Only recently have studies observed alterations in the trimethylation of lysine 27 (K27) of histone H3 (H3K27me3) in meningioma, a histone modification linked to the silencing of genes in the surrounding region (Katz *et al.*, 2018; Kondo *et al.*, 2008). Katz *et al*. (2018) demonstrated loss of H3K27me3 by immunohistochemistry (IHC) staining to be significantly associated with increased risk of tumour progression and recurrence most notably in grade I and II meningiomas (Katz *et al.*, 2018). Further, the authors showed H3K27me3-negative tumours to be affiliated with a DNA methylation pattern reflecting that of the more aggressive methylation subgroups among the recent DNA methylation classification of meningioma (Katz *et al.*, 2018; Sahm *et al.*, 2017). These findings propose the use of the epigenetic modification

H3K27me3 as a diagnostic marker to predict the progression and recurrence of this meningioma subset may prove to be clinically beneficial (Katz *et al.*, 2018). In contrast, Vasudevan *et al*. (2018) reported an enrichment of H3K27me3 in aggressive meningioma following DNA methylation profiling, suggesting further investigation into this epigenetic alteration is required to determine its importance in meningioma progression (Vasudevan *et al.*, 2018).

1.8.2.3 Transcriptomics

Transcriptomic analyses have been performed in meningioma in order to elucidate alterations in their gene expression profiles. Similar to other omics-based studies of meningioma, transcriptomic analyses have correlated transcriptional profiles with grade, histopathological subtype, progression, recurrence and aggressive tendencies (Aarhus *et al.*, 2008; Fevre-Montange *et al.*, 2009; Perez-Magan *et al.*, 2012; Watson *et al.*, 2002; Wrobel *et al.*, 2005). These investigations have facilitated the discovery of individual candidate genes associated with a specific meningioma subset and thus may hold potential as prognostic biomarkers.

The first gene expression profiling of meningiomas was performed by Watson *et al*. (2002) in which 15 meningiomas covering all WHO grades and three post-mortem leptomeninges were analysed (Watson *et al.*, 2002). The main outcome of the study was the differential expression of 133 genes that could distinguish grade I from higher-grade meningiomas (Watson *et al.*, 2002). Subsequent to this investigation, many transcriptomic studies also identified differential expression between low and high-grade meningiomas. In a study of 30 meningiomas, Wrobel *et al*. (2005) reported the expression of 37 and 27 genes in high-grade meningioma to decrease and increase respectively, compared to benign grade I (Wrobel *et al.*, 2005). Following this, analysis of 17 meningiomas by Fèvre-Montange and colleagues in 2009 identified the upregulation of

genes related to cell division and the downregulation of genes related to differentiation in high-grade compared to benign meningiomas (Fevre-Montange *et al.*, 2009).

Although previous expression analyses of meningioma have highlighted WHO grade-specific gene signatures with diagnostic potential, these studies have suffered from low sample numbers, particularly of the rarer grade III meningiomas (Fevre-Montange *et al.*, 2009). In 2016, Schmidt *et al*. (2016) addressed this limitation by performing comparative transcriptomics with a microarray study consisting of 62 meningiomas, of which 28 were grade III, the largest cohort of grade III analysed to date (Schmidt *et al.*, 2016). In the study, clinically more aggressive meningioma subgroups, including recurrent or malignantly progressing grade I and II, and all grade III tumours were found to share a common malignancy signature of 332 differentially expressed transcripts compared to non-recurrent benign grade I meningioma (Schmidt *et al.*, 2016). The authors went on to validate differential expression of a 10 gene subset derived from this malignancy signature in an independent meningioma cohort and following this, confirmed that the expression of two genes, *PTTG1* (*securin*) and *LEPR* (*leptin receptor*), were associated with significantly reduced PFS time and demonstrated strong prognostic power to predict aggressive tumour behaviour independent of WHO grade (Schmidt *et al.*, 2016).

More recently still, Dalan *et al*. (2017) conducted an integrated miRNA-mRNA analysis of 14 fresh-frozen meningioma and discovered an inverse correlation between expression of miR-29c-3p and the tumour suppressor *PTX3* (*pentraxin-related protein PTX3*) (Dalan *et al.*, 2017). Specifically, upregulation of miR-29c-3p was associated with downregulation of its target *PTX3* in meningioma tissue when compared to a healthy human meningeal cell line (Dalan *et al.*, 2017). Moreover, inhibition of miR-29c in primary meningioma cells led to an increase of *PTX3* expression and induced apoptosis (Dalan *et al.*, 2017). This study, among others such as the DNA methylation-based

classification system described by Sahm *et al.* (2017) (Sahm *et al.*, 2017), demonstrates the future importance of integrating omics studies to elucidate the interactive molecular landscape of meningioma and define molecular relationships that may hold clinical relevance as therapeutic targets or biomarkers.

While defining the transcriptional landscape of meningioma has revealed promising prognostic biomarker candidates, variations in experimental design have made it difficult to compare between transcriptome analyses. Many studies have endured small sample sizes and used different types of control from arachnoid cells to whole human brain (Aarhus *et al.*, 2008; Fevre-Montange *et al.*, 2009). Differential expression being investigated has also varied among microarray studies including between grades (Watson *et al.*, 2002), between tumour tissue and corresponding *in vitro* primary cultures (Sasaki, Hankins & Helm, 2003), or between meningioma and other brain tumours including glioblastoma multiforme (GBM) (Castells *et al.*, 2009). These variations have resulted in relatively poor overlap between transcriptomic datasets making the identification of shared candidate genes challenging (Aarhus, Lund-Johansen & Knappskog, 2011).

1.8.2.4 Proteomics

Proteomics is generally defined as the large-scale analysis of the protein complement of a biological sample (Graves & Haystead, 2002). The term proteome thus refers to the complete set of proteins expressed by a cell, tissue or organism. Proteomics has become a powerful and widely applied technique used to reveal the biological processes occurring in a given sample through characterisation of the proteome. It is proteins that exert the intended function of genes, performing many cellular operations at the molecular level dictating the phenotype of a cell (Graves & Haystead, 2002). Although defining the genome and transcriptome of a sample can provide important information about gene expression, quantification of mRNA levels is not directly proportional to protein

abundance and turnover (Graves & Haystead, 2002). There are numerous mechanisms involved in the process of protein synthesis that result in the generation of multiple protein products from a single gene. Figure 1.5 illustrates some aspects of this process. Among these mechanisms are post-translational modifications (PTMs), which add a further level of complexity and specialisation to the protein complement of a cell and may include the phosphorylation, glycosylation, acetylation, methylation and ubiquitination of a protein (Han & Martinage, 1992). Proteomic studies are thus fundamental in understanding the array of proteins expressed in a cell at any given time, as well as their dynamic regulation and dysregulation.

In the context of disease, alterations of the proteome play a substantial role in pathogenesis and cannot be identified from genomic analyses alone. Aberrations in protein function disrupt the normal structure and function of a cell ultimately leading to a disease state. This has led to the growth of a field within proteomics termed ‘disease proteomics’, which aims to describe the abnormal expression, function and structure of proteins involved in disease (Kavallaris & Marshall, 2005). As the majority of drugs target proteins, disease proteomics has become increasingly important in the identification of proteins and signalling pathways that can be exploited as therapeutic targets, as well as establishing proteins that can act as diagnostic or prognostic markers (Hanash, 2003).

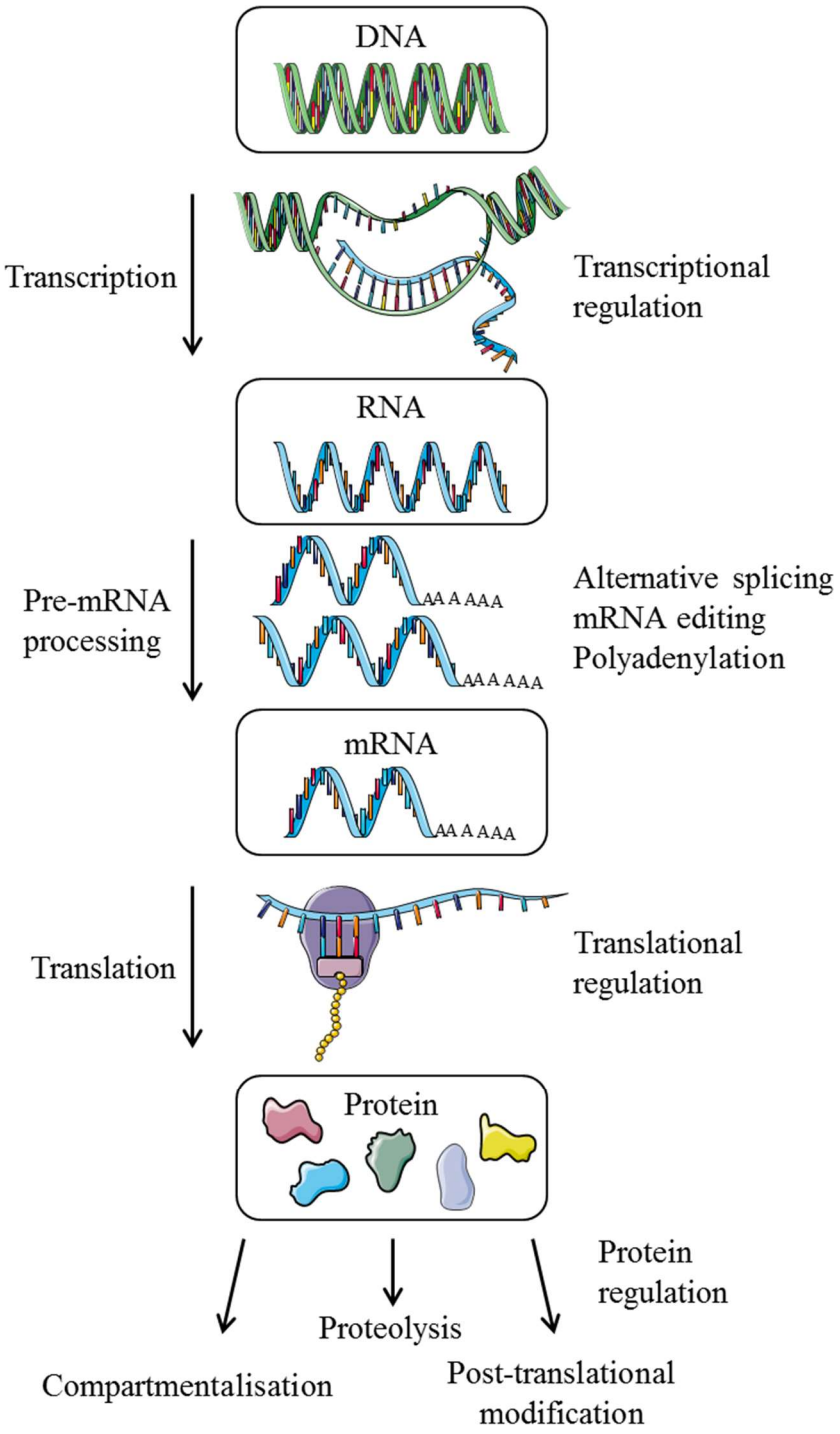

Figure 1.5 Regulation and mechanisms of protein synthesis. Schematic representation of the sequence of events by which multiple protein products can be generated from a single gene. After transcription, pre-mRNA may be subjected to alternative splicing or editing before forming mature mRNA. Once translated, proteins are regulated by several processes including post-translational modifications (PTMs) and may undergo PTMs such as phosphorylation, ubiquitination or glycosylation. These mechanisms all give rise to the dynamic nature of the proteome at any given time. Adapted from Graves *et al*. (2002) (Graves & Haystead, 2002).

There are several approaches used to study proteins including protein microarrays, large-scale two-hybrid analyses, high-throughput protein production and crystallization, and mass spectrometry (MS) (Cravatt, Simon & Yates, 2007). Among these, MS-based proteomics is now the preferred method for the comprehensive identification of proteins in biological systems (Cravatt, Simon & Yates, 2007). MS has greatly enhanced not only the sensitivity and precision of protein identification itself but can be further utilised for establishing protein quantification, modification and localisation (Cravatt, Simon & Yates, 2007). These features have permitted MS-based proteomics with the ability to provide a global overview of the complex network of interacting proteins in a cell.

In the molecular landscape of meningioma, proteomics attempts to bridge the gap between the increasing expanse of genomic, epigenomic and transcriptomic knowledge of these tumours and the execution of these instructions at the proteome level. Several studies have previously performed proteomic analysis of meningiomas although substantial variation between them exists concerning aims, methodology and the type of controls used.

Okamoto *et al*. (2006) conducted the first proteomic profiling of meningioma comparing the expression patterns of 24 tumours covering all WHO grades (Okamoto *et al.*, 2006). By using selective tissue microdissection followed with two-dimensional gel electrophoresis (2D-GE) and liquid chromatography tandem mass spectrometry (LC-MS/MS), the authors determined the significant differential expression of 15 proteins between grade I and II, whilst nine proteins were found to discriminate between grade II and III tumours (Okamoto *et al.*, 2006). However, the study did not include a control and only validated one protein by IHC on an independent cohort of meningioma (Okamoto *et al.*, 2006). A later analysis by Cui *et al*. (2014) also used 2D-GE and MS to define a protein expression signature indicative of meningioma (Cui *et al.*, 2014). Ten samples of

benign grade I meningioma were analysed from frozen along with arachnoid tissues adjacent to tumours used as control. Cui and colleagues identified 43 proteins to be differentially expressed between tumours and arachnoid tissue, validating three upregulated and three downregulated proteins on a further three meningiomas by Western blot (WB). Although the study included the use of control tissue, this was adjacent to the tumour and thus may have contained tumour cells. Further the study was limited by small sample size and focussed only on grade I meningioma.

Wibom *et al*. (2009) showed it was possible to distinguish between bone invasive and noninvasive behaviour in fibrous and meningothelial grade I meningioma based on protein expression patterns derived from MS analysis (Wibom *et al.*, 2009). The authors did not identify the proteins comprising these behaviour-specific protein signatures, however, the findings suggested MS to hold promise as a technique to predict tumours with progressive tendencies based on protein expression patterns (Wibom *et al.*, 2009).

Proteomics has been employed in an attempt to identify diagnostic and prognostic markers of meningioma. Saydam *et al*. (2010) completed MS-based proteomics on the benign meningioma cell line SF4433 compared to primary arachnoidal cells (Saydam *et al.*, 2010). The study identified the differential expression of 281 proteins and focussed on the minichromosome maintenance (MCM) family of proteins found to be significantly upregulated in meningioma cells (Saydam *et al.*, 2010). The authors validated all MCM members by qRT-PCR in meningioma tissue of all WHO grades concluding the MCM family may be able to act as diagnostic markers of these tumours (Saydam *et al.*, 2010).

Two further studies by Sharma and colleagues used quantitative proteomic analyses to investigate alterations in the protein composition of meningioma patient serum and tumour tissue (Sharma *et al.*, 2014; Sharma *et al.*, 2015). Both studies analysed 14 grade I, five grade II and one grade III meningioma and described differential expression of

proteins between tumours *vs*. healthy controls as well as among grades (Sharma *et al.*, 2014; Sharma *et al.*, 2015). Several differentially expressed proteins were found to be common to both studies that could act as possible predictive markers, while functional annotation revealed alterations of signalling pathways including the integrin, Ras and Wnt pathways to be associated with differentially expressed proteins of meningiomas (Sharma *et al.*, 2014; Sharma *et al.*, 2015). However, both studies were limited by inclusion of only a single grade III patient to characterise the rarest form of this tumour; as well as the use of 'glial tissues' in place of meninges to represent healthy control tissue when comparing against meningioma tissue (Sharma *et al.*, 2014; Sharma *et al.*, 2015).

To our knowledge, our group published the first study characterising the global and phosphoproteome of meningioma, analysing the expression of both proteins and phosphoproteins in grade I meningioma by MS. The study investigated potential novel therapeutic targets common to *NF2*-deficient meningioma and schwannoma using label free quantitative proteomics to analyse primary tumour cells (Bassiri *et al.*, 2017). Following analysis of differential expression, we identified the phosphoprotein PDLIM2 (PDZ and LIM domain protein 2) to be commonly overexpressed and to play a role in the proliferation of *NF2*-deficient meningioma and schwannoma (Bassiri *et al.*, 2017). The current project aimed to expand upon this work by analysing meningioma tissue of all WHO grades to explore the global proteome and phosphoproteome. However, since its commencement, one further study has also investigated the meningioma phosphoproteome from tissue. Parada *et al*. (2018) used a combination of a kinase peptide array and MS to analyse 14 frozen meningioma across all WHO grades (Parada *et al.*, 2018). Although the authors did not analyse normal meninges as a control, they identified 42 phosphopeptides to be differentially phosphorylated among the grades and validated grade-dependent expression patterns in five out of six proteins (Parada *et al.*, 2018). Of these five, the study demonstrated the potential of reduced AKAP12 (A-kinase anchor

protein 12) expression as a prognostic marker of high-grade meningioma as well as harbouring a possible role in tumour progression (Parada *et al.*, 2018).

Ultimately, these phosphoproteomic investigations reveal the importance of elucidating changes in not only protein expression, but also of aberrant protein phosphorylation and its resulting dysregulation of protein activity in order to establish potential therapeutic targets and biomarkers of meningioma.

1.8.3 Phosphoproteomic analysis

Protein phosphorylation is arguably one of the most common and important PTMs in eukaryotic cells (Harsha & Pandey, 2010). This transient modification acts as a 'molecular switch', fundamental in the regulation of a plethora of biological cellular processes (Fila & Honys, 2012). At any one time approximately 30% of the protein complement of a cell may be phosphorylated (Cohen, 2000). Phosphorylation primarily takes place on serine (S), threonine (T) and tyrosine (Y) residues; although it has also become apparent that phosphorylation of histidine residues plays a role in cellular functions but its detection by MS remains a challenge (Fuhs & Hunter, 2017). The aberrant phosphorylation of proteins and resultant dysregulation of signalling pathways is frequently implicated in disease (Harsha & Pandey, 2010). Therefore, analysis of the phosphoproteome in parallel with the global proteome is critical in understanding the mechanisms controlling healthy and diseased states.

Protein phosphorylation is generally studied using the MS-based proteomic approach termed 'phosphoproteomics'. This approach enables the study of the 'phosphoproteome' that consists of a comprehensive analysis of all phosphoproteins in a given sample (Graves & Haystead, 2002). Yet, the relatively low proportion of phosphorylated proteins amongst an abundance of non-phosphorylated proteins at any given time can make the detection of phosphoproteins somewhat challenging (Mann *et al.*, 2002). To overcome

this issue, enrichment techniques at either the protein or peptide level are necessary to eliminate non-phosphorylated proteins or peptides from complex samples prior to MS (Fila & Honys, 2012).

Phosphoprotein enrichment is performed immediately following protein extraction starting from intact phosphoproteins (Fila & Honys, 2012). Phosphoproteins are separated by 2D-GE or sodium dodecyl sulphate polyacrylamide gel electrophoresis (SDS-PAGE), excised and subjected to in-gel digestion with a protease, usually trypsin. Peptides are then purified before MS analysis (Fig. 1.6, left) (Fila & Honys, 2012). Enrichment of phosphopeptides similarly begins with protein extraction but proteins are subjected to in-solution digestion prior to enrichment, often using multiple proteases in a serial digestion for optimal digestion efficiency (Giansanti *et al.*, 2016). Peptides are then enriched for phosphopeptides before being purified and analysed by MS (Fig. 1.6, right) (Fila & Honys, 2012).

1.8.3.1 Phosphoprotein enrichment

Approaches to isolate intact phosphorylated proteins against a background of non-phosphorylated proteins include phosphospecific antibodies and affinity chromatography. Phosphospecific antibodies directed against phosphorylated tyrosine, serine and threonine residues can be used to immunoprecipitate phosphorylated proteins for quantification by MS. Although anti-phosphotyrosine antibodies have demonstrated effective enrichment of tyrosine phosphorylated proteins, antibodies against serine and threonine phosphorylated proteins have proved less successful (Fila & Honys, 2012). Moreover, utilising immunoprecipitation for global phosphoproteome analysis is not feasible due to its reliance upon individual immunoprecipitations for each antibody (Fila & Honys, 2012).

To study the full complement of phosphoproteins in a sample, affinity chromatography, particularly immobilised metal affinity chromatography (IMAC) is employed (Dunn, Reid & Bruening, 2010). IMAC exploits the affinity of negatively charged phosphate groups for positively charged metal ions immobilised on a resin of a solid matrix situated within a column (Fila & Honys, 2012). Phosphorylated proteins are retained on the column whilst non-phosphorylated proteins are removed by washing, followed by elution of the enriched fraction (Dunn, Reid & Bruening, 2010). Phosphoprotein enrichment is limited in its ability to provide phosphosite specific detail compared to phosphopeptide enrichment. Yet, following phosphoprotein enrichment protein identification is generally greater as the peptide spectrum is derived from both phosphorylated and non-phosphorylated peptides relating to one protein, whereas identification after phosphopeptide enrichment may often be based on a single peptide submitted to MS (Fila & Honys, 2012).

In particular, several studies have performed phosphoprotein enrichment using a commercially available purification kit from Qiagen® (Makrantoni *et al.*, 2005; Meimoun *et al.*, 2007; Metodiev, Timanova & Stone, 2004; Santamaria *et al.*, 2012). Similarly based on affinity chromatography, phosphorylated proteins are retained on a Qiagen® PhosphoProtein Purification Column (Fig. 1.6, left). Two studies have previously validated the use of this kit in yeast concluding the technique to be highly specific for phosphorylated proteins. Metodiev *et al*. (2004) used an antibody against phospho-threonine-proline motifs, confirming flow-through did not harbour any proteins with this motif, whilst the eluted fraction exhibited a strong retention of threonine phosphorylated proteins (Metodiev, Timanova & Stone, 2004). Following separation of phosphoprotein eluate by 2D-GE, Makrantoni *et al*. (2005) reported enrichment efficiency by confirming 11 of 13 protein spots taken at random to be associated with phosphorylation or ATP binding (Makrantoni *et al.*, 2005). More recent studies in plant and mammalian cells have

further corroborated the kit as an effective method to enrich for phosphoproteins (Meimoun *et al.*, 2007; Santamaria *et al.*, 2012). Specifically, Meimoun and colleagues were able to recover 88% of all ^{32}P-phosphate-labelled proteins captured by the column in the elution fraction (Meimoun *et al.*, 2007).

Overall, these studies verified the Qiagen® PhosphoProtein Purification Kit to be a technically straightforward, sensitive, quick and effective method to isolate phosphoproteins for MS analysis. We therefore decided to utilise this kit for the global phosphoprotein enrichment of meningioma tissue in this project.

1.8.3.2 Phosphopeptide enrichment

The primary enrichment methods employed to isolate phosphopeptides due to their increased selectivity and sensitivity are IMAC, also used in phosphoprotein enrichment, and metal oxide affinity chromatography (MOAC) (Fila & Honys, 2012). Although phosphopeptide enrichment is limited in its identification of proteins, often reliant upon a single phosphopeptide, it is advantageous in its ability to identify exact phosphorylation sites (Fila & Honys, 2012). Similar to IMAC, MOAC exploits the affinity of phosphate groups for metal ions. Specifically, MOAC utilises metal oxides that directly form the matrix without the need for a resin, unlike IMAC (Fila & Honys, 2012). Both methods are subject to variation in binding affinity of phosphopeptides depending on the metal ion or oxide used (Jensen & Larsen, 2007). However, unlike IMAC, MOAC displays resistance against harsh washing conditions, including low pH and use of detergents, that are encountered during enrichment without loss of phosphopeptide affinity or recovery (Jensen & Larsen, 2007).

The most commonly used metal oxide in MOAC is titanium dioxide (TiO_2) although others including zirconium dioxide (ZrO_2) have also been developed (Beltran & Cutillas, 2012). TiO_2 and ZrO_2 have been described as equally effective in the purification of singly

phosphorylated peptides. However, compared with ZrO_2, TiO_2 has shown improved enrichment efficiency of multiply phosphorylated peptides as well as reduced binding of unspecific non-phosphorylated peptides from complex samples (Aryal & Ross, 2010). The first studies to purify phosphopeptides by MOAC using TiO_2 microspheres were performed by Pinkse *et al*. (2004) and Sano *et al*. (2004) (Pinkse *et al.*, 2004; Sano & Nakamura, 2004). Both studies concluded TiO_2 as an effective metal oxide for phosphopeptide enrichment with Pinkse *et al*. (2004) reporting more than 90% recovery (Pinkse *et al.*, 2004). Since these studies, Fukuda *et al*. (2013) described optimisation of phosphopeptide enrichment by TiO_2 MOAC (Fukuda *et al.*, 2013). The authors achieved optimisation firstly by using glycerol as an additive reagent to increase phosphopeptide selectivity to the TiO_2 column and secondly by performing a two-step elution of NH_4OH and bis-Tris propane to enhance phosphopeptide recovery (Fukuda *et al.*, 2013).

Based on these studies TiO_2 MOAC appears a more robust and effective technique for phosphopeptide enrichment compared to IMAC. Thus, with the incorporation of optimised conditions established by Fukuda *et al*. (2013), we selected TiO_2 MOAC to enrich protein digests of meningioma tissue lysate for phosphopeptides in this project (Fukuda *et al.*, 2013). Figure 1.6 (right) provides an overview of phosphopeptide enrichment by MOAC.

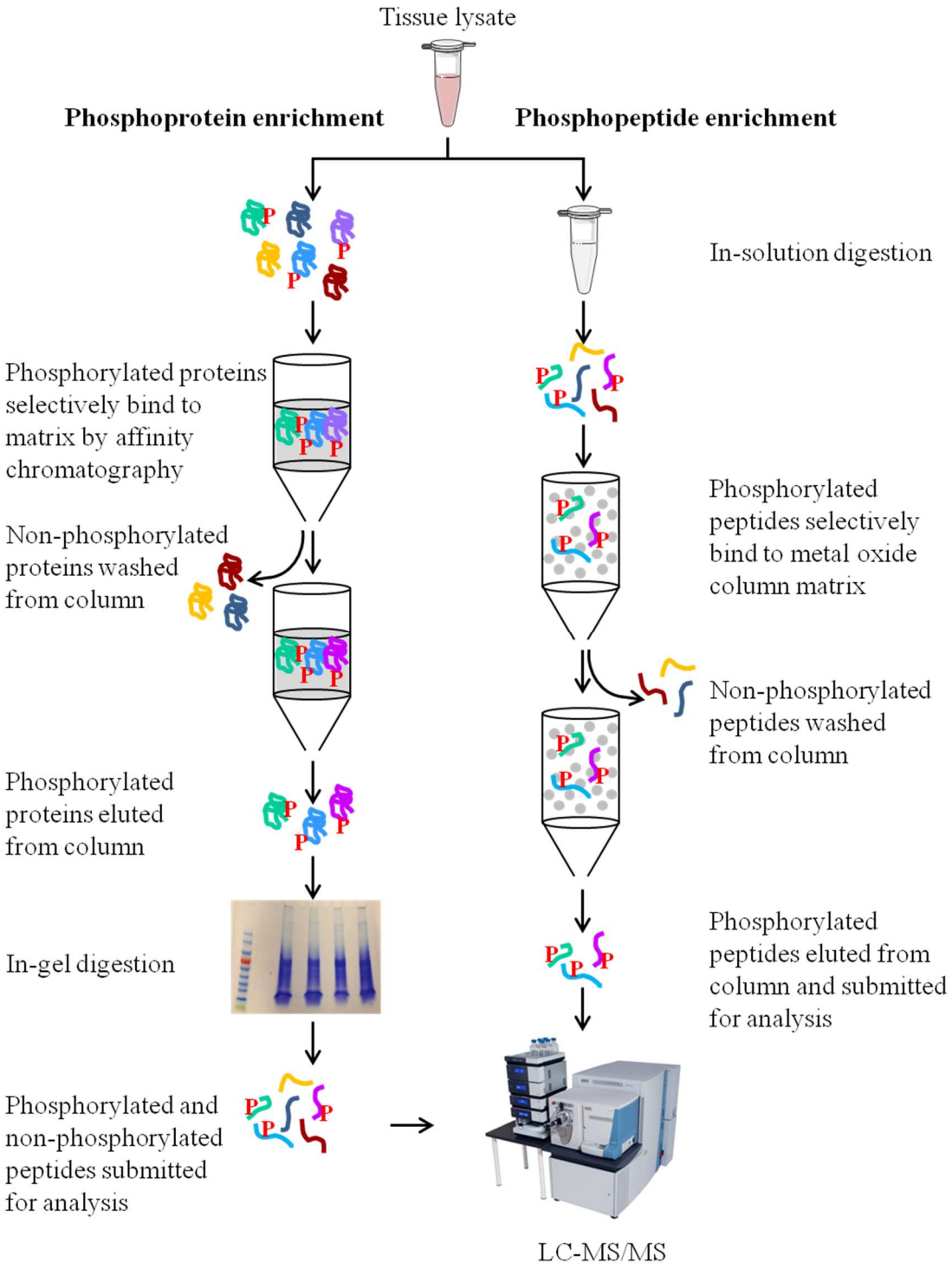

Figure 1.6 Schematic representation of phosphoprotein and phosphopeptide enrichments. Both enrichments start from extracted proteins in tissue lysate and utilise affinity chromatography to selectively isolate either phosphoproteins or phosphopeptides. Phosphoprotein enrichment (left) enriches from the protein level, whilst phosphopeptide enrichment (right) first digests proteins followed by enrichment from the peptide level that allows for detection of phosphorylation sites.

1.9 Project aim

The aim of this project is to elucidate the molecular landscape of meningioma by defining the proteomic signature of these tumours. By performing comparative proteomic analysis across 22 meningioma of all WHO grades *vs*. three healthy human meninges we aim to better understand the molecular pathogenesis of these tumours and identify key proteins common to all meningioma or grade-specific. In addition to global proteome analysis, we will use a phosphoproteomic approach in order to investigate aberrant protein phosphorylation in meningioma. By starting from tumour tissue as opposed to a pure tumour cell population we will ensure that the impact of signalling from the surrounding tumour microenvironment is captured.

Following MS, protein, phosphoprotein and phosphopeptide datasets will be analysed to establish differential expression between tumours and healthy controls. Differentially expressed proteins and phosphoproteins will be subjected to functional annotation to decipher associated biological processes and signalling pathways. Following this, experimental validation studies of differential expression in tumours analysed by MS as well as in an additional independent cohort of 15 meningiomas spanning all WHO grades will be performed. Ultimately, these studies will identify a panel of proteins and phosphoproteins that hold potential as biomarkers or novel therapeutic targets in meningioma. Figure 1.7 shows a schematic representation of the study design.

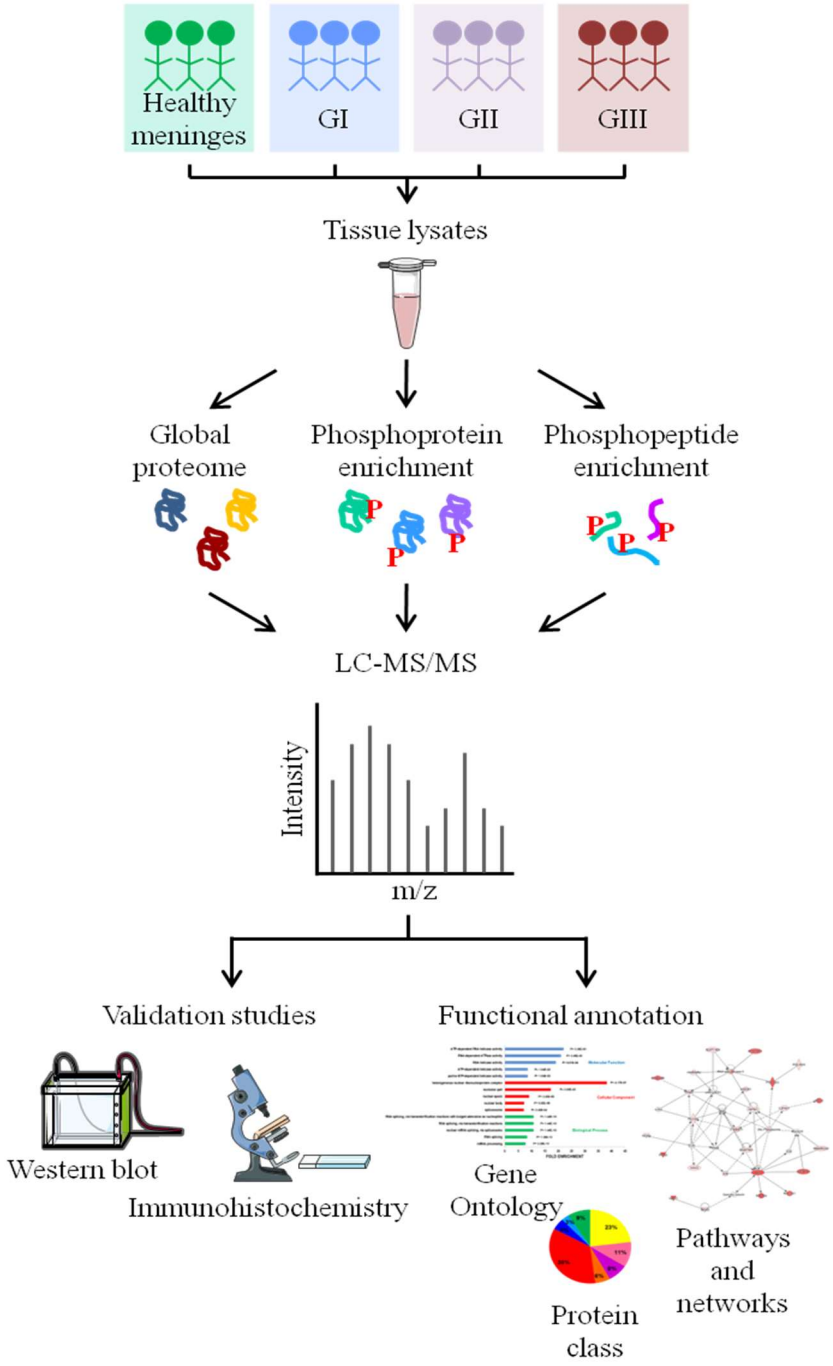

Figure 1.7 Schematic representation of the study design. Frozen tissue samples are collected from healthy meninges and all WHO grades of meningioma. Tissues are homogenised to form lysates from which protein is extracted and any necessary enrichment techniques performed. Samples are subjected to liquid chromatography tandem mass spectrometry (LC-MS/MS) followed by analysis of differential expression between tumours and healthy meninges, and between WHO grades. Functional annotation of differentially expressed proteins and phosphoproteins to identify associated biological processes as well as experimental validation studies to confirm expression will then be performed.

2 Materials and methods

2.1 Clinical material

Anonymised meningioma tissue samples under the ‘MN’ series were collected during planned surgical procedures and surplus frozen tissue was available after diagnostic testing. Patients were consented to the 'Identifying and validating molecular targets in low grade brain tumours' study and given a unique molecular target identification number (MN). This study was granted full national ethics approval by the South West research ethics committee (REC No: 14/SW/0119; IRAS project ID: 153351) and local research and development approval (Plymouth Hospitals NHS Trust: R&D No: 14/P/056 and North Bristol NHS Trust: R&D No: 3458). Anonymised meningioma samples under the ‘J’ series as well as the remainder of anonymised meningioma and normal meninges used for IHC studies were provided by the BRain Archive and Information Network (BRAIN UK, http://www.southampton.ac.uk/brainuk/) with ethical approval by the South West research ethics committee (REC No: 14/SC/0098; IRAS project ID: 143874), BRAIN UK Ref: 15/011). All tumours were classified according to the 2007 WHO Classification of Tumours of the Central Nervous System. Twenty-two meningioma were used in LC-MS/MS analysis and a further 15 in validation studies alone. Clinical and histological details about all the tumour specimens used in the project are presented in Tables 2.1 and 2.2. Two frozen flat normal meninges were obtained from Analytical Biological Services Inc. as custom collection and one human brain cerebral meninges whole tissue lysate was purchased from Novus Biologicals® (NB820-59183; lot B105014).

Sample code	WHO grade	Age	Sex	Histopathological subtype	Location
J5	I	50	F	Fibroblastic	Occipital
J6	I	37	F	Transitional	Parasagittal
J7	I	72	F	Transitional	Parasagittal
J8	I	68	F	Transitional	Parasagittal
J14	I	80	F	Fibroblastic	Frontal
J15	I	75	F	Meningothelial	Olfactory groove
MN005	I	59	F	Fibroblastic	Brain stem
MN017	I	51	F	Transitional	Frontal
J1	II	62	F	Atypical	Sphenoid wing
J2	II	51	F	Atypical	Parafalcine
J3	II	64	M	Atypical	Frontal
J4	II	66	M	Atypical	Occipital
J13	II	59	M	Atypical	Parietal
MN001	II	50	M	Atypical	Frontal
MN018	II	71	M	Atypical	Lateral posterior fossa
MN020	II	39	F	Atypical	Parietal
J9	III	82	F	Anaplastic	Occipital
J10	III	85	M	Anaplastic	Occipital
J11	III	85	M	Anaplastic	Occipital
J12	III	87	M	Anaplastic	Parasagittal
J16	III	67	F	Anaplastic	Occipital
J17	III	76	M	Anaplastic	Frontal

Table 2.1 Clinical and histological data of 22 patients by LC-MS/MS.

Sample code	WHO grade	Age	Sex	Histopathological subtype	Location
J18	I	67	F	Transitional	Parietal
J19	I	47	F	Secretory	Petrous apex
J20	I	71	M	Fibroblastic	Parasagittal
J26	I	56	M	Fibroblastic	Parasagittal
J27	I	81	F	Transitional	Sphenoid wing
J21	II	58	F	Atypical	Parasagittal
J22	II	69	M	Atypical	Occipital
J23	II	62	F	Atypical	Temporal
J24	II	60	F	Atypical	Frontal
J25	II	65	F	Atypical	Frontal
J28	III	48	M	Anaplastic	Left frontal
J29	III	68	F	Anaplastic	Frontal
J30	III	64	F	Anaplastic	Left posterior fossa
J31	III	76	F	Anaplastic	Left frontal
J32	III	70	F	Anaplastic	Left posterior fossa

Table 2.2 Clinical and histological data for an additional cohort of 15 patient samples used in Western blot validation.

2.2 DNA purification and genotyping

DNA purification for each tumour sample was performed with Qiagen® DNeasy® Blood & Tissue Kit (Qiagen, Hilden, Germany; #69504) following manufacturer's instructions. DNA concentration and purity were determined using a NanoDrop™ 2000 spectrophotometer (Thermo Scientific™) and 2 μg of DNA was sent to the Manchester Centre for Genomic Medicine for detection of *NF2* mutations using NGS and Multiplex Ligation-dependent Probe Amplification (MLPA®) dosage test. NGS was used to identify single nucleotide polymorphisms (SNP) in *NF2* and MLPA® to identify whole exon deletions and duplications. Heterozygosity analysis was not carried out as patient peripheral lymphocytes were not available.

Mutational screening of $AKT1^{E17K}$, $KLF4^{K409Q}$, $TRAF7^{N520S}$, SMO^{L412F}, SMO^{W535L}, $SMARCB1^{R374Q}$, $SMARCB1^{R377H}$ and $POLR2A^{Q403K}$ was completed in-house using the kompetitive allele specific PCR genotyping system, KASP™ (LGC Genomics) (He, Holme & Anthony, 2014). KASP genotyping assay is based on a competitive allele-specific polymerase chain reaction (PCR) to enable bi-allelic discrimination of a single nucleotide polymorphism (SNP) at a specific locus. It requires an SNP-specific KASP Assay mix, a universal KASP Master mix and sample DNA. The KASP Assay mix contains three oligonucleotides; two non-labelled allele-specific forward primers (one for each SNP) each with a unique tail sequence that corresponds with a universal FRET (Fluorescence resonant energy transfer) cassette and one common reverse primer. The KASP Master mix contains: the universal FRET cassettes consisting of two 5' fluor-labelled oligonucleotides, one labelled with FAM™ dye and the other with HEX™ dye; two oligonucleotides harbouring quenchers at the 3' ends and are complementary to the fluor-labelled oligonucleotides; ROX™ passive reference dye; taq polymerase; free nucleotides and $MgCl_2$ in an optimised buffer solution.

Fluorescent signals are quenched by complementary binding of quencher oligonucleotides to fluor-labelled oligonucleotides. During PCR, allele-specific forward primers compete to bind with the target SNP region and together with the common reverse primer amplify the region. As PCR proceeds, the allele-specific tail sequence is incorporated into the template and its complement generated. Following this, the complementary fluor-labelled oligonucleotide is incorporated into the template, SNP homozygosity is depicted by generation of only one of the two possible fluorescent signals and heterozygosity by a mixed fluorescent signal (HEX™ Em λ_{max} = 556 nm; FAM™ Em λ_{max} = 520 nm) (He, Holme & Anthony, 2014).

DNA purification was carried out on frozen meningioma tissue. Approximately 40 ng of DNA was added in duplicate to LightCycler 480 96-well plates (Roche; #04729692001) and synthetic DNA controls (Integrated DNA Technologies®; gBlocks® Gene Fragments) for each mutation were also added in duplicate as appropriate. Plates were sealed and spun at 1000 rpm for 1 minute. Next, 0.14 µL KASP Assay mix (primer sequences are detailed in Table 2.3) and 5 µL 2X KASP Master mix (standard concentration 2.5 mM $MgCl_2$) were added per well, plates were sealed with an optically clear seal (Roche; #04729692001) and again spun at 1000 rpm for 1 minute. Plates were then subjected to PCR using a LightCycler® 480 II (Roche) under the conditions listed in Table 2.4.

SNP ("rs#" = NCBI reference SNP ID number)	Primer Allele FAM (x-axis)	Primer Allele HEX (y-axis)	Primer common
AKT1 E17K (rs121434592)	CACCCGCACGTCTGTAGGGA	ACCCGCACGTCTGTAGGGG	GTGGCCGCCAGGTCTTGATGTA
KLF4 K409Q	GTGCCTTGATGGGAACTCTT	GTGCCTTGAGATGGGAACTCTG	GATTACGCGGGCTGCGGCAAAA
TRAF7 N520S	AGAAGGAGCTCACAGGCCTCAA	GAAGGAGCTCACAGGCCTCAG	GGTAGGAGCCGCTGTACAGGTA
SMO L412F	GAAGTAGCCTCCCACGATGAG	GGAAGTAGCCTCCCACGATGAA	GGGCTTCGTGCTGGCCCCAA
SMO W535L (rs121918347)	GGCATCGCCATGAGCACCTG	GGCATCGCCATGAGCACCTT	TCCAGATGAGCAGCGTGGCCTT
SMARCB1 R374Q	GTGTTGGCAAGACGCCTCATCT	GTTGGCAAGACGCCTCATCC	CATTGCCCTCCCCACTCCTCTT
SMARCB1 R377H (rs387906812)	CGGGGCCGTGTTGGCAAGAT	GGGGCCGTGTTGGCAAGAC	CCACTCCTCTTCCAGGCGGAT

POLR2A Q403K	CCTCTTTCCTTCC TAGACTTAAAGA ACTAGTGCGCAG GGGG	CCTCTTTCCTTCC TAGACTTCAAGA ACTAGTGCGCAG GGGG	NOT SUPPLIED

Table 2.3 Allele-specific forward primer sequences used in KASP genotyping assay.

Protocol Stage	Temperature	Duration	Number of cycles for each stage
Stage 1 Hot-start Taq activation	94°C	15 minutes	x 1 cycle
Stage 2 Touchdown	94°C	20 seconds	x 10 cycles
	61°C (61°C decreasing 0.6°C per cycle to achieve a final annealing/extension temperature of 55°C)	60 seconds	
Stage 3 Amplification	94°C	20 seconds	x 26 cycles
	55°C	60 seconds	
Optional Stage 4 (read stage for qPCR instruments only)	30°C (any temperature below 40°C is suitable for the read stage)	60 seconds	x 1 cycle

Table 2.4 KASP thermal cycling conditions for 61-55 °C touchdown protocol.

2.3 Phosphoprotein enrichment

Phosphoproteins were enriched from frozen tumour tissue using the commercially available Qiagen® PhosphoProtein Purification Kit (Qiagen, Hilden, Germany; #37101). The kit utilises affinity chromatography for the complete separation of the phosphorylated from the unphosphorylated fraction of tumour lysate. Phosphorylated proteins are bound to the affinity column matrix while unbound unphosphorylated proteins are collected in the flow-through fraction. Previous studies using this kit have reported an 88% elution recovery of phosphoproteins (Meimoun *et al.*, 2007).

The protocol was performed according to the manufacturer's instructions with the following modifications. Tissue was manually homogenised in 1 mL of 'PhosphoProtein Lysis Buffer', provided with the kit, containing 0.25% CHAPS detergent, the DNase/RNase Benzonase® Nuclease and protease inhibitors. Phosphatase inhibitor cocktails were also added to the lysis buffer at a concentration of 1:100 (Santa Cruz Biotechnology, Inc.; sc-45045; sc-45065). A further 1 mL 'PhosphoProtein Lysis Buffer' was then added to the tissue homogenate before incubating for 30 minutes at 4 °C, vortexing briefly every 10 minutes.

Following incubation, the homogenate was centrifuged at 16,000 x *g* for 30 minutes at 4 °C. During centrifugation, 'PhosphoProtein Purification Columns' were equilibrated with 4 mL 'PhosphoProtein Lysis Buffer' allowed to flow through the column. Supernatant was collected in Eppendorf® Protein LoBind 1.5 ml microcentrifuge tubes (Eppendorf, Hamburg, Germany; #0030108116). Protein concentration of lysate was determined using the Pierce™ BCA Protein Assay Kit (Thermo Fisher Scientific, Massachusetts, US; #23225), a detergent compatible protein assay at a bicinchoninic acid (BCA) working reagent ratio of 1:8 (v/v) with colorimetric detection measuring absorbance at 562 nm on a FLUOstar® Omega microplate reader. Sample absorbencies

were compared to a response curve generated from bovine serum albumin (BSA) protein standards, starting from a stock concentration of 2 mg/mL and halving the concentration.

A volume of lysate containing approximately 2.5 mg of total protein for phosphoprotein purification was adjusted to a protein concentration of 0.1 mg/mL by addition of 'PhosphoProtein Lysis Buffer'. This adjustment ensured that phosphate groups were accessible during purification and were not hidden within protein complexes. For each sample, half of the tissue lysate was then added to a 'PhosphoProtein Purification Column' and allowed to pass through, followed by the second half of lysate. Once all lysate had passed through, columns were washed with 6 mL 'PhosphoProtein Lysis Buffer', followed by elution of phosphoproteins from columns with 3 mL 'Phosphoprotein Elution Buffer' containing 0.25% CHAPS detergent. The eluted phosphoprotein fraction was then concentrated to approximately 30 µL using a Nanosep ultrafiltration column provided with the kit. Concentrated phosphoproteins were then recovered, added to 6X loading buffer (375 mM Tris-HCl pH 6.8, 6% SDS, 50% glycerol, 9% β-mercaptoethanol, 0.03% bromophenol blue) and stored at -20 °C prior to separation by SDS-PAGE.

2.4 Phosphopeptide enrichment

Meningioma tissue samples were manually homogenised from frozen in 1 mL lysis buffer (8 M urea, 100 mM Tris-HCl, pH 8.0). Lysates were frozen at -80 °C for at least 24 hours before being thawed on ice and spun down at 16,000 x *g* for 15 minutes at 4 °C. Supernatant was collected in Eppendorf® Protein LoBind microcentrifuge tubes and protein concentration determined as before using the Pierce™ BCA Protein Assay Kit.

Prior to phosphopeptide enrichment using TiO_2 beads, 2.5 mg of protein lysate was subjected to in-solution digestion. Proteins were reduced and alkylated by incubation with 0.1 M DL-Dithiothreitol (DTT) for 30 minutes at room temperature (RT), followed by

further incubation with 50 mM 2-iodoacetamide in the dark for 15 minutes at RT. Lys-C protease (Lysyl Endopeptidase®, Mass Spectrometry Grade, Wako) was then added at a protease: protein ratio of 1: 100 (w/w) in 50 mM ammonium bicarbonate (ABC) and incubated overnight at 37 °C.

Next, samples were diluted in 50 mM ABC to a final concentration of 2 M urea and incubated overnight at 37 °C with trypsin (Promega, Wisconsin, US), added at a protease: protein ratio of 1: 50 (w/w). Digested samples were acidified to a final concentration of 0.1% trifluoroacetic acid (TFA; LC/MS grade; Thermo Scientific™; #85183) and peptides desalted using HyperSep™ C18 Cartridges (Thermo Fisher Scientific, Massachusetts, US). Columns were washed with buffer A (1% TFA, 0.5% acetic acid (Fisher Scientific; #10644982)), peptides eluted in buffer B (80% acetonitrile (ACN), 0.5% acetic acid, 1% TFA) and dried in a vacuum concentrator (Labconco Centri®Vap DNA Concentrator).

Peptides were enriched for phosphopeptides by batch-wise incubation with Titansphere 10 µm TiO_2 beads (GL Sciences) as described by Lasonder *et al*. (2012) (Lasonder *et al.*, 2012) with the following modifications. Initially, TiO_2 beads (1 mg beads per incubation) were incubated in wash buffer A (80% ACN, 5% TFA, 15% LC/MS grade water) followed by incubation in buffer B (60% ACN, 5% TFA, 5% glycerol, 30% LC/MS grade water) for 5 minutes at 1000 rpm, at RT. TiO_2 beads were sedimented by centrifugation at 2,000 x *g* for 1 minute and buffer removed. Sample peptide digests were briefly sonicated to sheer DNA and minimise adsorption of peptides to the microcentrifuge tube, before subsequent incubation with TiO_2 beads under continuous shaking for 1 hour at RT. Next, the bead/peptide solution was transferred to a spin column, constructed from fused silica frits placed at the bottom of a pipette tip. Beads were then packed by centrifugation at 2,000 x *g* for 3 minutes allowing unbound peptides to flow through. Flow-through was collected and transferred to freshly prepared TiO_2

beads and incubated as before to maximise phosphopeptide enrichment. Packed TiO_2 beads were washed three times with 100 µl buffer B, followed by three washes with 100 µl buffer A, centrifuged at 3,000 x *g* for 1 minute each time. Silica frit columns were then placed into an Eppendorf® Protein LoBind 1.5 ml microcentrifuge tube and bound phosphopeptides eluted from the column using a two-step elution protocol by Fukuda *et al*. (2013) (Fukuda *et al.*, 2013). Phosphopeptides were eluted with 100 µl 5% ammonium hydroxide (NH_4OH) elution buffer (5% NH_4OH, 95% LC/MS grade water) followed by 100 µl 1 M 1,3-bis(tris-(hydroxymethyl)methylamino)propane (bis-Tris propane) elution buffer. Eluate was immediately acidified with 200 µl of 10% TFA and stored at 4 °C prior to peptide purification.

2.5 Total protein preparation

Following tissue lysis for phosphoprotein and phosphopeptide enrichments, a volume of tissue lysate containing 50 µg total protein was taken for global proteome analysis. Protein concentration was determined as before using the Pierce™ BCA Protein Assay Kit. Lysate volume for 50 µg total protein was added to 6X loading buffer and stored at -20 °C prior to separation by SDS-PAGE.

2.6 Protein fractionation and in-gel digestion

Proteins and phosphoproteins were separated using SDS-PAGE on 4-15% Mini-PROTEAN® TGX™ Precast Gels (Bio-Rad, Hercules, California, US). Gels were stained briefly with Coomassie Blue R-350 (GE Healthcare Life Sciences, Illinois, US) until sample lanes were visible. Destaining was performed using a destaining solution (50% LC/MS grade water (Fisher Scientific; #W6212), 40% LC/MS grade methanol (Fisher Scientific; #A456-1) and 10% acetic acid) overnight at RT. Sample lanes were excised from gels and sliced into 6 fractions that were further cut into 1 x 1 mm pieces before in-gel digestion.

In-gel digestion was performed following protocol adapted from Shevchenko *et al.* (2006) (Shevchenko *et al.*, 2006). Gel pieces were equilibrated with alternate incubations of 500 µl 100% ACN (LC/MS grade; Fisher Scientific; #10799704) and 500 µl ABC buffer (50 mM ABC, Sigma-Aldrich®; LC/MS grade water). Proteins were reduced by incubation with 10 mM DTT (Sigma-Aldrich®) in ABC buffer for 20 minutes at 56 °C shaking at 700 rpm and then alkylated by incubation with 50 mM 2-iodoacetamide (Sigma-Aldrich®) in ABC buffer for 20 minutes at RT in the dark. Gel pieces were again equilibrated with alternate incubations of 500 µl 100% ACN and 500 µl ABC buffer. Proteins were digested in 12.5 ng/µl trypsin (Promega, Wisconsin, US; #V5111) in ABC buffer overnight at 37 °C. Digested peptides were acidified with a final concentration of 2% TFA for 20 minutes at RT shaking at 1400 rpm and briefly sonicated to detach any peptides adhered to the microcentrifuge tubes. Supernatant was then transferred to fresh Eppendorf® Protein LoBind 1.5 ml microcentrifuge tubes. Remaining peptides were extracted from gel pieces by two 5 mintue incubations with 200 µl buffer B (80% ACN, 0.5% acetic acid, 1% TFA) shaking at 1400 rpm and supernatant pooled with previously collected peptides. Following this, ACN was evaporated from each fraction in a vacuum concentrator (Labconco Centri®Vap DNA Concentrator) prior to peptide purification.

2.7 Peptide purification

Digested peptides generated by all procedures described above were purified by stop and go extraction (STAGE) tips following protocol adapted from Rappsilber *et al.* (2003) (Rappsilber, Ishihama & Mann, 2003). StageTips were produced by cutting out small disks from larger polytetrafluoroethylene membrane disks containing embedded reversed-phase beads (Empore™ Solid Phase Extraction Disks C18, 3M™; Fisher Scientific). The cut-out disks were then inserted into a 200 µl pipette tip to function simultaneously as column material and frit, forming the StageTip. C_{18}-StageTips were

conditioned by 50 µl of LC/MS grade methanol and equilibrated using 50 µl buffer B (80% ACN, 0.5% acetic acid, 1% TFA) followed by 50 µl buffer A (1% TFA, 0.5% acetic acid). StageTips were placed into microcentrifuge tubes and loaded with sample, followed by centrifugation at 1-2000 x *g* until all sample had passed through the StageTip. Tips were then washed with 50 µl buffer A and peptides eluted in 40 µl of buffer B into Eppendorf® Protein LoBind 1.5 ml microcentrifuge tubes. Eluted peptides were dried down completely in a vacuum concentrator. Peptides were then resuspended in 25 µl of buffer A, transferred to LC/MS vials and stored at 4 °C prior to LC-MS/MS.

2.8 Liquid chomatography tandem mass spectrometry and protein identification

MS was carried out using an ultimate 3000 UPLC system (Thermo Fisher) connected to an Orbitrap Velos Pro mass spectrometer (Thermo Fisher). The prepared peptides were loaded on to a 2 cm Acclaim™ PepMap™ 100 Nano-Trap Column (Thermo Fisher) and separated by a 25 cm Acclaim™ PepMap™ 100 Nano LC column (Thermo Fisher) that is packed with C18 beads of 3 µm and running at 120 minute gradient of 95 % buffer A/ 5% buffer B (buffer A contains 0.5% acetic acid and buffer B contains 0.5% acetic acid in 100% ACN) to 65% buffer A/ 35 % buffer B and a flow rate of 300 nl/ minute. Eluted peptides were electrosprayed into the mass spectrometer at a spray voltage of 2.3 kV. Mass spectrometric data was acquired in a data dependent mode to switch between MS and MS2. Full-scan MS spectra of intact peptides (m/z 350–1500) were acquired in orbitrap cell at a resolution of 60,000 using an automated gain control accumulation target value of 1,000,0000 ions. In the linear ion trap the ten most abundant ions are isolated and fragmented by applying collision induced dissociation using an accumulation target value of 10,000, a capillary temperature of 275 °C, and normalized collision energy of 35%. A dynamic exclusion of ions previously sequenced within 45 seconds was applied.

Any singly charged ions and unassigned charged states were excluded from sequencing and a minimum of 10,000 counts was required for MS2 selection. This protocol was kindly provided by Dr. Vikram Sharma.

MS data was analysed to identify proteins with the Andromeda peptide database search engine (Cox *et al.*, 2011) integrated into the computational proteomics platform MaxQuant version (1.5.0.30) (Cox *et al.*, 2014; Tyanova *et al.*, 2016). Peptide mass spectra were searched against the UniProt database (http://www.uniprot.org/downloads, November 2015) and supplemented with sequences of frequently observed contaminants. Andromeda search parameters for protein identification specified a first search mass tolerance of 20 ppm and a main search tolerance of 4.5 ppm for the parental peptide and 0.5 Da mass tolerance for fragmentation spectra with a trypsin protease specificity allowing up to two mis-cleaved sites. Carboxyamidomethylation of cysteines was specified as a fixed modification, oxidation of methionine, deamidation of glutamine and asparagine, and protein N-terminal acetylation were set as variable modifications. The required minimal peptide length was set at 6 amino acids. MaxQuant performed an internal mass calibration of measured ions and peptide validation by the target decoy approach as described (Cox *et al.*, 2014). Proteins detected by at least two 'razor and unique' peptides in one of the samples with a 1% false discovery rate (FDR) for proteins and peptides were accepted. Proteins were label free quantified with label free quantification (LFQ) values representing normalised summed peptide intensities correlating with protein abundances, where the 'match between run' option was permitted between runs with a 0.7 minute elution time interval. Venn diagrams depicting the distribution of identified proteins and phosphoproteins were created with Venny 2.1 (http://bioinfogp.cnb.csic.es/tools/venny/index.html).

2.9 Protein quantification analysis and functional annotation analysis

LFQ values for proteins and phosphoproteins were $\log_2$ transformed using the Perseus software suite 1.5.0.31 (Tyanova *et al.*, 2016). Proteins and phosphoproteins identified in at least three runs were considered for LFQ and entries with an LFQ equal to zero were kept. Statistical significance of changes in abundance levels for proteins and phosphoproteins between meningioma grade sample groups and normal meningeal tissue (NMT) sample groups were calculated using Perseus software by a two-tailed *t*-test, with *p*-values adjusted for multiple testing by a permutation-based FDR at 1%. Microsoft Excel was used to calculate ratios and fold changes (FCs) for each meningioma grade *vs*. NMT from LFQ values, followed by $\log_2$ transformation of calculated FC. A $\log_2 FC \geq 1.5$ was considered to indicate upregulation and $\log_2 FC \leq -1.5$ to indicate downregulation. Proteins and phosphoproteins that were identified to be specific to one of the two groups being compared (i.e. were not detected in one group) were assigned a FC of infinity. Proteins and phosphoproteins with adjusted *p*-value< 0.05 were considered differentially expressed and included in further downstream analysis. Differentially expressed proteins and phosphoproteins for hierarchical clustering were obtained by submitting relative expression profiles of proteins and phosphoproteins identified in at least three runs to the Perseus software and performing a four-group one-way ANOVA (*p*-value< 0.05) on imputation supplemented protein data. Hierarchical clustering was then performed in Perseus.

Pathway analyses were generated with Ingenuity® Pathway Analysis (IPA®) (QIAGEN Inc., https://www.qiagenbioinformatics.com/products/ingenuity-pathway-analysis). GO enrichment analyses were performed using the knowledgebase of DAVID (the database for annotation, visualization and integrated discovery) version 6.8 (https://david.ncifcrf.gov/) (Huang da, Sherman & Lempicki, 2009) with a background

set of all human proteins. Enrichment of gene ontology (GO) FAT terms was considered statistically significant when corrected for multiple testing by the Benjamini-Hochberg method with adjusted *p*-values< 0.05. Cytoscape plugin Enrichment Map (Merico, Isserlin & Bader, 2011) was used to visualise enriched GO terms in an enrichment map. Protein-protein interactions were identified using the STRING (Search Tool for the Retrieval of Interacting Genes/Proteins) database version 10.5 (https://string-db.org/) for known and predicted *H. sapiens* protein–protein interactions (Szklarczyk *et al.*, 2017). Volcano plots were generated in the statistical software R version 3.4.2 by plotting $\log_2$ FC against corresponding *p*-value for each grade *vs*. grade comparison.

Molecular signatures for higher grade meningiomas were generated with the GeneSign module in BubbleGUM software (Spinelli *et al.*, 2015). Grade II and III samples were defined as subsets of interest (test classes), while NMT and grade I samples were defined as references. The Mean (test)/ Mean method was applied for extracting molecular signatures. This method calculates the ratio between the mean expression values of test and reference populations from data expressed in $\log_2$ scale, where missing values were imputed with the lowest expression value observed prior to analysis. Proteins or phosphoproteins with a minimal FC of 2 and a maximal FDR of 0.05, obtained from 10,000 random permutations were then subjected to hierarchical clustering performed in Perseus.

2.10 Phosphorylation motif analysis

Phosphorylation sites were classified by their chemical properties as acidic, basic, proline-directed, tyrosine or other by a binary decision tree method as follows: (1) get the 6 neighbouring amino acids before and after the phosphorylation site; (2) pY at position 0 then classify as “Tyrosine”; (3) P at +1 then classify as “Proline-directed”; (4) positions +1 to +6 contain five or more D/E then classify as “Acidic”; (5) K/R at position -3 then

classify as “Basic”; (6) D/E at +1/+2 or +3 then classify as “Acidic”; (7) two or more R/K at -6 to -1 then classify as “Basic”; (8) remaining peptides classify as “Other” (Villen *et al.*, 2007).

2.11 Data availability

MS proteomics data have been deposited to the ProteomeXchange Consortium via the PRIDE (Vizcaino *et al.*, 2016) partner repository with the following dataset identifiers and reviewer account details: global proteome PXD007073; phosphoproteome PXD007044; phosphopeptides PXD007125.

2.12 Tumour tissue and cell lysate preparation

Additional frozen tumour tissue samples that were obtained for validation studies and not used in MS analyses were manually homogenised from frozen in approximately 400 µl lysis buffer consisting of radioimmunoprecipitation assay (RIPA) buffer (50 mM Tris-HCl pH 7.4, 0.1% SDS, 1% NP-40, 150 mM NaCl, 1 mM ethylenediaminetetraacetic acid (EDTA), 0.5% sodium deoxycholate) and protease inhibitor used at 1:20 (cOmplete™, EDTA-free Protease Inhibitor Cocktail, Sigma-Aldrich®; #11873580001) and phosphatase inhibitor cocktails used at 1:100 (Santa Cruz Biotechnology, Inc.; sc-45045; sc-45065). Cells were similarly lysed in a volume of lysis buffer appropriate for the size of cell culture dish. All lysates were placed at -80 °C for at least 24 hours before being thawed on ice and spun down at 16,000 x *g* for 15 minutes at 4 °C. Supernatant was transferred to fresh 1.5 ml microcentrifuge tubes and protein concentration determined as before using the Pierce™ BCA Protein Assay Kit.

2.13 Western blotting

Appropriate volume of sample lysate for equal protein loading were added to 6X loading buffer and boiled for five minutes at 95 °C. Samples were then loaded onto the

polyacrylamide gel of applicable acrylamide percentage according to the molecular weight of the protein of interest. Gel recipes are shown in Table 2.5. Proteins were then separated via SDS-PAGE at 120 V constant for 100 minutes at RT or until proteins were adequately resolved in 1X running buffer (25 mM Tris base, 1.92 M glycine, 3.47 mM SDS). Following SDS-PAGE, proteins were transferred to a polyvinylidene difluoride membrane (Immun-Blot® PVDF membrane, Bio-Rad) at 400 mA constant for 70 minutes at RT via a wet transfer in transfer buffer (27.5 mM Tris base, 0.21 M glycine, 15% methanol). Membranes were blocked for one hour at RT in blocking milk (5% dried skimmed milk, PBST (phosphate-buffered saline (PBS; Thermo Fisher Scientific), 0.05% Tween-20)), before incubation with specific primary antibodies overnight at 4 °C. Table 2.6 lists all antibodies used in this study. Membranes were then washed three times in PBST followed by incubation for one hour at RT with appropriate anti-mouse or anti-rabbit horseradish peroxidase (HRP)-conjugated secondary antibodies (Bio-Rad) diluted 1:5000 in blocking milk. After incubation, membranes were again washed three times in PBST and detection was achieved using the enhanced chemiluminescence (ECL) or ECL Plus Western Blotting substrate (Pierce™). Membranes were exposed to Amersham Hyperfilm ECL to detect chemiluminescence signal of specific antigen-antibody interaction (GE Healthcare Life Sciences). GAPDH (glyceraldehyde-3-phosphate dehydrogenase) was used as loading control in all cases.

2.13.1 Peptide neutralization of DDX17 protein

WB protocol was followed as described above until primary antibody incubation. Subsequent to blocking, membrane was placed in a ratio of five-fold (by weight) excess of DDX17 (probable ATP-dependent RNA helicase DDX17) specific blocking peptide to optimum primary DDX17 antibody dilution (Table 2.6). Membrane was incubated in the mixture overnight at 4 °C and WB protocol continued as normal.

	Percentage acrylamide (resolving gel)				Stacking gel
Reagent	6%	8%	10%	15%	4%
40% acrylamide	1.5 mL	2 mL	2.5 mL	3.75 mL	0.5 mL
1.5 M Tris-HCl pH 8.8	2.5 mL	2.5 mL	2.5 mL	2.5 mL	X
0.5 M Tris-HCl, 0.4% SDS pH 6.8	X	X	X	X	1.25 mL
10% SDS	100 µl	100 µl	100 µl	100 µl	X
10% ammonium persulfate (APS)	100 µl	100 µl	100 µl	100 µl	50 µl
TEMED	10 µl	10 µl	10 µl	10 µl	10 µl
Distilled H_2O	5.79 mL	5.29 mL	4.79 mL	4.29 mL	3.19 mL

Table 2.5 Gel recipes for SDS-PAGE.

Antigen	Antibody	Type	WB dilution	IHC dilution
STAT2	#72604, Cell Signaling Technology®	Rabbit monoclonal	1:1000	
Akt	#4691, Cell Signaling Technology®	Rabbit monoclonal	1:250	
pAkt1 (Ser473)	#9018, Cell Signaling Technology®	Rabbit monoclonal	1:500	
pAkt1 (Thr308)	#4056, Cell Signaling Technology®	Rabbit monoclonal	1:500	
Akt2	#3063, Cell Signaling Technology®	Rabbit monoclonal	1:250	
pAkt2 (Ser474)	#8599, Cell Signaling Technology®	Rabbit monoclonal	1:500	
Paxillin	#2542, Cell Signaling Technology®	Rabbit polyclonal	1:500	
pPaxillin (Tyr118)	#2541, Cell Signaling Technology®	Rabbit polyclonal	1:500	
S100-A10	#5529, Cell Signaling Technology®	Mouse monoclonal	1:2000	1:3000
pRb (Ser780)	#8180, Cell Signaling Technology®	Rabbit monoclonal	1:500	
pRb (Ser807/811)	#8516, Cell Signaling Technology®	Rabbit monoclonal	1:500	1:1000

Rb	#9309, Cell Signaling Technology®	Mouse monoclonal	1:250	
EGFR	#4267 Cell Signaling Technology®	Rabbit monoclonal	1:1000	1:200
NF2	#6995 Cell Signaling Technology®	Rabbit monoclonal	1:1000	
NF2 (Ser518)	#9163 Cell Signaling Technology®	Rabbit polyclonal	1:500	
pPRAS40 (Thr246)	#13175 Cell Signaling Technology®	Rabbit monoclonal	1:500	
PRAS40	#2610 Cell Signaling Technology®	Rabbit polyclonal	1:500	
pGSK3β (Ser9)	#9323 Cell Signaling Technology®	Rabbit monoclonal	1:500	
GSK3β	#9315 Cell Signaling Technology®	Rabbit monoclonal	1:1000	
SET	#sc-133138, Santa Cruz Biotechnology, Inc.	Mouse monoclonal	1:1000	1:3000
Nek9	#sc-100401, Santa Cruz Biotechnology, Inc.	Mouse monoclonal	1:500	
CKAP4	#sc-393544, Santa Cruz Biotechnology, Inc.	Mouse monoclonal	1:500	1:200
TRIP6	#sc-166311, Santa Cruz Biotechnology, Inc.	Mouse monoclonal	1:250	

TRIP6	#sc-365122, Santa Cruz Biotechnology, Inc.	Mouse monoclonal		1:100
HK2	#sc-374091, Santa Cruz Biotechnology, Inc.	Mouse monoclonal	1:500	1:600
SF2/ASF	#sc-33652, Santa Cruz Biotechnology, Inc.	Mouse monoclonal	1:500	1:100
DDX17	#sc-398168, Santa Cruz Biotechnology, Inc.	Mouse monoclonal	1:500	1:300
AKT1	#sc-5298, Santa Cruz Biotechnology, Inc.	Mouse monoclonal		1:100
AKT2	#sc-5270, Santa Cruz Biotechnology, Inc.	Mouse monoclonal		1:300
Rb	#sc-102, Santa Cruz Biotechnology, Inc.	Mouse monoclonal		1:300
ATOX1	#H00000475-M02, Novus Biologicals®	Mouse monoclonal	1:500	
EPS8L2	#NBP1-83613, Novus Biologicals®	Rabbit polyclonal		1:200
EPS8L2	#ab126155, Abcam plc.	Rabbit polyclonal	1:500	
NEK9	#ab138488, Abcam plc.	Rabbit monoclonal		1:300
pNEK9 (Thr210)	#ab63553, Abcam plc.	Rabbit polyclonal	1:250	1:4000

pAKT1 (Ser473)	#ab81283, Abcam plc.	Rabbit monoclonal		1:400
STAT2	#ab53149, Abcam plc.	Rabbit polyclonal		1:800
Paxillin	#ab191007, Abcam plc.	Rabbit polyclonal		1:300
pPaxillin (Tyr118)	#ab194738, Abcam plc.	Rabbit polyclonal		1:2500
ATOX1	#ab176993, Abcam plc.	Rabbit polyclonal		1:500
pRb (Ser780)	#710296, ThermoFisher Scientific	Rabbit oligoclonal		1:200
GAPDH	#MAB374, Merk Millepore	Mouse monoclonal	1:50.000	

Table 2.6 Specifications of primary antibodies used for Western blot (WB) and immunohistochemistry (IHC).

2.13.2 Protein quantification and statistical analysis

Films were scanned in greyscale at a resolution of 600 dpi using a HP Scanjet 2400. Immunoreactive bands were quantified using Scion Image software and each band normalised to corresponding loading control values. The average value for the control samples was then calculated and taken as the reference value of one for quantification. Tumour samples were then each divided by the average value for control and significance determined between sample groups by performing a one-way ANOVA in Microsoft Excel. Average quantification values for each tumour grade were then calculated and plotted in a bar chart representing expression FC *vs*. NMT=1.

2.14 Immunohistochemistry

Formalin Fixed Paraffin Embedded (FFPE) tissue sections were cut at 4 μm by the Department of Cellular and Anatomical Pathology at University Hospitals Plymouth. For each antibody staining, 10 biological repeats were cut for NMT, grade I, II and III meningioma. Optimisation of primary antibody was performed on tonsil sections. Staining of ATOX1 (copper transport protein ATOX1), AKT2 (RAC-beta serine/threonine-protein kinase), EPS8L2 (epidermal growth factor receptor kinase substrate 8-like protein 2) and pRB-S780 (retinoblastoma-associated protein) was performed by the Department of Cellular and Anatomical Pathology at University Hospitals Plymouth. Negative controls were completed in parallel on tonsil and normal brain by omission of primary antibody. Following optimisation, tonsil sections were used as a positive control and routinely stained in each antibody run.

Sections were dewaxed and rehydrated by incubation at 60 °C for one hour, followed by two five minute washes in xylene (Fisher Scientific) and two further five minute washes in 100% ethanol (VWR®). Sections were then washed in running water for five minutes before blocking by submersion in 3% hydrogen peroxide (Fisher Scientific) in

methanol (VWR®) for 30 minutes at RT and subsequently washed in running water for 10 minutes. Antigen retrieval was performed by pre-treatment with either EDTA buffer (6.8 mM EDTA, 19.81 mM Tris base) pH 9.0 or citrate buffer (10 mM citric acid) pH 6.0. Sections were boiled in the appropriate pre-treatment buffer for 30 minutes and then washed under running water for 10 minutes before equilibration in Tris buffered saline-Tween-20 (TBST) buffer (0.05 M Tris base, 8% NaCl, 0.045% Tween-20) pH 7.6 for five minutes. Next, sections were blocked in 1% normal horse serum in TBST buffer for 30 minutes at RT followed by an avidin-biotin block (Vector Laboratories Ltd; #SP-2001) to block nonspecific binding of endogenous biotin consisting of a 15 minute incubation with Avidin D solution at RT, a brief one minute wash in TBST and then a 15 minute incubation with biotin solution. Finally, sections were drained of biotin solution and incubated in primary antibody, appropriately diluted in TBST overnight at 4 °C (specific primary antibody dilutions are listed in Table 2.6).

Sections were washed twice by immersion in TBST for five minutes and biotinylated secondary antibody (Vectastain® Universal Elite ABC kit; #PK-6200; Vector Laboratories Ltd) applied for 30 minutes at RT. Sections were washed twice by immersion in TBST for five minutes and incubated with biotinylated HRP (Vectastain® Elite ABC Reagent; Vectastain® Universal Elite ABC kit) for 30 minutes at RT according to manufacturer's protocol. Sections were again washed twice by immersion in TBST for five minutes before incubation in 3,3'-diaminobenzidine (DAB) solution (Sigma-Aldrich®; #D4293) for 5 minutes to allow detection of protein and then washed for 10 minutes under running water. If required, sections were immersed in DAB enhancer solution (25 mM copper sulphate, 124 mM sodium chloride) for five minutes followed by a five minute wash under running water. Counterstaining of sections was performed with application of Mayer's haematoxylin solution (Sigma-Aldrich®; #MHS1) for two minutes and excess removed by washing under running water for 10 minutes. Finally,

sections were washed twice for five minutes in 100% ethanol, followed by two five minute washes in xylene and then mounted onto coverslips using DPX mountant, (Sigma-Aldrich®; #06522), sections applied facedown.

Images were acquired using a Leica DMRB and the intensity of staining was assessed semi-quantitatively with the help of consultant neuropathologist, Dr David Hilton (Department of Cellular and Anatomical Pathology at University Hospitals Plymouth).

2.15 Cell culture

2.15.1 Cell lines

Cell lines used in this project included the immortalised benign meningioma cell line, Ben-Men-1 (BM1), derived from a human WHO grade I meningothelial meningioma (Puttmann *et al.*, 2005) and the malignant meningioma cell line KT21-MG1 (KT21), established from a human malignant meningioma transplanted into nude mice (Tanaka *et al.*, 1989). Cells were cultured in meningioma medium (Dulbecco's Modified Eagle's Media (DMEM; Thermo Fisher Scientific), supplemented with 10% foetal bovine serum (FBS; Sigma-Aldrich®), 1% D-(+)-glucose (Sigma-Aldrich®), 100 U/mL penicllin/streptomycin (Thermo Fisher Scientific) and 2 mM L-glutamine (Thermo Fisher Scientific)) at 37 °C in humidified 5% CO_2. Human meningeal cells (HMC) were obtained from ScienCell™ and routinely cultured in the manufacturer's recommended medium and growth supplements at 37 °C in humidified 5% CO_2.

2.15.2 Primary meningioma cells

Tumours were cut into small pieces and incubated in DMEM with 10% FBS, 100 U/mL penicillin/streptomycin and 20 U/mL Collagenase III (Worthington Biochemical Corp.) overnight at 37 °C in humidified 5% CO_2. Tumour pieces were then further disaggregated after incubation by manual pipetting to release cells. All media was collected and cells

were pelleted at 2000 rpm for five minutes, resuspended in meningioma medium (previously described in section 2.15.1), seeded in the appropriate tissue culture dish and grown at 37 °C in humidified 5% CO_2, keeping cell confluence above ~60%.

2.15.3 Passaging of cells

Cell lines and primary meningioma cells were washed once with PBS and incubated with trypsin-EDTA (0.05%) (Thermo Fisher Scientific) at 37 °C for approximately three minutes until cells detached. Trypsin was then neutralised with meningioma media and an appropriate volume of media added to the cell suspension for seeding in required tissue culture dish (Greiner Bio-One).

2.15.4 Cell viability assay

BM1 and KT21 cell lines were plated in 96-well culture plates (Greiner Bio-One; #655088) at approximately 3000 cells per well. Cells were allowed to adhere and proliferate for 24 hours. AZD5363, BKM120 (Buparlisib, NVP-BKM120) and Ku-0063794 (Selleckchem.com) were resuspended in dimethyl sulfoxide (DMSO; Sigma-Aldrich®) and serially diluted to the appropriate concentration in meningioma medium. Vehicle-treated control cells were grown with the addition of 0.1% DMSO. Cells were treated every 24 hours by careful removal of media from wells, as not to detach cells, followed by addition of fresh drug during a 72 hour incubation period at 37 °C in humidified 5% CO_2. Cell viability was determined using the 'CellTiter-Glo® Luminescent Cell Viability Assay' (Promega; #G7570). Upon application of the assay cells are lysed releasing ATP. The assay generates a luminescent signal proportional to the quantity of ATP present. The quantity of ATP is directly proportional to the number of viable cells in culture. Each drug concentration was tested in triplicate. Cell viability was calculated as a percentage of control cells, untreated cells as negative control and media alone as positive control. Graphs were generated using GraphPad Prism 5.

3 Global proteome analysis of meningioma

3.1 Introduction

Meningiomas constitute up to 36% of all brain tumours and are the most common intracranial tumour (Louis, 2016). They can occur sporadically and are a hallmark tumour of the predisposing familial syndrome NF2 along with schwannoma and ependymoma (Petrilli & Fernandez-Valle, 2016). Currently, there are no effective drugs for the treatment of these tumours. Primary therapies consisting of surgery and radiotherapy can cause significant morbidity and although resection can be curative, total tumour resection is not accomplished in approximately half of newly diagnosed meningioma (Fathi & Roelcke, 2013). Moreover, chemotherapies show poor, if any, activity in meningioma. The growing trend towards omics based techniques has greatly enhanced our knowledge of the molecular landscape of these tumours. By using an unbiased proteomic approach, tumour tissue and healthy tissue can be screened to identify proteins that may represent novel biomarkers or druggable therapeutic targets in meningioma.

Previous proteomic studies have highlighted some possible biomarkers and therapeutic targets of meningioma by following a MS approach (Cui *et al.*, 2014; Okamoto *et al.*, 2006; Saydam *et al.*, 2010; Sharma *et al.*, 2014; Sharma *et al.*, 2015). However, those studies were often limited by absence of appropriate control tissue and low sample numbers of high-grade meningiomas (Cui *et al.*, 2014; Sharma *et al.*, 2015). This chapter will provide a global proteome analysis of tissue from 22 meningioma specimens encompassing all WHO grades (eight grade I, eight grade II and six grade III) and three healthy human meninges, the most complete proteomic analyses from meningioma tissue to date.

Here, we performed in-depth global protein expression profiling of human meningiomas compared to healthy meningeal tissue by LC-MS/MS to identify differentially expressed proteins as well as dysregulated cellular pathways and processes in meningioma. We generated a large proteomic dataset revealing many differentially expressed proteins by comparative analysis of sample groups (grade I, II, III meningioma and NMT). In order to discover molecular targets and biomarkers for meningioma, we preferentially focussed on significantly upregulated proteins against which therapies can be targeted rather than significantly downregulated proteins. The initial analysis of downregulated proteins in meningioma discussed in this chapter will be expanded upon in future studies conducted by our research group.

Ultimately, this chapter will aim to describe the differential expression of proteins common to all meningioma grades compared to healthy meninges and additionally investigate grade-specific protein expression. These analyses will provide the basis from which a subset of differentially expressed proteins will be selected and their expression validated by the use of different techniques.

3.2 Mutational screening of meningioma

The recent surge in studies describing new genomic alterations of meningioma led us to define the genetic background of the 22 meningiomas analysed by MS using a combination of in-house and external genotyping approaches. To determine the mutational status of *NF2*, the gene most frequently implicated in meningioma pathogenesis, external NGS and MLPA was performed on tumour DNA whilst tumour lysates were subjected to in-house Western blotting. Full details of NGS and MLPA analysis are displayed in Supplementary Table S1. All supplementary tables are contained on the CD provided.

In all but five tumours, we confirmed mutations in the *NF2* gene by NGS and MLPA. Thirteen meningiomas were identified to have a deletion encompassing the whole of the *NF2* gene accompanied by a pathogenic mutation in the remaining *NF2* allele. These 13 tumours were therefore assigned an $NF2^{-/-}$ genotype. Four tumours (J7, MN018, J11 and J16) were established $NF2^{+/-}$ subsequent to detection of pathogenic *NF2* mutations of at least one allele in three tumours, and deletion of the majority of the *NF2* gene by MLPA in the remaining tumour. However, in three of these cases, MLPA failed and thus it cannot be disregarded these tumours may also harbour a deletion in the *NF2* gene resulting in an $NF2^{-/-}$ genotype. Wild-type *NF2* status was confirmed for five meningiomas (J8, J15, J1, J2 and J17) that did not reveal any genetic aberrations following either NGS or MLPA. We did not establish a correlation between *NF2* genotype with tumour grade.

We additionally used Western blotting to determine the expression of NF2 and pNF2-S518. This allowed us to understand how NGS and MLPA results were reflected at the protein level of NF2 in the tumours. In general, all 22 tumour lysates showed some expression of NF2 protein except for the grade III sample, J17 (Fig. 3.1A). This finding may be seen to conflict with the $NF2^{-/-}$ tumour genotypes confirmed by NGS and MLPA. However, in these cases it is likely that NF2 expression detected by WB originates from cells of the tumour microenvironment. Indeed, meningiomas are described as heterogeneous tumours comprising mainly of tumour cells alongside a variable presence of infiltrating immune cells, most frequently macrophages (Domingues *et al.*, 2012). Further, expression of pNF2-S518 could not be detected for these $NF2^{-/-}$ tumour genotypes (Fig. 3.1A). In contrast, four of the five $NF2^{+/+}$ meningiomas could clearly be seen to show higher NF2 expression with concomitant pNF2-S518 expression (J8, J15, J1 and J2) compared to all other tumours and NMT in WB (Fig. 3.1A).

Following mutational screening for *NF2*, we used the KASP genotyping system to perform in-house screening to check many of the other genes now described in some non-*NF2* meningioma to contain mutational hotspots. The mutational hotspots investigated included $AKT1^{E17K}$, $KLF4^{K409Q}$, $TRAF7^{N520S}$, SMO^{L412F}, SMO^{W535L}, $SMARCB1^{R374Q}$, $SMARCB1^{R377H}$ and $POLR2A^{Q403K}$. All tumours returned a wild-type genotype of the hotspots checked except for two, MN018 and J11 that were found to harbour a heterozygous genotype for *TRAF7* at the N520S hotspot. Full details of these results are displayed in Supplementary Table S1.

Although we identified five meningiomas as $NF2^{+/+}$ in our MS sample cohort by NGS and MLPA, we chose not to exclude these tumours from $NF2^{-/-}$ or $NF2^{+/-}$ genotyped meningiomas in downstream proteomic profiling analyses. Whilst it is of interest to characterise the genetic background of these tumours, by taking this approach we were able to analyse the largest meningioma cohort to date spanning all WHO grades. Moreover, following WB analysis of $NF2^{+/+}$ meningiomas, we were confident that if NF2 expression was detected concurrently with pNF2-S518, NF2 may be present. We did not detect any additional mutations in $NF2^{+/+}$ meningiomas by KASP genotyping. Future studies by our research group will aim to stratify proteomic analyses based on *NF2* status and if sample numbers permit, further stratify non-*NF2* meningiomas by the additional mutations described above.

We were not able to confirm the mutational background for the additional cohort of 15 meningiomas by NGS, MLPA or KASP as the amount of sample material was very limited in some instances. Therefore, we were only able to suggest an *NF2* genotype for these tumours by WB (Fig. 3.1B). NF2 expression was seen in the majority of tumours and did not appear to be grade dependent, whilst only the grade II tumour J21 showed weak expression of pNF2-S518 (Fig. 3.1B). Although expression of NF2 was detected in

many of the tumours this may arise from non-neoplastic cells of the tumour microenvironment as discussed above. Thus an *NF2*$^{-/-}$ genotype specific to tumour cells cannot be ruled out for these meningioma.

Similarly to our additional 15 meningioma cohort, we were only able to suggest an *NF2* genotype for NMT samples by WB. Expression of NF2 was found to be variable among NMT samples when run in parallel with both the MS meningioma sample cohort (Fig. 3.1A) and the additional cohort (Fig. 3.1B). This variation in NF2 expression may have arisen from the use of two independent tissue lysates for each NMT sample between screening of the MS meningioma cohort and the additional meningioma cohort. NMT samples did not display pNF2-S518 expression in either screening (Fig. 3.1), suggesting if NF2 was present it was in its active form.

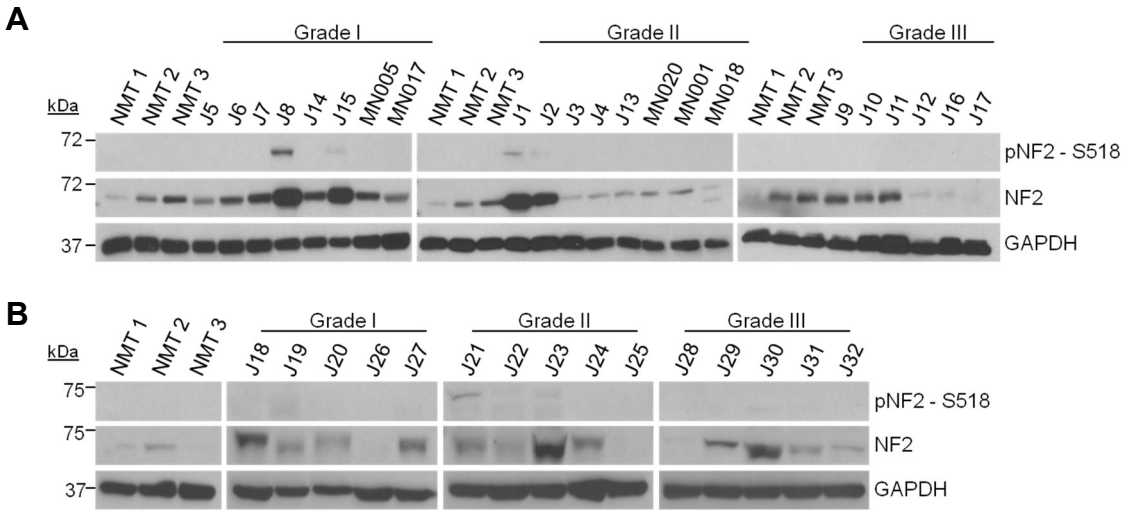

Figure 3.1 Expression of NF2 and pNF2-S518 in meningioma and NMT by Western blot. (**A**) Immunoreactivity of meningiomas and NMT used in MS analysis. (**B**) Immunoreactivity of additional cohort of 15 meningiomas used in WB validation studies. GAPDH was used as loading control. Clinical details of all meningiomas are presented in Tables 2.1 and 2.2.

3.3 Protein identification and quantification

In total, we sequenced and identified 3905 proteins across 25 samples; three normal meninges and 22 meningiomas. Proteins were identified by at least two 'razor and unique' peptides with an FDR of 1% using LC-MS/MS LFQ proteomics (Supplementary Table S2A). Figure 3.2 depicts the distribution of the 3905 identified proteins amongst the sample groups of NMT, grade I, II and III. We identified 3619 proteins within normal meninges (*n*=3), whilst in meningioma tissue we identified 3850 proteins across grade I (*n*=8), 3852 across grade II (*n*=8) and 3855 across six grade III (*n*=6). Proteins identified in at least 3 runs (3888 out of 3905) were then subjected to label-free quantitative analysis and analysed further for significant differential expression (Supplementary Table S3A).

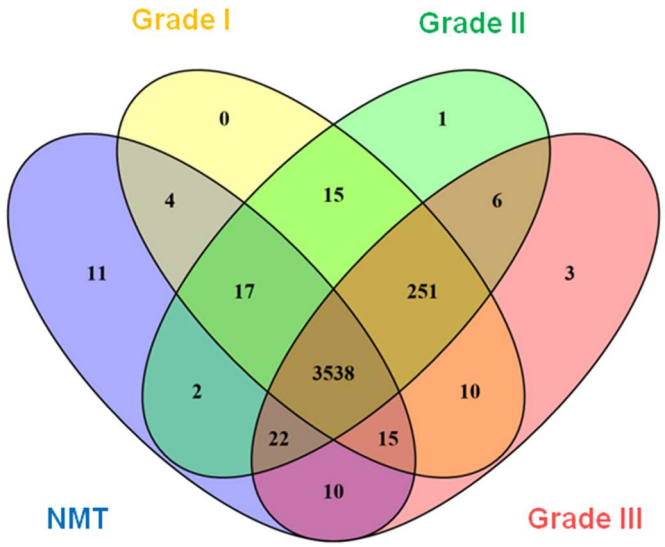

Figure 3.2 Venn diagram depicting the distribution of 3905 proteins identified across NMT and meningiomas. Label free quantitative (LFQ) proteomics by LC-MS/MS was used to identify proteins and quantify in three NMT, eight grade I, eight grade II and six grade III meningioma. Proteins were identified by at least two 'razor and unique' peptides with an FDR of 1% and are detailed in Supplementary Table S2A. Venn diagrams created using Venny 2.1.

3.4 Comparative proteomic analysis of the meningioma global proteome

3.4.1 Hierarchical clustering of differentially expressed proteins

Initially, we produced a heat map to obtain an overview of differentially expressed proteins of the global proteome dataset. This enabled us to visualise clusters of proteins that showed differential expression between tumours and healthy meninges. To generate a heat map we first transformed LFQ values for each of the 3888 quantified proteins into relative expression values between 0 and 1, where 0 is absence of protein expression and 1 represents the highest LFQ value detected for a protein across all samples. Relative expression profiles were then submitted to Perseus software to perform a one-way ANOVA. Significantly differentially expressed proteins (p-value< 0.05) were subsequently extracted and submitted for generation of a heat map with associated hierarchical clustering of samples. Hence, this analysis also allowed us to identify if samples clustered into their respective sample groups (NMT, grade I, II or III meningiomas) based on protein expression profiles.

Hierarchical clustering revealed a clear separation of tumour from control based on global proteomic profiles (Fig. 3.3A). Meningiomas clustered into their respective WHO grades, with the exception of the grade III sample J9, which was assigned to the grade II cluster (Fig. 3.3A). Three clusters of proteins displayed higher expression in at least one grade compared to NMT. The cluster showing increased expression across all grades included proteins such as EGFR, PRKDC (DNA-dependent protein kinase catalytic subunit), XRCC5 (X-ray repair cross-complementing protein 5), TOP1 (DNA topoisomerase 1), TOP2B (DNA topoisomerase 2-beta), SON (protein SON) and the DEAD-box RNA helicases DDX5 (probable ATP-dependent RNA helicase DDX5), DDX6 (probable ATP-dependent RNA helicase DDX6), DDX17 and DDX42 (ATP-dependent RNA helicase DDX42); whilst two smaller clusters with increased grade III-

specific expression contained mainly mitochondrial related proteins (Fig. 3.3A). One cluster of differentially expressed proteins was found to exhibit reduced expression common to all meningioma grades compared to NMT. Among this cluster were the proteins DKK3 (dickkopf-related protein 3) and SFRP3 (secreted frizzled-related protein 3) that function in modulation of the Wnt signalling, a pathway frequently dysregulated in cancer (Fig. 3.3A). Further proteins identified as downregulated in all tumours were the glycolytic enzyme HK1 (hexokinase-1) and the metalloproteinase inhibitor TIMP3 (Fig. 3.3A).

3.4.2 Commonly upregulated proteins amongst meningioma grades

Next, we focussed on identifying proteins upregulated in each meningioma grade compared to control, enabling us to identify proteins that were overexpressed unique to a grade or commonly overexpressed among grades. To describe a protein as up or downregulated we defined relatively stringent criteria; proteins with a $\log_2$ FC$\geq$ 1.5 were designated upregulated and those with a $\log_2$ FC$\leq$ -1.5 designated downregulated. Significant quantitative differences between sample groups were assessed by Student's *t*-tests using the Perseus software and significance was set at p-value$<$ 0.05.

To identify a subset of proteins that were commonly and significantly upregulated in all meningioma grades we first determined significantly upregulated proteins of each grade compared to control. Following this, we overlapped these three protein lists and identified 181 proteins to be commonly and significantly upregulated among all grades *vs.* NMT as depicted by the Venn diagram in Figure 3.3B. By initially concentrating on commonly overexpressed proteins we were able to obtain an overview of global dysregulation of protein expression occurring in meningioma irrespective of WHO grade. Table 3.1 presents the top 50 commonly and significantly upregulated proteins. Full lists

of quantified proteins detailing fold changes and significance are contained in Supplementary Table S3A.

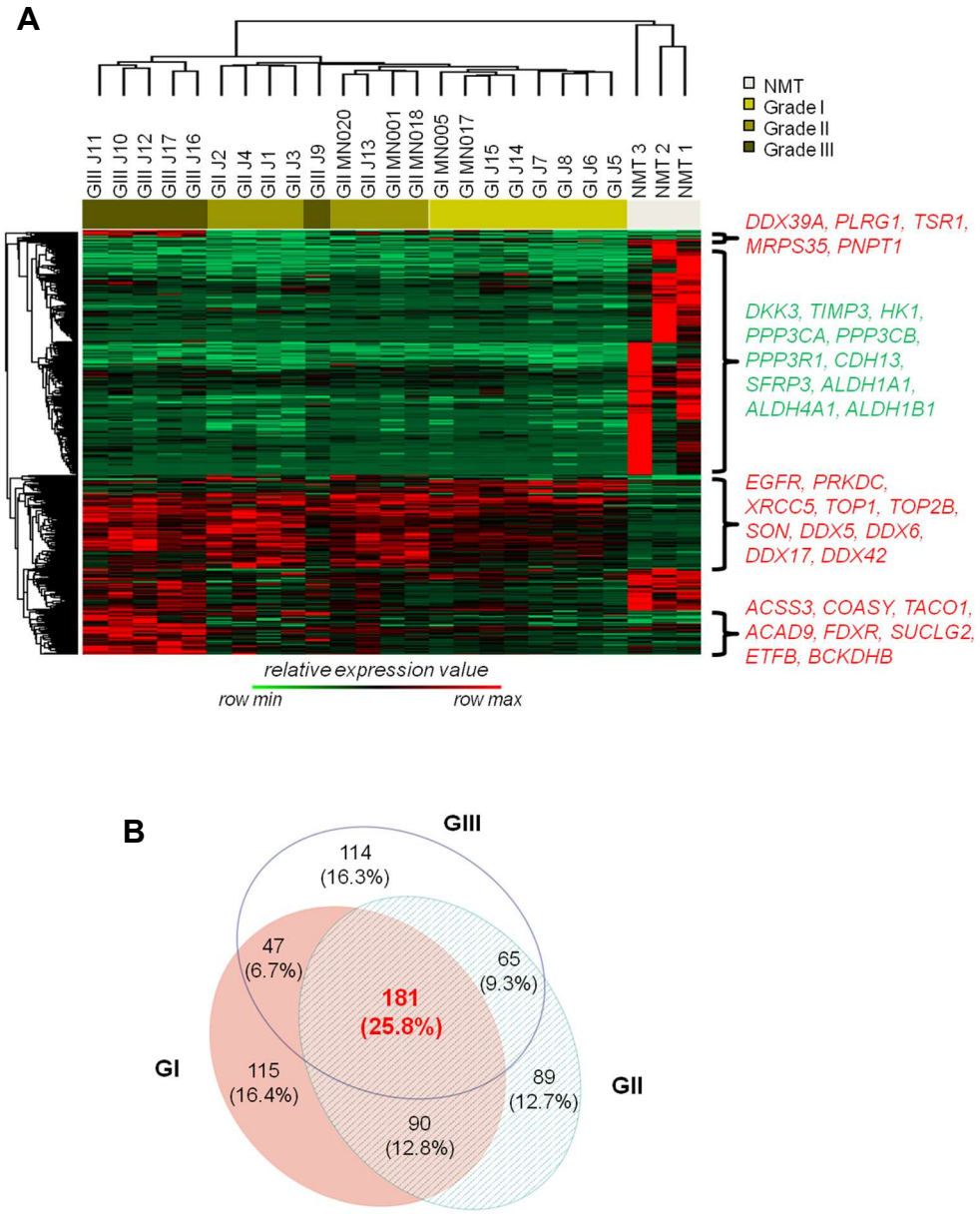

Figure 3.3 Comparative quantitative analysis of the meningioma global proteome. (**A**) Unsupervised hierarchical clustering of 481 differentially expressed proteins based on relative expression values (meningiomas *n*=22; NMT *n*=3). Meningiomas clustered separately from NMT in their protein profiles and into their respective WHO grades. Three protein clusters showing higher relative expression in at least one or more meningioma grade compared to NMT are annotated in red. A cluster of proteins showing lower relative expression across meningioma grades compared to NMT are annotated in green. Clustering was generated using Perseus 1.5.0.31 software suite, based on four-group one-way ANOVA, *p*-value< 0.05, corrected for multiple testing. (**B**) Venn diagram depicting unique and commonly upregulated proteins among different meningioma grades *vs*. NMT.

Protein name	Gene	Log_2 FC (GI *vs.* NMT)	Log_2 FC (GII *vs.* NMT)	Log_2 FC (GIII *vs.* NMT)
DnaJ homolog subfamily C member 8	DNJC8	∞	∞	∞
Protein SET	SET	∞	∞	∞
Isoform 2 of Signal transducer and activator of transcription 2	STAT2	∞	∞	∞
Histone H2AX	H2AX	∞	∞	∞
Copper transport protein ATOX1	ATOX1	∞	∞	∞
Vacuolar protein sorting-associated protein 28 homolog (Fragment)	VPS28	∞	∞	∞
Isoform J of Protein SON	SON	∞	∞	∞
U6 snRNA-associated Sm-like protein LSm6	LSM6	∞	∞	∞
Zinc finger CCCH-type antiviral protein 1-like	ZCCHL	∞	∞	∞
Thyroid receptor-interacting protein 6	TRIP6	∞	∞	∞
Splicing factor 3B subunit 5	SF3B5	∞	∞	∞

Isoform 2 of Forkhead box protein P1	FOXP1	∞	∞	∞
Ubiquitin-like modifier-activating enzyme 7	UBA7	∞	∞	∞
Isoform 3 of Eukaryotic translation initiation factor 2A	EIF2A	∞	∞	∞
Isoform 3 of Nuclear pore complex protein Nup153	NU153	∞	∞	∞
Exosome complex exonuclease RRP44	RRP44	∞	∞	∞
Uncharacterized protein FLJ45252	YJ005	∞	∞	∞
Isoform 5 of Neuron navigator 1	NAV1	∞	∞	∞
Ubiquitin carboxyl-terminal hydrolase 10	UBP10	∞	∞	∞
E3 ubiquitin-protein ligase TRIM22 (Fragment)	TRIM22	∞	∞	∞
Thrombospondin type-1 domain-containing protein 4	THSD4	8.38	7.91	5.41
Interferon-induced GTP-binding protein Mx1	MX1	7.86	5.97	8.14

Allograft inflammatory factor 1	AIF1	6.18	3.11	4.15
Deoxynucleoside triphosphate triphosphohydrolase SAMHD1	SAMH1	5.33	4.71	4.30
Isoform 2 of General transcription factor II-I	GTF2I	5.18	5.79	5.03
HLA class II histocompatibility antigen, DR alpha chain	HLA-DRA	5.10	3.75	3.43
Serine/threonine-protein kinase Nek9	NEK9	4.83	4.33	2.89
Isoform 3 of Centromere protein V	CENPV	4.57	4.62	4.60
Isoform 6 of Tight junction protein ZO-2	ZO2	4.38	5.16	3.93
Isoform Short of RNA-binding protein FUS	FUS	4.37	4.13	4.24
Protein S100-A10	S10AA	4.33	3.66	4.13
Serpin H1	SERPH	4.29	4.43	3.82
Sulfotransferase 1A1	ST1A1	4.28	4.37	4.09

Isoform 3 of KN motif and ankyrin repeat domain-containing protein 2	KANK2	4.21	4.59	3.46
Ubiquitin/ISG15-conjugating enzyme E2 L6	UB2L6	4.20	4.04	9.24
Transcription intermediary factor 1-beta	TIF1B	4.10	4.77	5.02
Histone H4	H4	4.08	3.17	3.17
Peptidyl-prolyl cis-trans isomerase FKBP9	FKBP9	4.03	4.12	4.36
Thymidine phosphorylase (Fragment)	TYMP	3.97	3.99	3.63
Small nuclear ribonucleoprotein F	RUXF	3.94	3.61	4.47
Splicing factor 3B subunit 2	SF3B2	3.89	4.48	4.23
Isoform 4 of Perilipin-3	PLIN3	3.86	3.21	3.34
Isoform 3 of Acyl-CoA synthetase family member 2, mitochondrial	ACSF2	3.85	3.67	5.41

Thyroid hormone receptor-associated protein 3	TR150	3.84	3.96	3.38
Coatomer subunit delta	COPD	3.77	3.76	2.89
Isoform 2 of Protein SET	SET	3.74	3.99	4.18
Heterogeneous nuclear ribonucleoprotein H	HNRH1	3.71	4.22	3.98
Signal transducer and activator of transcription 1-alpha/beta	STAT1	3.67	3.67	4.46
Heterogeneous nuclear ribonucleoprotein A0	HNRNPA0	3.67	4.78	3.08
Heterogeneous nuclear ribonucleoprotein D-like	HNRNPDL	3.63	3.33	4.14

Table 3.1 Top 50 of the most commonly and significantly upregulated proteins among all WHO grades of meningiomas compared to NMT. Corresponding $\log_2$ FCs for each meningioma grade compared to NMT are shown. Significant upregulation defined by $\log_2$ fold-change≥1.5; *p*-value<0.05. Proteins specific to one of the two groups compared were assigned a fold change of infinity. Full details of the 181 proteins commonly and significantly upregulated can be found in Supplementary Table S3A.

Next, we wanted to ascertain the overlap of our proteomic analyses with previously generated proteomes of meningioma. Comparing our global proteome dataset with that of Sharma *et al*. (2015), who similarly analysed the proteome of all meningioma grades (Sharma *et al.*, 2015), we identified 1428 proteins to be common to both studies. Of the 181 upregulated proteins we established from the analysis above to be common to all grades, 28 were also found by Sharma *et al*. (2015) to be commonly upregulated among all meningioma grades compared to control and are displayed in Table 3.2.

Protein name	Gene	Log_2 FC (GI *vs.* NMT)	Log_2 FC (GII *vs.* NMT)	Log_2 FC (GIII *vs.* NMT)
Annexin A2	ANXA2	1.73	2.10	1.78
X-ray repair cross-complementing protein 6	XRCC5	1.59	2.56	3.68
X-ray repair cross-complementing protein 5	XRCC6	1.81	2.38	6.01
Histone H2AX	H2AX	∞	∞	∞
Heterogeneous nuclear ribonucleoproteins A2/B1	HNRNPA2B1	2.79	2.76	2.42
Leukocyte elastase inhibitor	SERPINB1	1.87	1.71	1.92
Serpin H1	SERPINH1	4.29	4.43	3.82
Heterogeneous nuclear ribonucleoprotein A3	HNRNPA3	2.46	2.15	1.83
Allograft inflammatory factor 1	AIF1	6.18	3.11	4.15
Protein SEC13 homolog	SEC13	2.26	2.81	2.35
Cytoskeleton-associated protein 4	CKAP4	2.63	2.22	2.97
Endoplasmic reticulum resident protein 44	ERP44	1.71	2.16	2.05
Eukaryotic translation initiation factor 5A	EIF5A	1.73	1.60	1.56

Chloride intracellular channel protein 1	CLIC1	1.75	1.90	2.26
Ubiquitin/ISG15-conjugating enzyme E2 L6	UBE2L6	4.20	4.04	9.24
Adenine phosphoribosyltransferase	APRT	1.56	1.66	1.52
Coatomer subunit delta	ARCN1	3.77	3.76	2.89
Protein S100-A10	S100A10	4.33	3.66	4.13
Small nuclear ribonucleoprotein E	SNRPE	1.91	1.95	2.36
Small nuclear ribonucleoprotein F	SNRPF	3.94	3.61	4.47
40S ribosomal protein S25	RPS25	2.90	2.69	1.76
Elongation factor 1-alpha 1	EEF1A1	2.54	2.65	2.41
Spliceosome RNA helicase DDX39B	DDX39B	2.11	2.84	2.80
Thrombospondin type-1 domain-containing protein 4	THSD4	8.38	7.91	5.41
Peptidyl-prolyl cis-trans isomerase FKBP10	FKBP10	3.58	4.08	3.68
Aminopeptidase B	RNPEP	2.70	1.99	2.55

Epidermal growth factor receptor kinase substrate 8-like protein 2	EPS8L2	1.66	3.26	3.04
Echinoderm microtubule-associated protein-like 4	EML4	2.94	2.94	2.36

Table 3.2 Proteins identified as commonly upregulated among all WHO grades of meningiomas found to overlap with previous proteomic meningioma studies. Displayed are proteins identified by Sharma *et al*. (2015) that overlap with the 181 proteins identified to be significantly and commonly upregulated among all meningioma grades compared to NMT (Sharma *et al.*, 2015). Corresponding $\log_2$ FCs for each meningioma grade compared to NMT are shown. Proteins specific to one of the two groups compared were assigned a fold change of infinity.

3.4.3 Functional annotation of commonly upregulated proteins in meningioma

In order to interpret and extract the biological meaning behind a protein dataset there are various bioinformatic computational tools that can be employed. Functional annotation is used to predict the functional role of proteins identified in a sample as well as to detect the biological processes and pathways most represented by a set of proteins. Specifically, enrichment analysis is often performed to identify biological annotations that are overrepresented or 'enriched' in a protein dataset and may therefore play a role in pathogenesis. One of the most widespread approaches to annotate proteomic datasets involves the use of ontologies. Gene ontologies are comprised of a hierarchy of terms that are assigned to the classes of 'Biological Process', 'Molecular Function' and 'Cellular Component' that are then associated with a gene to describe its role in a biological system (Carnielli, Winck & Paes Leme, 2015).

In this project we performed functional annotation analysis using the web-based bioinformatic resource DAVID (https://david.ncifcrf.gov/). Following submission of a gene list, DAVID maps the genes of interest to related GO terms and subsequently presents which of these terms are statistically enriched (Huang da, Sherman & Lempicki, 2009). Enrichment analysis is based on the principle that if a biological process is altered in a given condition, the genes functioning in that process should more likely be detected (enriched) and assigned to the process. Enrichment is then calculated by comparison of the user's submitted gene list with the relevant gene population background dataset chosen in DAVID. For instance, if 10% of the user's genes are annotated as kinases compared to 1% of genes that comprise the human genome (set as the background dataset), then kinases will represent a higher proportion of the user's gene list than that of the background (Huang da, Sherman & Lempicki, 2009). Thus, kinases would be

concluded to be statistically enriched 10-fold relative to the human genome and have potentially important implications in the study (Huang da, Sherman & Lempicki, 2009).

We submitted the 181 proteins found to be commonly and significantly upregulated in all meningioma grades *vs*. control to DAVID to determine enriched GO terms and elucidate upon the dysregulated biological processes that may be underlying all meningioma grades. Figure 3.4A presents a histogram of significantly enriched GO terms in order of fold enrichment. Among terms classed under 'Molecular Function', double-stranded telomeric DNA binding gave the highest enrichment (46-fold) followed by telomeric DNA binding (15-fold). These terms are reflective of previous studies in meningioma reporting mutations in the promoter region of the *TERT* gene coding for the ribonucleoprotein enzyme, telomerase, essential for chromosome telomere replication (Goutagny *et al.*, 2014; Sahm *et al.*, 2016).

GO terms related to splicing were distributed throughout the classes of 'Cellular Component' and 'Biological Process'. The pICln-Sm protein complex GO term showed the highest enrichment (51-fold) of the 'Cellular Component' class in addition to enrichment of spliceosome components; U6 snRNP (small nuclear ribonucleoprotein) (43-fold) and U4 snRNP (37-fold) (Fig. 3.4A). Among the 'Biological Process' class, regulation of alternative mRNA splicing via spliceosome GO term was found to have a 12-fold enrichment (Fig. 3.4A). Proteins that we identified to be commonly upregulated in the meningioma proteome related to these enriched splicing GO terms included components of the spliceosome; SNRPD3 (small nuclear ribonucleoprotein Sm D3), SNRPF (small nuclear ribonucleoprotein F), SNRPE (small nuclear ribonucleoprotein E), SF3B2 (splicing factor 3B subunit 2), SF3B5 (splicing factor 3B subunit 5) and the splicing factors SRSF3 (serine/arginine-rich splicing factor 3), SRSF7 (serine/arginine-rich splicing factor 7) and SF2/ASF (serine/arginine-rich splicing factor 1; also SRSF1).

Other enriched terms associated with commonly upregulated proteins included COPI vesicle coat (51-fold) and transport vesicle (8-fold) suggesting an increase in vesicle-mediated transport in meningiomas compared to normal meninges (Fig. 3.4A). The remainder of identified enriched terms were generally related to functions surrounding transcription and RNA processing (Fig. 3.4A). A full list of all GO terms associated with the 181 upregulated proteins can be found in Supplementary Table S4A.

To obtain a global view of the biological functions associated with commonly upregulated proteins, enriched GO terms were visualised in an 'enrichment map', where each term is represented by a node with edges showing degree of overlap between GO term sets (Fig. 3.4B; Supplementary Table S4B). Five clusters of GO terms were identified in the protein enrichment map. The largest cluster, comprised of 36 nodes, was associated with transcription/post-transcriptional modifications, including mRNA processing and spliceosomal complex. Complementary to this, two further clusters contained terms related specifically to splicing machinery and the spliceosomal complex, indicating an enhanced activity of transcriptional and post-transcriptional processes. Other clusters included cell adhesion (3 nodes) and vesicle-mediated transport (9 nodes).

We next wanted to establish signalling pathways associated with commonly and significantly upregulated proteins. This enabled us to highlight dysregulated pathways that may show therapeutic promise throughout all meningioma grades. Due to the relatively low number of common proteins (181), following pathway enrichment analysis we were only able to identify 11 pathways, of which two were found to be significantly enriched with adjusted p-value< 0.05 (Fig. 3.4C; Supplementary Table S4C). In line with previous functional annotation that demonstrated commonly upregulated proteins to be associated with aspects of splicing (Fig 3.4A and 3.4B), the spliceosome pathway was shown to be the most enriched (12-fold) (Fig 3.4C). A schematic representation of the

spliceosome pathway is also shown in figure 3.4C highlighting proteins of spliceosome components found to be upregulated in meningioma. Taken together, these results suggest an upregulation of factors related to splicing may play a role in meningioma pathogenesis.

A

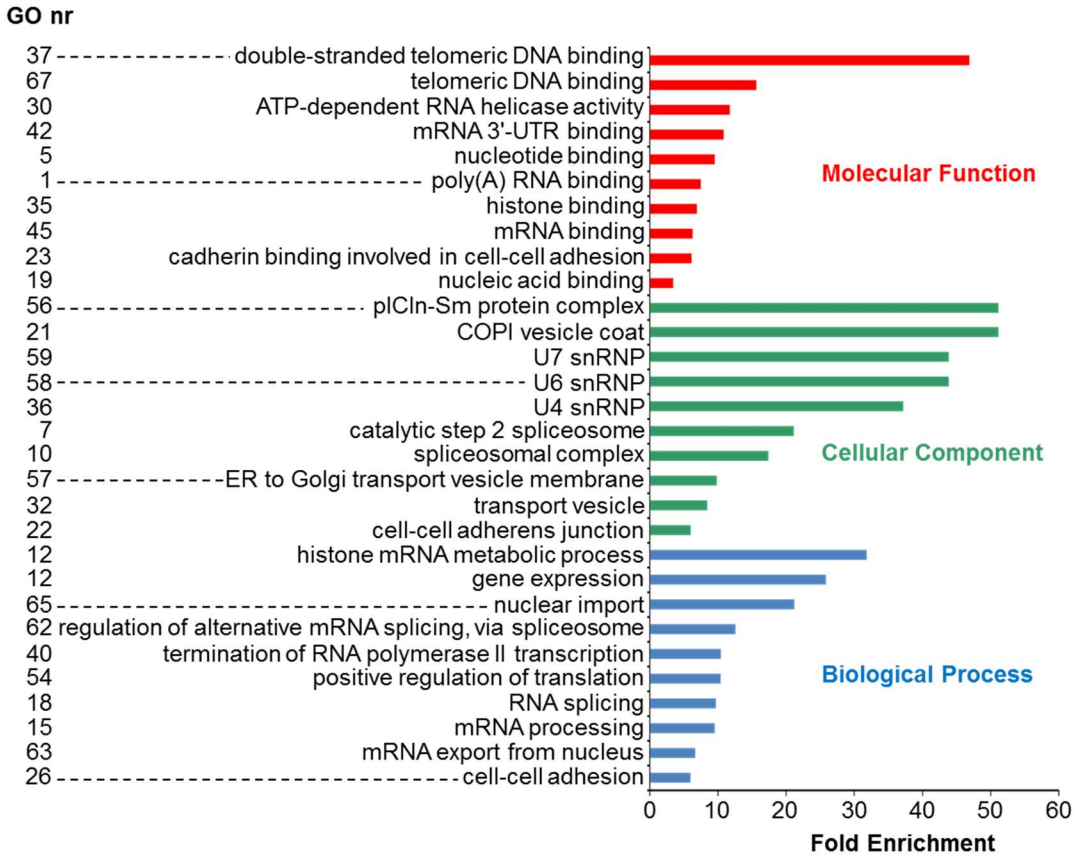
GO nr
37 double-stranded telomeric DNA binding
67 telomeric DNA binding
30 ATP-dependent RNA helicase activity
42 mRNA 3'-UTR binding
5 nucleotide binding
1 poly(A) RNA binding
35 histone binding
45 mRNA binding
23 cadherin binding involved in cell-cell adhesion
19 nucleic acid binding
Molecular Function
56 plCln-Sm protein complex
21 COPI vesicle coat
59 U7 snRNP
58 U6 snRNP
36 U4 snRNP
7 catalytic step 2 spliceosome
10 spliceosomal complex
57 ER to Golgi transport vesicle membrane
32 transport vesicle
22 cell-cell adherens junction
Cellular Component
12 histone mRNA metabolic process
12 gene expression
65 nuclear import
62 regulation of alternative mRNA splicing, via spliceosome
40 termination of RNA polymerase II transcription
54 positive regulation of translation
18 RNA splicing
15 mRNA processing
63 mRNA export from nucleus
26 cell-cell adhesion
Biological Process
0 10 20 30 40 50 60
Fold Enrichment

B

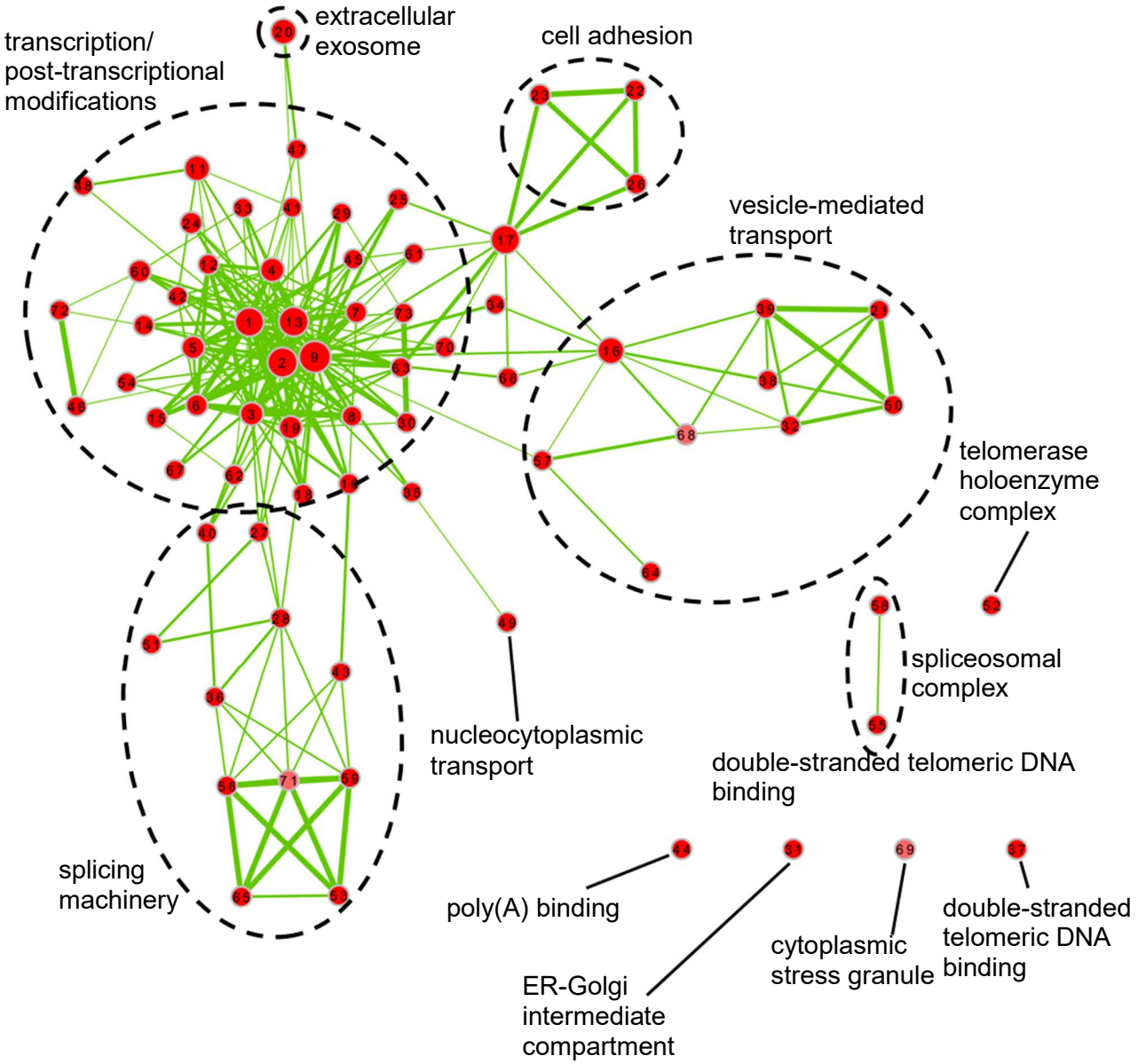
transcription/
post-transcriptional
modifications
extracellular
exosome
cell adhesion
vesicle-mediated
transport
telomerase
holoenzyme
complex
spliceosomal
complex
nucleocytoplasmic
transport
double-stranded telomeric DNA
binding
splicing
machinery
poly(A) binding
ER-Golgi
intermediate
compartment
cytoplasmic
stress granule
double-stranded
telomeric DNA
binding

C

Category	Pathway	Protein Count	Fold Enrichment	Benjamini-Hochberg *p*-value
KEGG	Spliceosome	23	12.57855164	1.49E-16
KEGG	Herpes simplex infection	10	3.974690825	0.04068571
BIOCARTA	RNA polymerase III transcription	3	30.46875	0.187580127
KEGG	Influenza A	8	3.344222626	0.273428601
KEGG	Non-homologous end-joining	3	16.7854251	0.285206644
BIOCARTA	Granzyme A mediated Apoptosis Pathway	3	13.84943182	0.414706538
BIOCARTA	Spliceosomal Assembly	3	10.88169643	0.436289463
KEGG	RNA transport	7	2.960220318	0.458091116
KEGG	Systemic lupus erythematosus	6	3.256873527	0.461541418
KEGG	RNA degradation	4	3.778537252	0.689918982
KEGG	Protein processing in endoplasmic reticulum	6	2.582373092	0.705847283

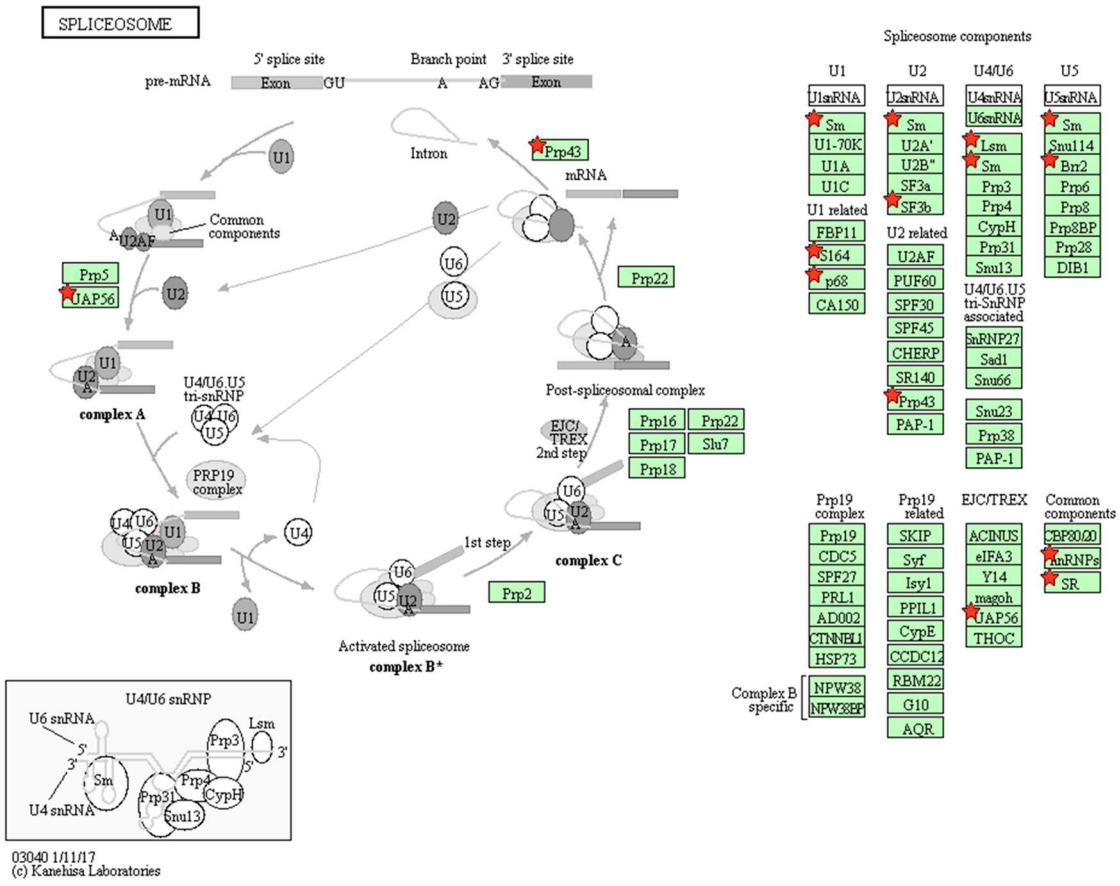

Figure 3.4 Functional annotation of proteins significantly upregulated and common to all meningioma grades *vs.* NMT. (**A**) Gene ontology (GO) enrichment analysis of 181 proteins commonly upregulated to all meningioma grades by the web tool DAVID version 6.8. Terms containing at least three proteins with Benjamini-Hochberg $p < 0.05$ are shown. Gene Ontologies representing 'Molecular Function' are presented in red, 'Cellular Component' in green and 'Biological Process' in blue. Fold enrichment relative to the *H. sapiens* proteome is displayed at the *x*-axis. Full details of GO analysis output are detailed in Supplementary Table S4A (**B**) Enrichment map of GO terms found to be enriched among upregulated proteins. Nodes represent enriched GO terms, colour intensities reflecting statistical significance and line thickness correlating to the degree of overlap. Numbers refer to GO terms some of which are seen in (A) with full list of terms detailed in Supplementary Table S4B. Image created with Cytoscape plugin Enrichment Map. (**C**) Pathway enrichment analysis of commonly upregulated proteins by DAVID version 6.8. Shown are identified enriched pathways associated with upregulated proteins and corresponding Benjamini-Hochberg *p*-values. Spliceosome and herpes simplex infection pathways were found to be enriched with p-value< 0.05. Representative schematic of the spliceosome pathway extracted from DAVID is displayed. Red stars highlight upregulated proteins mapped to the pathway. Full pathway enrichment output is detailed in Supplementary Table S4C.

3.4.4 Commonly downregulated proteins amongst all meningioma grades

Similar to our approach for the identification of upregulated proteins, we first determined significantly downregulated proteins (log_2 FC≤ -1.5; *p*-value< 0.05) of each grade compared to control. Following this, we overlapped these three protein lists and identified 94 proteins to be commonly and significantly downregulated among all grades *vs.* NMT. Table 3.3 displays the top 50 commonly and significantly downregulated proteins. Full lists of quantified proteins detailing fold changes and significance are contained in Supplementary Table S3A.

Protein name	Gene	Log_2 FC (GI *vs.* NMT)	Log_2 FC (GII *vs.* NMT)	Log_2 FC (GIII *vs.* NMT)
Proline-rich transmembrane protein 2	PRRT2	-∞	-7.05	-8.01
Neurexin-1-beta	NRXN1	-∞	-4.19	-4.08
Isoform 2 of Cochlin	COCH	-∞	-5.98	-∞
Isoform 2 of Regucalcin	RGN	-∞	-∞	-∞
Lymphocyte antigen 6H	LY6H	-∞	-1.87	-2.52
Membrane primary amine oxidase	AOC3	-13.20	-12.64	-12.65
Guanine deaminase	GUAD	-11.35	-11.32	-6.65
Calponin-1	CNN1	-11.13	-12.46	-13.33
Isoform 3 of Sorbin and SH3 domain-containing protein 2	SRBS2	-10.32	-8.36	-10.26
Protein kinase C and casein kinase substrate in neurons protein 1	PACN1	-10.14	-7.54	-7.30
Isoform 2 of Neuronal-specific septin-3	SEPT3	-9.92	-9.06	-6.92
Sushi domain-containing protein 2	SUSD2	-9.90	-8.70	-7.91
Amyloid-like protein 1	APLP1	-9.85	-10.78	-5.59
Isoform 3 of Neuronal cell adhesion molecule	NRCAM	-9.45	-11.60	-7.21
Sodium/potassium-transporting ATPase subunit beta-2	AT1B2	-9.42	-8.90	-8.18

Neural cell adhesion molecule L1-like protein	NCHL1	-9.40	-9.17	-8.78
C-reactive protein	CRP	-9.35	-11.50	-9.89
Oligodendrocyte-myelin glycoprotein	OMGP	-9.29	-10.47	-9.68
Isoform 8 of Tropomyosin alpha-1 chain	TPM1	-9.20	-9.66	-9.13
Pleiotrophin	PTN	-8.66	-10.30	-11.56
Neural cell adhesion molecule 2	NCAM2	-8.62	-7.99	-7.15
Isoform 3 of Liver carboxylesterase 1	EST1	-8.49	-10.73	-8.24
Isoform 2 of Sodium- and chloride-dependent GABA transporter 2	S6A13	-8.22	-7.02	-9.02
Neurocan core protein	NCAN	-7.54	-7.46	-4.73
Isoform 6 of Neurofascin	NFASC	-7.43	-9.16	-7.32
Contactin-associated protein-like 2	CNTP2	-7.41	-7.12	-7.76
Neurosecretory protein VGF	VGF	-6.98	-7.66	-6.24
Contactin-1	CNTN1	-6.70	-6.43	-6.04
Alpha-actinin-2	ACTN2	-6.62	-7.26	-6.58
1-phosphatidylinositol 4,5-bisphosphate phosphodiesterase beta-1	PLCB1	-6.38	-7.34	-6.83
Spondin-1	SPON1	-6.03	-5.02	-6.94
Cytoplasmic FMR1-interacting protein 2	CYFIP2	-5.78	-5.65	-5.33

Protocadherin-1	PCDH1	-5.77	-3.40	-5.83
Actin, aortic smooth muscle	ACTA	-5.67	-5.05	-4.58
Myosin-11	MYH11	-5.65	-5.95	-5.73
Dickkopf-related protein 3	DKK3	-5.65	-5.99	-4.59
Isoform 3B of Myosin light chain kinase, smooth muscle	MYLK	-4.99	-5.08	-3.14
Glycogen phosphorylase, muscle form	PYGM	-4.97	-2.70	-4.29
Isoform 3 of Collagen alpha-1(XVIII) chain	COIA1	-4.93	-2.86	-3.00
Ribonuclease pancreatic	RNAS1	-4.89	-6.03	-3.24
Isoform 2 of TBC1 domain family member 24	TBC24	-4.88	-4.59	-2.82
Isoform 2 of 4F2 cell-surface antigen heavy chain	4F2	-4.87	-3.45	-3.06
Solute carrier family 13 member 3 (Fragment)	SLC13A3	-4.78	-3.90	-4.26
Protein FAM49A	FA49A	-4.72	-4.78	-5.07
Transgelin	TAGL	-4.71	-5.38	-4.86
Succinate-semialdehyde dehydrogenase, mitochondrial	SSDH	-4.50	-5.19	-2.34
Isoform 3 of Erythrocyte membrane protein band 4.2	EPB42	-4.49	-6.69	-5.00
Basal cell adhesion molecule	BCAM	-4.46	-4.81	-5.50
Fructose-bisphosphate aldolase C	ALDOC	-4.41	-3.75	-2.47

Tyrosine-protein phosphatase non-receptor type substrate 1	SHPS1	-4.40	-4.25	-4.33

Table 3.3 Top 50 of the most commonly and significantly downregulated proteins among all grades of meningiomas compared to NMT. Corresponding $\log_2$ FCs for each meningioma grade compared to NMT are shown. Significant downregulation defined as $\log_2$ FC$\leq$ -1.5; *p*-value$<$ 0.05. Proteins specific to one of the two groups compared were assigned a fold change of infinity. Full details of the 94 proteins commonly and significantly downregulated can be found in Supplementary Table S3A.

3.4.5 Functional annotation of commonly downregulated proteins in meningioma

As discussed at the beginning of this chapter we decided to concentrate on a more extensive bioinformatic analyses of upregulated rather than downregulated proteins. In addition, it is not ideal to perform functional annotation of such a small amount of commonly downregulated proteins (94) due to limited coverage. However, we submitted commonly downregulated proteins to STRING and DAVID in order to obtain a general overview of the protein-protein interactions occurring as well as enriched GO terms relative to the *H. sapiens* proteome (Fig. 3.5).

We performed a STRING clustering analysis of the meningioma interactome to observe the associations between downregulated proteins. To identify the most reliable protein network, we defined protein interactions by selecting 'known interactions' that have been previously experimentally determined or curated from databases and removing 'predicted interactions'. Figure 3.5A shows a protein interaction network highlighted with five clusters of downregulated proteins and their associated biological functions.

The largest cluster of proteins identified by STRING analysis was related to cell adhesion (Fig. 3.5A), a biological process also identified by GO enrichment analysis of downregulated proteins to show a 7-fold significant enrichment (Fig. 3.5B; Supplementary Table S5A). The most enriched GO term was aldehyde dehydrogenase (nicotinamide adenine dinucleotide (NAD)) activity in the 'Molecular Function' class with a 46-fold enrichment (Fig. 3.5B). This molecular function was also associated with a cluster of interacting proteins defined by STRING (Fig. 3.5A). Proteins comprising the aldehyde dehydrogenase (NAD) activity cluster included members belonging to the superfamily of aldehyde dehydrogenases such as ALDH1A1 (retinal dehydrogenase 1) and ALDH5A1 (succinate-semialdehyde dehydrogenase, mitochondrial); previously

identified as downregulated and a biomarker of poor prognosis in various cancers (Okudela *et al.*, 2013; Tian *et al.*, 2017).

Remaining protein-protein interaction clusters were related to G-protein coupled receptor (GPCR) signalling, the cortical cytoskeleton and the calcineurin complex (Fig. 3.5A). Specifically, within the calcineurin complex we identified the component proteins PPP3CA (serine/threonine-protein phosphatase 2B catalytic subunit alpha isoform), PPP3CB (serine/threonine-protein phosphatase 2B catalytic subunit beta isoform) and PPP3R1 (calcineurin subunit B type 1) (Fig. 3.5A). These proteins were identified in our previous analysis to exhibit significantly reduced expression across meningioma grades, as highlighted in Figure 3.3A.

A

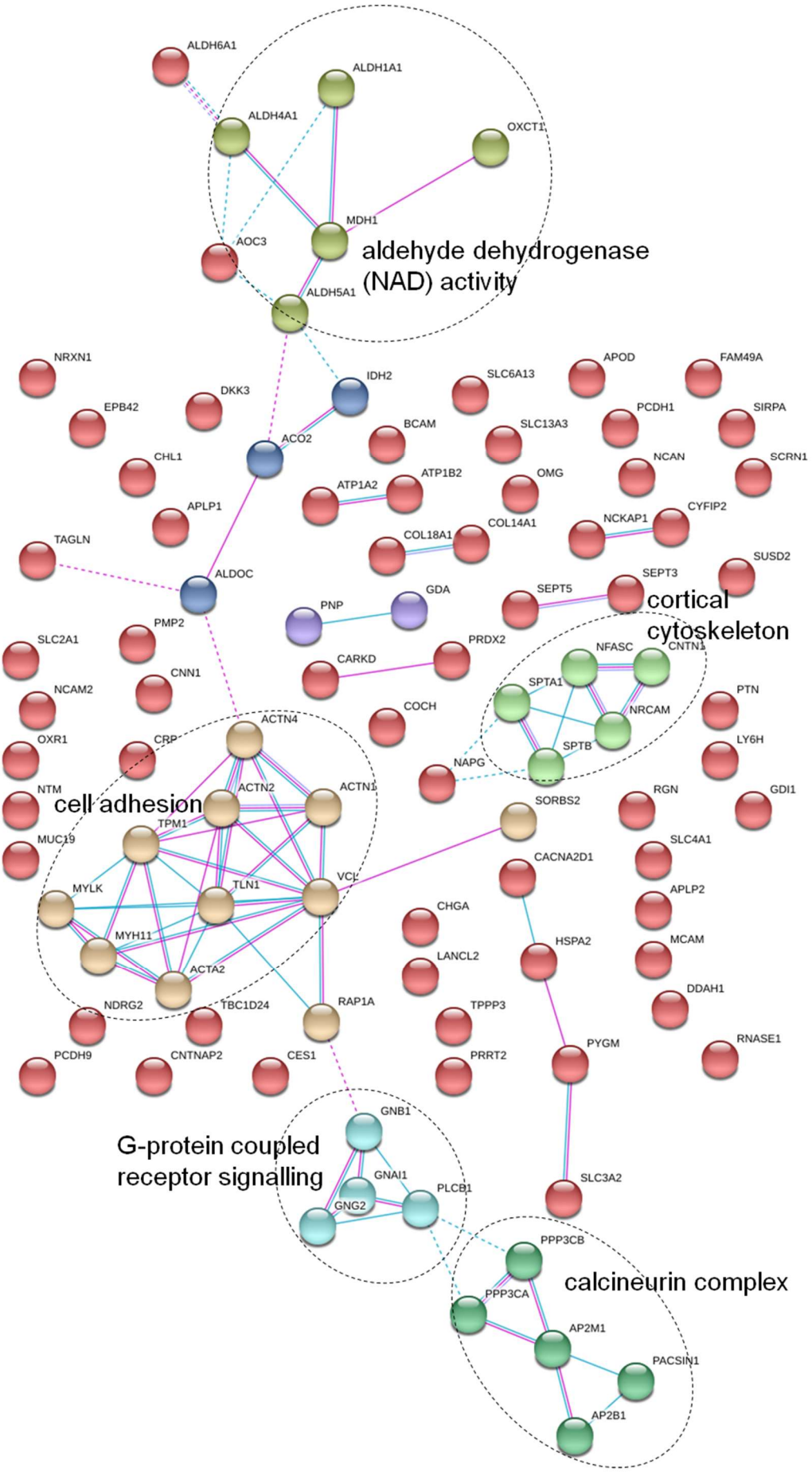
ALDH6A1
ALDH1A1
ALDH4A1
OXCT1
MDH1
AOC3
ALDH5A1
aldehyde dehydrogenase (NAD) activity
NRXN1
IDH2
SLC6A13
APOD
FAM49A
EPB42
DKK3
PCDH1
SIRPA
BCAM
SLC13A3
ACO2
CHL1
NCAN
SCRN1
ATP1A2
ATP1B2
OMG
APLP1
CYFIP2
NCKAP1
COL18A1
COL14A1
TAGLN
SUSD2
ALDOC
SEPT5
SEPT3
GDA
PNP
cortical cytoskeleton
PMP2
SLC2A1
PRDX2
CARKD
NFASC
CNTN1
CNN1
SPTA1
NCAM2
PTN
COCH
NRCAM
ACTN4
OXR1
CRP
SPTB
LY6H
NAPG
NTM
ACTN2
ACTN1
RGN
GDI1
cell adhesion
SORBS2
TPM1
MUC19
SLC4A1
CACNA2D1
MYLK
TLN1
VCL
APLP2
CHGA
MYH11
HSPA2
MCAM
LANCL2
ACTA2
DDAH1
NDRG2
TBC1D24
RAP1A
TPPP3
PYGM
RNASE1
PCDH9
CNTNAP2
CES1
PRRT2
GNB1
G-protein coupled receptor signalling
GNAI1
SLC3A2
GNG2
PLCB1
PPP3CB
calcineurin complex
PPP3CA
AP2M1
PACSIN1
AP2B1

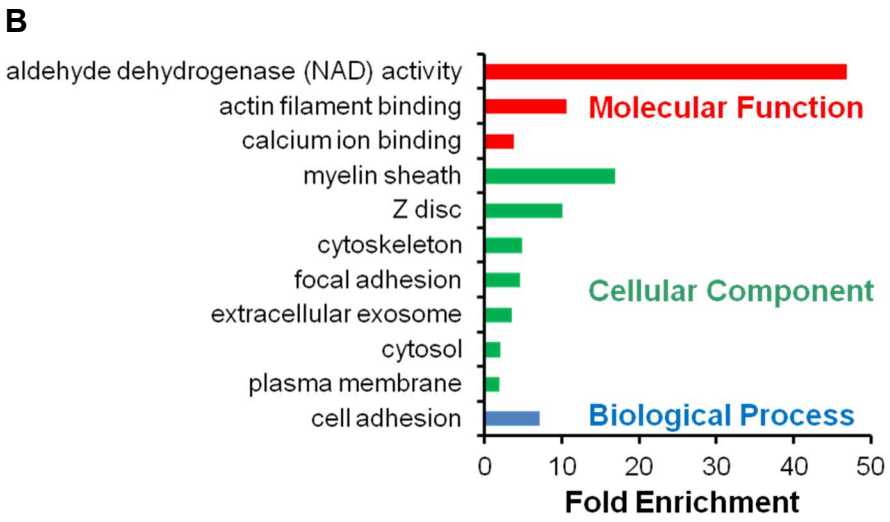

Figure 3.5 Functional annotation of proteins significantly downregulated and common to all meningioma grade *vs.* NMT. (**A**) Protein-protein interaction network of proteins commonly downregulated in all meningioma grades. Highlighted are clusters of proteins with known interactions each associated to a biological function. Network derived from the STRING database version 10.5 and analysed with the kmeans clustering method. Proteins are represented by network nodes. Protein-protein associations are shown by connecting lines and are derived from curated databases and/or experimentally determined. (**B**) Gene ontology (GO) enrichment analysis of 94 proteins commonly downregulated in all meningioma grades by the web tool DAVID version 6.8. Terms containing at least three proteins with Benjamini-Hochberg adjusted $p< 0.05$ are shown. Gene Ontologies representing 'Molecular Function' are presented in red, 'Cellular Component' in green and 'Biological Process' in blue. Fold enrichment relative to the *H. sapiens* proteome is displayed at the *x*-axis. Full details of GO analysis output are detailed in Supplementary Table S5A.

3.4.6 Grade-specific comparative proteomic analysis of meningiomas

In addition to establishing proteomic signatures common to all meningioma it is also of interest to investigate altered protein expression between WHO grades in order to identify grade-specific proteins that may act as potential biomarkers or therapeutic targets. We decided to concentrate our analysis on describing the differential expression of proteins specific to high-grade meningiomas. These aggressive tumours are often more therapeutically challenging with a higher rate of recurrence than slower growing grade I meningiomas.

To obtain an overview of the differentially expressed proteins between grades, we assessed significant quantitative differences in large datasets composed of replicate data from each meningioma grade by Student's *t*-tests and visualised differentially expressed proteins in Volcano plots (Fig. 3.6; Supplementary Table S6A). We identified 260 proteins to be significantly differentially expressed between grade II *vs*. grade I (Fig. 3.6A), 424 proteins between grade III *vs*. grade I (Fig. 3.6B) and 243 proteins between grade III *vs*. grade II (Fig. 3.6C).

Proteins significantly upregulated in grade II meningiomas *vs*. grade I included the DNA damage response protein MRE11 (double-strand break repair protein MRE11), the topoisomerase TOP1 that functions to remove DNA supercoils during transcription and DNA replication and NCBP1 (nuclear cap-binding protein subunit 1), a component of the cap-binding complex that binds the 5'-cap of pre-mRNAs and plays a role in RNA biogenesis (Fig. 3.6A). Among those proteins that were significantly downregulated in grade II meningiomas compared to grade I were the tumour suppressor BIN1 (Myc box-dependent-interacting protein 1) (Wechsler-Reya, Elliott & Prendergast, 1998) and the protein kinase PRKCG (protein kinase C gamma type), also known to possess tumour suppressive activity (Dashzeveg, Yogosawa & Yoshida, 2016) (Fig. 3.6A).

Following comparisons of grade III meningioma with grade I and II, we identified several proteins involved in energy production including the glycolytic enzyme HK2 (hexokinase-2) and the mitochondrial related proteins HSPE1 (10 kDa heat shock protein, mitochondrial) and IDH3B (isocitrate dehydrogenase [NAD] subunit beta, mitochondrial) as significantly upregulated in grade III (Fig. 3.6B and 3.6C). Proteins found to be significantly upregulated in the grade III *vs*. grade II comparison alone included the serine proteases SERPINE1 (plasminogen activator inhibitor 1; also PAI1) and SERPINE2 (glia-derived nexin; also GDN) both known to play a role in tumour progression (Andreasen, 2007; Wu, 2016). Similarly to upregulated proteins, we found some proteins to be significantly downregulated in both the grade III meningiomas *vs*. grade I and the grade III *vs*. grade II comparisons (Fig. 3.6B and 3.6C). Among these were the cell adhesion protein CDH11 (cadherin-11) that functions as a tumour suppressor, inhibiting the proliferation and invasion of head and neck cancer (Piao *et al.*, 2017) and CAST (calpastatin), a negative regulator of the intracellular cysteine protease calpain, which upon loss of CAST expression has been shown to demonstrate enhanced tumour-promoting activity in acute myelogenous leukaemia cells (Niapour *et al.*, 2012).

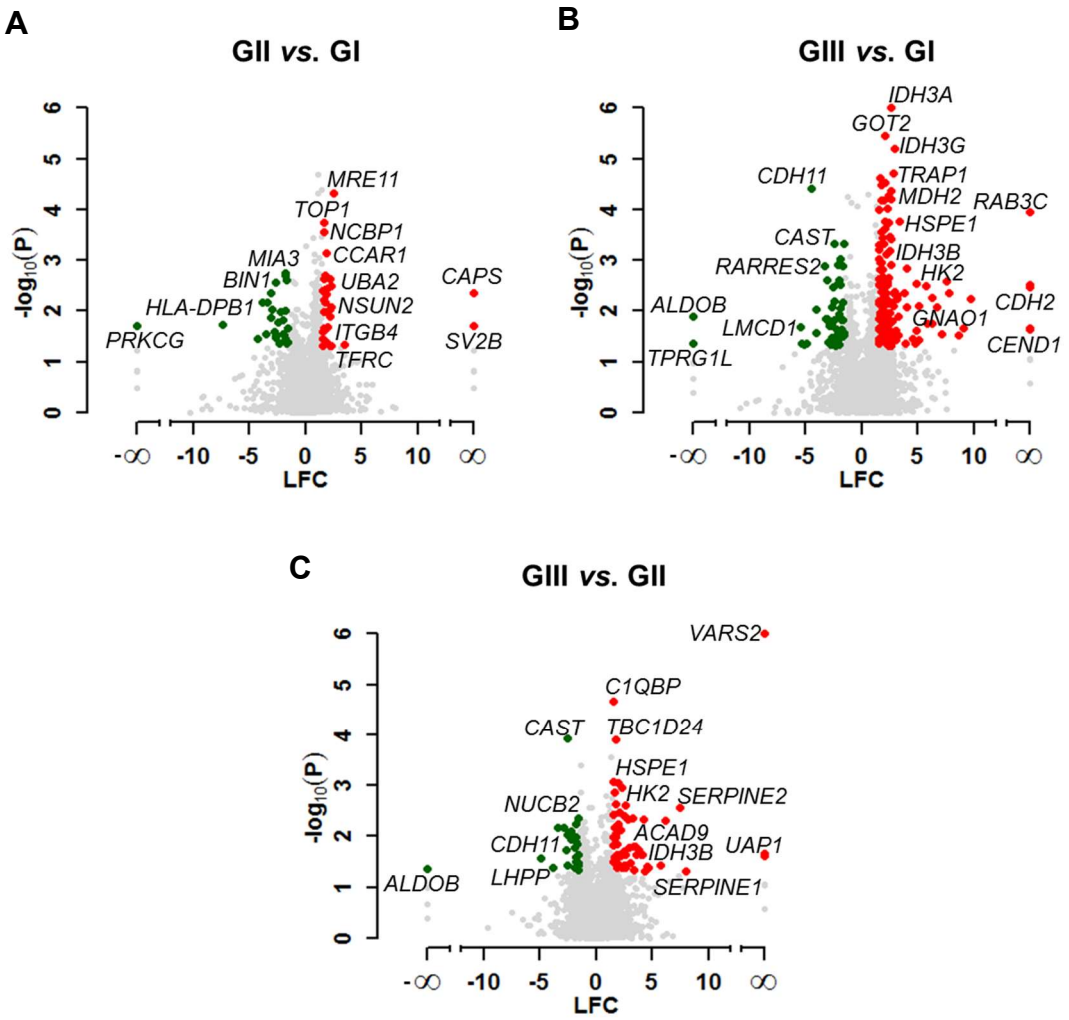

Figure 3.6 Differential protein expression between meningioma grades. Fold changes in protein abundance between different grades of meningiomas is depicted in Volcano plots. Differential expression of proteins is shown: (**A**) grade II *vs*. grade I; (**B**) grade III *vs*. grade I and (**C**) grade III *vs*. grade II. Depicted in the plots are the comparisons of $\log_2$ fold changes (LFC) versus *p*-values (Student's *t*-test between replicate measurements). Red dots: Upregulated proteins ($\log_2$ FC≥ 1.5; *p*-value< 0.05). Green dots: Downregulated proteins ($\log_2$ FC≤ 1.5; *p*-value< 0.05). Grey dots: Proteins that did not meet these criteria. Proteins specific to one of the two groups compared were assigned a fold change of infinity. See also Supplementary Table S6A for full analysis.

To further characterise the proteomic landscape of aggressive meningiomas we extracted individual molecular signatures for grade II and grade III meningiomas using the computational tool BubbleGUM (Spinelli *et al.*, 2015). This tool enabled us to determine increased protein expression specific to a sample group by comparison with one or more other sample groups. In contrast to the Volcano plots described previously, we were able to incorporate the protein expression profile of normal meninges into this comparative analysis. Consequently, this enabled the generation of molecular signatures that would provide us with improved possibilities to identify grade-specific biomarkers or molecular therapeutic targets. Increased expression of a protein by a sample group was determined by a FC≥ 2 selected in BubbleGUM. At this time, we did not extract molecular signatures representing loss of protein expression as we wanted to focus on identifying abundant proteins that could act as biomarkers or molecular targets of meningioma, as previously discussed.

The molecular signature of grade II meningiomas was generated by comparison of the proteomic profile of grade II tumours with those of grade I and NMT, and a grade III signature by comparison with grade II, grade I and NMT. We identified a grade II molecular signature of 191 proteins and a grade III molecular signature of 192 proteins with FC> 2. Hierarchical clustering of extracted signatures showed clustering of samples into their respective grades, again with the exception of the grade III sample, J9, seen to reside between grade I and II tumours (Fig. 3.7). Grade II and III signatures could be clearly visualised by differences in relative expression between the sample groups, generating expression profiles that reflect the ability to distinguish between high and low-grade meningiomas. Among the grade II signature were proteins that overlapped with those identified in the Volcano plot of Figure 3.6A, such as MRE11 and NSUN2 (tRNA (cytosine(34)-C(5))-methyltransferase), as well as additional proteins specifically increased in grade II meningiomas including MUC4 (mucin-4) and the minichromosome

maintenance protein, MCM6 (Fig. 3.7). Similarly, we identified proteins in the grade III meningioma signature that overlapped with those seen in the Volcano plots, such as SERPINE1 and HK2 in addition to other proteins such as the mitochondrial related protein, SUCLG2 (succinate--CoA ligase [GDP-forming] subunit beta, mitochondrial) (Fig.3.6B and 3.6C; Fig. 3.7). Complete protein lists generated by BubbleGUM analyses are shown in Supplementary Tables S7A and S7B.

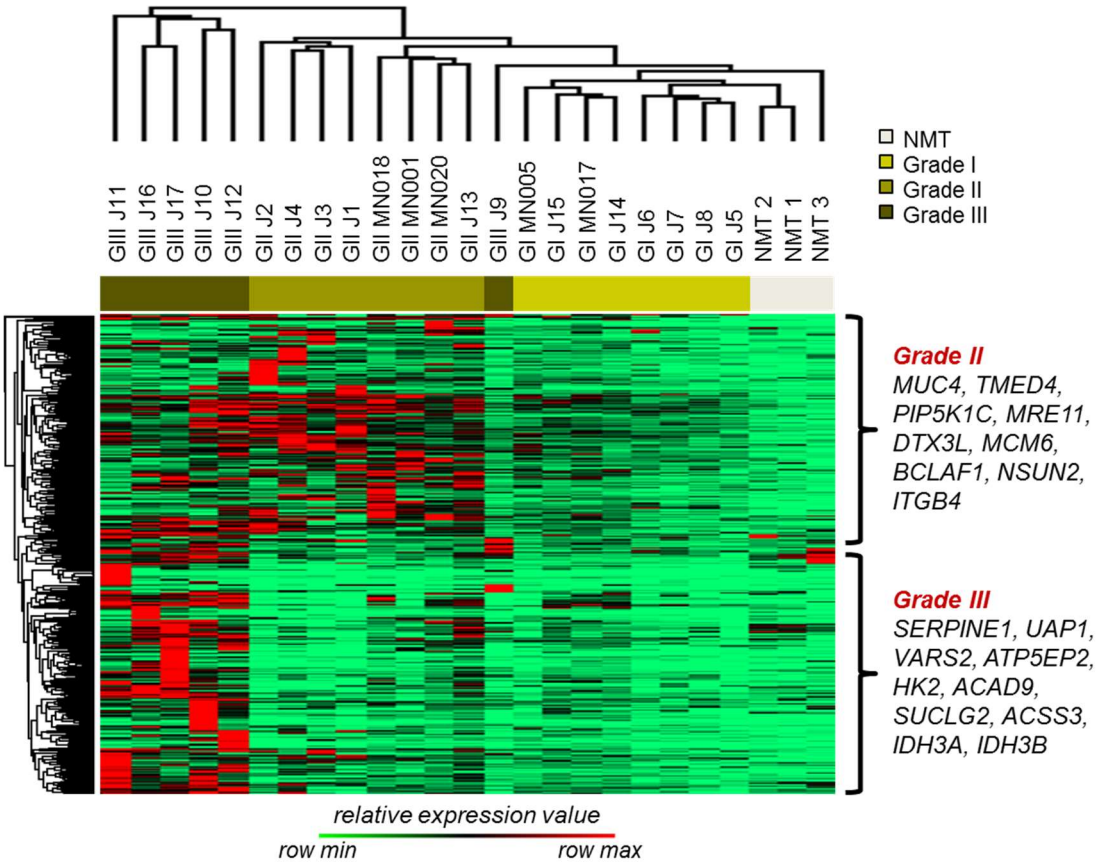

Figure 3.7 Global proteome signatures of grade II and III meningiomas. Individual protein signatures of grade II and III meningiomas were generated by the computational tool BubbleGUM and are visualised in a heatmap (Spinelli *et al.*, 2015). The GeneSign module was used to generate a grade II signature by comparison with grade I and NMT, and a grade III signature by comparison with grade II, grade I and NMT. A grade II molecular signature of 191 proteins and a grade III signature of 192 proteins with FC> 2 were identified. Hierarchical clustering of extracted signatures based on relative expression values is shown. A collection of proteins found within each signature is presented. Clustering was created using Perseus 1.5.0.31 software suite. Supplementary Tables S7A and S7B provide details of BubbleGUM output for molecular signatures.

3.4.7 Gene ontology analysis of grade II and III protein molecular signatures

GO enrichment analysis was performed to functionally annotate proteins identified by the grade II and III molecular signatures. All significantly enriched GO terms are displayed for both signatures (Fig. 3.8A and 3.8B; Supplementary Tables S7C and 7D). Grade II proteins showed the greatest fold enrichments in RNA helicase activity (27-fold) in the 'Molecular Function' class, whilst the 'Cellular Component' with the strongest enrichment of grade II proteins was the podosome (16-fold) and in the 'Biological Process' class mRNA splicing via spliceosome produced the highest enrichment (6-fold) (Fig. 3.8A). Other enriched terms included three terms related to cell-cell adhesion, with one GO term per class (Fig. 3.8A).

Analysis of the grade III molecular signature returned 28 significantly enriched GO terms. The majority of terms identified under the three categories were related to energy production and mitochondria, reflecting the increased metabolic requirements of these malignant tumours (Fig 3.8B). These terms included acyl-CoA dehydrogenase activity (23-fold) and tricarboxylic acid cycle (25-fold) with the highest fold enrichments under the 'Molecular Function' and 'Biological Process' classes, respectively (Fig 3.8B). Remaining enriched GO terms included those associated with splicing, such as precatalytic spliceosome (19-fold), the most enriched term under 'Cellular Component', and similarly to the grade II molecular signature analysis, mRNA splicing via spliceosome (5-fold) (Fig 3.8B).

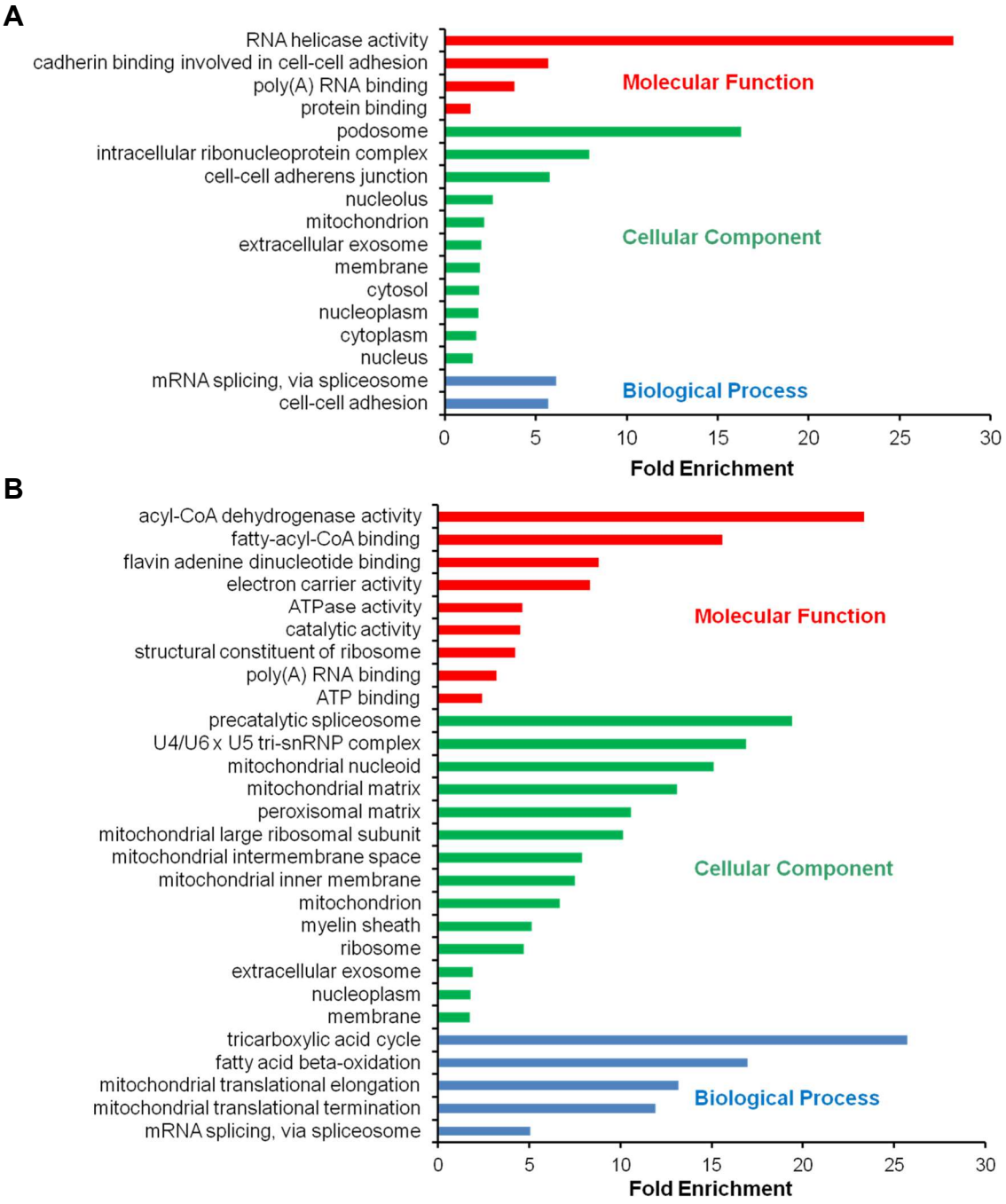

Figure 3.8 GO enrichment analysis of grade II and grade III meningioma molecular signatures. Histogram displays all significantly enriched GO terms returned by the web tool DAVID version 6.8 following submission of 191grade II protein signature (**A**) and 192 grade III protein signature (**B**). Terms containing at least three proteins with Benjamini-Hochberg adjusted $p< 0.05$ are shown. Gene Ontologies representing 'Molecular Function' are presented in red, 'Cellular Component' in green and 'Biological Process' in blue. Fold enrichment relative to the *H. sapiens* proteome is displayed at the *x*-axis. Full details of GO analyses output are detailed in Supplementary Tables S7C and S7D.

3.5 Discussion

To investigate the proteomic profile of meningioma we analysed the global proteome of 22 meningiomas across all WHO grades and three healthy normal meninges. From MS we identified nearly 4000 proteins among all the samples and focussed firstly on establishing proteins that were commonly and significantly upregulated in each grade compared to NMT. This approach gave us 181 upregulated proteins common to all meningioma grades. Functional annotation analyses revealed many of these proteins to be associated with transcription and post-transcriptional modifications, in particular splicing.

The pathological alteration of alternative splicing patterns is now widely recognised in cancer, highlighting the possibility that targeting it in cancer might hold therapeutic value. Splice site sequence mutations often lead to proto-oncogene activation, whilst dysregulated expression and somatic mutations of splicing factors alters splice site preference in favour of an oncogenic splicing program (Lee & Abdel-Wahab, 2016). Specifically, we identified several components of the spliceosome as upregulated in meningioma including SNRPD3, SNRPF, SNRPE, SF3B2, SF3B5 as well as the splicing factors SRSF3, SRSF7 and SF2/ASF. Various compounds used to inhibit components of the spliceosome have shown anti-tumour activity including reduction of cell proliferation, demonstrating their therapeutic benefit in cancer (Kotake *et al.*, 2007). In meningioma, tumour-specific alternative splicing of the tumour suppressor gene *CHEK2* (*serine/threonine-protein kinase Chk2*) has been shown to reduce function of the proteins involved in DNA repair, thus resulting in genomic instability and tumour progression (Yang *et al.*, 2012). Further characterisation of dysregulated splicing and its role in meningioma pathogenesis could help to elucidate the potential of this biological process as a therapeutic target.

We also conducted bioinformatic analyses of 94 proteins identified as commonly and significantly downregulated in each grade compared to NMT. Functional annotation showed these proteins to be related to biological functions including aldehyde dehydrogenase (NAD) activity and the phosphatase complex of calcineurin. Interestingly, the calcineurin complex is a calcium-dependent protein serine/threonine phosphatase complex that has been shown to act in a tumour suppressive or tumour promoting manner depending on cancer type. Upon elevated levels of intracellular calcium, calcineurin is activated and dephosphorylates target proteins including NFAT (nuclear factor of activated T cells) transcription factors that upregulate expression of targets genes including cytokines (Quang *et al.*, 2015). Studies have identified calcineurin activation to play a protective role against squamous cell carcinoma by promoting mechanisms of cell senescence; whilst in breast cancer, its activation has been shown to enhance tumour progression and metastatic potential (Quang *et al.*, 2015; Wu *et al.*, 2010). We thus propose that additional investigation into the downregulation of this complex in meningioma could enhance our knowledge of a possible tumour suppressor role in these tumours.

By performing grade-specific comparative analysis we were able to define proteomic signatures indicative of high-grade meningiomas. In particular, we wanted to identify proteins with increased expression specific to grade II and III meningioma, as these tumours frequently pose the most challenging to treat. We generated Volcano plots displaying differential protein expression of grade-wise comparisons as well as molecular signatures of proteins with increased abundance specific to either grade II or III meningioma.

Proteins established as upregulated in grade II meningioma included the transmembrane mucin, MUC4, shown in many cancers to be differentially expressed

(Singh, Chaturvedi & Batra, 2007). MUC4 overexpression has been previously found to enhance the proliferation and invasive potential of GBM cells by upregulating EGFR expression (Li *et al.*, 2014b); indeed, silencing EGFR in pancreatic cancer cells decreased MUC4 expression by reducing the phosphorylation of STAT1 (signal transducer and activator of transcription 1-alpha/beta) (Seshacharyulu *et al.*, 2015). Interestingly, EGFR was identified as commonly overexpressed among all meningioma grades in our global proteome analysis, whilst phosphorylation of STAT1 was shown in previous work by our group as a common target in *NF2*-negative schwannomas and meningioma BM1 cells (Bassiri *et al.*, 2017). We conclude these findings warrant future investigation to determine potential interaction between MUC4, EGFR and phosphorylated STAT1 in grade II meningioma with the possibility of a grade-specific combinatorial therapeutic approach.

Among the grade III-specific molecular signature the serine protease inhibitor SERPINE1 was found to be the most abundant protein. SERPINE1 is often overexpressed in cancers known to play a role in EMT facilitating tumour cell invasion and angiogenesis (Andreasen, 2007; Bajou *et al.*, 1998). In agreement with our data, elevated SERPINE1 expression has previously been linked to the malignant progression, brain invasion and recurrence of meningiomas, demonstrating its potential value as a prognostic marker in these aggressive tumours (Kandenwein *et al.*, 2011).

Finally, functional annotation of proteins comprising high-grade molecular signatures revealed both grade II and III associated proteins to be enriched in terms related to splicing, once again highlighting that this biological process may play a fundamental role in meningioma pathogenesis. Grade II proteins also showed enrichment in the ‘Cellular Component’ GO term of podosome, a functional structure that protrudes from the outer plasma membrane and promotes degradation of the extracellular matrix (Flynn *et al.*,

2008). Podosomes have been suggested to be the precursor to invadopodia, protrusions of similar structure associated with matrix degradation and directional movement of cancer cells, thus playing a role in tumour invasion and metastasis (Flynn *et al.*, 2008; Paz, Pathak & Yang, 2014). We could therefore speculate that grade II-specific proteins may contribute to tumour progression by the formation of invadopodia. Indeed, inhibition of invadopodia has gained recognition in recent years as a plausible therapeutic target in cancer metastasis (Stoletov & Lewis, 2015).

Grade III-specific proteins demonstrated a clear enrichment in processes related to metabolism and energy production reflecting the abundance of mitochondrial associated proteins that were identified in these more aggressive tumours. Although many of these mitochondrial proteins function in the tricarboxylic acid cycle such as IDH3A (isocitrate dehydrogenase [NAD] subunit alpha, mitochondrial) and IDH3B, the alpha and beta subunits of the isocitrate dehydrogenase IDH3; we also identified HK2 that has a key role in aerobic glycolysis and therefore the "Warburg effect" commonly associated with invasive and metastasising cancers. Taken together, these findings reflect the energy requirements expected of rapidly growing, malignant grade III meningioma. Further studies may indicate the plausibility of inhibiting energy production pathways as a treatment strategy in this malignant phenotype.

Overall, in this chapter we have been able to identify proteins and biological processes in meningioma that with additional investigation could lead to potential biomarkers or candidates for the targeted treatment of these tumours. We will select some of the proteins highlighted in these analyses for experimental validation studies, the results of which are presented later in this project.

4 Phosphoproteome analysis of meningioma

4.1 Introduction

The reversible phosphorylation of proteins is one of the most frequent and important PTMs. Protein phosphorylation is responsible for the regulation of many cellular processes. Aberrant phosphorylation results in altered protein activity and the dysregulation of signalling pathways often associated with diseases including cancer. Quantitative analysis of the phosphoproteome permits the investigation of alterations in protein phosphorylation and related pathways in diseased and healthy states enabling the detection of potential therapeutic targets, druggable pathways or biomarkers (Harsha & Pandey, 2010).

The majority of previous studies have focussed on characterising the global proteome in meningioma without exploring alterations in PTMs, thus overlooking the potential role of PTMs, such as protein phosphorylation, in the pathogenesis of these tumours. Prior to the start of this work, there were no published works detailing phosphoproteome analyses of meningioma tissue by MS-based techniques. This project was designed to expand upon previous analysis by our research group describing the global proteome and phosphoprotein landscape of grade I *NF2*-deficient meningioma cells, work that has since been published (Bassiri *et al.*, 2017). More recently, Parada *et al*. (2018) completed analysis also from meningioma tissue of all WHO grades by MS following phosphopeptide enrichment and combined these findings with a kinase peptide array to establish prognostic biomarkers (Parada *et al.*, 2018). However, the authors concentrated on grade-wise comparisons only and were not able to identify commonly upregulated phosphoproteins among all meningioma grades compared to healthy meninges.

In comparison to these studies, the research in this chapter aims to expand further upon the phosphoprotein environment of meningioma in two respects. Firstly, by conducting

analysis from tissue we aim to preserve tumour microenvironment signalling, and secondly, by analysing healthy human meninges as well as meningioma tissue we intend to identify possible tumour-specific therapeutic targets or biomarkers.

Here, we present a phosphoproteomic analysis of meningiomas detailing phosphoprotein expression profiles and differentially expressed phosphoproteins that may pose potential therapeutic targets. We have focussed mainly on the identification and analysis of significantly upregulated rather than downregulated phosphoproteins in meningiomas compared to healthy meninges. We undertook this approach in order to elucidate dysregulated phosphorylation in meningioma with the potential for pharmaceutical intervention, targeting either phosphorylation sites themselves or upstream kinase activity. However, the role of aberrant protein dephosphorylation in meningioma pathogenesis should not be overlooked. For this reason future studies of our research group will expand upon the implications of downregulated phosphoproteins in meningioma.

In addition to phosphoprotein analysis, this chapter will describe the phosphopeptide analysis of eight meningiomas covering all grades, providing an overview of protein phosphorylation sites detected in these tumours. This dataset acts as a complementary analysis to the phosphoprotein dataset for the identification of possible phosphorylation sites associated with differentially expressed phosphoproteins.

4.2 Analysis of phosphoproteins in meningioma

4.2.1 Phosphoprotein identification and quantification

In total, we sequenced and identified 3162 phosphoproteins across 17 samples; three normal meninges and 14 meningiomas. Phosphoproteins were identified by at least two 'razor and unique' peptides with an FDR of 1% using LC-MS/MS LFQ proteomics (Supplementary Table S2B). Figure 4.1 depicts the distribution of the 3162 identified phosphoproteins amongst the sample groups of NMT, grade I, II and III. We identified 2793 phosphoproteins within normal meninges (*n*=3), whilst in meningioma tissue we identified 2965 phosphoproteins across grade I (*n*=5), 2934 across grade II (*n*=5) and 2868 across grade III (*n*=4). Phosphoproteins identified in at least 3 runs (3074 out of 3162) were then subjected to label-free quantitative analysis and analysed further for significant differential expression (Supplementary Table S3B).

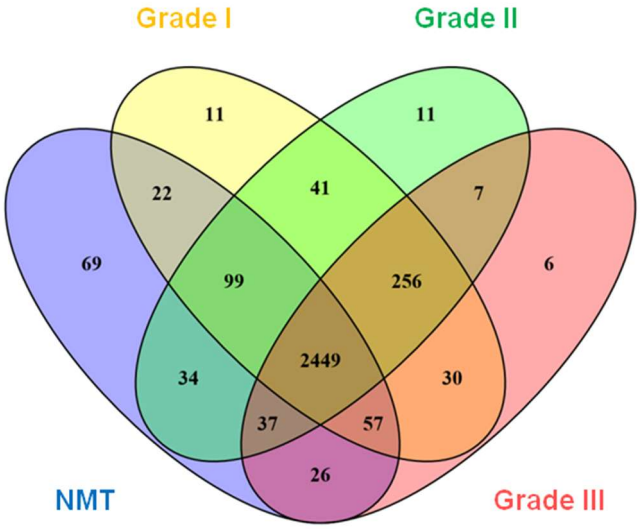

Figure 4.1 Venn diagram depicting the distribution of 3162 phosphoproteins identified across three NMT and 22 meningiomas (grade I *n*=5; grade II *n*=5 and grade III *n*=4) by LC-MS/MS LFQ proteomics. Proteins were identified by at least two 'razor and unique' peptides with an FDR of 1% and are detailed in Supplementary Table S2B. Venn diagrams created using Venny 2.1.

4.2.2 Hierarchical clustering of differentially expressed phosphoproteins

In order to obtain an overview of differentially expressed phosphoproteins we generated a heat map as previously created for the global proteome dataset. This allowed us to visualise clusters of phosphoproteins that showed differential expression between samples. Again as for global proteome data, we transformed LFQ values for each of the 3074 quantified phosphoproteins into relative expression values between 0 and 1. Following this, we performed a one-way ANOVA that enabled us to submit differentially expressed phosphoproteins (p-value< 0.05) to Perseus software and extract a heatmap with associated hierarchical clustering of samples (Fig. 4.2A). Hierarchical clustering revealed if samples clustered into their respective sample groups (NMT, grade I, II or III meningioma) based on their differential phosphoprotein expression profiles.

Hierarchical clustering of differentially expressed phosphoproteins showed a marked separation of tumours *vs.* NMT (Fig. 4.2A). Moreover, meningiomas were seen to cluster into their respective WHO grade (Fig. 4.2A). We identified three main clusters of phosphoproteins that displayed higher expression in at least one grade compared to NMT. Among phosphoproteins present in the largest cluster were AKT1 and 2, NEK7 (serine/threonine-protein kinase Nek7), NEK9 (serine/threonine-protein kinase Nek9; also Nercc1), PDGFRB, NFKB1 (nuclear factor NF-kappa-B p105 subunit), MAPK2 (mitogen-Activated Protein Kinase 2), mTOR and members of the DOCK (dedicator of cytokinesis)-family of guanine nucleotide exchange factors (GEFs) (Fig. 4.2A). One phosphoprotein cluster that was found to reveal grade III-specific increased expression contained the serine/threonine protein kinase ATR (serine/threonine-protein kinase ATR), the minichromosome maintenance proteins MCM3 and MCM6, and the DEAD-box RNA helicases DDX10 (probable ATP-dependent RNA helicase DDX10) and DDX24 (ATP-dependent RNA helicase DDX24) (Fig. 4.2A). Another cluster showed

phosphoproteins with generally lower expression across all meningioma grades compared to NMT. Present in this cluster were proteins also found to be differentially downregulated in the global proteome dataset across all meningiomas such as DKK3 and CDH13 (cadherin-13) (Fig. 3.3A and 4.2A). Other phosphoproteins located within this cluster included the mitotic checkpoint protein BUB3 (mitotic checkpoint protein BUB3) as well as HEPACAM (hepatocyte cell adhesion molecule), involved in the control of cell adhesion and cell growth and also found to be downregulated in bladder cancer (He *et al.*, 2010).

4.2.3 Commonly upregulated phosphoproteins amongst all meningioma grades

Next, we focussed on identifying phosphoproteins upregulated in each meningioma grade compared to control, enabling us to identify phosphoproteins that were overexpressed unique to a grade or commonly overexpressed among grades. We used the same criteria as for global proteome analysis to describe a phosphoprotein as up or downregulated. Phosphoproteins with a $\log_2$ FC$\geq$ 1.5 were designated upregulated and those with a $\log_2$ FC$\leq$ -1.5 designated downregulated. Significant quantitative differences between sample groups were assessed by Student's *t*-tests using the Perseus software and significance was set at *p*-value$<$ 0.05.

Similarly to global proteome analysis, we looked to identify a subset of phosphoproteins that were commonly and significantly upregulated in all meningioma grades. We overlapped significantly upregulated phosphoproteins of each grade compared to control and identified 338 phosphoproteins to be commonly and significantly upregulated among all grades *vs.* NMT as depicted by the Venn diagram in Figure 4.2B. By initially concentrating on commonly upregulated phosphoproteins we were able to obtain an overview of global dysregulation of protein phosphorylation occurring in meningioma irrespective of WHO grade. Table 4.1 presents the top 50

commonly and significantly upregulated phosphoproteins. The full quantified phosphoprotein dataset detailing fold changes and significance can be found in Supplementary Table S3B.

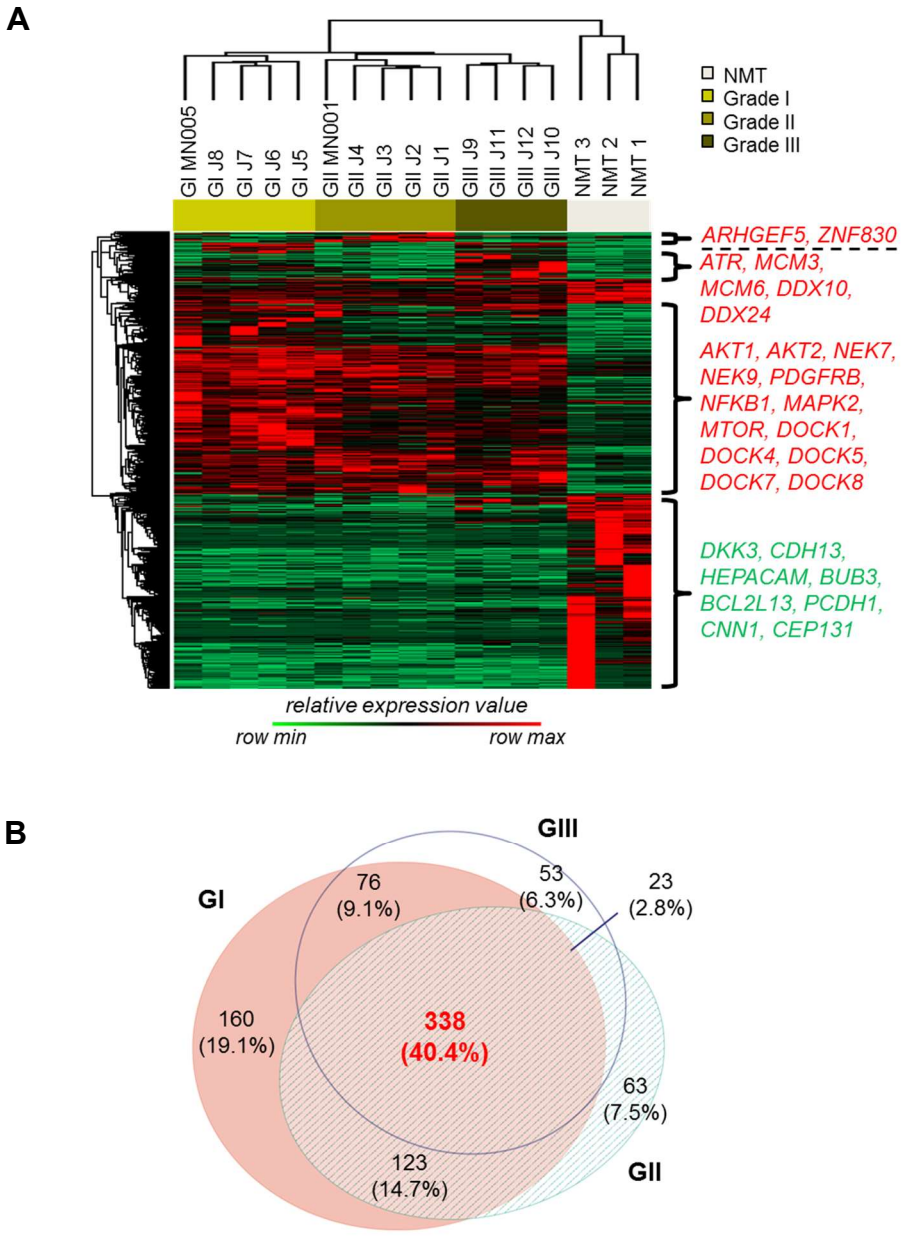

Figure 4.2 Comparative proteomic analysis of the meningioma phosphoproteome. (**A**) Unsupervised hierarchical clustering of 1296 differentially expressed phosphoproteins based on relative expression values (meningiomas *n*=14; NMT *n*=3). Meningiomas clustered separately from NMT in their phosphoprotein profiles and into their respective WHO grades. Three phosphoprotein clusters showing higher relative expression in at least one or more meningioma grade compared to NMT are annotated in red. A cluster of proteins showing lower relative expression across meningioma grades compared to NMT are annotated in green. Clustering was generated using Perseus 1.5.0.31 software suite, based on four-group one-way ANOVA, *p*-value< 0.05, corrected for multiple testing. (**B**) Venn diagram depicting unique and commonly upregulated phosphoproteins among different meningioma grades *vs*. NMT.

Protein name	Gene	Log_2 FC (GI *vs.* NMT)	Log_2 FC (GII *vs.* NMT)	Log_2 FC (GIII *vs.* NMT)
Protein phosphatase Slingshot homolog 3	SSH3	∞	∞	∞
Isoform 2 of Band 4.1-like protein 1	E41L1	∞	∞	∞
Carboxypeptidase D	CBPD	∞	∞	∞
Paladin	PALD	∞	∞	∞
Isoform 2 of AP2-associated protein kinase 1	AAK1	∞	∞	∞
Zinc finger CCCH-type antiviral protein 1	ZCCHV	∞	∞	∞
Isoform 10 of Partitioning defective 3 homolog	PARD3	∞	∞	∞
Fragile X mental retardation syndrome-related protein 1	FXR1	∞	∞	∞
Polynucleotide 5-hydroxyl-kinase NOL9	NOL9	∞	∞	∞
DEP domain-containing mTOR-interacting protein	DPTOR	∞	∞	∞
45 kDa calcium-binding protein	CAB45	∞	∞	∞
Phostensin	PPP1R18	∞	∞	∞
Acetyl-coenzyme A synthetase, cytoplasmic	ACSA	∞	∞	∞

HLA class II histocompatibility antigen, DR alpha chain	HLA-DRA	∞	∞	∞
Isoform 2 of Serine/threonine-protein kinase N2	PKN2	∞	∞	∞
Serine/threonine-protein kinase 4	STK4	∞	∞	∞
Isoform 2 of Protein-tyrosine kinase 2-beta	FAK2	∞	∞	∞
Pre-mRNA-splicing factor ATP-dependent RNA helicase PRP16	PRP16	∞	∞	∞
Rho guanine nucleotide exchange factor 10 (Fragment)	H0YAN8	∞	∞	∞
Serine/threonine-protein kinase Nek7	NEK7	∞	∞	∞
Serine/threonine-protein phosphatase 4 catalytic subunit	PP4C	∞	∞	∞
Protein THEMIS2	THMS2	∞	∞	∞
FERM, RhoGEF and pleckstrin domain-containing protein 2	FARP2	∞	∞	∞
Peptidyl-prolyl cis-trans isomerase-like 4	PPIL4	∞	∞	∞
Serine/threonine-protein kinase MRCK beta	MRCKB	∞	∞	∞
Tripartite motif-containing protein 26	TRI26	∞	∞	∞

Phosphatidylinositol 4-phosphate 3-kinase C2 domain-containing subunit alpha	P3C2A	∞	∞	∞
GABARAP-a	GABARAP	∞	∞	∞
RAC-beta serine/threonine-protein kinase	AKT2	∞	∞	∞
Isoform 3 of Ribosomal protein S6 kinase beta-1	KS6B1	∞	∞	∞
Signal recognition particle receptor subunit alpha	SRPR	∞	∞	∞
Isoform 4 of Ubiquitin-associated protein 2-like	UBP2L	∞	∞	∞
Translational activator GCN1	GCN1L	∞	∞	∞
Isoform 4 of Pyridoxal-dependent decarboxylase domain-containing protein 1	PDXD1	∞	∞	∞
Rhotekin	RTKN	∞	∞	∞
DBIRD complex subunit ZNF326	ZN326	∞	∞	∞
Rab3 GTPase-activating protein non-catalytic subunit	RBGPR	∞	∞	∞
Ras GTPase-activating protein 3	RASA3	∞	∞	∞
Serine-protein kinase ATM	ATM	∞	∞	∞
Protein pelota homolog	PELO	∞	∞	∞
Isoform 2 of Sickle tail protein homolog	SKT	∞	∞	∞

ARF GTPase-activating protein GIT2	GIT2	∞	∞	∞
Chromatin complexes subunit BAP18	C17orf49	∞	∞	∞
Leucine-rich repeat and WD repeat-containing protein 1	LRWD1	∞	∞	∞
Isoform 4 of Inactive tyrosine-protein kinase 7	PTK7	∞	∞	∞
HEAT repeat-containing protein 6	HEAT6	∞	∞	∞
Coatomer subunit zeta-1	COPZ1	∞	∞	∞
Isoform 3 of NF-kappa-B inhibitor-interacting Ras-like protein 2	KBRS2	∞	∞	∞
Pleckstrin homology-like domain family B member 2 (Fragment)	PHLDB2	∞	∞	∞
Nuclear factor NF-kappa-B p105 subunit	NFKB1	∞	∞	∞

Table 4.1 Top 50 of the most commonly and significantly upregulated phosphoproteins among all WHO grades of meningiomas compared to normal meningeal tissue. Corresponding $\log_2$ FCs for each meningioma grade compared to NMT are shown. Significant upregulation defined by $\log_2$ fold-change≥1.5; *p*-value<0.05. Phosphoproteins specific to one of the two groups compared were assigned a fold change of infinity. Full details of the 338 phosphoproteins commonly and significantly upregulated can be found in Supplementary Table S3B.

4.2.4 Functional annotation of commonly upregulated phosphoproteins

We performed functional annotation analysis using the bioinformatic resources DAVID and IPA to establish biological processes, molecular functions and signalling pathways associated with commonly upregulated phosphoproteins. We compared significantly enriched terms of phosphoproteins with corresponding fold enrichments of proteins to identify GO terms predominantly targeted by phosphorylation. Some of the most enriched GO terms are depicted as a histogram plot with bars representing fold enrichments (Fig. 4.3A; Supplementary Table S4D).

Following this comparison, we were able to identify several phosphoprotein-specific enriched GO terms including PIP_3 (phosphatidylinositol-3,4,5-trisphosphate) binding (8-fold), EGFR (6-fold) and VEGFR (6-fold) signalling pathways, and the most enriched phosphoprotein term in the 'Biological Process' class, signal complex assembly (33-fold) (Fig. 4.3A). GO terms with the strongest enrichment from upregulated phosphoproteins in the classes of 'Molecular Function' and 'Cellular Component' were RNA helicase activity (23-fold) and COPI vesicle coat (51-fold), respectively (Fig. 4.3A). However, these particular terms were also found to show even higher enrichment from commonly upregulated proteins (Fig. 4.3A).

To obtain a global view of the biological functions associated with significantly commonly upregulated phosphoproteins, enriched GO terms were then visualised in an 'enrichment map' as performed previously for commonly upregulated proteins (Fig. 4.3B; Supplementary Table S4E). The map displayed five clusters of GO terms representing biological functions including signal transduction, transport vesicle, transcription/pre-mRNA processing, cell adhesion and Rho GTPase activity, suggesting the regulation of these functions by aberrant protein phosphorylation in meningiomas.

Finally, we annotated the 338 commonly upregulated phosphoproteins to elucidate associated signalling pathways. Further, by comparing these pathways with those related to the 181 commonly upregulated proteins we would be able to define pathways that may be regulated by protein phosphorylation. We used IPA to identify canonical pathways significantly associated with upregulated proteins and phosphoproteins. IPA revealed 22 and 198 pathways associated with proteins and phosphoproteins, respectively (Supplementary Tables S4F and S4G provide details of all identified pathways). Pathways containing ≥2 proteins or phosphoproteins were grouped under broader functional pathway classes according to Ingenuity Canonical Pathways and pathway counts for each class displayed in a bar chart (Fig. 4.3C).

Classes associated with upregulated proteins included 'cellular immune response', 'cellular stress and injury' and 'intracellular and second messenger signaling', with no more than four pathways identified in a class at any time (Fig. 4.3C). Upregulated phosphoproteins were most frequently associated with pathways related to 'cellular growth, proliferation and development', 'cellular immune response', 'disease-specific pathways' and 'cancer'; within these groups we identified the integrin, EIF2 (eukaryotic initiation factor 2), FAK, ERK (extracellular signal–regulated kinase)/MAPK, paxillin, Rho Family GTPases and GPRC signalling pathways (Fig. 4.3C; Supplementary Table S4G).

A

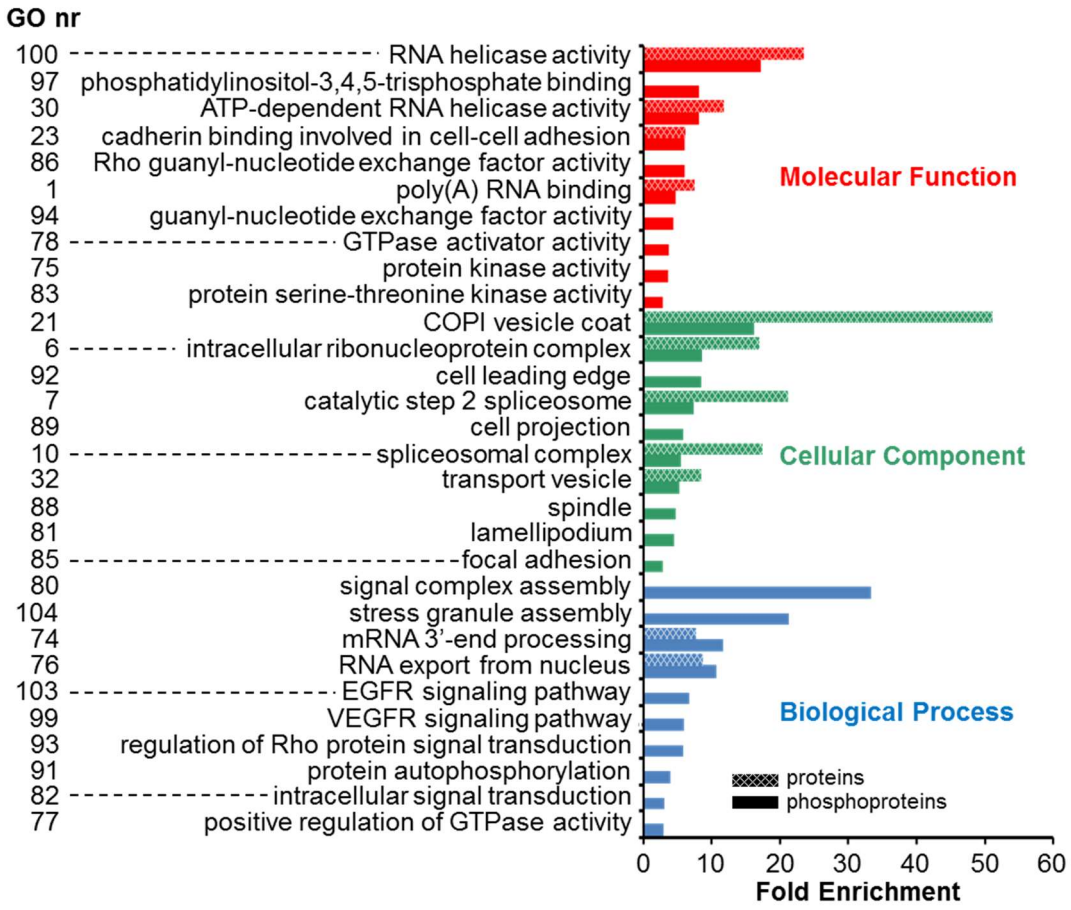
GO nr
100 RNA helicase activity
97 phosphatidylinositol-3,4,5-trisphosphate binding
30 ATP-dependent RNA helicase activity
23 cadherin binding involved in cell-cell adhesion
86 Rho guanyl-nucleotide exchange factor activity
1 poly(A) RNA binding
94 guanyl-nucleotide exchange factor activity
78 GTPase activator activity
75 protein kinase activity
83 protein serine-threonine kinase activity
21 COPI vesicle coat
6 intracellular ribonucleoprotein complex
92 cell leading edge
7 catalytic step 2 spliceosome
89 cell projection
10 spliceosomal complex
32 transport vesicle
88 spindle
81 lamellipodium
85 focal adhesion
80 signal complex assembly
104 stress granule assembly
74 mRNA 3'-end processing
76 RNA export from nucleus
103 EGFR signaling pathway
99 VEGFR signaling pathway
93 regulation of Rho protein signal transduction
91 protein autophosphorylation
82 intracellular signal transduction
77 positive regulation of GTPase activity
Molecular Function
Cellular Component
Biological Process
proteins
phosphoproteins
0 10 20 30 40 50 60
Fold Enrichment

B

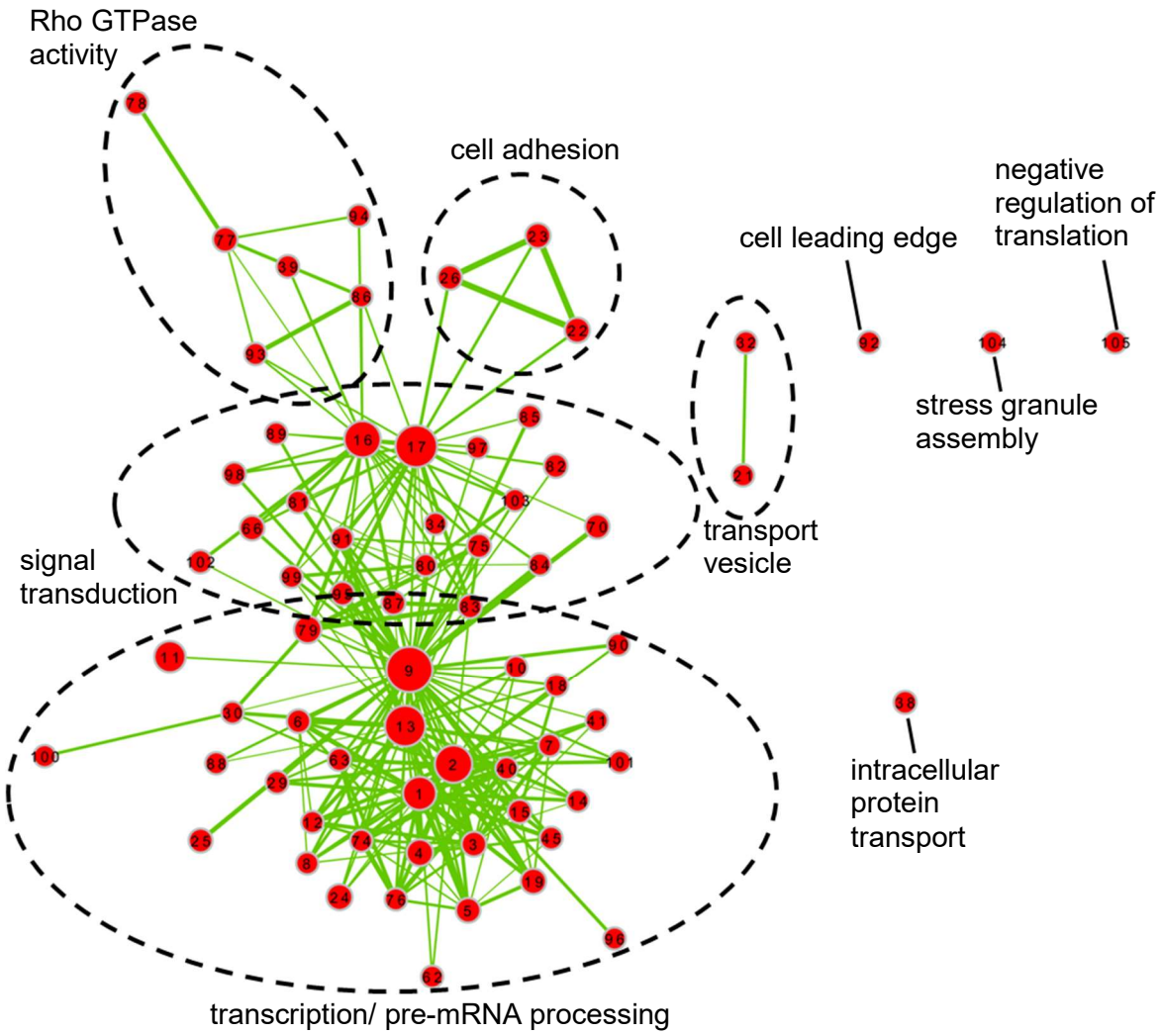
Rho GTPase activity
cell adhesion
cell leading edge
negative regulation of translation
stress granule assembly
transport vesicle
signal transduction
intracellular protein transport
transcription/ pre-mRNA processing

C

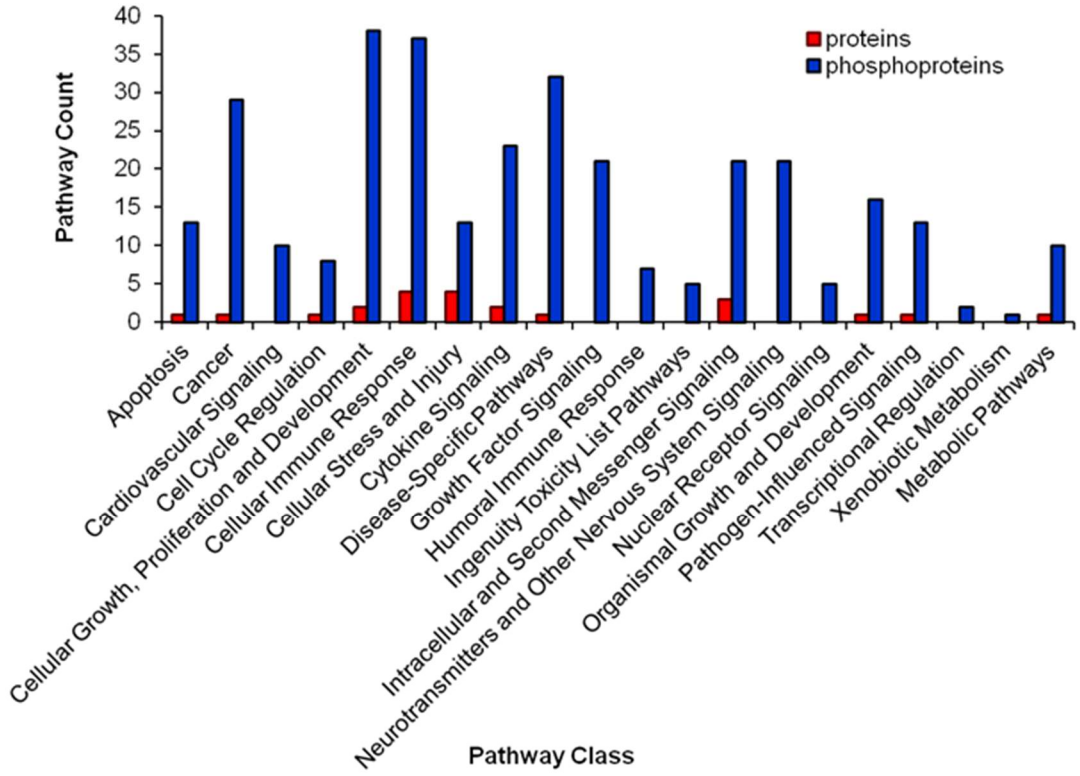

Figure 4.3 Functional annotation of phosphoproteins significantly upregulated and common to all meningioma grades *vs*. NMT. (**A**) Gene ontology (GO) enrichment analysis of significantly upregulated proteins and phosphoproteins common to all grades of meningiomas *vs*. NMT ($\log_2$ fold change≥ 1.5; $p< 0.05$) by the web tool DAVID version 6.8. Terms containing at least three proteins with Benjamini-Hochberg adjusted $p< 0.05$ are shown. Gene Ontologies representing 'Molecular Function' are presented in red, 'Cellular Component' in green and 'Biological Process' in blue. Fold enrichment relative to the *H. sapiens* proteome is displayed at the *x*-axis. Full details of GO analysis output are detailed in Supplementary Tables S4A and S4D. (**B**) Enrichment map of GO terms found to be enriched among upregulated phosphoproteins. Nodes represent enriched GO terms, colour intensities reflecting statistical significance and line thickness correlating to the degree of overlap. Numbers refer to GO terms some of which are seen in (A) with full list of terms detailed in Supplementary Table S4E. Image created with Cytoscape plugin Enrichment Map. (**C**) Ingenuity Pathway Analysis (IPA) of commonly upregulated proteins and phosphoproteins. Pathways significantly associated with two or more proteins or phosphoproteins (Fisher's exact test right-tailed, *p*-value< 0.05) were grouped into pathway

classes according to Ingenuity Canonical Pathways. Classes containing the most pathways associated with proteins were ‘cellular immune response’ and ‘cellular stress and injury’ with 4 pathways in each. Phosphoproteins included ‘cellular growth, proliferation and development’, ‘cellular immune response’, ‘disease-specific pathways’ and ‘cancer’ with 38, 37, 32 and 29 pathways, respectively. Supplementary Tables S4F and S4G provide details of IPA pathway analysis and pathway classification.

4.2.5 Commonly downregulated phosphoproteins amongst all meningioma grades

In addition to unravelling the increased phosphorylation of proteins in cancer, it is also of interest to ascertain the dephosphorylation of proteins. Dephosphorylation of a protein, among other functions, can serve to inactivate a tumour suppressor protein or activate an oncoprotein. We therefore sought to establish phosphoproteins that were commonly downregulated across all WHO grades. To do this three lists of commonly and significantly downregulated phosphoproteins ($\log_2$ FC$\leq$ -1.5; *p*-value$<$ 0.05) of each grade compared to control were generated. Following this, phosphoprotein lists were overlapped resulting in the identification of 161 phosphoproteins as commonly and significantly downregulated among all grades *vs.* NMT. Table 4.2 displays the top 50 most commonly and significantly downregulated phosphoproteins. Full lists of quantified phosphoproteins detailing fold changes and significance are contained in Supplementary Table S3B.

Protein name	Gene	Log_2 FC (GI *vs.* NMT)	Log_2 FC (GII *vs.* NMT)	Log_2 FC (GIII *vs.* NMT)
Isoform 4 of Cytosolic acyl coenzyme A thioester hydrolase	BACH	-∞	-7.82	-6.21
Dickkopf-related protein 3	DKK3	-∞	-∞	-∞
Isoform 2 of Synaptoporin	SYNPR	-∞	-∞	-∞
Guanine nucleotide-binding protein G(i) subunit alpha-1	GNAI1	-∞	-∞	-6.24
Chromogranin-A	CMGA	-∞	-∞	-∞
Protein bassoon	BSN	-∞	-∞	-∞
Isoform 2 of Peroxisomal membrane protein PEX14	PEX14	-∞	-8.07	-3.68
Dihydropteridine reductase	DHPR	-∞	-2.97	-∞
Isoform 2 of 6-phosphogluconate dehydrogenase, decarboxylating	6PGD	-∞	-∞	-∞
Isoform Tau-D of Microtubule-associated protein tau	TAU	-∞	-∞	-∞
Beta-centractin	ACTY	-∞	-∞	-∞
Cytochrome b-c1 complex subunit 7	UQCRB	-∞	-∞	-∞
2-oxoglutarate dehydrogenase, mitochondrial	OGDH	-∞	-3.64	-∞

NADH dehydrogenase [ubiquinone] 1 beta subcomplex subunit 9	NDUFB9	-∞	-3.88	-∞
Isoform 2 of Major prion protein	PRIO	-∞	-∞	-∞
Prenylcysteine oxidase 1 (Fragment)	C9K055	-∞	-∞	-∞
Isoform 2 of Protocadherin-1	PCDH1	-∞	-∞	-∞
60S ribosomal protein L30 (Fragment)	RPL30	-∞	-2.71	-2.44
Isoaspartyl peptidase/L-asparaginase	ASGL1	-∞	-1.91	-∞
Secretogranin-1	SCG1	-∞	-3.72	-4.91
MICOS complex subunit MIC19	MIC19	-∞	-6.33	-∞
Low molecular weight phosphotyrosine protein phosphatase	PPAC	-∞	-3.98	-4.84
NADH dehydrogenase [ubiquinone] 1 alpha subcomplex subunit 8	NDUA8	-∞	-4.30	-∞
Sodium- and chloride-dependent GABA transporter 1	SC6A1	-∞	-3.00	-∞
Isoform 2 of Armadillo repeat-containing protein 1	ARMC1	-∞	-∞	-1.91

Isoform 2 of EGF-like repeat and discoidin I-like domain-containing protein 3	EDIL3	-∞	-∞	-∞
Secretory carrier-associated membrane protein 1	SCAM1	-∞	-∞	-∞
Haloacid dehalogenase-like hydrolase domain-containing protein 2	HDHD2	-∞	-2.12	-∞
Electron transfer flavoprotein subunit beta	ETFB	-∞	-∞	-∞
Hydroxymethylglutaryl-CoA lyase, mitochondrial	HMGCL	-∞	-∞	-∞
Isoform 3 of Centrosomal protein of 131 kDa	CP131	-∞	-∞	-∞
Glycerol-3-phosphate dehydrogenase 1-like protein	GPD1L	-∞	-∞	-1.98
Cadherin-13	CDH13	-∞	-∞	-∞
Isoform 4 of Inter-alpha-trypsin inhibitor heavy chain H4	ITIH4	-∞	-∞	-∞
Fermitin family homolog 2 (Fragment)	FERMT2	-∞	-∞	-∞
Isoform 5 of Sulfatase-modifying factor 2	SUMF2	-∞	-2.36	-∞
SH3 domain-binding glutamic acid-rich-like protein 2	SH3L2	-∞	-∞	-2.07

Sushi domain-containing protein 2	SUSD2	-∞	-∞	-∞
Isoform 2 of Vesicle-associated membrane protein 4	VAMP4	-∞	-∞	-1.62
60S ribosomal protein L23a	RL23A	-∞	-∞	-∞
Beta-1-syntrophin	SNTB1	-∞	-2.70	-3.04
Troponin I, slow skeletal muscle	TNNI1	-∞	-∞	-∞
Isocitrate dehydrogenase [NADP] cytoplasmic	IDHC	-∞	-∞	-∞
Isoform 2 of Arylsulfatase B	ARSB	-∞	-∞	-∞
Carbonyl reductase [NADPH] 3	CBR3	-∞	-∞	-∞
Proline-rich transmembrane protein 2	PRRT2	-14.26	-12.68	-∞
Clathrin coat assembly protein AP180	SNAP91	-13.57	-9.67	-7.88
Syntaxin-1A	STX1A	-13.27	-12.99	-12.38
Isoform 2-4 of Alpha-synuclein	SYUA	-12.08	-8.20	-9.47
SPARC-like protein 1	SPRL1	-11.13	-11.09	-9.22

Table 4.2 Top 50 of the most commonly and significantly downregulated phosphoproteins among all grades of meningiomas compared to NMT. Corresponding $\log_2$ FCs for each meningioma grade compared to NMT are shown. Significant downregulation defined as $\log_2$ FC≤ -1.5; *p*-value< 0.05. Phosphoproteins specific to one of the two groups compared were assigned a FC of infinity. Full details of the 161 phosphoproteins commonly and significantly downregulated can be found in Supplementary Table S3B.

4.2.6 Functional annotation of commonly downregulated phosphoproteins in meningioma

We performed functional annotation of downregulated phosphoproteins analogous to that of downregulated proteins. STRING clustering analysis was used to observe the associations between sub networks of downregulated phosphoproteins. We again defined protein interactions by selecting 'known interactions' that have been previously experimentally determined or curated from databases and removing 'predicted interactions'. In this way we retained only the most reliable protein-protein interactions. Figure 4.4A shows an interaction network highlighted with six clusters of downregulated proteins and associated biological functions. Next, we submitted the 161 commonly downregulated phosphoproteins to DAVID for GO enrichment analysis (Fig. 4.4B).

STRING analysis revealed three clusters of protein-protein interactions were related to metabolic processes and energy production; metabolic pathways, oxidation-reduction process and cellular respiration (Fig. 4.4A). The biological functions associated with these three clusters were also reflected in many of the significantly enriched GO terms of commonly downregulated phosphoproteins subsequent to analysis by DAVID (Fig. 4.4B; Supplementary Table S5B). Enriched GO terms linked to metabolic processes and energy production included NAD binding (17-fold) and NADH (NAD + hydrogen (H)) dehydrogenase (ubiquinone) activity (13-fold) within the 'Molecular Function' class; mitochondrial respiratory chain complex I (16-fold) within the 'Cellular Component' class; as well as tricarboxylic acid cycle (22-fold) and glycolytic process (22-fold) within the 'Biological Process' class (Fig. 4.4B). Remaining clusters of downregulated phosphoproteins defined by STRING were associated with synaptic transmission, cytoskeletal protein binding and nonsense mediated mRNA decay (Fig. 4.4A).

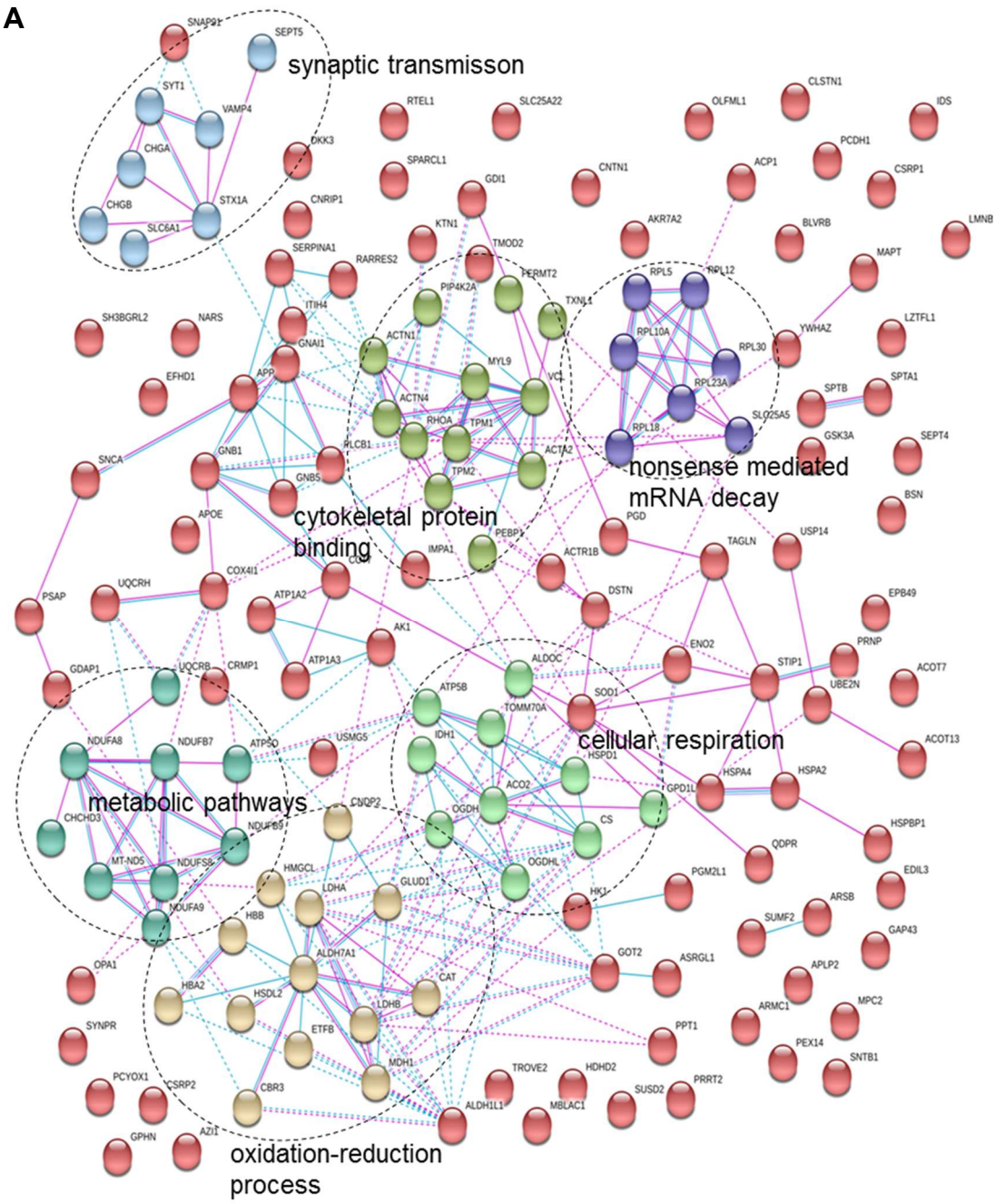
A
synaptic transmisson
nonsense mediated mRNA decay
cytokeletal protein binding
cellular respiration
metabolic pathways
oxidation-reduction process
SNAP91
SEPT5
SYT1
VAMP4
CHGA
CHGB
STX1A
SLC6A1
OKK3
CNRIP1
SERPINA1
RARRES2
ITIH4
GNAI1
APP
EFHD1
SH3BGRL2
NARS
SNCA
GNB1
GNB5
PLCB1
APOE
COX4I1
UQCRH
PSAP
ATP1A2
ATP1A3
AK1
GDAP1
UQCRB
CRMP1
NDUFA8
NDUFB7
ATP5O
CHCHD3
NDUFB9
MT-ND5
NDUFS8
NDUFA9
OPA1
HBB
HBA2
HSDL2
SYNPR
PCYOX1
CSRP2
CBR3
AZI1
GPHN
HMGCL
LDHA
ALDH7A1
ETFB
MDH1
LDHB
CAT
GLUD1
CNDP2
USMG5
IDH1
ACO2
OGDH
OGDHL
CS
ATP5B
TOMM70A
ALDOC
SOD1
HSPD1
GPD1L
HSPA4
HSPA2
HSPBP1
QDPR
PGM2L1
HK1
EDIL3
ARSB
SUMF2
GAP43
APLP2
MPC2
ARMC1
PEX14
SNTB1
PPT1
GOT2
ASRGL1
TROVE2
HDHD2
SUSD2
PRRT2
ALDH1L1
MBLAC1
RTEL1
SLC25A22
SPARCL1
GDI1
KTN1
TMOD2
PERMT2
PIP4K2A
TXNL1
ACTN1
MYL9
VCL
ACTN4
RHOA
TPM1
TPM2
ACTA2
IMPA1
PEBP1
CFL1
ACTR1B
DSTN
PGD
TAGLN
USP14
ENO2
STIP1
PRNP
UBE2N
EPB49
ACOT7
ACOT13
CNTN1
AKR7A2
RPL5
RPL12
RPL10A
RPL30
RPL23A
SLC25A5
RPL18
OLFML1
CLSTN1
IDS
PCDH1
CSRP1
ACP1
BLVRB
LMNB1
MAPT
YWHAZ
LZTFL1
SPTB
SPTA1
GSK3A
SEPT4
BSN

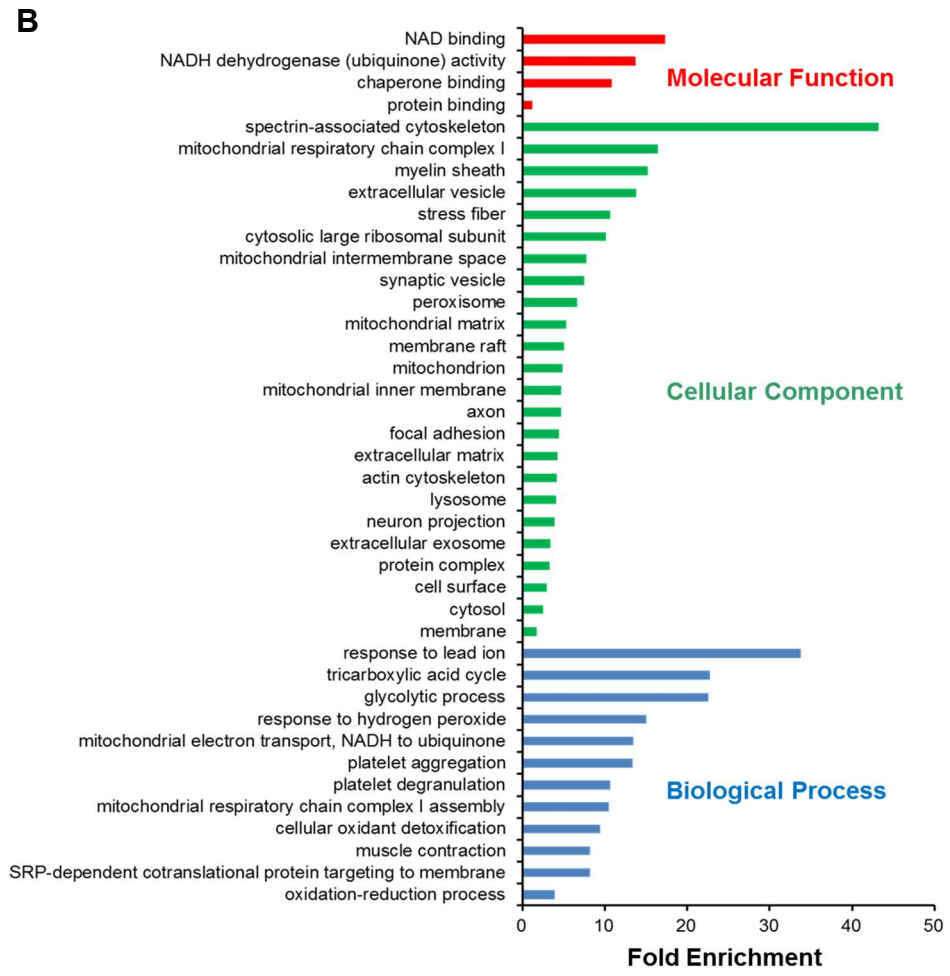

Figure 4.4 Functional annotation of phosphoproteins significantly downregulated and common to all meningioma grade *vs.* NMT. (**A**) Protein-protein interaction network of phosphoproteins commonly downregulated in all meningioma grades. Highlighted are clusters of phosphoproteins with known interactions each associated to a biological function. Network derived from the STRING database version 10.5 and analysed with the kmeans clustering method. Phosphoproteins are represented by network nodes. Protein-protein associations are shown by connecting lines and are derived from curated databases and/or experimentally determined. (**B**) Gene ontology (GO) enrichment analysis of 161 phosphoproteins commonly downregulated in all meningioma grades by the web tool DAVID version 6.8. Terms containing at least three phosphoproteins with Benjamini-Hochberg adjusted $p< 0.05$ are shown. Gene Ontologies representing 'Molecular Function' are presented in red, 'Cellular Component' in green and 'Biological Process' in blue. Fold enrichment relative to the *H. sapiens* proteome is displayed at the *x*-axis. Full details of GO analysis output are detailed in Supplementary Table S5B.

4.2.7 Grade-specific phosphoprotein analysis of meningiomas

To investigate dysregulated protein phosphorylation between meningioma WHO grades we explored the differential expression of phosphoproteins specific to high-grade meningiomas. This analysis enabled us to determine those proteins that are aberrantly phosphorylated in these aggressive tumours and may act as potential therapeutic targets. Additionally, it allowed us to elucidate upon the biological processes that may be regulated by phosphorylation in these meningioma.

Similarly to analysis of our global proteome dataset, we assessed significant quantitative differences in large datasets composed of replicate data from each meningioma grade by Student's *t*-tests and visualised differentially expressed phosphoproteins in Volcano plots (Fig. 4.5; Supplementary Table S6B). We identified 404 phosphoproteins to be significantly differentially expressed between grade II *vs*. grade I (Fig. 4.5A), 423 between grade III *vs*. grade I (Fig. 4.5B) and 346 between grade III *vs*. grade II (Fig. 4.5C).

Significantly upregulated phosphoproteins in grade II meningiomas compared to grade I included EFNB2 (ephrin-B2), a ligand for the EPH family of RTKs, recently identified to be activated in *NF2*-deficient meningioma (Angus *et al.*, 2018); whilst the MAPK-specific phosphatase PTPN7 (tyrosine-protein phosphatase non-receptor type 7; also HePTP) was shown to be downregulated (Fig. 4.5A) (Pettiford & Herbst, 2000). Among significantly upregulated phosphoproteins in grade III *vs*. grade I meningiomas we identified CDH2 (cadherin-2; also N-cadherin) known to play a role in EMT during tumour progression (Fig. 4.5B) (Mariotti *et al.*, 2007). Following comparison of grade III with grade II tumours, we established the DEAD-box RNA helicase DDX24 as significantly upregulated in grade III meningiomas (Fig. 4.5C), also identified in a grade III cluster of overexpressed proteins seen in Figure 4.2A.

Differential expression between grade III *vs*. grade I meningiomas and grade III *vs.* grade II meningiomas also demonstrated some phosphoproteins to be common to both comparisons. Significantly upregulated phosphoproteins overlapping between these comparisons included the cell cycle checkpoint protein ATR, often critical for tumour cell survival during increased levels of DNA replication stress (Fig. 4.5B and 4.5C). We also identified several significantly downregulated phosphoproteins to overlap between these comparisons including MRC2 (C-type mannose receptor 2), SVIL (supervillin), CPPED1 (serine/threonine-protein phosphatase CPPED1) and SSH1 (protein phosphatase Slingshot homolog 1) (Fig. 4.5B and 4.5C).

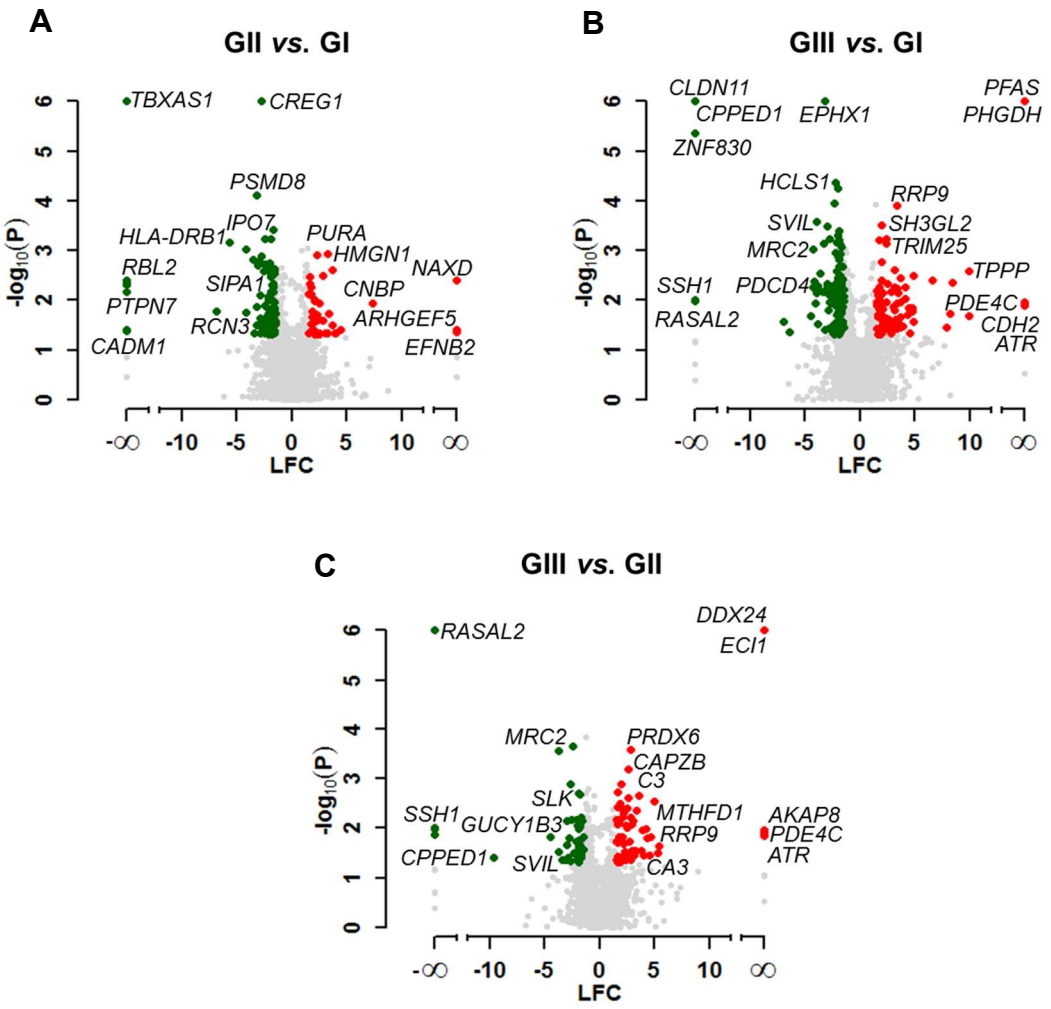

Figure 4.5 Differential phosphoprotein expression between meningioma grades. Fold changes in protein abundance between different grades of meningiomas is depicted in Volcano plots. Differential expression of phosphoproteins is shown: (**A**) grade II vs. grade I; (**B**) grade III vs. grade I and (**C**) grade III vs. grade II. Depicted in the plots are the comparisons of $\log_2$ fold changes (LFC) versus *p*-values (Student's t-test between replicate measurements). Red dots: Upregulated phosphoproteins ($\log_2$ FC≥ 1.5; *p*-value< 0.05). Green dots: Downregulated phosphoproteins ($\log_2$ FC≤ 1.5; *p*-value< 0.05). Grey dots: Phosphoproteins that did not meet these criteria. Phosphoproteins specific to one of the two groups compared were assigned a fold change of infinity. See also Supplementary Table S6B for full analysis.

Next, we used the computational tool BubbleGUM to extract individual molecular signatures for grade II and grade III meningiomas based on the relative expression of phosphoproteins. This enabled us to further elucidate increased expression of phosphoproteins specific to a sample group that may hold therapeutic potential or could act as biomarkers.

The molecular signature of grade II meningiomas was generated by comparison of the proteomic profile of grade II tumours with those of grade I and NMT, and a grade III signature by comparison with grade II, grade I and NMT. We identified a grade II molecular signature of 88 phosphoproteins and a grade III molecular signature of 84 phosphoproteins with FC> 2. Hierarchical clustering of extracted signatures showed clustering of samples into their respective grades, again with the exception of the grade III sample, J9, seen to reside between grade I and II tumours (Fig. 4.6). Grade II and III phosphoprotein signatures exhibited a clear difference to grade I meningiomas and NMT (Fig. 4.6).

Grade II-specific phosphoproteins included the tumour suppressor PTEN (phosphatase and tensin homologue deleted on chromosome 10) whose function is inactivated by its phosphorylation, as well as the transcription factor CREB1 (cyclic AMP-responsive element-binding protein 1) (Fig. 4.6). In grade III meningiomas we identified increased expression of the DEAD-box RNA helicase DDX19B (ATP-dependent RNA helicase DDX19B). Phosphorylated DDX19B has been shown to function in an ATR/CHEK1 (serine/threonine-protein kinase Chk1)-dependent manner in the DNA damage response upon its phosphorylation by CHEK1 (Hodroj *et al.*, 2017); indeed, ATR was identified in our previous analyses as a grade III-specific phosphoprotein (Fig. 4.2A; 4.5B and 4.5C). Complete phosphoprotein lists generated by BubbleGUM analyses are shown in Supplementary Tables S7E and S7F.

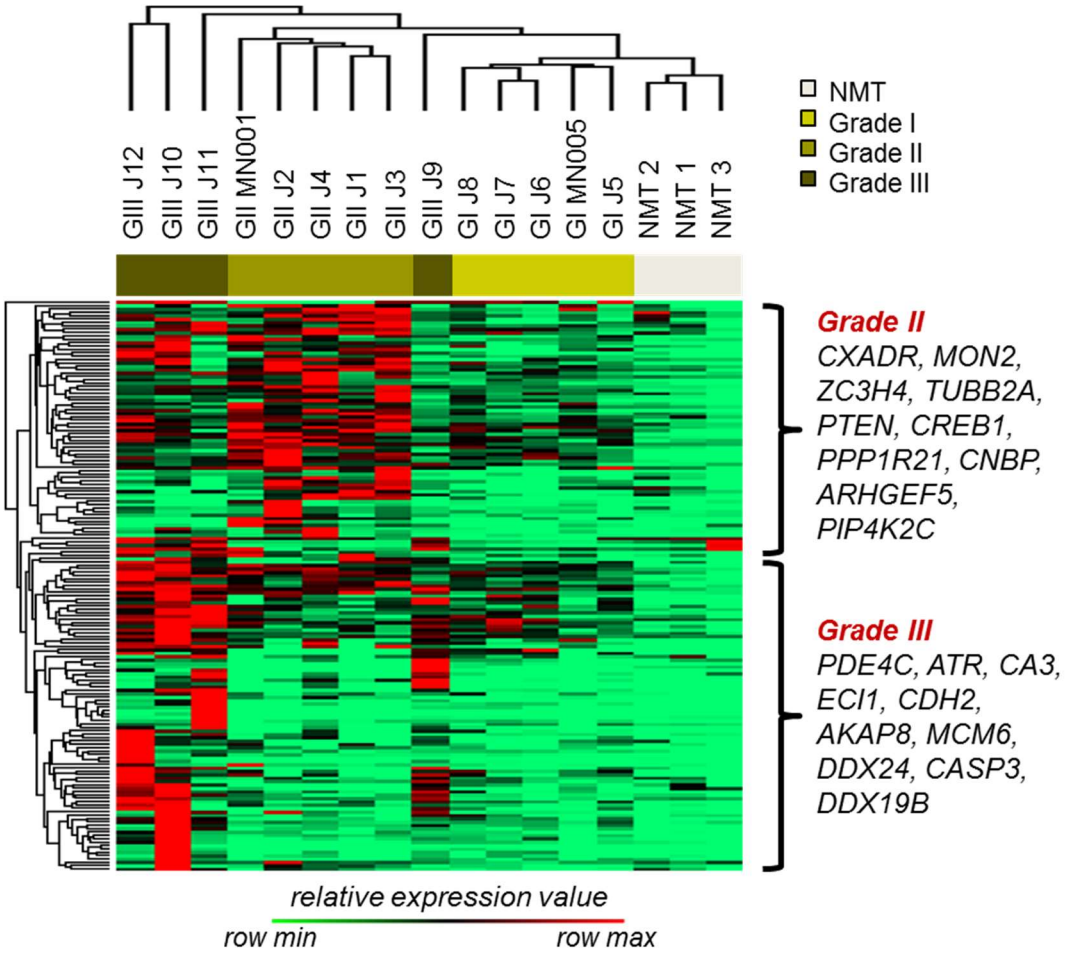

Figure 4.6 Phosphoprotein signatures of grade II and III meningiomas. Individual phosphoprotein signatures of grade II and III meningiomas were generated by the computational tool BubbleGUM and are visualised in a heatmap (Spinelli *et al.*, 2015). The GeneSign module was used to generate a grade II signature by comparison with grade I and NMT, and a grade III signature by comparison with grade II, grade I and NMT. A grade II molecular signature of 88 phosphoproteins and a grade III signature of 84 phosphoproteins with FC> 2 were identified. Hierarchical clustering of extracted signatures based on relative expression values is shown. A collection of proteins found within each signature is presented. Clustering was created using Perseus 1.5.0.31 software suite. Supplementary Tables S7E and S7F provide details of BubbleGUM output for molecular signatures.

4.2.8 Gene ontology analysis of grade II and III phosphoprotein molecular signatures

GO enrichment analysis was performed to functionally annotate phosphoproteins identified in the grade II and III molecular signatures. All significantly enriched GO terms are displayed for both signatures (Fig. 4.7A and 4.7B; Supplementary Tables S7G and S7H). Phosphoproteins comprising the molecular signature of grade II meningiomas revealed the highest fold enrichment under the GO term of mRNA splicing via spliceosome (8-fold) in the 'Biological Process' class (Fig. 4.7A). Identified terms also demonstrated strong enrichment related to cell-cell adhesion and included the terms cadherin binding involved in cell-cell adhesion (7-fold), cell-cell adherens junction (7-fold) and cell-cell adhesion (7-fold) in the 'Molecular Function', 'Cellular Component' and 'Biological Process' classes, respectively (Fig. 4.7A).

Among grade III-specific phosphoproteins, terms with the strongest enrichments included RNA helicase activity (65-fold), small-subunit processome (26-fold) and RNA secondary structure unwinding (29-fold) in the 'Molecular Function', 'Cellular Component' and 'Biological Process' classes, respectively, with terms mainly linked to RNA activity and ribosome biogenesis (Fig. 4.7B).

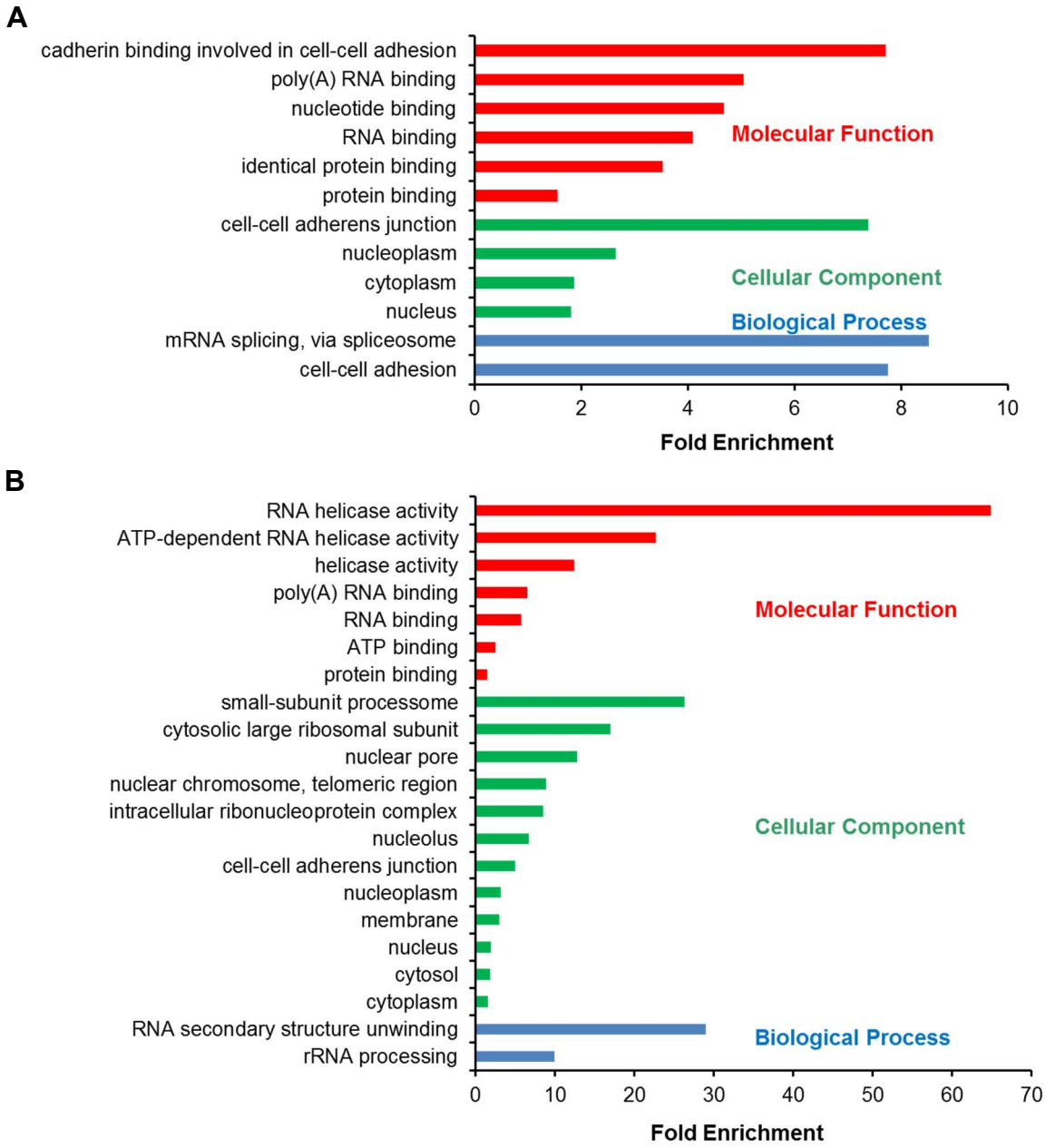

Figure 4.7 GO enrichment analysis of grade II and grade III meningioma molecular signatures. Histogram displays all significantly enriched GO terms returned by the web tool DAVID version 6.8 following submission of 88 grade II phosphoprotein signature (**A**) and 84 grade III phosphoprotein signature (**B**). Terms containing at least three phosphoproteins with Benjamini-Hochberg adjusted $p< 0.05$ are shown. Gene Ontologies representing 'Molecular Function' are presented in red, 'Cellular Component' in green and 'Biological Process' in blue. Fold enrichment relative to the *H. sapiens* proteome is displayed at the *x*-axis. Full details of GO analyses output are detailed in Supplementary Tables S7G and S7H.

4.3 Analysis of phosphorylation sites in meningioma

In order to identify specific phosphorylation sites in meningioma we enriched for phosphorylated peptides in eight meningioma tissue specimens (three grade I, three grade II and two grade III) using a TiO_2-based affinity enrichment step and analysed phosphopeptides by LC-MS/MS. We sequenced and identified 3622 phosphopeptides, of which 2729 (75%) were identified with a phosphosite PTM localization probability score greater than 0.75 (Supplementary Table S8A). Our distribution of serine (~90%), threonine (~9%) and tyrosine (~1%) phosphorylation sites were similar to previous studies (Fig. 4.8A) (Zhou *et al.*, 2013). We further classified phosphopeptides based on their chemical properties using a binary decision tree (Villen *et al.*, 2007). The majority of sites were classified as either proline-directed (33%) or basic (32%), followed by acidic (21%), other (13%) and tyrosine (1%) (Fig. 4.8B).

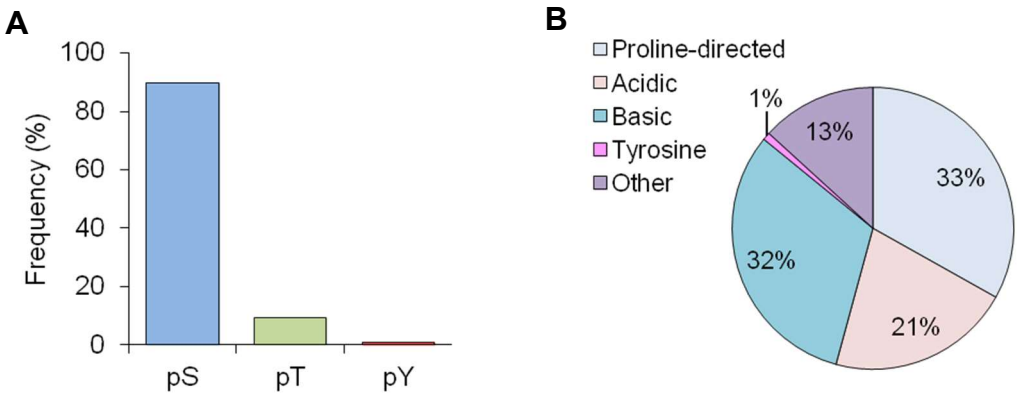

Figure 4.8 Protein phosphorylation sites in meningiomas. (**A**) Distribution of amino acid phosphorylation for serine (pS), threonine (pT) and tyrosine (pY) across meningiomas. See Supplementary Table S8A for all phosphorylation sites. (**B**) Distribution of phosphorylation site classes in meningiomas. The phosphorylated residue is located at the central position within a sequence window of 13 amino acids. Classes were defined by the chemical properties of the sequence window peptide as acidic, basic, proline-directed, tyrosine or other by a binary decision tree method (Villen *et al.*, 2007).

The 3622 identified phosphopeptides covered a total of 1320 proteins of which 56% (738) were found to overlap with the phosphoprotein dataset. We next performed analyses to functionally annotate the phosphoproteins common to both datasets using DAVID and IPA. GO analysis of the overlap showed a strong enrichment in terms related to the cellular membrane and its adhesion properties (e.g. basal cortex, zonula adherens, podosome assembly), microtubule regulation, cytoskeletal organization and DNA binding (Fig. 4.9A; Supplementary Table S8B). Additionally, we analysed the 1320 proteins associated with identified phosphopeptides using IPA and identified 211 significantly associated canonical pathways (Fig. 4.9B; Supplementary Table S8C). Pathways were grouped under broader functional classes as before and compared with analyses previously generated from 338 commonly and significantly upregulated phosphoproteins across meningioma grades. Phosphoproteins identified by phosphopeptides showed a similar trend of pathway classification when compared to that of commonly upregulated phosphoproteins; the majority of pathways were associated with ‘cellular growth, proliferation and development’ (34 pathways) and ‘cellular immune response’ (34 pathways) (Fig. 4.9B).

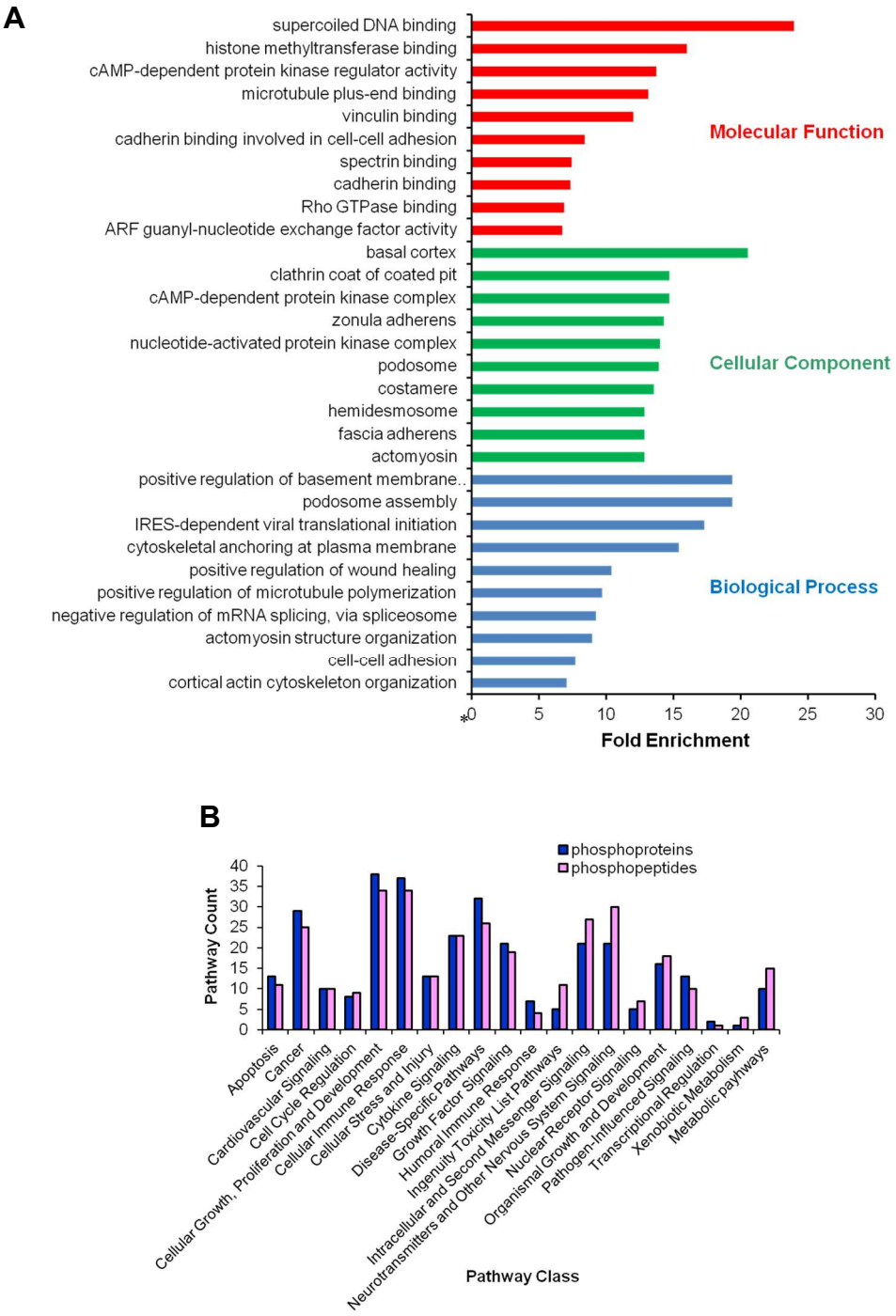

Figure 4.9 Functional annotation of protein phosphorylation sites in meningiomas. (**A**) GO enrichment analysis of 738 phosphoproteins common to the phosphoprotein and phosphopeptide datasets performed by the web tool DAVID version 6.8. Terms containing at least three phosphoproteins with Benjamini-Hochberg adjusted $p< 0.05$ are shown. Gene Ontologies representing 'Molecular Function' are presented in red, 'Cellular Component' in green and 'Biological Process' in blue. Fold enrichment relative to the *H. sapiens* proteome is displayed at the *x*-axis. *positive regulation of basement membrane assembly = positive regulation of

basement membrane assembly involved in embryonic body morphogenesis. Phosphoproteins associated with these terms are provided in Supplementary Table S8B. (**B**) Ingenuity Pathway Analysis of commonly upregulated phosphoproteins and of proteins associated with identified phosphopeptides. Pathways significantly associated with two or more phosphoproteins (Fisher's exact test right-tailed, *p*-value< 0.05) were grouped into pathway classes according to Ingenuity Canonical Pathways. Supplementary Tables S4G and S8C provide details of pathway analysis and classification.

Subsequent to performing phosphoprotein and phosphopeptide enrichments in meningioma, we aimed to identify abundant phosphoproteins in meningioma compared to healthy meninges (as shown earlier in this Chapter). Following this, we utilised our phosphopeptide dataset to establish associated protein phosphorylation sites of upregulated phosphoproteins. We successfully found 738 phosphorylated proteins common to both datasets. We identified phosphosites for SET (protein SET; also phosphatase 2A inhibitor I2PP2A), PXN (paxillin), EPS8L2 and NEK9 that were established as upregulated in meningioma compared to NMT in both phosphoprotein and global proteome datasets (Table 4.3). Among phosphoproteins highlighted from analyses earlier in this Chapter and also seen in the phosphopeptide dataset were members of the DOCK-family of GEFs; DOCK1, DOCK4, DOCK7 and DOCK8, previously found to be significantly upregulated in all meningioma grades (Fig. 4.2A; Table 4.3). In addition, we also detected phosphosites for DOCK2 (S1177, S1198), DOCK6 (S176, S1308) and DOCK9 (S167, S229) that although were not significantly upregulated in every meningioma grade, were each identified in all 14 meningioma samples analysed for the phosphoprotein dataset (Supplementary Tables S3B and S8A).

Unfortunately, we were unable in this project to verify identified protein phosphorylation sites associated with the phosphoproteins shown in Table 4.3 due to

many being novel and not yet described in the literature, as well as lacking phosphosite-specific antibodies for validation experiments.

Protein name	Gene	Phosphosite
Protein SET*	SET	S7
Isoform Alpha of Paxillin*	PXN	S85, S499
Epidermal growth factor receptor kinase substrate 8-like protein 2*	EPS8L2	S48
Serine/threonine-protein kinase Nek9*	NEK9	S868
Serine/threonine-protein kinase Nek7*	NEK7	S195
Mammalian target of rapamycin*	MTOR	T1162
Dedicator of cytokinesis protein 1*	DOCK1	S130
Dedicator of cytokinesis protein 4*	DOCK4	S121
Dedicator of cytokinesis protein 7*	DOCK7	S439, S888, S1392, S1398
Dedicator of cytokinesis protein 8*	DOCK8	S383, S836
Cyclic AMP-responsive element-binding protein 1+	CREB1	S102

*Phosphoproteins commonly and significantly upregulated in all meningioma WHO grades compared to NMT.
+Grade II-specific phosphoproteins.

Table 4.3 Protein phosphorylation sites detected following phosphopeptide enrichment and MS analysis for a selection of phosphoproteins significantly differentially expressed in meningioma compared to NMT. See Supplementary Table S8A for all phosphorylation sites.

4.4 Discussion

This Chapter has enabled us to build upon our knowledge surrounding dysregulated protein activity in meningioma by exploring the phosphoproteome of these tumours. Phosphoprotein enrichment and MS analysis of 14 meningioma and three healthy meninges provided us with the successful quantification of over 3000 phosphoproteins, whilst phosphopeptide enrichment of eight meningioma identified over 2700 phosphorylation sites for downstream analysis.

Analogous to our global proteome analysis we initially focussed on determining a phosphoprotein profile common to all grades of meningioma. Although a recent study published by Parada *et al*. (2018) also observed differential expression of the meningioma phosphoproteome, as discussed at the beginning of this chapter, the authors did not compare findings with the phosphoproteome of normal meninges (Parada *et al.*, 2018). The work here went beyond describing the phosphoprotein landscape of meningioma in isolation, also comparing it with that of healthy meninges to seek out novel therapeutic targets abundant in tumour cells.

We were able to detect 338 phosphoproteins as commonly and significantly upregulated in all grades of meningioma compared to NMT. Functional annotation of commonly upregulated phosphoproteins was associated with signal transduction, as would likely be expected following phosphoprotein enrichment prior to MS. More specifically, functional annotation by GO enrichment and IPA Ingenuity Canonical Pathways highlighted Rho GTPase activity to be linked to upregulated phosphoproteins. Interestingly, upregulated phosphoproteins contained many GEFs, including members of the DOCK-family of GEFs, DOCK1, DOCK4, DOCK5, DOCK7 and DOCK8. The DOCK-family of GEFs activate the Rho GTPases Rac(1/2/3) and/or Cdc42 and have been previously implicated in cancer (Gadea & Blangy, 2014). Phosphorylation of DOCK1 on

S1250 by protein kinase A in GBM has been shown to be important for glioma cell growth and invasion, while phosphorylation of DOCK4 by GSK3β (glycogen synthase kinase 3β) was found to increase Wnt-induced Rac activation of the canonical Wnt/β-catenin pathway in colon cancer cell lines (Feng *et al.*, 2014; Upadhyay *et al.*, 2008). To our knowledge, the phosphorylation of DOCK proteins and their role in meningioma pathogenesis has yet to be described. Future clarification of DOCK protein function in these tumours could therefore yield them as a targetable family of proteins for treatment.

Among the top significantly downregulated phosphoproteins we observed a strong decrease across all meningioma grades of the tumour suppressor DKK3. We also previously identified DKK3 as commonly downregulated in the global proteome dataset. In addition to our findings, a recent study of grade I and II meningioma also confirmed the reduced expression of DDK3 by IHC and WB (Caffo *et al.*, 2017). DKK3 is an antagonist of the Wnt signalling pathway and methylation of its promoter has led to its epigenetic silencing in various cancers, resulting in increased Wnt/ β-catenin signalling as well as reduced apoptosis (Xiang *et al.*, 2013; Yin *et al.*, 2013). Taken together, these findings suggest that further exploration of DKK3 downregulation in meningioma could reveal possible dysregulation of Wnt pathway activity and new therapeutic strategies for these tumours.

Following functional annotation of commonly downregulated phosphoproteins, we found many were related to metabolic processes and energy production. In contrast to this finding, we previously observed enrichment of metabolic processes by upregulated grade III-specific proteins (section 3.4.7). Further investigation into the dysregulation of metabolic pathways in meningioma pathogenesis and progression is required to determine if they play tumour promoting or tumour suppressing roles in these tumours.

Comparison of the phosphoprotein dataset with that of the phosphopeptides allowed us to detect protein phosphorylation sites associated with several differentially expressed phosphoproteins in meningioma. Although we did not compare phosphopeptides between tumour and normal meningeal cells, this analysis provides a complementary source of information to identify phosphosites in meningioma that might act as therapeutic targets. Interestingly, we detected phosphosites for seven DOCK-family members further implicating these proteins with a possible role in meningioma pathogenesis. We also identified phosphosites for SET, PXN, EPS8L2, NEK9, NEK7 and mTOR. However, phosphosites associated with these proteins appeared to be novel and not yet described in literature, hampering further validation studies at this time.

We also detected the phosphosite S102 for the transcription factor CREB1 (cyclic AMP-responsive element-binding protein 1) identified as a grade-II specific phosphoprotein. In agreement with our results, Barresi *et al.* (2015) also showed expression of phosphorylated CREB1 to be significantly higher in grade II meningiomas compared to grade I (Barresi *et al.*, 2015). CREB1 phosphorylation on S133 by kinases including AKT1, also identified in our phosphoprotein analyses as overexpressed in meningioma, has been shown to activate CREB1 leading to transcription of target genes that participate in proliferation, survival and development (Du & Montminy, 1998). Although phosphorylation of CREB1 on S102 appears to be novel and not yet confirmed as a regulatory mechanism of CREB1 activity, additional investigation could define its function in grade II meningioma.

Similarly to our global proteome analysis, we completed grade-specific comparisons to establish phosphoprotein signatures indicative of high-grade meningiomas that are the most therapeutically challenging. We generated Volcano plots as well as molecular

signatures of phosphoproteins with increased abundance specific to either grade II or III meningioma.

From grade II-specific analyses we identified the upregulation of several phosphoproteins, including CREB1 as discussed above, that might hold promise as targets for therapy in meningioma. Other upregulated grade II phosphoproteins included EFNB2, a ligand of the EPH family of RTKS. Signalling via EPH RTKs and their ephrin ligands plays a role in the control of cell morphology, adhesion, migration and invasion and their involvement in cancer pathogenesis has been described for several years (Pasquale, 2010). Specifically, overexpression of EFNB2 and its phosphorylation on tyrosine residues has been previously identified in the invading GBM cells of patient biopsies (Nakada *et al.*, 2010). In addition, the authors demonstrated phosphorylated EFNB2 to promote cell migration and invasion in the GBM cell line U251 (Nakada *et al.*, 2010). Interestingly, increased expression and activation of several members of the EPH family of RTKs have recently been described in *NF2*-deficient meningioma (Angus *et al.*, 2018). These studies suggest our grade II-specific discovery of EFNB2 expression may be important for meningioma progression and EPH-ephrin signalling should be further explored in these tumours.

In this Chapter we showed upregulation of members of the DEAD-box helicase family as was previously observed in our global proteome dataset. In particular, expression of phosphorylated DDX19B and DDX24 was increased in grade III meningiomas. Phosphorylation of DDX19B as described earlier is known to play a role in the DNA damage response, and whilst phosphosites for DDX24 have been reported in literature, their role on the modulation of protein activity has in general not yet been elucidated (Gustafson & Wessel, 2010; Hodroj *et al.*, 2017). Overall, the aberrant expression of several members of the DEAD-box helicase family across both the phosphoprotein and

global proteome datasets strongly implies that future investigation of this protein family in meningioma could reveal their potential as biomarkers or molecular targets for treatment.

From functional annotation we observed a strong enrichment of grade II-specific phosphoproteins in terms related to cell adhesion, reflecting our identification of proteins such as CDH2. Previous studies have shown phosphorylation of CDH2 on Y860 by the tyrosine kinase SRC, a phosphoprotein we also identified as significantly overexpressed in meningioma, to facilitate CDH2 dissociation from β-catenin in melanoma cells (Qi *et al.*, 2006). Disassembly of the β-catenin-N-cadherin complex results in a reduction of cell-cell adhesion and enhances transendothelial migration of cancer cells, a critical step in metastasis, as well as releasing β-catenin for nuclear translocation and activation of gene transcription (Qi *et al.*, 2006). Phosphorylation of CDH2 might therefore play a role in tumour progression and invasion of meningioma and further studies exploring the inhibition of SRC may provide therapeutic opportunities.

In summary, by investigating the phosphoproteome we have been able to identify the differential expression of phosphorylated proteins in meningioma compared to normal meninges. In addition, we have revealed biological functions and signalling pathways associated with differentially expressed phosphoproteins that with further study might be found to play a role in meningioma pathogenesis. We will select some of the phosphoproteins highlighted in the analyses presented here for experimental validation studies, the results of which are presented in the following chapter.

5 Experimental validation of differentially expressed proteins and phosphoproteins in meningiomas

5.1 Introduction

The use of unbiased omics-based screening techniques has enhanced our knowledge of the molecular landscapes that underlie biological samples. Omics approaches have enabled the investigation of healthy *vs*. diseased states in order to elucidate molecular abnormalities that play a role in pathogenesis. Following initial analysis and functional annotation of large datasets produced by a screening, it is common practice to perform experimental verification on a selection of identified molecules. Differential expression established by data analysis is often verified on a sample set, preferably an independent cohort, using techniques such as WB or IHC, to provide confidence about the previously generated dataset.

This Chapter begins by displaying the results of WB and IHC validation studies of a subset of proteins and phosphoproteins we found to be differentially expressed in meningioma compared to NMT by proteomic analyses. For this project, we decided to concentrate on the validation of significantly upregulated proteins and phosphoproteins compared to NMT. We considered these proteins and phosphoproteins to possess the best potential for establishing novel candidates that may hold promise as molecular therapeutic targets or biomarkers in meningioma. Our selection of significantly upregulated proteins and phosphoproteins for validation was based on a previous association with cancer and the availability of commercial antibodies. Proteomic expression patterns were verified on a subset of the samples screened by MS and an independent cohort of meningioma tissues to substantiate the validity of our results. Following this, we suggest a panel of proteins and phosphoproteins that subsequent to

further investigation may show potential as biomarkers or therapeutic targets of meningioma.

Although we prioritised the validation of a selection of upregulated proteins or phosphoproteins in this project, this does not disregard the importance of investigating the consequences of downregulated proteins or phosphoproteins in meningioma pathogenesis, or indeed their plausibility as meningioma biomarkers upon further studies.

High-throughput omics techniques such as MS-based approaches are able to produce large proteomic datasets often yielding many proteins for investigation. In essence, these approaches are hypothesis generating tools. Identification of a protein of interest is often established by statistical and enrichment analyses of the dataset followed by validation studies to confirm expression in biological samples. Following this, additional evidence is required by performing functional validation studies to demonstrate that identified differences in protein expression have a measurable phenotypic effect relating to the disease state being investigated. Functional validation studies are generally performed *in vitro* and may include the use of inhibitors to block protein function or gene knockdown to reduce expression of a protein of interest. Biological assays like these provide measurable effects on cellular processes such as proliferation or apoptosis that can be used to garner evidence for the importance of a protein in a pathological state and its potential as a therapeutic target.

Here, we also display initial functional validation of the phosphoprotein AKT1 that is upregulated in grade I and II meningioma whilst downregulated in grade III using three inhibitors to determine its potential as a therapeutic target of meningioma.

5.2 Western blot validation of identified proteins and phosphoproteins

We validated our proteomic results firstly using WB on a subset of proteins and phosphoproteins found to be significantly upregulated in meningioma compared to NMT subsequent to analyses of MS datasets. Proteins and phosphoproteins selected for validation studies and their associated $\log_2$ FCs are detailed in Table 5.1. It should be noted that only a minimal amount of tissue lysate was available for some samples to use in validation studies post-MS analysis. This was due to the variability in the amount of frozen tissue we received for each sample as well as the relatively large quantity of starting material (2.5 mg) required for MS. Taking this into consideration, we initially performed WB validation on a selection of those tissue lysates subjected to MS including all three NMT, and three samples each of grade I, II and III meningiomas. To increase confidence in our findings we expanded upon our WB validation studies by sourcing an additional independent cohort of 15 frozen meningioma tissues, five grade I, five grade II and five grade III. Clinical details of all meningiomas used in WB validation are displayed in Tables 2.1 and 2.2. Finally, we performed quantification of the immunoreactive bands and used a one-way ANOVA to ascertain if overexpression of proteins and phosphoproteins visualised by WB was significantly different between tumour grades and NMT.

Protein name	Gene	Log_2 FC (GI *vs.* NMT)	Log_2 FC (GII *vs.* NMT)	Log_2 FC (GIII *vs.* NMT)
Epidermal growth factor receptor	EGFR	1.96	3.33	2.03
Serine/threonine-protein kinase Nek9	pNEK9	5.40	4.16	3.42
Serine/threonine-protein kinase Nek9	NEK9	4.83	4.33	2.89
Retinoblastoma-associated protein	pRB	∞	∞	∞
Isoform 2 of Signal transducer and activator of transcription 2	STAT2	∞	∞	∞
Hexokinase-2	HK2	∞*	∞	∞
Epidermal growth factor receptor kinase substrate 8-like protein 2	EPS8L2	1.66	3.26	3.04
Isoform Alpha of Paxillin	pPXN	3.70	4.26	3.02
Isoform Alpha of Paxillin	PXN	2.65	3.36	2.72
Thyroid receptor-interacting protein 6	TRIP6	∞	∞	∞
Cytoskeleton-associated protein 4	CKAP4	2.63	2.22	2.97
RAC-beta serine/threonine-protein kinase	pAKT2	∞	∞	∞
RAC-alpha serine/threonine-protein kinase	pAKT1	7.00	5.74	4.97

Protein SET	SET	∞	∞	∞
Isoform 2 of Protein SET	SET	3.74	4.00	4.18
Serine/arginine-rich splicing factor 1	SF2/ASF	2.12	1.85	1.95
Protein S100-A10	S100-A10	4.33	3.66	4.13
Copper transport protein ATOX1	ATOX1	∞	∞	∞

*Log_2 FC did not reach significance by Student's two-tailed *t*-test $p < 0.05$.

Table 5.1 Proteins and phosphoproteins selected for validation by WB and IHC. Shown are associated log_2 FC for each meningioma grade compared to NMT.

WB validation on a subset of the 181 proteins identified in proteomic analyses as commonly and significantly upregulated to all meningioma grades compared to NMT included EGFR, NEK9, STAT2 (signal transducer and activator of transcription 2), EPS8L2, PXN, TRIP6 (thyroid receptor-interacting protein 6), CKAP4 (cytoskeleton-associated protein 4), SET, SF2/ASF, S100-A10 (protein S100-A10) and ATOX1. The proteins listed above demonstrated immunoreactivity in the majority of meningiomas across all grades with a weak or absent expression in NMT in both the MS sample subset and in the independent meningioma cohort (Fig. 5.1A and Fig. 5.1C).

Following quantification of WB immunoreactivity, just STAT2 was found to be significantly overexpressed by an average of ~24 fold across all meningioma grades compared to NMT in the MS sample subset (Fig. 5.1B). EPS8L2, PXN, TRIP6 and CKAP4 were all shown to be significantly overexpressed in at least two out of three meningioma grades; whilst SF2/ASF, S100-A10 and ATOX1 were significantly overexpressed in one grade only (Fig. 5.1B). EGFR and SET did not reach significant

overexpression in any meningioma grade compared to NMT subsequent to quantification (Fig. 5.1B).

From WB quantification of the same commonly upregulated proteins described above in the independent meningioma cohort, we established significant overexpression across all meningioma grades with an average of ~15 fold for EGFR, ~6 fold for NEK9, ~10 fold for STAT2, ~4 fold for EPS8L2, ~8 fold for CKAP4 and ~16 fold for SET in all grades compared to NMT (Fig. 5.1D). Significant overexpression was shown by SF2/ASF and ATOX1 in two of three meningioma grades compared to NMT; PXN and TRIP6 were significantly overexpressed in one grade; whilst S100-A10 failed to reach significant overexpression by WB quantification (Fig. 5.1D).

Further, we confirmed by WB the grade-specific significant overexpression of HK2 in grade II and III meningioma compared to both grade I and NMT in the independent cohort (Fig. 5.1C and 5.1D). Significant overexpression was also observed in grade III meningioma compared to grade I and NMT in the MS sample subset (Fig. 5.1A and 5.1B). Indeed, HK2 was identified as a potential biomarker of high-grade meningioma in our previous data analysis (Fig.3.5B and 3.5C; Fig. 3.6).

Among the phosphoproteins, we validated the phosphorylation of pNEK9-T210, pRB-S780, pRB-S807/811, pPXN-Y118, pAKT1-S473 and pAKT2-S474 by WB and discovered a similar pattern of expression by both the MS sample subset and the independent cohort of tumours (Fig. 5.1A and 5.1C). Overexpression of pNEK9-T210 was observed in the majority of tumours across all meningioma grades in the MS sample subset, and was clearly seen in every tumour sample of the independent cohort with an absence of immunoreactivity in NMT (Fig. 5.1A and 5.1C). The phosphorylation of RB on S780 and S807/811 was identified in the majority of grade I and II meningiomas but showed variable immunoreactivity in grade III. We also investigated the presence of total

RB by WB. Consistent expression of RB was established across all tumours of the independent cohort and most tumours of the MS sample set except the grade III meningiomas; whilst in NMT expression was weak or absent (Fig. 5.1A and 5.1C).

The overexpression of pPXN-Y118 was seen in all but one of the MS tumour subset WB (Fig. 5.1A) and was also found overexpressed among all tumour grades of the independent cohort compared to NMT, although immunoreactivity was more variable within each grade (Fig. 5.1C). We detected consistent expression of pAKT1-S473 in mainly grade I and II tumours with minimal expression in grade III or NMT, whilst protein levels of AKT1 remained constant across all grades with weaker or absent expression in NMT (Fig. 5.1A and 5.1C). Immunoreactivity of pAKT2-S474 was also found predominantly in grade I and II meningiomas but with greater variability of expression than pAKT1-S473. Expression of AKT2, like AKT1, was strong across tumours in all grades with weak presence in NMT (Fig. 5.1A and 5.1C).

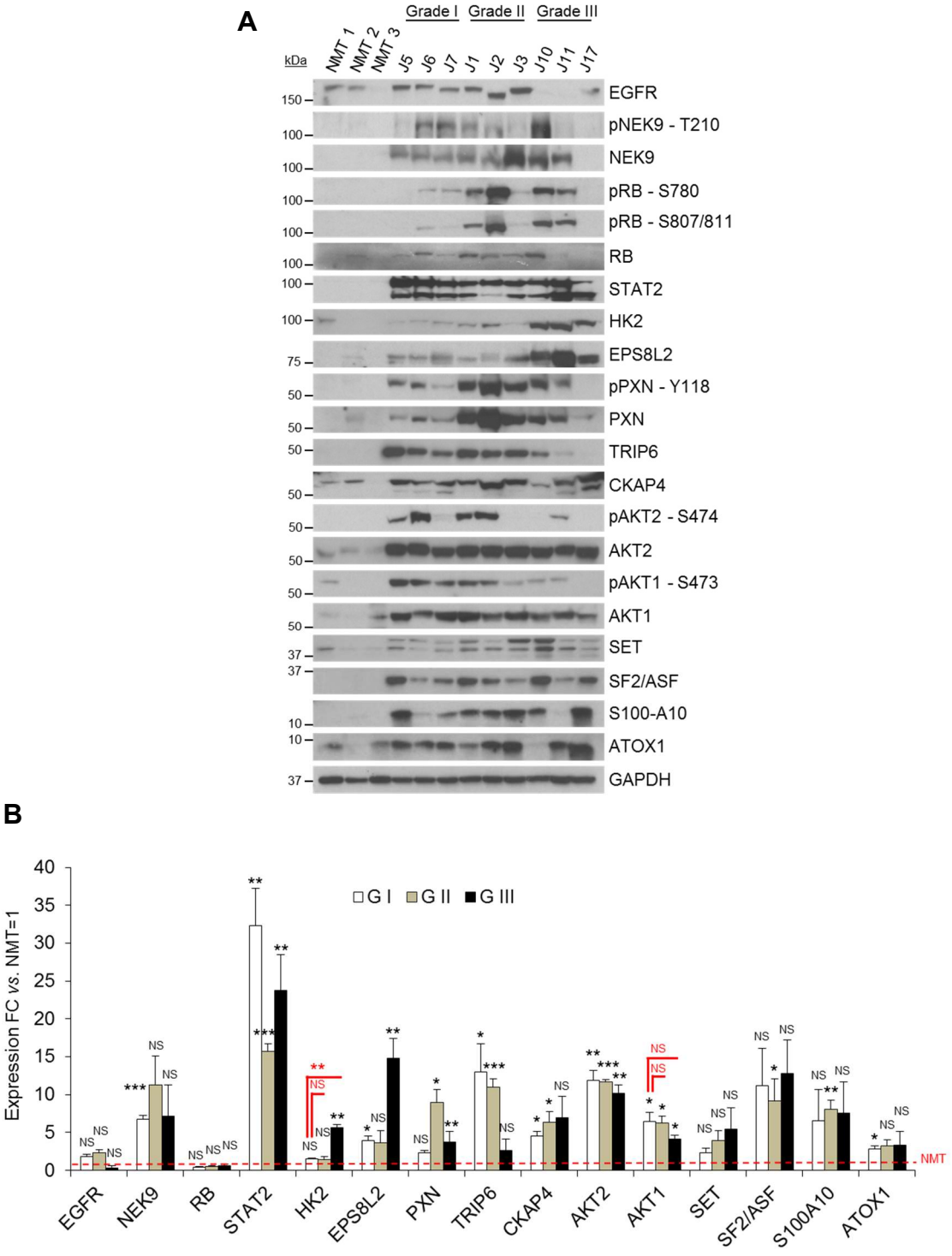
A
Grade I
Grade II
Grade III
kDa
NMT 1
NMT 2
NMT 3
J5
J6
J7
J1
J2
J3
J10
J11
J17
150
EGFR
100
pNEK9 - T210
100
NEK9
100
pRB - S780
100
pRB - S807/811
100
RB
100
STAT2
100
HK2
75
EPS8L2
50
pPXN - Y118
50
PXN
50
TRIP6
50
CKAP4
50
pAKT2 - S474
50
AKT2
50
pAKT1 - S473
50
AKT1
37
SET
37
SF2/ASF
10
S100-A10
10
ATOX1
37
GAPDH
B
Expression FC vs. NMT=1
G I
G II
G III
NMT
EGFR
NEK9
RB
STAT2
HK2
EPS8L2
PXN
TRIP6
CKAP4
AKT2
AKT1
SET
SF2/ASF
S100A10
ATOX1

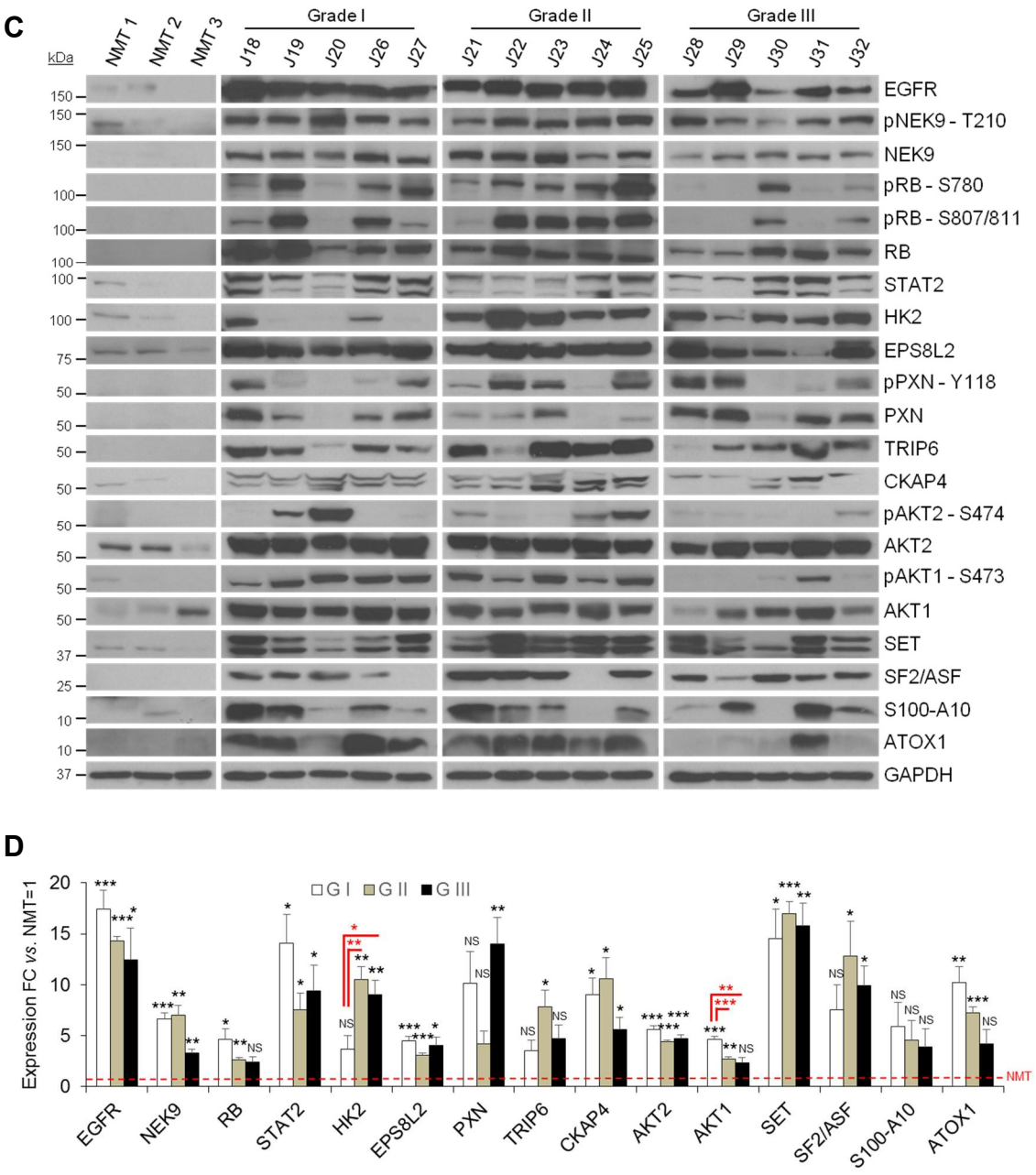

Figure 5.1 Western blot validation of proteins and phosphoproteins. WB analysis of a subset of proteins and phosphoproteins identified as significantly upregulated in meningiomas *vs*. NMT by MS analysis. GAPDH was used as loading control. (**A**) Selection of meningiomas analysed by MS with clinical details presented in Table 2.1. NMT *n*=3; grade I *n*=3, grade II *n*=3 and grade III *n*=3. (**B**) Histogram representing WB quantification of EGFR, NEK9, RB, STAT2, HK2, EPS8L2, PXN, TRIP6, CKAP4, AKT2, AKT1, SET, SF2/ASF, S100-A10 and ATOX1 shown in (A) compared to levels in NMT. Data are presented as mean ± SEM. (**C**) Independent cohort of meningiomas. Clinical details of the cohort are presented in Table 2.2. NMT *n*=3; grade I *n*=5, grade II *n*=5 and grade III *n*=5. (**D**) Histogram representing WB quantification of EGFR, NEK9,

RB, STAT2, HK2, EPS8L2, PXN, TRIP6, CKAP4, AKT2, AKT1, SET, SF2/ASF, S100-A10 and ATOX1 shown in (B) compared to levels in NMT. Data are presented as mean ± SEM. Red bars in histograms show grade-specific quantification. Statistical significance is shown by: NS $p \geq 0.05$; * $p < 0.05$; ** $p < 0.01$; *** $p < 0.001$.

In addition to the proteins and phosphoproteins validated above, we also validated the overexpression of the DEAD-box RNA helicase DDX17, identified as commonly and significantly upregulated across all meningioma grades following MS analysis. WB revealed several immunoreactive bands between 100 and 50 kDa after probing for DDX17 expression. Isoforms of DDX17 are described to have molecular weights of 72 and 82 kDa (Uhlmann-Schiffler, Rossler & Stahl, 2002); to determine the specificity of the observed bands we applied a blocking peptide specific for DDX17. By using a single NMT sample alongside one sample each of grade I, II and III meningiomas we confirmed bands visualised between 100 kDa and 50 kDa were specific for DDX17, whilst no expression was detected upon addition of blocking peptide (Fig. 5.2A).

Next, we validated the expression of DDX17 in the meningioma panel analysed by MS as well as the independent meningioma cohort (Fig 5.2B and 5.2D). The most prominent band seen in all tumour samples by WB was situated above the 75 kDa molecular marker representative of the 82 kDa isoform of DDX17. This band was also detected in some NMT. We then quantified the expression of the heaviest band for both blots and identified significant overexpression by ~3 folds in grade III meningioma compared to NMT in the independent cohort only (Fig. 5.2C and 5.2E). However, additional bands representing DDX17 isoforms at lower molecular weights could also be seen in many of the tumours across all grades with no expression observed in NMT samples following WB validation of both cohorts (Fig 5.2B and 5.2D).

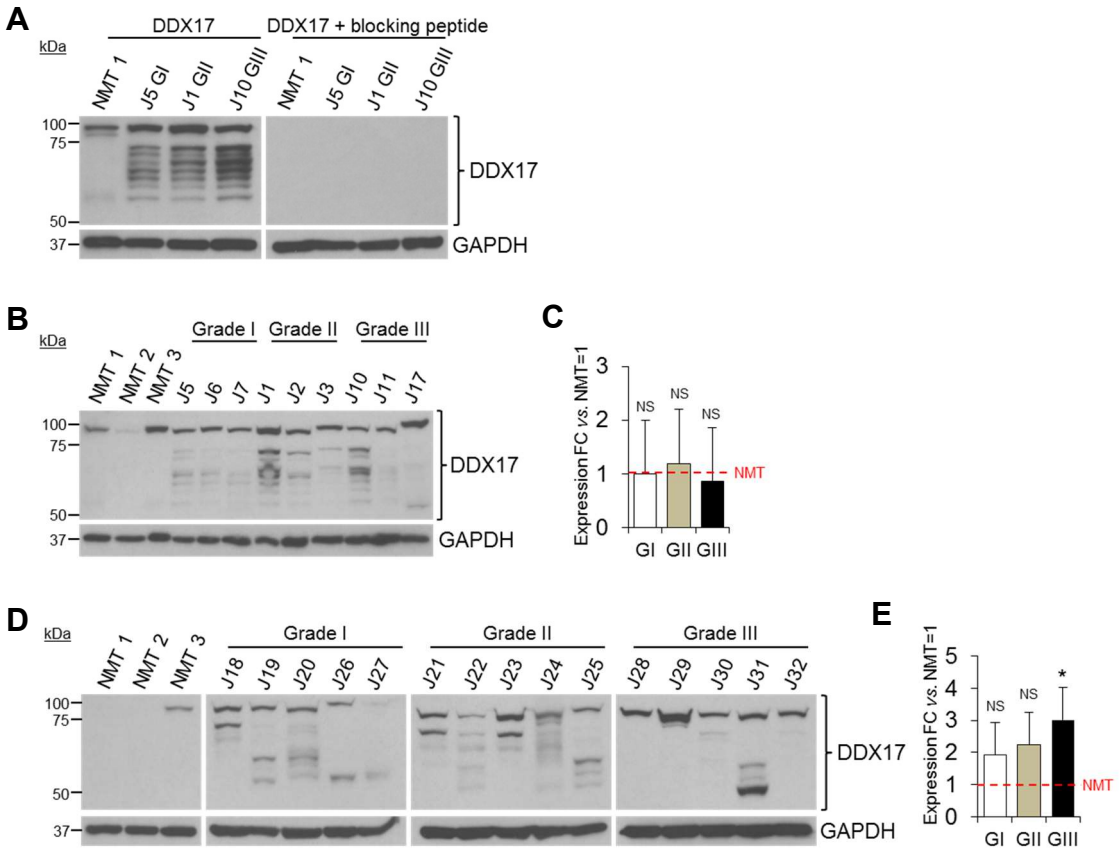

Figure 5.2 Validation of the commonly and significantly upregulated protein DDX17. (**A**) WB analysis was performed on a single tissue lysate from each sample group analysed by MS and probed with anti-DDX17 antibody alone or combined anti-DDX17 antibody and DDX17 specific blocking peptide. (**B**) WB validation of DDX17 on a selection of meningiomas analysed by MS with clinical details presented in Table 2.1. NMT *n*=3; grade I *n*=3, grade II *n*=3 and grade III *n*=3. (**C**) Histogram representing WB quantification of DDX17 shown in (B) compared to NMT. Data are presented as mean ± SEM. (**D**) WB validation of DDX17 on an independent cohort of meningiomas. Clinical details of the cohort are presented in Table 2.2. NMT *n*=3; grade I *n*=5, grade II *n*=5 and grade III *n*=5. (**E**) Histogram representing WB quantification of DDX17 shown in (D) compared to NMT. GAPDH used as loading control in all WB. Data are presented as mean ± SEM. Statistical significance in histograms is shown by: NS $p \geq 0.05$; * $p < 0.05$; ** $p < 0.01$; *** $p < 0.001$.

5.3 Immunohistochemistry validation of identified proteins and phosphoproteins

In addition to WB, we also used IHC to validate the differential expression of proteins and phosphoproteins in meningioma compared to NMT. By performing IHC we were also able to expand our cohorts of meningioma and non-neoplastic human meninges. This was of particular importance for the control, as all prior experiments throughout the project were conducted with three normal meningeal tissues. Whilst an *n* number of three does allow statistical analyses to be applied, we wanted to add robustness to our results by expanding the control cohort. Overall, we used 10 sections per sample group (NMT, grade I, II and III) to examine the expression levels of a selected protein or phosphoprotein. To eliminate the possibility of false positive immunostaining due to nonspecific binding of secondary antibody, negative controls were completed by omission of primary antibody. Presented in this section will be representative images of each sample group following protein or phosphoprotein immunostaining. Semi-quantitative scoring of immunostaining intensities can be found in Supplementary Table S9.

The majority of proteins that demonstrated significant overexpression in every grade compared to NMT after WB quantification (EGFR, NEK9, STAT2, CKAP4 and SET) (Fig. 5.1D) also showed a similar trend by IHC and are displayed in Figure 5.3A. Immunostaining scoring of EGFR, NEK9, STAT2, CKAP4 and SET was absent or weak in normal meninges with higher expression in the majority of meningiomas across all grades (Supplementary Table S9). Immunostaining revealed a largely cytoplasmic localisation for NEK9, STAT2 and CKAP4; SET was found to be predominantly nuclear, while EGFR localised to the cytoplasm and plasma membrane (Fig. 5.3A). HK2 demonstrated an expression pattern strongest in high-grade meningioma and largely

absent in normal meninges with widespread cytoplasmic and some macrophage staining (Fig. 5.3A). This expression pattern was consistent with previous data analyses and WB validation of HK2 in high-grade tumours (Fig.3.5B and 3.5C; Fig. 3.6; Fig. 5.1A-D).

Of the phosphoproteins, those that demonstrated expression most reflective of WB validation results included pNEK9-T210 and pAKT1-S473. Immunostaining of pNEK9-T210 was found to be predominantly nuclear and stronger across tumours compared to normal meninges; whilst pAKT1-S473 showed increased staining in lower grade meningioma compared to grade III, localising mainly to the cytoplasm and sometimes nuclear, with generally weaker staining in normal meninges (Fig. 5.3A). Staining of the AKT2 isoform for phosphorylation on S474 can often not be distinguished from staining for the phosphosites of AKT1 and AKT3 and so immunostaining of pAKT2-S474 was not conducted at this time. We also completed staining for total AKT1 and AKT2 to determine if expression was consistent across tumours as seen by WB. Expression of AKT1 was localised to the cytoplasm of cells and frequently higher across tumours compared to a weaker or absent expression in normal meninges, a pattern also seen by WB (Fig. 5.3A). AKT2 could not be observed in normal meninges, whilst in meningioma it was present only at low levels in under half of all tumours stained with a granular cytoplasmic appearance (Fig. 5.3A). This is in contrast to strong detection of AKT2 across all tumours observed in WB with weaker expression in NMT (Fig. 5.1A and 5.1C).

IHC validation for the remaining proteins and phosphoproteins validated by WB are displayed in Figure 5.3B. These proteins and phosphoproteins may not have produced a significant overexpression in each meningioma WHO grade compared to NMT following WB analysis and quantification, but were validated by IHC to obtain additional insight of their presence in tumours compared to normal meninges.

The proteins TRIP6, SF2/ASF, ATOX1 and DDX17 each displayed a general increase in immunostaining across tumours of all WHO grades compared to normal meninges (Fig. 5.3B). These results were analogous to immunoreactivity seen by WB despite significance not always being reached between each grade compared to NMT following quantification (Fig. 5.1A-D and Fig. 5.2B-E). TRIP6 immunostaining showed widespread cytoplasmic and some focal membrane expression, whilst SF2/ASF exhibited nuclear presence with weaker widespread cytoplasmic staining (Fig. 5.3B). DDX17 largely displayed a strong nuclear and cytoplasmic localisation although nuclear expression was occasionally lost in some grade III meningiomas (Fig. 5.3B). Finally, ATOX1 immunostaining was not detected among the 10 normal meninges, whilst tumour cells showed weak staining that appeared to be mainly localised to tumour-associated macrophages (Fig. 5.3B).

Finally, proteins and phosphoproteins including pRB-S780, pRB-S807/811, RB, EPS8L2, pPXN-Y118, PXN and S100-A10 did not display a clear correlation between protein expression observed in WB validation and that seen by IHC.

pRB-S780 and pRB-S807/811 produced the strongest immunostaining in grade III meningiomas with weaker expression in lower grades and weak or absent staining in normal meninges (Fig. 5.3B). This observation was in contrast with WB validation of the independent meningioma cohort in which pRB-S780 and pRB-S807/811 showed inconsistent expression in grade III tumours (Fig. 5.1C). Localisation of pRB-S807/811 was strongly nuclear, whilst pRB-S780 localisation was generally weak staining occasionally localised to dividing tumour cells (Fig. 5.3B). Immunostaining for RB was low in both grade I meningioma and normal meninges, increasing in intensity with increasing grade, with grade III tumours producing the strongest staining for RB showing a cytoplasmic and nuclear presence (Fig. 5.3B). Again this observation was not reflective

of WB validation for RB, which exhibited high expression of RB across all grades, especially from the independent meningioma cohort (Fig. 5.1C).

EPS8L2 staining did not produce a clear difference between meninges and tumours by IHC, with both showing low level diffuse cytoplasmic expression (Fig. 5.3B). These results were not reflective of the significant overexpression of EPS8L2 found between each meningioma grade compared to NMT by WB quantification of the independent cohort (Fig. 5.1D).

Validation of pPXN-Y118 and total PXN by WB showed variable expression across all meningioma grades with minimal or absent expression in NMT. However, neither staining of PXN nor pPXN-Y118 produced a detectable difference in expression between tumours and normal meninges following IHC validation (Fig. 5.3B). Immunostaining was high across tumours and control for both total PXN and pPXN-Y118, of note pPXN-Y118 showed strong nuclear localisation whilst PXN displayed scattered staining of nuclei with some cytoplasmic localisation. Similar to pPXN-Y118 and total PXN, S100-A10 displayed strong staining across tumours and normal meninges with no observable differences (Fig. 5.3B).

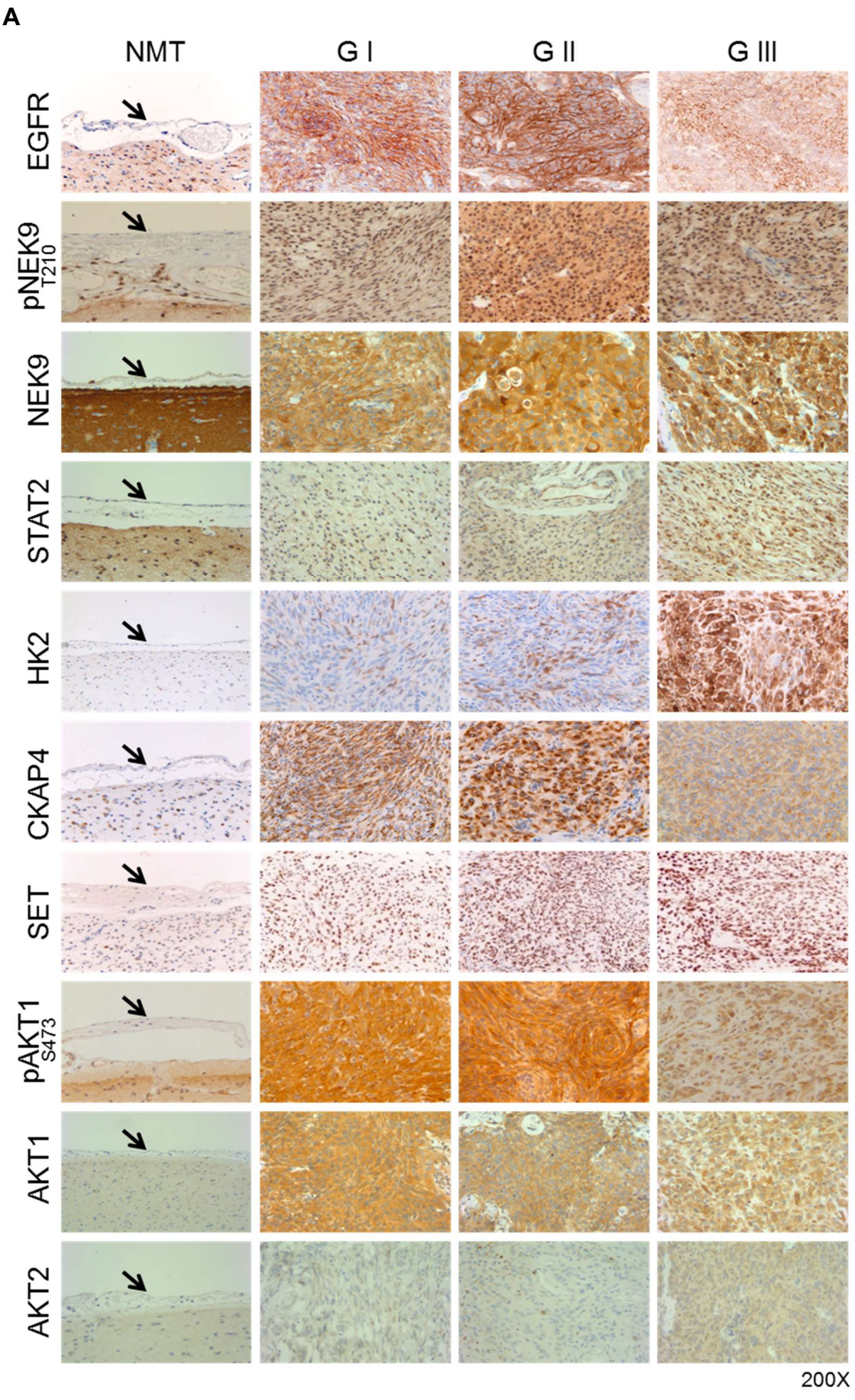
A
NMT
G I
G II
G III
EGFR
pNEK9 T210
NEK9
STAT2
HK2
CKAP4
SET
pAKT1 S473
AKT1
AKT2
200X

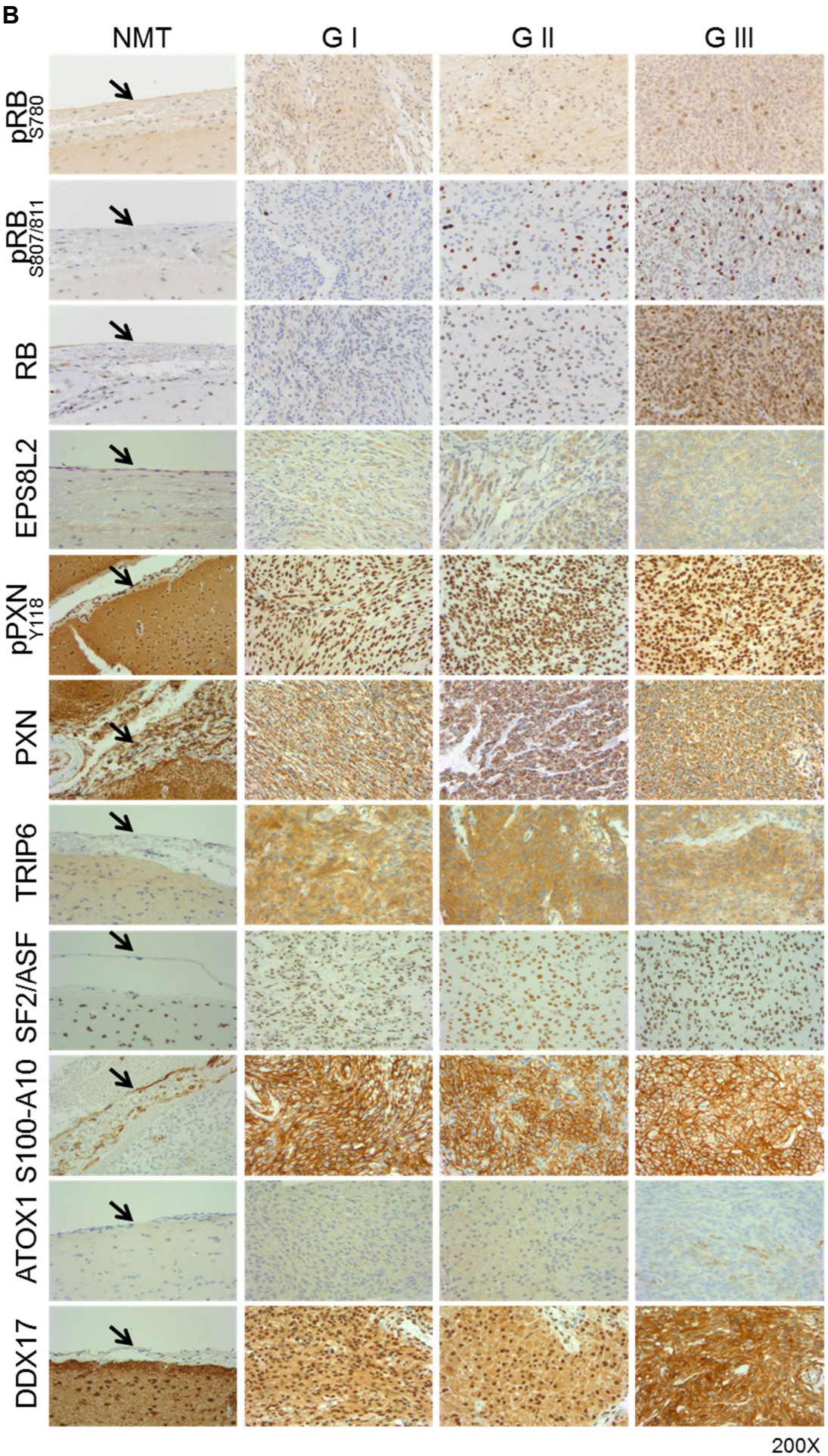
B
NMT
G I
G II
G III
pRB S780
pRB S807/811
RB
EPS8L2
pPXN Y118
PXN
TRIP6
SF2/ASF
S100-A10
ATOX1
DDX17
200X

Figure 5.3 Immunohistochemistry validation of proteins and phosphoproteins. Representative images showing the immunohistochemical staining of a subset of proteins and phosphoproteins identified as significantly upregulated in meningiomas *vs*. NMT by MS analysis. (**A**) Immunostaining of proteins and phosphoproteins that displayed a trend of expression similar to that seen in WB validation including EGFR, pNEK9-T210, NEK9, STAT2, HK2, CKAP4, SET, pAKT1-S473. (**B**) Immunostaining of proteins and phosphoproteins that did not display significant overexpression in each meningioma WHO grade compared to NMT by WB. Proteins shown are pRB-S780, pRB-S807/811, RB, EPS8L2, pPXN-Y118, PXN, TRIP6, SF2/ASF, S100-A10, ATOX1, DDX17. Black arrows annotate normal meninges. Images were taken at x200 magnification. NMT n=10; grade I n=10; grade II n=10 and grade III n=10. Semi-quantitative scoring of immunostaining intensities can be found in Supplementary Table S9.

5.4 Functional validation of pAKT1 S473 as a grade-specific target in meningioma

In the final stage of this project, we wanted to expand upon the panel of proteins and phosphoproteins successfully validated as overexpressed in meningiomas by performing some preliminary functional validation studies of a specific candidate. From validation using WB and IHC we identified the significant overexpression of pAKT1-S473 in lower grade meningioma compared to grade III with minimal expression in NMT. We therefore decided to explore the potential of phospho-AKT1 as a grade-specific therapeutic target in lower grade meningioma by functional validation studies. As a pilot experiment, we investigated the effects of an AKT inhibitor *in vitro* in the benign grade I meningioma cell line, BM1, and the malignant meningioma cell line, KT21.

First, we confirmed the activation of the PI3K/AKT/mTOR pathway in the three grades of meningioma *vs*. NMT by analysing two downstream targets: GSK3β and proline-rich AKT substrate of 40 kDa (PRAS40). The PI3K/AKT/mTOR pathway is

activated by stimulation of RTKs or GPCRs at the plasma membrane and the subsequent activation of PI3K, which then converts phosphatidylinositol (4, 5)-bisphosphate (PIP_2) to PIP_3 (Manning & Toker, 2017). AKT1 is recruited to the membrane by interaction with PIP_3 where it is phosphorylated on T308 by PDK1 (3-phosphoinositide-dependent protein kinase 1) (Alessi *et al.*, 1997). Phosphorylation of T308 in the catalytic domain of AKT1 is one of two residues key for AKT1 activation (Alessi *et al.*, 1996). In order for AKT1 to achieve full kinase activation, phosphorylation of S473 is also required (Alessi *et al.*, 1996). The primary kinase of S473 is mTORC2 whose activity is generally known to be stimulated in a PI3K-dependent manner at the plasma membrane (Sarbassov *et al.*, 2005); however a recent study has also showed mTORC2 activity at the plasma membrane in a PI3K-independent manner (Ebner *et al.*, 2017). Activated AKT1 phosphorylates downstream substrates including GSK3β and PRAS40 inhibiting their activity, preventing their inhibition of downstream cellular functions such as cell survival, proliferation, metabolism and growth (Wang *et al.*, 2012). Figure 5.4 provides an overview of the PI3K/AKT/mTOR pathway.

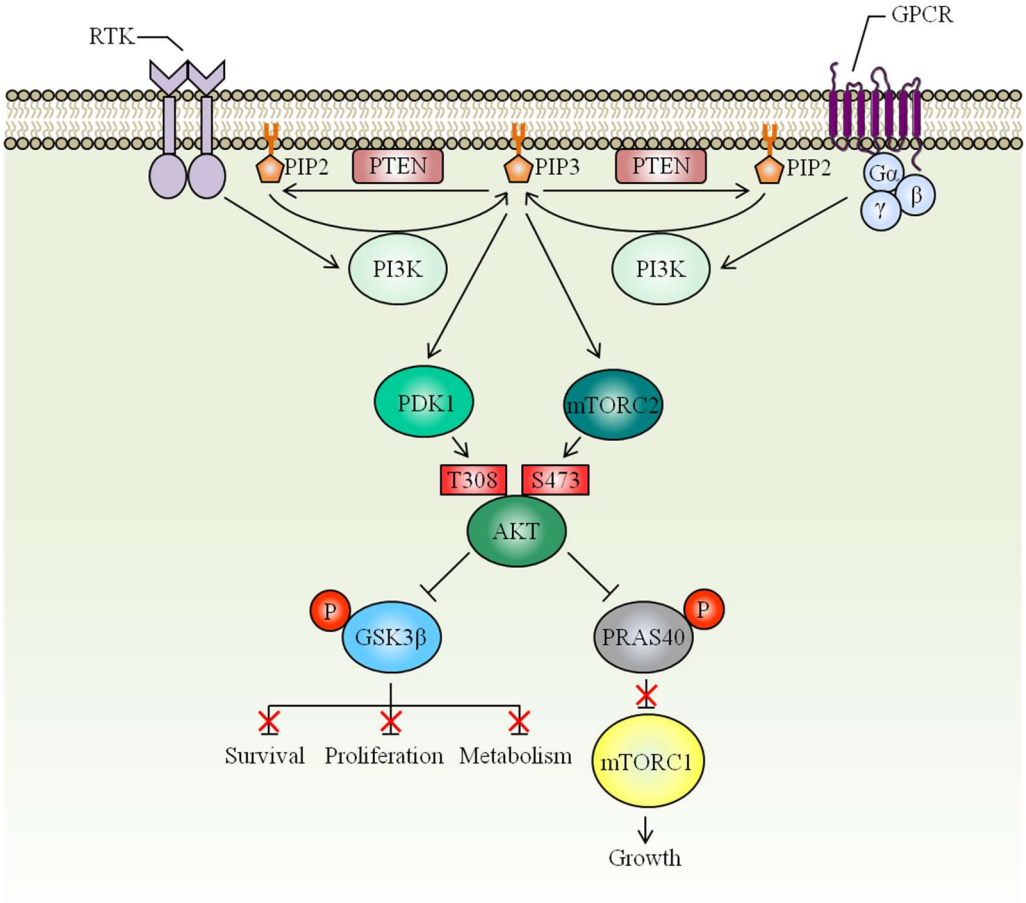

Figure 5.4 Schematic representation of the activation and regulation of AKT. Stimulation of GPCRs and RTKs at the plasma membrane activates PI3K leading to the phosphorylation of PIP_2 to generate PIP_3. Co-localisation of PDK1 and inactive AKT at the plasma membrane by PIP_3 results in phosphorylation of AKT on T308 by PDK1. Phosphorylation of AKT on S473 by mTORC2 is required for full kinase activity and is suggested to occur in a PI3K-dependent manner at the plasma membrane. Activated AKT phosphorylates downstream substrates GSK3β and PRAS40 resulting in their inhibition and subsequent inhibitory release on downstream cellular processes. GPCR, G-protein coupled receptor; RTK, receptor tyrosine kinase; PIP2, phosphatidylinositol (4, 5)-bisphosphate; PIP3, phosphatidylinositol (3, 4, 5)-trisphosphate; PTEN, phosphatase and tensin homologue deleted on chromosome 10; PI3K, phosphoinositide 3-kinase; PDK1, 3-phosphoinositide-dependent protein kinase 1; mTORC2, mammalian target of rapamycin complex 2; GSK3β, glycogen synthase kinase 3β; PRAS40, proline-rich AKT substrate of 40 kDa; mTORC1, mammalian target of rapamycin complex1. Image adapted from Manning *et al*. (2017) and Wang *et al*. (2012) (Manning & Toker, 2017; Wang *et al.*, 2012).

We completed WB analysis on the independent meningioma cohort for GSK3β phosphorylated on serine 9 and PRAS40 phosphorylated on threonine 246 by AKT1 (Fig. 5.5). Expression of pGSK3β-S9 and pPRAS40-T246 followed a trend similar to pAKT1-S473, showing lower expression in grade III compared to grade I and II meningiomas (Fig. 5.5A). Presence of GSK3β and PRAS40 were also reduced in grade III meningioma whilst generally displaying stronger immunoreactivity in grade I and II (Fig. 5.5A). WB quantification of GSK3β and PRAS40 showed significant overexpression in both grade I and grade II *vs*. NMT but not between grade III *vs*. NMT (Fig. 5.5B). Moreover, expression of GSK3β and PRAS40 were both significantly overexpressed in grade I and II meningioma compared to grade III (Fig. 5.5B). These results thus warranted further investigation into the potential of pAKT1-S473 as a therapeutic target of low-grade meningiomas.

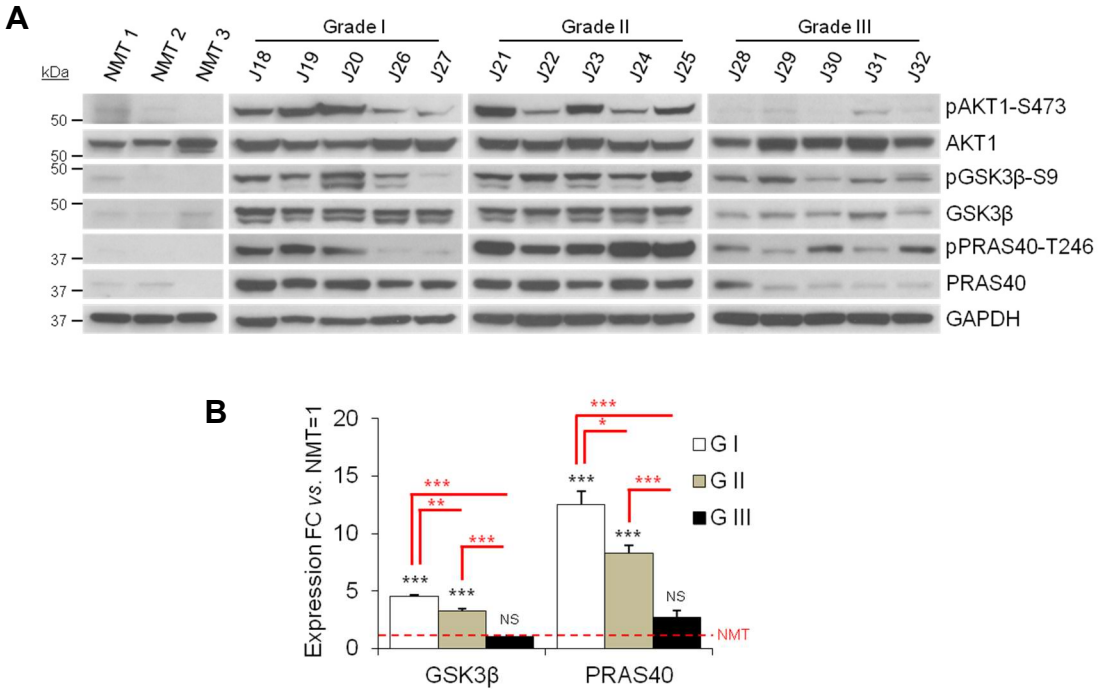

Figure 5.5 Phosphorylation of downstream AKT substrates in meningioma. (**A**) WB analysis of the cellular AKT substrates pGSK3β-S9 and pPRAS40-T246 in NMT and meningioma tumour lysates of all WHO grades (NMT *n*=3; grade I *n*=5, grade II *n*=5 and grade III *n*=5). GAPDH was used as loading control. (**B**) Histogram representing WB quantification of GSK3β and PRAS40 compared to levels in NMT. Data are presented as mean ± SEM. Red bars show grade-specific quantification. Statistical significance is shown by: NS $p \geq 0.05$; * $p < 0.05$; ** $p < 0.01$; *** $p < 0.001$.

Next, we examined pAKT1-S473 expression in HMC, BM1 and KT21 cell lines by WB and determined that whilst both BM1 and KT21 showed increased pAKT1-S473 levels compared to HMC, KT21 demonstrated a significant reduction in pAKT1-S473 compared to BM1 (Fig. 5.6A and 5.6B). These results were reflective of pAKT1-S473 expression levels seen earlier in patient-derived grade I and III meningiomas (Fig. 5.5) and justified our use of BM1 and KT21 as model systems for functional validation studies of pAKT1-S473.

To decipher if elevated levels of pAKT1-S473 in lower grade meningiomas could be a potential target for therapy we tested the pan-AKT kinase inhibitor, AZD5363. This inhibitor has previously shown efficacy in the treatment of metastatic grade I meningothelial meningioma harbouring the $AKT1^{E17K}$ mutation (Weller *et al.*, 2017). In addition, AZD5363 was well tolerated and demonstrated tumour regression in a recent phase I trial of *PIK3CA*-mutated breast and gynaecological cancers, and is further being used in a phase II trial of combinatorial treatment for castration-resistant prostate cancer that is now recruiting (NCT02525068) (Banerji *et al.*, 2018).

AZD5363 activity is determined by its ability to prevent the phosphorylation of the AKT substrates GSK3β and PRAS40 (Davies *et al.*, 2012). Based on pilot experiments using 1 μM and 5 μM AZD5363, we observed a more pronounced effect on downstream AKT substrates following treatment with 5 μM AZD5363. Thus, we used this concentration to further assess the efficacy of the drug in meningioma cells. We treated BM1 and KT21 cells with 5 μM AZD5363 for 30 minutes, 3, 6 and 24 hours (Fig. 5.6C). The inhibitor was effective in reducing phosphorylation of GSK3β and PRAS40 at 30 minutes post-treatment in both BM1 and KT21 cells, with a greater overall reduction in BM1 cells (Fig. 5.6C). Following the initial reduction at 30 minutes, levels of pGSK3β-S9 began to recover over time in both BM1 and KT21 cells whereas pPRAS-T246 expression remained low during the 24 hours (Fig. 5.6C). Total amounts of GSK3β and PRAS40 did not change over the 24 hours. We did however observe an increase in both pAKT1-S473 and pAKT1-T308 compared to vehicle following administration of AZD5363. This is an expected effect of AZD5363, which when bound to AKT is reported to increase its phosphorylation (Davies *et al.*, 2012). This action has been described to occur with other ATP competitive, catalytic inhibitors of AKT and results in the protein being kept in a hyperphosphorylated state that inactivates its catalytic function (Davies *et al.*, 2012; Okuzumi *et al.*, 2009).

To assess the effect of AZD5363 on cell viability we treated BM1 and KT21 cells with increasing concentrations of AZD5363 for 72 hours, including administration of fresh inhibitor every 24 hours, and measured viability at 72 hours (Fig. 5.6D). BM1 cells showed a more pronounced concentration-dependent reduction in cell viability than KT21 cells (Fig. 5.6D). However, the IC_{50} of BM1 and KT21 cells were high at 33.13 μM and 67.79 μM, respectively (Fig. 5.6D). Nonetheless, the IC_{50} of BM1 cells was observed to be approximately half that of KT21 suggesting that AKT1 inhibition may be more effective in reducing cell viability in lower rather than high-grade meningioma.

Following our previous result, we tested the efficacy of AZD5363 in grade I primary meningioma cells. Unfortunately, we were unable to perform treatments of primary grade III meningioma cells due to lack of samples for this very rare subtype. Initially, we checked the pAKT1-S473 expression in a selection of primary meningioma cells compared to HMC by WB (Fig. 5.6E). Primary cells included the genotypes: two $NF2^{-/-}$, two $NF2^{+/+}$ and two $AKT1^{E17K}$ mutants. We saw an increase of pAKT1-S473 expression compared to HMC in all primary meningioma cells except MN052 (Fig. 5.6E). Expression did not appear to be *NF2* dependent although was found to be ~6-fold higher in primary $AKT1^{E17K}$ mutant meningioma cells (Fig. 5.6E). Increased pAKT1-S473 expression would be expected of meningiomas harbouring the $AKT1^{E17K}$ mutation, known to cause pathological localisation of AKT1 to the plasma membrane, resulting in constitutive AKT1 activation and subsequent downstream pathway signalling (Carpten *et al.*, 2007).

Next, we treated four primary meningioma cells; MN102, MN080, MN109 and MN110 with AZD5363 for 72 hours, administering fresh inhibitor every 24 hours and measuring cell viability (Fig. 5.6F). In general, all four primaries followed a concentration-dependent reduction in viability. Treatment of the $NF2^{-/-}$ primary MN102

resulted in the least reduction of cell viability with an IC_{50} of 41.59 μM (Fig. 5.6F). Extrapolated IC_{50} values of MN080, MN109 and MN110 were lower than that previously seen for BM1 cells (33.13 μM) with the $AKT1^{E17K}$ mutant meningioma MN110 displaying the lowest IC_{50} of 5.24 μM (Fig. 5.6F).

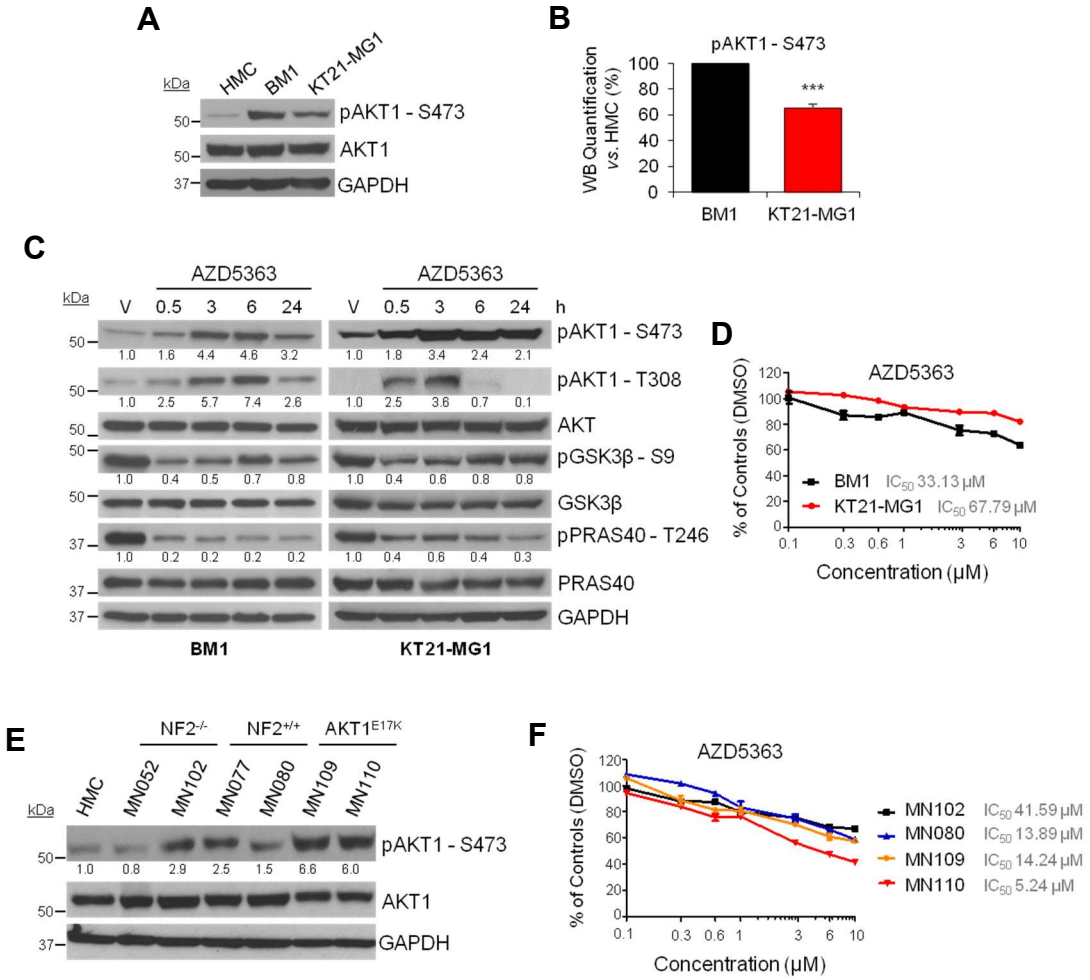

Figure 5.6 AKT inhibition by AZD5363 *in vitro*. (**A** and **B**) WB analysis and quantification of pAKT1-S473 expression in HMC, BM1 and KT21 cell lines. Statistical significance in (**B**) is shown by: NS $p \geq 0.05$; * $p < 0.05$; ** $p < 0.01$; *** $p < 0.001$. (**C**) WB analysis of BM1 and KT21 lysates following treatment with 5 μM AZD5363. Cells were lysed and extracts were analysed for expression of pAKT1-S473, pAKT1-T308 and cellular AKT substrates. Expression of pAKT1-S473, pAKT-T308, pGSK3β-S9 and pPRAS40-T246 was quantified after normalising for the corresponding GAPDH expression and is presented as a fold change of the vehicle. (**D**) Cell viability assay was performed in BM1 and KT21 cells after incubation with the indicated AZD5363 concentrations in triplicate for 72 hours. Fresh drug was administered every 24 hours by removal of media. Corresponding IC_{50} values are reported. Data are presented as mean ± SD. (**E**) WB analysis of pAKT1-S473 expression in HMC and six grade I primary meningioma cells with the following genotypes: two *NF2*$^{-/-}$, two *NF2*$^{+/+}$ and two *AKT1*^{E17K} mutants. Expression of pAKT1-S473 was quantified after normalising for the corresponding GAPDH expression and is

presented as a fold change of HMC. (**F**) Cell viability assay was performed in four grade I primary meningioma cells after incubation with the indicated AZD5363 concentrations in triplicate for 72 hours. Fresh drug was administered every 24 hours by removal of media. Corresponding IC_{50} values are reported. Data are presented as mean ± SD. GAPDH used as loading control in all WB. Cell viability determined using CellTiter-Glo® Luminescent Cell Viability Assay by quantification of ATP present.

To further investigate the constitutive activation of the PI3K/AKT/mTOR pathway in lower grade meningioma we decided to inhibit two well described activators of AKT1; PI3K and mTORC2 (Fig. 5.4). Further, we aimed to establish if targeting either PI3K or mTORC2 may prove more promising candidates for molecular targeted therapy in meningioma than our previous observation of AKT1 inhibition.

Currently, there are no commercially available mTORC2-specific inhibitors and thus we selected the dual mTOR inhibitor Ku-0063794 to inhibit mTORC2 activity in BM1 and KT21 cells (Garcia-Martinez *et al.*, 2009; Murray & Cameron, 2017). Ku-0063794 is a potent inhibitor of the mTOR kinase that sits within complexes mTORC1 and mTORC2 and has formerly shown preclinical efficacy including decreasing the viability and growth of renal cell carcinoma cell lines (Zhang *et al.*, 2013).

We treated BM1 and KT21 cells with 5 μM Ku-0063794 for 30 minutes, 3, 6 and 24 hours (Fig. 5.7A). At 30 minutes post-treatment the inhibitor did not reduce the phosphorylation of GSK3β on S9 in BM1 cells, whilst in contrast, pGSK3β-S9 levels decreased in KT21 cells to less than half that of vehicle-treated cells at 30 minutes following Ku-0063794 application. Detection of pGSK3β-S9 began to recover in KT21 cells at three hours onwards and at 24 hours was at 80% expression of vehicle-treated cells (Fig. 5.7A). Levels of pPRAS40-T246 displayed a similar reduction in BM1 and KT21 cells after treatment with Ku-0063794. The inhibitor was effective at 30 minutes

with around 80% reduction of pPRAS40-T246 expression compared to vehicle in both cell lines. In KT21 cells pPRAS40-T246 levels were restored to approximately 50% of that seen in vehicle at three hours post-treatment and stayed at this level through to 24 hours. Expression of pPRAS40-T246 in BM1 cells at three hours had recovered to double compared to the 30 minutes post-treatment time point and climbed to 60% of vehicle by 24 hours. Overall amounts of GSK3β and PRAS40 did not change in BM1 or KT21 during treatment with Ku-0063794 over the 24 hour period (Fig. 5.7A).

To assess the effect of Ku-0063794 on cell viability, BM1 and KT21 cells were treated with Ku-0063794 at increasing concentrations for 72 hours with fresh inhibitor administered every 24 hours. Cell viability was measured at 72 hours and found to decrease in a concentration-dependent manner in both BM1 and KT21 cells (Fig. 5.7B). However, reduction of viability was found to be greater in BM1 cells with an IC_{50} of 1.14 μM whereas KT21 cells reached IC_{50} at 3.63 μM, over double that of BM1 (Fig. 5.7B).

Next, we investigated the inhibition of PI3K in meningioma using the selective pan-class I PI3K inhibitor BKM120. This drug inhibits PI3K in an ATP competitive manner, leaving other protein or lipid kinases unaffected and does not have significant mTOR inhibitory activity (Maira *et al.*, 2012). Preclinical studies have demonstrated BKM120 to have anti-tumour effects as a single agent therapy or in combination with other therapies (Wang *et al.*, 2016; Zhao *et al.*, 2017). BKM120 has also entered clinical trials for several cancers including GBM (NCT01339052).

BM1 and KT21 cells were treated with 5 μM BKM120 for 30 minutes, 3, 6 and 24 hours (Fig. 5.7C). Expression of pGSK3β-S9 did not decrease following administration of BKM120 in BM1 cells and even demonstrated a 2-fold increase at 24 hours post-treatment compared to vehicle (Fig. 5.7C). However, in KT21 cells BKM120 was effective 30 minutes post-treatment reducing pGSK3β-S9 levels to 50% of vehicle-treated

cells and maintained this decrease until 24 hours when levels began to recover (Fig. 5.7C). Inhibition of PI3K produced pPRAS40-T246 reduction in BM1 analogous to that seen in KT21 cells (Fig. 5.7C). The largest decrease was observed 30 minutes post-treatment with levels of pPRAS40-T246 around 20% that of vehicle (Fig. 5.7C). Levels then gradually increased and at 24 hours had recovered 50% expression of vehicle (Fig. 5.7C). Total amounts of GSK3β and PRAS40 remained constant over the 24 hour period (Fig. 5.7C).

Finally, BM1 and KT21 cells were treated with BKM120 at increasing concentrations for 72 hours applying fresh inhibitor every 24 hours. Although BKM120 produced a concentration-dependent decrease in cell viability in both BM1 and KT21 cells, we did not observe a noticeable difference in efficacy between cell lines (Fig. 5.7D). BM1 cells showed an IC_{50} of 2.30 μM whilst that of KT21 cells was lower at 2.03 μM (Fig. 5.7D).

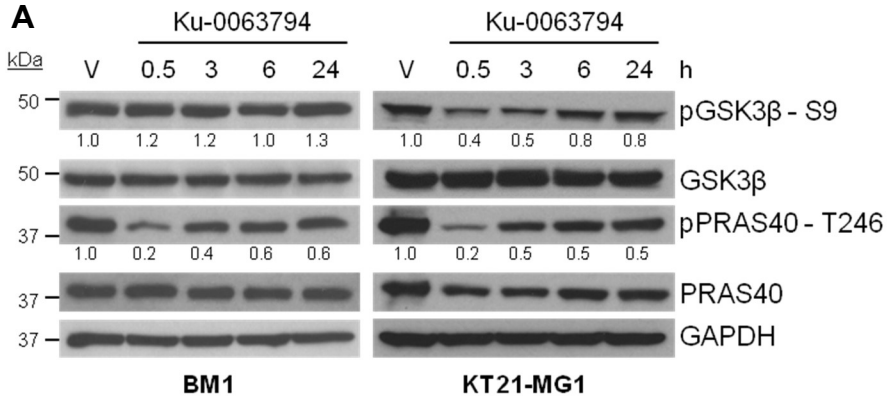
A
Ku-0063794
Ku-0063794
kDa
V 0.5 3 6 24 V 0.5 3 6 24 h
50
pGSK3β - S9
1.0 1.2 1.2 1.0 1.3 1.0 0.4 0.5 0.8 0.8
50
GSK3β
37
pPRAS40 - T246
1.0 0.2 0.4 0.6 0.6 1.0 0.2 0.5 0.5 0.5
37
PRAS40
37
GAPDH
BM1
KT21-MG1

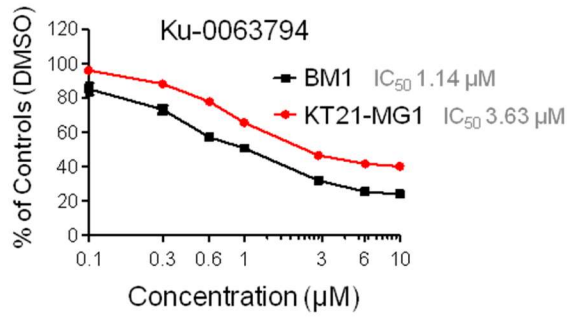
B
Ku-0063794
% of Controls (DMSO)
120
100
80
60
40
20
0
BM1 IC50 1.14 μM
KT21-MG1 IC50 3.63 μM
0.1 0.3 0.6 1 3 6 10
Concentration (μM)

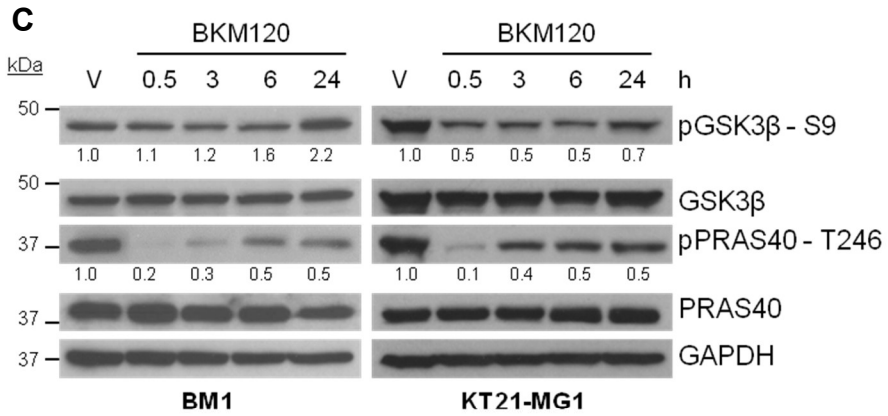
C
BKM120
BKM120
kDa
V 0.5 3 6 24 V 0.5 3 6 24 h
50
pGSK3β - S9
1.0 1.1 1.2 1.6 2.2 1.0 0.5 0.5 0.5 0.7
50
GSK3β
37
pPRAS40 - T246
1.0 0.2 0.3 0.5 0.5 1.0 0.1 0.4 0.5 0.5
37
PRAS40
37
GAPDH
BM1
KT21-MG1

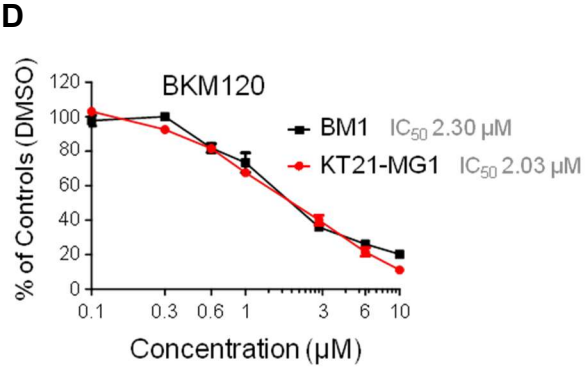
D
BKM120
% of Controls (DMSO)
120
100
80
60
40
20
0
BM1 IC50 2.30 μM
KT21-MG1 IC50 2.03 μM
0.1 0.3 0.6 1 3 6 10
Concentration (μM)

Figure 5.7 Inhibition of PI3K and mTORC2 in BM1 and KT21 cell lines. BM1 and KT21 cells were treated with 5 μM of the dual mTOR inhibitor Ku-0063794 (**A**) or the pan-class I PI3K inhibitor BKM120 (**C**) and cells collected at the indicated time points. Vehicle cells were treated with DMSO for 24 hours. Cell lysates were used for Western blotting to analyse phosphorylation of the downstream effectors GSK3β and PRAS40. Expression of pGSK3β-S9 and pPRAS40-T246 was quantified after normalising for the corresponding GAPDH expression and is presented as a fold change of the vehicle. GAPDH used as loading control in all WB.

BM1 and KT21 cells were plated on 96-well tissue culture plates and then treated with the Ku-0063794 (**B**) or BKM120 (**D**) at the indicated concentrations in triplicate for 72 hours. Fresh drug was administered every 24 hours by removal of media. Cell viability assay was performed at 72 hours. Corresponding IC_{50} values are reported. Data are presented as mean ± SD. Cell viability determined using CellTiter-Glo® Luminescent Cell Viability Assay by quantification of ATP present.

5.5 Discussion

In this chapter we have completed successful experimental validation of several proteins and phosphoproteins identified as overexpressed across all grades of meningioma compared to NMT by MS analyses. Proteins significantly overexpressed in WB quantification of the independent meningioma sample cohort and also upregulated in all WHO grades compared to normal meninges following IHC included EGFR, NEK9, STAT2, CKAP4 and SET. Of these, only STAT2 was significantly overexpressed in all three meningioma grades in the MS sample subset following WB quantification. However, expression of EGFR, NEK9, CKAP4 and SET was clearly present in the majority of tumours even though significance was not always reached. We also validated increased phosphorylation of NEK9 on T210 in all meningioma grades by both WB and IHC, reflecting MS analysis.

We therefore propose the overexpression of EGFR, NEK9, STAT2, CKAP4, SET and pNEK9-T210 as a panel of proteins indicative of meningioma independent of WHO grade. Further investigation should be performed to elucidate upon the consequences of their aberrant expression in meningioma pathogenesis and their potential as candidates for targeted therapy or biomarkers.

Several proteins including TRIP6, SF2/ASF, ATOX1 and DDX17 demonstrated a strong tumour presence across all grades by IHC and WB, although not always significantly overexpressed in all three grades compared to NMT following WB quantification.

Of interest, ATOX1 appeared to localise to tumour-associated macrophages by IHC validation. ATOX1 is expressed during wound healing by macrophages that infiltrate into damaged tissue and function in promoting angiogenesis and tissue repair of the wounded site (Das *et al.*, 2016). Meningiomas are frequently described as highly vascular brain

tumours (Miller *et al.*, 2014). Here, identification of ATOX1 in tumour-associated macrophages of meningioma may suggest a role for its participation in promoting tumour angiogenesis and its potential as a therapeutic target of the tumour microenvironment. Moreover, this finding demonstrates the importance of analysing the tumour microenvironment using tissue proteomics and complementing these analyses with validation techniques such as IHC.

We also identified and validated the grade-specific overexpression of HK2 and pAKT1-S473. Subsequent to MS analyses we previously established HK2 to be significantly upregulated in high-grade meningioma and observed the same expression pattern by WB and IHC validation. In contrast, the phosphoprotein AKT1 was initially identified as commonly and significantly upregulated among all meningioma grades compared to NMT. However, following WB and IHC, levels of pAKT1-S473 were found to be predominantly higher in grade I and II meningioma compared to grade III and NMT. These findings indicate HK2 and pAKT1-S473 as possible grade-specific molecular targets or biomarkers for high-grade and low-grade meningioma, respectively.

Finally, pRB-S780, pRB-S807/811, RB, EPS8L2, pPXN-Y118, PXN and S100-A10 expression did not exhibit a correlation between patterns observed in WB compared to that seen by IHC validation. Here, it must be considered that although WB and IHC are complementary validation techniques, an absolute overlap of results between them cannot be expected. Both techniques are heavily antibody dependent and as the same antibody was not always applicable for both techniques, the outcome observed for the proteins described above could reflect differences in antibody binding and possibly unspecific binding. However, further experimental validation with additional antibodies may therefore reveal a correlation with MS analysis not observed by those used in this project.

In the latter part of this chapter we performed preliminary functional validation studies of pAKT1-S473 to elucidate its potential as a therapeutic target in lower grade meningioma. Initially, we used the specific AKT inhibitor AZD5363 to determine whether AKT inhibition produced a larger reduction in cell viability in grade I than in grade III meningioma cell lines. Here, we confirmed that AZD5363 is effective in its inhibition of AKT seen by the reduced phosphorylation of the downstream substrates GSK3β and PRAS40. In addition, AZD5363 was more effective on grade I cells than grade III cells producing a greater decrease in cell viability. Grade I primary meningioma cells also demonstrated a reduction in viability following AKT inhibition although variable and with high IC_{50} values. These findings would suggest AKT inhibition by AZD5363 alone would not have efficacy as a targeted therapy in meningioma.

Next, we inhibited the AKT1 activators PI3K and mTORC2 to determine if these showed more promise as molecular targets in lower grade meningioma. In general, inhibition of PI3K or mTORC2 was more effective in reducing cell viability of grade I and III cell lines, with much lower IC_{50} values than AKT inhibition. However, it must be considered that the increased efficacy we observe here may not be due to the inhibition of PI3K or mTORC2 alone. Both the PI3K inhibitor BKM120 and the mTOR inhibitor Ku-0063794 are described to have off-target effects that may account for the improved efficacy, as well as the similar responses we observe between grade I and III meningioma cell lines. Indeed, Ku-0063794 is a dual mTOR inhibitor, thus the improved efficacy we detect likely results from the combined inhibition of both mTOR complexes (Garcia-Martinez *et al.*, 2009). Further, we used a cell viability assay to determine the amount of healthy, metabolically active cells as an indicator of inhibitor efficacy following treatment; however, further studies should be performed to fully elucidate whether the inhibitors are exerting a cytotoxic or cytostatic effect on the cells.

In summary, our preliminary studies of pAKT1-S473 in meningioma indicate that targeting key upstream AKT1 activators may be more effective than direct inhibition of AKT1. However, with further investigation it is possible that a combinatorial approach of AKT inhibition with inhibition of PI3K, mTOR or alternative pivotal signalling pathways involved in meningioma pathogenesis may demonstrate increased efficacy as a therapeutic strategy.

6 Discussion

6.1 Introduction

The aim of this project was to define the proteomic signature of all grades of meningioma by employing an MS-based approach, analysing both the global proteome and phosphoproteome to find a panel of proteins and phosphoproteins with potential as molecular targets or biomarkers of these tumours. Omics-based screenings are now frequently utilised to elucidate molecular alterations between healthy and disease states and are undeniably indispensable tools in the move toward developing personalised targeted therapies in cancer. In the case of meningioma, there are currently no drugs approved for treatment by either the FDA (US Food and Drug Administration) or EMA (European Medicines Agency). Surgical resection and radiotherapy remain the predominant treatment options whilst chemotherapeutics show minimal efficacy underlining the urgent need for effective targeted therapies of meningioma.

The research presented here is comparing for the first time both the global and phosphoproteome across all three WHO grades of meningioma to healthy meningeal tissue. Prior to this study, comparative global proteome studies from meningioma tissue specimens have suffered from low sample numbers of the rarest grade III tumours and none have analysed normal meningeal tissue as control in parallel. Further, there were no former comparative analyses of the meningioma phosphoproteome from tissue prior to the start of this work. Only recently has a study by Parada *et al*. (2018) utilised phosphopeptide enrichment to analyse the phosphoproteome of all meningioma grades from tissue, although, the authors did not include a comparison to control tissue as we have here and were thus not able to identify phosphoproteins commonly upregulated to all grades compared to control (Parada *et al.*, 2018). The inclusion of control tissue enabled us to perform not just grade-wise comparisons but to really focus in on proteins

and phosphoproteins that showed abundance in meningioma, whilst absent or less abundant in healthy meninges. In this project we have analysed healthy meninges that include the dura, arachnoid and pia mater. To our knowledge this approach represents the first study to analyse frozen healthy meningeal tissue not adjacent to tumour.

The following sections of this Chapter will discuss the results obtained during the course of this project and their relevance in relation to meningioma pathogenesis, as well as suggest future research to build upon these findings.

6.2 Challenges in sample preparation for MS analysis

MS-based techniques are now used routinely in many laboratories for the identification of proteins, phosphoproteins and phosphopeptides; however complete proteome coverage in cells and tissues is still not entirely possible. The generation of a high quality proteomic dataset achieving comprehensive coverage of protein identification is subject to several challenges in sample preparation.

A sufficient quantity of high quality biological sample is required to obtain an adequate amount of protein for phosphoproteomic analysis, usually in the range of milligrams (Feist & Hummon, 2015). This is not always achievable when analysing patient-derived tumour specimens that vary in mass. In this project we were therefore limited by the amount of patient tissue received from which we could extract a sufficient amount of protein to perform phosphoproteomic analyses. A large amount of starting material enables efficient enrichment of phosphopeptides that are at a much lower abundance in a sample than non-phosphorylated peptides (Mann *et al.*, 2002). Here, we performed phosphoprotein and phosphopeptide enrichments from 2.5 mg of total protein and identified just over 3000 phosphoproteins and 2700 phosphorylation sites. In contrast, a former study of mouse brain starting from 8 mg of total protein detected over 12000

phosphorylation sites following TiO_2 enrichment, thus demonstrating the coverage that can be achieved with ample starting material (Wisniewski *et al.*, 2010).

A further challenge when employing an MS-based proteomic approach are losses endured in steps such as washes and elution during sample preparation (Feist & Hummon, 2015). Sample loss is less prevalent when starting material is not limited and also varies based on the sample preparation method employed (Feist & Hummon, 2015). For instance, sample recovery following in-gel digests has been described to have reduced efficiency than in-solution digestion, with approximately 70-90% of the recovery achieved by in-solution digestion (Shevchenko *et al.*, 2006).

Unfortunately, for a project analysing patient tumour tissue derived during surgical resection, quantity of starting material received is an uncontrollable factor and the most effective sample preparation method to minimise sample loss must be carefully selected.

6.3 Mutational status of meningioma

The growing number of genetic alterations now identified in meningioma, initially led by the defining studies of Clark *et al*. (2013) and Brastianos *et al*. (2013), suggest that omics-based screening approaches of meningioma should be integrated with the mutational background of samples moving forward (Brastianos *et al.*, 2013; Clark *et al.*, 2013). In this way, a more complete overview of the molecular landscape of these tumours will be achieved. Indeed, the recently proposed DNA methylation-based classification system by Sahm *et al*. (2017) took this approach; integrating DNA methylation profiling with known recurrent mutations, copy-number aberrations as well as histology of meningioma to define a stratification system predictive of clinical outcome (Sahm *et al.*, 2017). Taking these studies into consideration we investigated the mutational status of 22 meningioma specimens subjected to MS in this project by NGS and MLPA. We identified 13 tumours with an $NF2^{-/-}$ genotype and five $NF2^{+/+}$ meningiomas, of which none were found to

harbour any further mutations tested for in-house (*AKT1*^{E17K}, *KLF4*^{K409Q}, *TRAF7*^{N520S}, *SMO*^{L412F}, *SMO*^{W535L}, *SMARCB1*^{R374Q}, *SMARCB1*^{R377H} and *POLR2A*^{Q403K}). Four tumours were designated an *NF2*$^{+/-}$ genotype. Of these, two were found to harbour heterozygous *TRAF7*^{N520S} mutations. However, as MLPA failed for three of these cases, it is possible these tumours may also possess a deletion in *NF2* and thus harbour an *NF2*$^{-/-}$ genotype. Based on these findings we did not stratify our proteomic analyses by genotype at this time. We took this decision in order to maintain the maximum sample number within each WHO grade and focus on proteomic profiling stratified by tumour grade and not by mutational status for this project.

Moreover, the mutational background of meningioma does not currently impact on patient treatment options. To date, only one patient with metastatic meningioma has been administered treatment based on the mutational status of the tumour, in this instance the *AKT*^{E17K} mutation (Weller *et al.*, 2017). Indeed, the contributions of recurrent non-*NF2* mutations to meningioma pathogenesis have not yet been characterised (Smith, 2015). Stratification of proteomic profiling by mutational status should certainly be considered as a future extension to this project if adequate sample numbers are reached.

6.4 Global proteome analyses of meningioma

We were able to quantify 3888 proteins across 22 meningioma and three normal meninges by MS. Initially, we analysed data by unsupervised hierarchical clustering based on differentially expressed proteins across all grades of meningioma and NMT. We observed a clear separation of tumours *vs.* controls, as well as a separation between tumour grades. The only exception was the grade III sample J9, which was grouped together with grade II tumours; however, since meningiomas can progress from a grade II to a grade III, we cannot exclude that this tumour may still retain some grade II features. Although hierarchical clustering demonstrated proteomic profiles of meningioma grades were

distinct from each other, the heatmap also displayed a cluster of proteins with increased expression across all meningioma grades compared to NMT. We initially focussed our global proteome analyses around 181 commonly and significantly upregulated proteins identified among all meningioma grades compared to NMT. In doing so, we optimised the potential for discovering proteins targetable for therapy or for use as biomarkers common to all meningioma.

By comparison of our global proteome dataset with the previously generated meningioma proteomes of Sharma *et al*. (2015) we identified 1428 proteins common to both studies and 2460 proteins unique to our dataset (Sharma *et al.*, 2015). Of these 1428 proteins, we established an overlap of 28 proteins also commonly upregulated among all meningioma grades. Among these were CKAP4, S100-A10 and EPS8L2 that we subjected to experimental validation studies discussed later in this chapter. Further, we identified MX1 (interferon-induced GTP-binding protein Mx1), ANP32E (acidic leucine-rich nuclear phosphoprotein 32 family member E), SUPT16H (FACT complex subunit SPT16), NEK9 and DDX42 as commonly upregulated among all grades, which were previously shown by Saydam *et al*. (2010) to be expressed in a human benign meningioma cell line *vs*. human primary arachnoidal cells (Saydam *et al.*, 2010). Identification of an overlap with previous studies strengthens confidence in our findings and in the potential of these overexpressed proteins as targets for meningioma treatment.

Functional annotation analyses of the 181 commonly upregulated proteins allowed us to identify the significant enrichment of biological functions largely related to transcription and post-transcriptional modifications, including a strong enrichment of splicing associated terms. It must be noted here that the relatively low number of proteins (181) submitted for functional annotation limits the coverage of GO terms that can be attained. Therefore, it is a compromise of submitting a more stringent, smaller subset of

significantly relevant proteins with reduced coverage; or submitting a larger protein list, of which not all may be differentially expressed but attain a more comprehensive overview of enriched biological functions. Here, we used only significantly upregulated proteins to establish enriched biological functions at the risk of identifying fewer GO terms, in order to identify dysregulated cellular processes most likely to be a direct consequence of upregulated proteins.

In addition to identifying common molecular signatures between grades, we wanted to characterise protein signatures specific to grade II and III meningiomas as these tumours are the most therapeutically challenging. We performed grade-specific comparisons of proteomic profiles to reveal proteins that might be able to define grade II and III meningiomas.

Proteins upregulated in grade II meningioma included several already associated with tumour progression in other cancers. These included MUC4 as described earlier to be overexpressed in GBM cells (Li *et al.*, 2014b); and the RNA methyltransferase NSUN2 involved in cell proliferation and stem cell differentiation, shown to be overexpressed in many human cancers (Okamoto *et al.*, 2012; Yi *et al.*, 2017). In particular, hypomethylation of the NSUN2 promoter and resultant upregulation of NSUN2 expression was found to enhance cell migration and invasion of breast cancer cells thus promoting tumour progression (Yi *et al.*, 2017). As the DNA methylation profile of meningioma has recently been characterised (Sahm *et al.*, 2017), it would be interesting to determine if grade II meningioma are associated with hypomethylation of NSUN2 as a possible diagnostic biomarker. Here, we report overexpression of MUC4 and NSUN2 for the first time in meningioma as well as their grade II-specificity, warranting their further investigation as novel therapeutic targets or biomarkers of this WHO grade.

Among grade III-specific proteins we observed a significant enrichment in proteins associated with energy metabolism as identified by functional enrichment analysis. Reprogramming of metabolism and associated pathways to support the demands of malignant cells is considered a hallmark of cancer and it has been suggested targeting a combination of metabolic pathways may prove beneficial (DeBerardinis & Chandel, 2016). We identified several proteins associated with metabolic pathways such as ACAD9 (acyl-CoA dehydrogenase family member 9, mitochondrial), ACSS3 (acyl-CoA synthetase short-chain family member 3, mitochondrial) SUCLG2, IDH3A, IDH3B and HK2. Of these, we validated the overexpression of HK2 in high-grade meningioma, which will be discussed later in this Chapter. Taken together, these findings provide the rationale for elucidating the metabolic alterations occurring in high-grade meningioma to identify suitable drug targets for these aggressive tumours.

6.5 Phosphoprotein and phosphopeptide analyses of meningioma

We analysed protein phosphorylation in meningioma as it is estimated that at any one time approximately 30% of the proteins in a cell are phosphorylated, and is a general mechanism of switching "on" and "off" pivotal enzymes and pathways (Cohen, 2000). Most of the signalling molecules whose activity is modulated by phosphorylation are present at very low abundance within the cell, requiring enrichment steps for MS detection; still, a comprehensive analysis of the phosphoproteome using the available enrichment techniques remains a challenge due to the complexity of biological samples (Chandramouli & Qian, 2009). Here, we used a dual approach, employing affinity chromatography to enrich phosphoproteins and TiO_2 to enrich phosphopeptides. The two datasets shared 56% of the identified proteins and several canonical pathways. The number of phosphoproteins identified by phosphoprotein enrichment was more than

double the number of phosphoproteins identified by phosphopeptide enrichment, thus we performed in-depth bioinformatics on the phosphoprotein dataset first.

Following quantification of just over 3000 phosphoproteins we performed unsupervised hierarchical clustering based on differentially expressed phosphoproteins across all grades of meningioma and NMT as control. As was observed for the global proteome dataset, there was a clear separation of tumours *vs.* controls, as well as a separation between tumour grades. Similarly to our global proteome analyses, we initially focussed on characterising the 338 phosphoproteins identified as commonly and significantly upregulated among all meningioma grades. Among these were phosphoproteins that have been well characterised in cancer such as phospho-RB, phospho-SRC or phospho-FAK, and others that are novel. We took several commonly upregulated phosphoproteins through to experimental validation stages including RB, AKT1, AKT2, NEK9 and PXN. In addition, we identified the upregulation of many members of the DOCK-family of GEFs and also detected phosphorylation sites for several DOCK proteins following phosphopeptide enrichment. These findings, together with the functional enrichment of Rho GTPase activity encompassing many DOCK proteins, propose that with further investigation this protein family could be attractive candidates for targeted therapy across meningioma grades.

Grade-wise comparisons of phosphoprotein profiles revealed the DEAD-box RNA helicase family members DDX19B and DDX24 to be phosphorylated and upregulated in grade III meningioma. Overexpression of several members of this family was also detected in our global proteome analyses. This family of proteins play key roles in RNA metabolism using ATP to unwind and separate complex secondary RNA structures thus altering the structure, folding and rearrangement of RNA, aiding in the remodelling of RNA-protein complexes (Jarmoskaite & Russell, 2011). DEAD-box RNA helicases are

reported to be heavily implicated in mRNA processing and translation (Heerma van Voss, van Diest & Raman, 2017). These functions are reflected by the GO terms 'RNA helicase activity', 'RNA secondary structure unwinding' and 'ATP-dependent RNA helicase activity' that we found to show the highest fold enrichment of grade III-specific phosphoproteins, as well as by clusters of enriched GO terms related to pre-mRNA modifications of both commonly upregulated proteins and phosphoproteins. In cancer cells, RNA helicases have been noted for their role in the enhanced protein synthesis requirements and translation of oncogenic mRNAs (Heerma van Voss, van Diest & Raman, 2017). As such, it is now recognised that inhibition of these proteins might hold potential in being exploited for cancer treatments, as could be the case for meningioma pending further research into this family of proteins (Heerma van Voss, van Diest & Raman, 2017).

Phosphopeptide enrichment of eight meningiomas provided us with a complementary dataset to the phosphoprotein enrichment of 14 meningiomas, providing an overlap of 56% phosphoprotein coverage between the two datasets. Whilst we were able to detect over 3600 phosphopeptides corresponding to 1320 phosphoproteins, we were unfortunately not able to validate phosphosites associated with differentially expressed phosphoproteins. Validation studies on phosphoproteins are more challenging as they rely on availability of phospho-specific antibodies and many of the phosphorylation sites identified in this project are yet to be described in literature. Among identified differentially expressed phosphoproteins, we detected phosphosites for several DOCK proteins, as well as NEK9, SET and EPS8L2; of which, the latter three proteins we validated expression on phosphorylation sites already confirmed in literature, or on total protein levels only. Future studies might look to explore the novel phosphorylation sites detected in this project to confirm their presence and any influence they may have on protein activity.

IPA analysis of the 1320 phosphoproteins associated with identified phosphopeptides showed an enrichment of canonical pathways analogous to that observed from the 338 phosphoproteins commonly upregulated among all meningioma grades. The pathway classes most frequently associated with phosphoproteins and phosphopeptides included 'cellular growth, proliferation and development', 'cellular immune response' and 'intracellular and second messenger signalling'. Phosphoprotein and phosphopeptide enrichments were performed on different meningioma cohorts of all grades. Therefore, the identification of canonical pathway upregulation common to both datasets provides us with confidence that these two techniques were complementary of each other. Further investigation could reveal possible targetable signalling pathways within these enriched canonical pathways of the meningioma phosphoproteome.

6.6 Validated proteins and phosphoproteins with potential as therapeutic targets or biomarkers in meningioma

Subsequent to MS analysis and functional annotation we performed experimental validation on a selection of differentially expressed proteins and phosphoproteins. Here, we will discuss proteins that demonstrate the most potential as candidates for targeted therapy or biomarkers of meningioma following experimental validation studies.

Among commonly upregulated proteins we validated the nuclear proto-oncogene SET, which participates in many cellular processes including cell-cycle regulation, gene transcription, epigenetic regulation and cell migration (Mukhopadhyay *et al.*, 2013). SET is overexpressed in various cancers, contributing to tumourigenesis in part through its inhibition of the tumour suppressor phosphatase PP2A (protein phosphatase 2A), which acts as a negative regulator of cellular growth and survival pathways (Mukhopadhyay *et al.*, 2013). Both SET isoforms are also components of the inhibitor of acetyltransferases (INHAT) complex shown to bind histones, predominantly histone H4, and inhibit histone

acetyltransferase activity thus regulating chromatin modification and transcriptional activity (Seo *et al.*, 2001). Interestingly, histone H4 was another commonly upregulated candidate identified by our global proteome analysis. Further, SET has been found to block the function of granzyme proteins released by cytotoxic T lymphocytes (CTLs), critical for the induction of CTL-mediated apoptosis of virally infected or cancer cells (Fan *et al.*, 2003; Trotta *et al.*, 2011). This protein has never been studied in meningioma, but deciphering the causes of its overexpression and identifying its binding partners could clarify which role it plays in the pathogenesis and whether this could lead to a therapeutic intervention.

Another commonly and significantly upregulated protein among all grades was STAT2, a STAT-family member involved in immune response through activation of the JAK/STAT pathway after stimulation with type I interferons (interferon-alpha and interferon-beta) (Au-Yeung, Mandhana & Horvath, 2013). Activated STAT2 forms heterodimers with STAT1, a protein which we also observed as commonly upregulated in all grades (Table 3.1). Phosphorylated STAT1 was previously identified by our group as a common target in *NF2*-negative schwannomas and meningioma BM1 cells and has since been further validated as overexpressed in meningioma by ongoing research in our group (Bassiri *et al.*, 2017). These results, together with the identification of 'cellular immune response' and 'cytokine signalling' as two of the most upregulated pathway classes identified by both phosphoprotein and phosphopeptide enrichment, suggest that the tumour microenviroment and immunomodulatory molecules could have a pivotal role in meningioma development and progression.

Previously, our group also identified EPS8L2 as a commonly phosphorylated protein in *NF2*-negative schwannomas and meningioma BM1 cells (Bassiri *et al.*, 2017). In the context of this project, EPS8L2 was found to be commonly and significantly upregulated

among all grades of meningioma as both total and phosphoprotein. Further, we identified a novel EPS8L2 phosphorylation site, S48, subsequent to phosphopeptide enrichment. Experimental validation of EPS8L2 was only performed at total protein levels as phosphorylation sites of EPS8L2 with known regulatory function have to date not been reported. By WB analysis we saw a strong overexpression of EPS8L2 across all grades compared to NMT; however, IHC showed weak positivity across tumours and normal meninges. Nonetheless, this protein should not yet be dismissed as a potential molecular target or biomarker without further validation studies.

EPS8L2 is a member of the EPS8 (EGF receptor kinase substrate 8) family of proteins that comprises an additional two EPS8-like proteins; EPS8L1 (epidermal growth factor receptor kinase substrate 8-like protein 1) and EPS8L3 (epidermal growth factor receptor kinase substrate 8-like protein 3) (Offenhauser *et al.*, 2004). EPS8 itself is involved in several cellular processes including as a signalling adapter protein implicated in signal transduction from Ras to Rac, regulation of actin-based cellular motility and organisation of actin-based structures (Giampietro *et al.*, 2015). Although the role of the EPS8–like forms is still unclear, it has been proposed they can substitute EPS8 function (Offenhauser *et al.*, 2004). High levels of EPS8 have been reported to induce the nuclear translocation and activation of the co-transcriptional regulator YAP (Yes-associated protein), a member of the Hippo pathway known to be active in *NF2*-negative meningiomas (Giampietro *et al.*, 2015; Striedinger *et al.*, 2008). EPS8 is also a substrate for EGFR and participates in both EGFR signalling through Rac, and vesicular trafficking through Rab5 (Lanzetti *et al.*, 2000), required for the fusion of plasma membranes and early endosomes (Hoffenberg *et al.*, 2000). Our functional annotation analyses identified GO terms reflecting EPS8 functions such as ‘cortical actin cytoskeleton organization’ and ‘cytoskeletal anchoring at plasma membrane’ to be enriched in the phosphopeptide dataset, as well as ‘transport vesicle’ in commonly upregulated proteins and

phosphoproteins. Combining these enrichment terms with the possible functional redundancy of EPS8 by EPS8-like proteins and the accompanying overexpression of EGFR identified in our global proteome dataset, the role of EPS8L2 and downstream EGFR signalling in meningioma pathogenesis certainly warrant further investigation.

In addition to EPS8L2, we validated the overexpression of another protein, CKAP4, identified as commonly upregulated among all meningioma grades by global proteome analysis and also known to associate with EGFR (Li *et al.*, 2014a). This protein is an epithelial cell surface receptor with high-affinity for the antiproliferative factor secreted by bladder epithelial cells (Matika *et al.*, 2012) and plays an important role in mediating the anchoring of the endoplasmic reticulum to microtubules (Vedrenne, Klopfenstein & Hauri, 2005). Dependent upon cancer type, CKAP4 has shown conflicting roles in tumour growth. In hepatocellular carcinoma CKAP4 was found to complex with EGFR and suppress downstream EGFR signalling (Li *et al.*, 2014a); whilst two studies have shown upon binding to DKK1 (dickkopf-1), an antagonist of the canonical Wnt pathway, CKAP4 enhances Wnt-independent cellular proliferation through PI3K/AKT activation in pancreatic, lung and esophageal cancers (Kimura *et al.*, 2016; Shinno *et al.*, 2018). Further, the use of an anti-CKAP4 antibody blocks DKK1-CKAP4 interaction and inhibits AKT activation demonstrating the potential of CKAP4 as a novel therapeutic target in cancer (Kimura *et al.*, 2016; Shinno *et al.*, 2018). The biological function of CKAP4 in meningioma is to date unknown but these studies suggest its role and suitability as a molecular therapeutic target should be further explored.

We also identified overexpression of phosphorylated AKT1 common to all meningioma grades. Clark *et al.* (2013) described a constitutively active mutation of AKT1 ($AKT1^{E17K}$) in *NF2*-positive meningiomas and other studies have shown that inhibition of pAKT1 by the Integrin-Linked Kinase inhibitor OSU-T315 in BM1 cells

was able to arrest cell cycle and induce cell death (Clark *et al.*, 2013; Mercado-Pimentel *et al.*, 2016). Following validation, overexpression of pAKT-S473 was consistently seen in grade I and II meningiomas, where CKAP4 was also strongly detected, again supporting the future investigation into the role of CKAP4 and its regulation of AKT activation by potential interaction with DKK1 in meningioma (Kimura *et al.*, 2016; Shinno *et al.*, 2018). In fact, we chose to perform preliminary functional validation experiments of pAKT1-S473 to determine its plausibility as a therapeutic target of lower grade meningioma. The findings of these experiments will be discussed later in this Chapter.

One additional validated protein, which was significantly overexpressed and phosphorylated across all grades but not expressed in NMT was NEK9, a serine/threonine-protein kinase of the NIMA family protein kinases that together with other members of the family functions in the regulation of mitosis (Roig *et al.*, 2002). In particular, NEK9 controls G1/S transition and S phase progression when phosphorylated on T210 and associated with the heterodimeric complex FACT, formed by the proteins SPT16 (FACT complex subunit SPT16) and SSRP1 (FACT complex subunit SSRP1) (Tan & Lee, 2004); indeed, both proteins were also identified in our proteome dataset as upregulated in all grades compared to NMT, like the validated pNEK9-T210. Although NEK9 has been previously identified to be exclusively expressed in a benign meningioma cell line compared to primary arachnoidal cells, its phosphorylated active form has not been shown in meningioma until now (Saydam *et al.*, 2010). By phosphopeptide analysis we identified the phosphorylation site S868 specific to NEK9, however, this site has not yet been described in literature and currently there are no commercial antibodies available. We therefore validated the phosphorylation of NEK9 on the site T210, confirmed to regulate NEK9 activation (Tan & Lee, 2004). Furthermore, NEK9 activates two additional family members, NEK6 (serine/threonine-protein kinase Nek6) and

NEK7, and together the three proteins function in mitotic progression with a role in mitotic spindle formation, a GO term established as enriched among phosphoproteins identified as commonly upregulated among all grades in our dataset (Belham *et al.*, 2003). Phosphorylated NEK7 was also identified as commonly overexpressed in all grades compared to NMT and detected in phosphopeptide analysis to be phosphorylated on S195. These findings thus present NEK9, as well as NEK7 and the FACT complex as potential novel drug targets in meningioma, proposing their further validation.

Our functional annotation of upregulated proteins among all meningioma grades showed a significant enrichment in GO terms related to splicing. Among identifying several components of the spliceosome, we also detected and validated overexpression of the oncogenic splicing factor SF2/ASF in all meningioma grades compared to NMT. Upregulation of SF2/ASF has been shown in many different human cancers and its overexpression causes oncogenic transformation of immortal rodent fibroblasts that can form sarcomas in nude mice (Karni *et al.*, 2007). SF2/ASF may contribute to tumourigenesis through aberrant splicing of its target genes including the tumour suppressor BIN1, identified as downregulated in our analysis of grade II *vs*. grade I meningioma. Aberrant splicing by SF2/ASF promotes an alternative BIN1 isoform lacking its tumour suppressive pro-apoptotic function (Karni *et al.*, 2007). It follows that SF2/ASF is now recognised as a possible target for cancer therapy demonstrated by a study showing siRNA-mediated downregulation of SF2/ASF induced apoptosis in non-small cell lung cancer cell lines (Ezponda *et al.*, 2010). Our data and previous studies highlight that splicing dysregulation in meningioma should be explored to determine if targeting SF2/ASF and spliceosome components together may represent attractive therapeutic targets in meningioma.

One family of proteins repeatedly identified by both global proteome and phosphoprotein analysis were the DEAD-box family of RNA helicases. Across both analyses we found DDX5, DDX6, DDX10, DDX17, DDX19B DDX24, DDX39A (ATP-dependent RNA helicase DDX39A) and DDX42 to be significantly upregulated in one or more grades of meningioma compared to NMT. Of these, we validated DDX17 by both WB and IHC. From WB analysis we observed multiple bands of expression for DDX17, reported to have two isoforms at 72 and 82 kDa. We confirmed specificity of these bands for DDX17 using a blocking peptide and found the majority were absent from NMT but present across many of the tumours. By IHC, all tumours demonstrated strong positivity for DDX17, with low or absent expression in normal meninges. Interestingly, DDX17 shares ~90% homology with DDX5, also identified as a commonly upregulated protein in our analysis. The two proteins are known to demonstrate functional redundancy of their roles in cell proliferation and ribosome biogenesis, in addition to non-redundant functions (Fuller-Pace & Moore, 2011; Jalal, Uhlmann-Schiffler & Stahl, 2007). Both proteins have been implicated in cancer through their functional role in multiple processes including transcriptional regulation, alternative splicing, as well as miRNA and ribosome biogenesis (Fuller-Pace, 2013). Simultaneous overexpression of DDX5 and DDX17 has been described in colorectal cancer as potentially causative of the disease, as well as a possible marker of progression and novel therapeutic target (Shin *et al.*, 2007). Taken together, our identification of the common upregulation of RNA helicases among all grades as well as experimental validation of DDX17 warrant the future investigation of DEAD-box RNA helicases in meningioma in order to determine their potential as a family of biomarkers or molecular targets.

Finally, we validated the grade-specific significant overexpression of the glycolytic enzyme HK2 in grade II and III meningiomas suggesting its potential as a diagnostic biomarker and possible molecular target of these high-grade tumours. There are four

hexokinase isoforms, HK1-4, that catalyse the phosphorylation of glucose in the first step of glycolysis (Xu *et al.*, 2018). Notably, in cancer it is the increased expression of HK2, predominantly expressed in embryonic tissues, that has been found to play a key role in aerobic glycolysis and thus, the "Warburg effect" in rapidly growing cancer cells (Lis *et al.*, 2016; Xu *et al.*, 2018). Indeed, we further identified high-grade protein signatures to be enriched in metabolic terms related to energy production. Former studies have associated HK2 with the promotion of tumour growth, migration and metastasis in GBM and pancreatic cancer (Anderson *et al.*, 2017; Wolf *et al.*, 2011). HK2 has been acknowledged as a favourable molecular target of HK2-positive cancers, in particular, those that do not also express the HK1 isoform (Xu *et al.*, 2018). Consequently, selective inhibitors of HK2 have shown promise in some cancer cell lines and importantly show selectivity over HK1, expressed by healthy cells, thus minimising systemic toxicity (Lin *et al.*, 2016; Xu *et al.*, 2018).

6.7 Phosphorylated AKT1 as a therapeutic target of low-grade meningioma

Detection of AKT1 by phosphoprotein enrichment and MS analysis of meningioma led us to validate the phosphorylation of AKT1 on S473. Subsequent to experimental validation we discovered pAKT1-S473 was predominantly seen in low-grade meningioma as described above. In addition, we showed the downstream AKT1 targets pGSK3β-S9 and pPRAS40-T246, as well as total protein levels of GSK3β and PRAS40 displayed stronger expression in grade I and II meningioma compared to grade III and NMT, similar to pAKT1-S473 expression. These findings prompted us to investigate the value of pAKT1-S473 as a grade-specific therapeutic target of low-grade meningioma.

Genomic studies in recent years have revealed recurrent mutations of *AKT1* and *PI3KCA* in mainly grade I non-*NF2* meningiomas generating interest in the possibility of targeting the PI3K/AKT/mTOR signalling pathway associated with these genes

(Abedalthagafi *et al.*, 2016; Brastianos *et al.*, 2013; Clark *et al.*, 2013). We first tested the AKT inhibitor AZD5363 using the BM1 and KT21 meningioma cell lines as models of grade I and grade III meningioma, respectively. Previously, AZD5363 has shown efficacy in a patient with metastatic meningioma harbouring the recurrent $AKT1^{E17K}$ mutation (Weller *et al.*, 2017); however, we did not observe a strong reduction in cell viability of either BM1 or KT21. Following administration of AZD5363 in four primary grade I meningioma cells, efficacy was improved with generally lower IC_{50} values than those seen in the cell lines. Future studies might test the efficacy of alternative AKT inhibitors such as the allosteric AKT inhibitor MK2206 that has demonstrated anti-tumour efficacy in colon cancer cells and has recently been tested in a phase II trial of advanced breast cancer (NCT01277757) (Agarwal *et al.*, 2014).

To further analyse the potential of AKT inhibition, we sought to elucidate the upstream activators of pAKT1-S473 by inhibiting two key components of the PI3K/AKT/mTOR pathway, PI3K and mTORC2. Although we observed improved efficacy by the application of a PI3K and a dual mTOR inhibitor in grade I and III cell lines, we were unable to determine the percentage of cell viability reduction that might be attributable to off-target effects. However, the role of both mTOR complexes in meningioma should be further investigated based on previous studies reporting the activation of mTORC1 and its substrates in meningioma of all grades, as well as the detection of mTOR expression across all meningiomas in our phosphoprotein dataset (Pachow *et al.*, 2013). Moreover, proliferation of meningioma cell lines *in vitro* and *in vivo* was reduced following the use of the mTORC1-specific inhibitors temsirolimus and everolimus (Pachow *et al.*, 2013). Thus, future studies may investigate the efficacy of alternative AKT inhibitors, as well as a possible combinatorial approach of inhibiting AKT and its upstream activators in meningioma.

6.8 Conclusion

The aim of this project was to characterise the proteomic and phosphoproteomic profiles of meningioma with a goal to identify and validate a panel of candidate proteins and phosphoproteins that show potential as biomarkers or therapeutic targets in these tumours. To our knowledge, this is the most comprehensive proteomic study of the meningioma proteome from tissue to date, covering 22 meningiomas, including six grade III samples, as well as an independent cohort used for Western blot validation. In addition, our analyses of the meningioma phosphoproteome, performing both phosphoprotein and phosphopeptide enrichments, has enabled us to explore not only aberrant protein expression but also dysregulated protein activity by focussing on protein phosphorylation. Moreover, by being the first proteomic study to analyse meningioma of all grades in parallel with three normal meningeal tissues, we were able to reveal differentially expressed proteins and phosphoproteins between meningioma and healthy meninges that may represent possible molecular targets for therapeutic intervention.

During this project we have described the enrichment of overexpressed proteins and phosphoproteins in biological functions associated with splicing and RNA metabolism not previously linked to meningioma pathogenesis. Upon further investigation these novel areas may represent opportunities to target entire cellular processes. We have also identified and performed successful validation on a panel of proteins and phosphoproteins including pNEK9-T210, NEK9, HK2, CKAP4, pAKT1-S473, SET, SF2/ASF and DDX17 that show promise as novel candidates for diagnostic biomarkers and potential therapeutic targets in meningioma. Further examination of these candidates may ultimately facilitate their translation into the clinic.

Finally, this body of work will act to provide the basis of future projects in unravelling the molecular mechanisms underlying meningioma pathogenesis.

Appendix

This section contains the following publications:

Collord G, Tarpey P, Kurbatova N *et al.* (2018) An integrated genomic analysis of anaplastic meningioma identifies prognostic molecular signatures. Sci Rep. 2018 Sep 10;8(1):13537. doi: 10.1038/s41598-018-31659-0.

Dunn J, Ferluga S, Sharma V *et al*. (2018) Proteomic analysis discovers the differential expression of novel proteins and phosphoproteins in meningioma including NEK9, HK2 and SET and deregulation of RNA metabolism. EBioMedicine. 2018 Dec 26;40:77. doi: 10.1016/j.ebiom.2018.12.048.

References

Aarhus, M., Bruland, O., Bredholt, G., Lybaek, H., Husebye, E. S., Krossnes, B. K., Vedeler, C., Wester, K., Lund-Johansen, M. & Knappskog, P. M. (2008) 'Microarray analysis reveals down-regulation of the tumour suppressor gene WWOX and up-regulation of the oncogene TYMS in intracranial sporadic meningiomas'. *J Neurooncol*, 88 (3), pp. 251-259.

Aarhus, M., Lund-Johansen, M. & Knappskog, P. M. (2011) 'Gene expression profiling of meningiomas: current status after a decade of microarray-based transcriptomic studies'. *Acta Neurochir (Wien)*, 153 (3), pp. 447-456.

Aavikko, M., Li, S. P., Saarinen, S., Alhopuro, P., Kaasinen, E., Morgunova, E., Li, Y., Vesanen, K., Smith, M. J., Evans, D. G., Poyhonen, M., Kiuru, A., Auvinen, A., Aaltonen, L. A., Taipale, J. & Vahteristo, P. (2012) 'Loss of SUFU function in familial multiple meningioma'. *Am J Hum Genet*, 91 (3), pp. 520-526.

Abedalthagafi, M., Bi, W. L., Aizer, A. A., Merrill, P. H., Brewster, R., Agarwalla, P. K., Listewnik, M. L., Dias-Santagata, D., Thorner, A. R., Van Hummelen, P., Brastianos, P. K., Reardon, D. A., Wen, P. Y., Al-Mefty, O., Ramkissoon, S. H., Folkerth, R. D., Ligon, K. L., Ligon, A. H., Alexander, B. M., Dunn, I. F., Beroukhim, R. & Santagata, S. (2016) 'Oncogenic PI3K mutations are as common as AKT1 and SMO mutations in meningioma'. *Neuro Oncol*, 18 (5), pp. 649-655.

Agarwal, E., Chaudhuri, A., Leiphrakpam, P. D., Haferbier, K. L., Brattain, M. G. & Chowdhury, S. (2014) 'Akt inhibitor MK-2206 promotes anti-tumor activity and cell death by modulation of AIF and Ezrin in colorectal cancer'. *BMC Cancer*, 14 pp. 145.

Alessi, D. R., Andjelkovic, M., Caudwell, B., Cron, P., Morrice, N., Cohen, P. & Hemmings, B. A. (1996) 'Mechanism of activation of protein kinase B by insulin and IGF-1'. *EMBO J*, 15 (23), pp. 6541-6551.

Alessi, D. R., James, S. R., Downes, C. P., Holmes, A. B., Gaffney, P. R., Reese, C. B. & Cohen, P. (1997) 'Characterization of a 3-phosphoinositide-dependent protein kinase which phosphorylates and activates protein kinase Balpha'. *Curr Biol*, 7 (4), pp. 261-269.

Alexiou, G. A., Gogou, P., Markoula, S. & Kyritsis, A. P. (2010) 'Management of meningiomas'. *Clin Neurol Neurosurg*, 112 (3), pp. 177-182.

Anderson, M., Marayati, R., Moffitt, R. & Yeh, J. J. (2017) 'Hexokinase 2 promotes tumor growth and metastasis by regulating lactate production in pancreatic cancer'. *Oncotarget*, 8 (34), pp. 56081-56094.

Andreasen, P. A. (2007) 'PAI-1 - a potential therapeutic target in cancer'. *Curr Drug Targets*, 8 (9), pp. 1030-1041.

Angus, S. P., Oblinger, J. L., Stuhlmiller, T. J., DeSouza, P. A., Beauchamp, R. L., Witt, L., Chen, X., Jordan, J. T., Gilbert, T. S. K., Stemmer-Rachamimov, A., Gusella, J. F., Plotkin, S. R., Haggarty, S. J., Chang, L. S., Johnson, G. L., Ramesh, V. & Children's Tumor Foundation Synodos for, N. F. C. (2018) 'EPH receptor signaling as a novel therapeutic target in NF2-deficient meningioma'. *Neuro Oncol*,

Apra, C., Peyre, M. & Kalamarides, M. (2018) 'Current treatment options for meningioma'. *Expert Rev Neurother*, 18 (3), pp. 241-249.

Aryal, U. K. & Ross, A. R. (2010) 'Enrichment and analysis of phosphopeptides under different experimental conditions using titanium dioxide affinity chromatography and mass spectrometry'. *Rapid Commun Mass Spectrom*, 24 (2), pp. 219-231.

Au-Yeung, N., Mandhana, R. & Horvath, C. M. (2013) 'Transcriptional regulation by STAT1 and STAT2 in the interferon JAK-STAT pathway'. *JAKSTAT*, 2 (3), pp. e23931.

Bacci, C., Sestini, R., Provenzano, A., Paganini, I., Mancini, I., Porfirio, B., Vivarelli, R., Genuardi, M. & Papi, L. (2010) 'Schwannomatosis associated with multiple meningiomas due to a familial SMARCB1 mutation'. *Neurogenetics*, 11 (1), pp. 73-80.

Bajou, K., Noel, A., Gerard, R. D., Masson, V., Brunner, N., Holst-Hansen, C., Skobe, M., Fusenig, N. E., Carmeliet, P., Collen, D. & Foidart, J. M. (1998) 'Absence of host plasminogen activator inhibitor 1 prevents cancer invasion and vascularization'. *Nat Med*, 4 (8), pp. 923-928.

Banerji, U., Dean, E. J., Perez-Fidalgo, J. A., Batist, G., Bedard, P. L., You, B., Westin, S. N., Kabos, P., Garrett, M. D., Tall, M., Ambrose, H., Barrett, J. C., Carr, T. H., Cheung, S. Y. A., Corcoran, C., Cullberg, M., Davies, B. R., de Bruin, E. C., Elvin, P., Foxley, A., Lawrence, P., Lindemann, J. P. O., Maudsley, R., Pass, M., Rowlands, V., Rugman, P., Schiavon, G., Yates, J. & Schellens, J. H. M. (2018) 'A Phase I Open-Label Study to Identify a Dosing Regimen of the Pan-AKT Inhibitor AZD5363 for Evaluation in Solid

Tumors and in PIK3CA-Mutated Breast and Gynecologic Cancers'. *Clin Cancer Res*, 24 (9), pp. 2050-2059.

Barresi, V., Branca, G., Caffo, M. & Tuccari, G. (2015) 'p-CREB expression in human meningiomas: correlation with angiogenesis and recurrence risk'. *J Neurooncol*, 122 (1), pp. 87-95.

Barski, D., Wolter, M., Reifenberger, G. & Riemenschneider, M. J. (2010) 'Hypermethylation and transcriptional downregulation of the TIMP3 gene is associated with allelic loss on 22q12.3 and malignancy in meningiomas'. *Brain Pathol*, 20 (3), pp. 623-631.

Bassiri, K., Ferluga, S., Sharma, V., Syed, N., Adams, C. L., Lasonder, E. & Hanemann, C. O. (2017) 'Global Proteome and Phospho-proteome Analysis of Merlin-deficient Meningioma and Schwannoma Identifies PDLIM2 as a Novel Therapeutic Target'. *EBioMedicine*, 16 pp. 76-86.

Belham, C., Roig, J., Caldwell, J. A., Aoyama, Y., Kemp, B. E., Comb, M. & Avruch, J. (2003) 'A mitotic cascade of NIMA family kinases. Nercc1/Nek9 activates the Nek6 and Nek7 kinases'. *J Biol Chem*, 278 (37), pp. 34897-34909.

Beltran, L. & Cutillas, P. R. (2012) 'Advances in phosphopeptide enrichment techniques for phosphoproteomics'. *Amino Acids*, 43 (3), pp. 1009-1024.

Benson, V. S., Pirie, K., Schuz, J., Reeves, G. K., Beral, V., Green, J. & Million Women Study, C. (2013) 'Mobile phone use and risk of brain neoplasms and other cancers: prospective study'. *Int J Epidemiol*, 42 (3), pp. 792-802.

Bi, W. L., Greenwald, N. F., Abedalthagafi, M., Wala, J., Gibson, W. J., Agarwalla, P. K., Horowitz, P., Schumacher, S. E., Esaulova, E., Mei, Y., Chevalier, A., Ducar, M., Thorner, A. R., van Hummelen, P., Stemmer-Rachamimov, A., Artyomov, M., Al-Mefty, O., Dunn, G. P., Santagata, S., Dunn, I. F. & Beroukhim, R. (2017) 'Genomic landscape of high-grade meningiomas'. *NPJ Genom Med*, 2

Bi, W. L., Mei, Y., Agarwalla, P. K., Beroukhim, R. & Dunn, I. F. (2016) 'Genomic and Epigenomic Landscape in Meningioma'. *Neurosurg Clin N Am*, 27 (2), pp. 167-179.

Black, P. M. (1993) 'Meningiomas'. *Neurosurgery*, 32 (4), pp. 643-657.

Black, P. M., Carroll, R., Glowacka, D., Riley, K. & Dashner, K. (1994) 'Platelet-derived growth factor expression and stimulation in human meningiomas'. *J Neurosurg*, 81 (3), pp. 388-393.

Boetto, J., Bielle, F., Sanson, M., Peyre, M. & Kalamarides, M. (2017) 'SMO mutation status defines a distinct and frequent molecular subgroup in olfactory groove meningiomas'. *Neuro Oncol*, 19 (3), pp. 345-351.

Bostrom, J., Meyer-Puttlitz, B., Wolter, M., Blaschke, B., Weber, R. G., Lichter, P., Ichimura, K., Collins, V. P. & Reifenberger, G. (2001) 'Alterations of the tumor suppressor genes CDKN2A (p16(INK4a)), p14(ARF), CDKN2B (p15(INK4b)), and

CDKN2C (p18(INK4c)) in atypical and anaplastic meningiomas'. *Am J Pathol*, 159 (2), pp. 661-669.

Brastianos, P. K., Horowitz, P. M., Santagata, S., Jones, R. T., McKenna, A., Getz, G., Ligon, K. L., Palescandolo, E., Van Hummelen, P., Ducar, M. D., Raza, A., Sunkavalli, A., Macconaill, L. E., Stemmer-Rachamimov, A. O., Louis, D. N., Hahn, W. C., Dunn, I. F. & Beroukhim, R. (2013) 'Genomic sequencing of meningiomas identifies oncogenic SMO and AKT1 mutations'. *Nat Genet*, 45 (3), pp. 285-289.

Burns, S. S., Akhmametyeva, E. M., Oblinger, J. L., Bush, M. L., Huang, J., Senner, V., Chen, C. S., Jacob, A., Welling, D. B. & Chang, L. S. (2013) 'Histone deacetylase inhibitor AR-42 differentially affects cell-cycle transit in meningeal and meningioma cells, potently inhibiting NF2-deficient meningioma growth'. *Cancer Res*, 73 (2), pp. 792-803.

Bush, M. L., Oblinger, J., Brendel, V., Santarelli, G., Huang, J., Akhmametyeva, E. M., Burns, S. S., Wheeler, J., Davis, J., Yates, C. W., Chaudhury, A. R., Kulp, S., Chen, C. S., Chang, L. S., Welling, D. B. & Jacob, A. (2011) 'AR42, a novel histone deacetylase inhibitor, as a potential therapy for vestibular schwannomas and meningiomas'. *Neuro Oncol*, 13 (9), pp. 983-999.

Caffo, M., Esposito, E., Barresi, V., Caruso, G., Cardali, S. M., Rinaldi, M., Mallamace, R., Campolo, M., Casili, G., Conti, A., Germano, A., Cuzzocrea, S. & Minutoli, L. (2017) 'Modulation of Dkk-3 and claudin-5 as new therapeutic strategy in the treatment of meningiomas'. *Oncotarget*, 8 (40), pp. 68280-68290.

Carnielli, C. M., Winck, F. V. & Paes Leme, A. F. (2015) 'Functional annotation and biological interpretation of proteomics data'. *Biochim Biophys Acta*, 1854 (1), pp. 46-54.

Carpten, J. D., Faber, A. L., Horn, C., Donoho, G. P., Briggs, S. L., Robbins, C. M., Hostetter, G., Boguslawski, S., Moses, T. Y., Savage, S., Uhlik, M., Lin, A., Du, J., Qian, Y. W., Zeckner, D. J., Tucker-Kellogg, G., Touchman, J., Patel, K., Mousses, S., Bittner, M., Schevitz, R., Lai, M. H., Blanchard, K. L. & Thomas, J. E. (2007) 'A transforming mutation in the pleckstrin homology domain of AKT1 in cancer'. *Nature*, 448 (7152), pp. 439-444.

Carroll, R. S., Black, P. M., Zhang, J., Kirsch, M., Percec, I., Lau, N. & Guha, A. (1997) 'Expression and activation of epidermal growth factor receptors in meningiomas'. *J Neurosurg*, 87 (2), pp. 315-323.

Castells, X., Garcia-Gomez, J. M., Navarro, A., Acebes, J. J., Godino, O., Boluda, S., Barcelo, A., Robles, M., Arino, J. & Arus, C. (2009) 'Automated brain tumor biopsy prediction using single-labeling cDNA microarrays-based gene expression profiling'. *Diagn Mol Pathol*, 18 (4), pp. 206-218.

Chamberlain, M. C. (1996) 'Adjuvant combined modality therapy for malignant meningiomas'. *J Neurosurg*, 84 (5), pp. 733-736.

Chamberlain, M. C. (2012) 'The role of chemotherapy and targeted therapy in the treatment of intracranial meningioma'. *Curr Opin Oncol*, 24 (6), pp. 666-671.

Chamberlain, M. C. & Johnston, S. K. (2011) 'Hydroxyurea for recurrent surgery and radiation refractory meningioma: a retrospective case series'. *J Neurooncol*, 104 (3), pp. 765-771.

Chamberlain, M. C., Tsao-Wei, D. D. & Groshen, S. (2004) 'Temozolomide for treatment-resistant recurrent meningioma'. *Neurology*, 62 (7), pp. 1210-1212.

Chamberlain, M. C., Tsao-Wei, D. D. & Groshen, S. (2006) 'Salvage chemotherapy with CPT-11 for recurrent meningioma'. *J Neurooncol*, 78 (3), pp. 271-276.

Chamoun, R., Krisht, K. M. & Couldwell, W. T. (2011) 'Incidental meningiomas'. *Neurosurg Focus*, 31 (6), pp. E19.

Chandramouli, K. & Qian, P. Y. (2009) 'Proteomics: challenges, techniques and possibilities to overcome biological sample complexity'. *Hum Genomics Proteomics*, 2009

Christiaans, I., Kenter, S. B., Brink, H. C., van Os, T. A., Baas, F., van den Munckhof, P., Kidd, A. M. & Hulsebos, T. J. (2011) 'Germline SMARCB1 mutation and somatic NF2 mutations in familial multiple meningiomas'. *J Med Genet*, 48 (2), pp. 93-97.

Clark, V. E., Erson-Omay, E. Z., Serin, A., Yin, J., Cotney, J., Ozduman, K., Avsar, T., Li, J., Murray, P. B., Henegariu, O., Yilmaz, S., Gunel, J. M., Carrion-Grant, G., Yilmaz, B., Grady, C., Tanrikulu, B., Bakircioglu, M., Kaymakcalan, H., Caglayan, A. O., Sencar, L., Ceyhun, E., Atik, A. F., Bayri, Y., Bai, H., Kolb, L. E., Hebert, R. M., Omay, S. B., Mishra-Gorur, K., Choi, M., Overton, J. D., Holland, E. C., Mane, S., State, M. W.,

Bilguvar, K., Baehring, J. M., Gutin, P. H., Piepmeier, J. M., Vortmeyer, A., Brennan, C. W., Pamir, M. N., Kilic, T., Lifton, R. P., Noonan, J. P., Yasuno, K. & Gunel, M. (2013) 'Genomic analysis of non-NF2 meningiomas reveals mutations in TRAF7, KLF4, AKT1, and SMO'. *Science*, 339 (6123), pp. 1077-1080.

Clark, V. E., Harmanci, A. S., Bai, H., Youngblood, M. W., Lee, T. I., Baranoski, J. F., Ercan-Sencicek, A. G., Abraham, B. J., Weintraub, A. S., Hnisz, D., Simon, M., Krischek, B., Erson-Omay, E. Z., Henegariu, O., Carrion-Grant, G., Mishra-Gorur, K., Duran, D., Goldmann, J. E., Schramm, J., Goldbrunner, R., Piepmeier, J. M., Vortmeyer, A. O., Gunel, J. M., Bilguvar, K., Yasuno, K., Young, R. A. & Gunel, M. (2016) 'Recurrent somatic mutations in POLR2A define a distinct subset of meningiomas'. *Nat Genet*, 48 (10), pp. 1253-1259.

Claus, E. B., Calvocoressi, L., Bondy, M. L., Schildkraut, J. M., Wiemels, J. L. & Wrensch, M. (2011) 'Family and personal medical history and risk of meningioma'. *J Neurosurg*, 115 (6), pp. 1072-1077.

Cohen, P. (2000) 'The regulation of protein function by multisite phosphorylation--a 25 year update'. *Trends Biochem Sci*, 25 (12), pp. 596-601.

Collord, G., Tarpey, P., Kurbatova, N., Martincorena, I., Moran, S., Castro, M., Nagy, T., Bignell, G., Maura, F., Young, M. D., Berna, J., Tubio, J. M. C., McMurran, C. E., Young, A. M. H., Sanders, M., Noorani, I., Price, S. J., Watts, C., Leipnitz, E., Kirsch, M., Schackert, G., Pearson, D., Devadass, A., Ram, Z., Collins, V. P., Allinson, K., Jenkinson, M. D., Zakaria, R., Syed, K., Hanemann, C. O., Dunn, J., McDermott, M. W., Kirollos, R. W., Vassiliou, G. S., Esteller, M., Behjati, S., Brazma, A., Santarius, T. & McDermott,

U. (2018) 'An integrated genomic analysis of anaplastic meningioma identifies prognostic molecular signatures'. *Sci Rep*, 8 (1), pp. 13537.

Commins, D. L., Atkinson, R. D. & Burnett, M. E. (2007) 'Review of meningioma histopathology'. *Neurosurg Focus*, 23 (4), pp. E3.

Cox, J., Hein, M. Y., Luber, C. A., Paron, I., Nagaraj, N. & Mann, M. (2014) 'Accurate proteome-wide label-free quantification by delayed normalization and maximal peptide ratio extraction, termed MaxLFQ'. *Mol Cell Proteomics*, 13 (9), pp. 2513-2526.

Cox, J., Neuhauser, N., Michalski, A., Scheltema, R. A., Olsen, J. V. & Mann, M. (2011) 'Andromeda: a peptide search engine integrated into the MaxQuant environment'. *J Proteome Res*, 10 (4), pp. 1794-1805.

Cravatt, B. F., Simon, G. M. & Yates, J. R., 3rd (2007) 'The biological impact of mass-spectrometry-based proteomics'. *Nature*, 450 (7172), pp. 991-1000.

Cui, G. Q., Jiao, A. H., Xiu, C. M., Wang, Y. B., Sun, P., Zhang, L. M. & Li, X. G. (2014) 'Proteomic analysis of meningiomas'. *Acta Neurol Belg*, 114 (3), pp. 187-194.

Curto, M., Cole, B. K., Lallemand, D., Liu, C. H. & McClatchey, A. I. (2007) 'Contact-dependent inhibition of EGFR signaling by Nf2/Merlin'. *J Cell Biol*, 177 (5), pp. 893-903.

Dalan, A. B., Gulluoglu, S., Tuysuz, E. C., Kuskucu, A., Yaltirik, C. K., Ozturk, O., Ture, U. & Bayrak, O. F. (2017) 'Simultaneous analysis of miRNA-mRNA in human

meningiomas by integrating transcriptome: A relationship between PTX3 and miR-29c'. *BMC Cancer*, 17 (1), pp. 207.

Das, A., Sudhahar, V., Chen, G. F., Kim, H. W., Youn, S. W., Finney, L., Vogt, S., Yang, J., Kweon, J., Surenkhuu, B., Ushio-Fukai, M. & Fukai, T. (2016) 'Endothelial Antioxidant-1: a Key Mediator of Copper-dependent Wound Healing in vivo'. *Sci Rep*, 6 pp. 33783.

Dashzeveg, N., Yogosawa, S. & Yoshida, K. (2016) 'Transcriptional induction of protein kinase C delta by p53 tumor suppressor in the apoptotic response to DNA damage'. *Cancer Lett*, 374 (1), pp. 167-174.

Davies, B. R., Greenwood, H., Dudley, P., Crafter, C., Yu, D. H., Zhang, J., Li, J., Gao, B., Ji, Q., Maynard, J., Ricketts, S. A., Cross, D., Cosulich, S., Chresta, C. C., Page, K., Yates, J., Lane, C., Watson, R., Luke, R., Ogilvie, D. & Pass, M. (2012) 'Preclinical pharmacology of AZD5363, an inhibitor of AKT: pharmacodynamics, antitumor activity, and correlation of monotherapy activity with genetic background'. *Mol Cancer Ther*, 11 (4), pp. 873-887.

DeBerardinis, R. J. & Chandel, N. S. (2016) 'Fundamentals of cancer metabolism'. *Sci Adv*, 2 (5), pp. e1600200.

Di Vinci, A., Brigati, C., Casciano, I., Banelli, B., Borzi, L., Forlani, A., Ravetti, G. L., Allemanni, G., Melloni, I., Zona, G., Spaziante, R., Merlo, D. F. & Romani, M. (2012) 'HOXA7, 9, and 10 are methylation targets associated with aggressive behavior in meningiomas'. *Transl Res*, 160 (5), pp. 355-362.

Domingues, P. H., Teodosio, C., Ortiz, J., Sousa, P., Otero, A., Maillo, A., Barcena, P., Garcia-Macias, M. C., Lopes, M. C., de Oliveira, C., Orfao, A. & Tabernero, M. D. (2012) 'Immunophenotypic identification and characterization of tumor cells and infiltrating cell populations in meningiomas'. *Am J Pathol*, 181 (5), pp. 1749-1761.

Du, K. & Montminy, M. (1998) 'CREB is a regulatory target for the protein kinase Akt/PKB'. *J Biol Chem*, 273 (49), pp. 32377-32379.

Du, Z., Abedalthagafi, M., Aizer, A. A., McHenry, A. R., Sun, H. H., Bray, M. A., Viramontes, O., Machaidze, R., Brastianos, P. K., Reardon, D. A., Dunn, I. F., Freeman, G. J., Ligon, K. L., Carpenter, A. E., Alexander, B. M., Agar, N. Y., Rodig, S. J., Bradshaw, E. M. & Santagata, S. (2015) 'Increased expression of the immune modulatory molecule PD-L1 (CD274) in anaplastic meningioma'. *Oncotarget*, 6 (7), pp. 4704-4716.

Dunn, J. D., Reid, G. E. & Bruening, M. L. (2010) 'Techniques for phosphopeptide enrichment prior to analysis by mass spectrometry'. *Mass Spectrom Rev*, 29 (1), pp. 29-54.

Ebner, M., Sinkovics, B., Szczygiel, M., Ribeiro, D. W. & Yudushkin, I. (2017) 'Localization of mTORC2 activity inside cells'. *J Cell Biol*, 216 (2), pp. 343-353.

Epstein, R. J. & Lin, F. P. (2017) 'Cancer and the omics revolution'. *Aust Fam Physician*, 46 (4), pp. 189-193.

Erdincler, P., Lena, G., Sarioglu, A. C., Kuday, C. & Choux, M. (1998) 'Intracranial meningiomas in children: review of 29 cases'. *Surg Neurol*, 49 (2), pp. 136-140; discussion 140-131.

Evans, D. G., Huson, S. M., Donnai, D., Neary, W., Blair, V., Newton, V., Strachan, T. & Harris, R. (1992) 'A genetic study of type 2 neurofibromatosis in the United Kingdom. II. Guidelines for genetic counselling'. *J Med Genet*, 29 (12), pp. 847-852.

Ezponda, T., Pajares, M. J., Agorreta, J., Echeveste, J. I., Lopez-Picazo, J. M., Torre, W., Pio, R. & Montuenga, L. M. (2010) 'The oncoprotein SF2/ASF promotes non-small cell lung cancer survival by enhancing survivin expression'. *Clin Cancer Res*, 16 (16), pp. 4113-4125.

Fan, Z., Beresford, P. J., Oh, D. Y., Zhang, D. & Lieberman, J. (2003) 'Tumor suppressor NM23-H1 is a granzyme A-activated DNase during CTL-mediated apoptosis, and the nucleosome assembly protein SET is its inhibitor'. *Cell*, 112 (5), pp. 659-672.

Fathi, A. R. & Roelcke, U. (2013) 'Meningioma'. *Curr Neurol Neurosci Rep*, 13 (4), pp. 337.

Feist, P. & Hummon, A. B. (2015) 'Proteomic challenges: sample preparation techniques for microgram-quantity protein analysis from biological samples'. *Int J Mol Sci*, 16 (2), pp. 3537-3563.

Feng, H., Hu, B., Vuori, K., Sarkaria, J. N., Furnari, F. B., Cavenee, W. K. & Cheng, S. Y. (2014) 'EGFRvIII stimulates glioma growth and invasion through PKA-dependent serine phosphorylation of Dock180'. *Oncogene*, 33 (19), pp. 2504-2512.

Fevre-Montange, M., Champier, J., Durand, A., Wierinckx, A., Honnorat, J., Guyotat, J. & Jouvet, A. (2009) 'Microarray gene expression profiling in meningiomas: differential expression according to grade or histopathological subtype'. *Int J Oncol*, 35 (6), pp. 1395-1407.

Fila, J. & Honys, D. (2012) 'Enrichment techniques employed in phosphoproteomics'. *Amino Acids*, 43 (3), pp. 1025-1047.

Flynn, D. C., Cho, Y., Vincent, D. & Cunnick, J. M. (2008) 'Podosomes and Invadopodia: Related structures with Common Protein Components that May Promote Breast Cancer Cellular Invasion'. *Breast Cancer (Auckl)*, 2 pp. 17-29.

Fuhs, S. R. & Hunter, T. (2017) 'pHisphorylation: the emergence of histidine phosphorylation as a reversible regulatory modification'. *Curr Opin Cell Biol*, 45 pp. 8-16.

Fukuda, I., Hirabayashi-Ishioka, Y., Sakikawa, I., Ota, T., Yokoyama, M., Uchiumi, T. & Morita, A. (2013) 'Optimization of enrichment conditions on TiO2 chromatography using glycerol as an additive reagent for effective phosphoproteomic analysis'. *J Proteome Res*, 12 (12), pp. 5587-5597.

Fuller-Pace, F. V. (2013) 'DEAD box RNA helicase functions in cancer'. *RNA Biol*, 10 (1), pp. 121-132.

Fuller-Pace, F. V. & Moore, H. C. (2011) 'RNA helicases p68 and p72: multifunctional proteins with important implications for cancer development'. *Future Oncol*, 7 (2), pp. 239-251.

Gadea, G. & Blangy, A. (2014) 'Dock-family exchange factors in cell migration and disease'. *Eur J Cell Biol*, 93 (10-12), pp. 466-477.

Garcia-Martinez, J. M., Moran, J., Clarke, R. G., Gray, A., Cosulich, S. C., Chresta, C. M. & Alessi, D. R. (2009) 'Ku-0063794 is a specific inhibitor of the mammalian target of rapamycin (mTOR)'. *Biochem J*, 421 (1), pp. 29-42.

Gelerstein, E., Berger, A., Jonas-Kimchi, T., Strauss, I., Kanner, A. A., Blumenthal, D. T., Gottfried, M., Margalit, N., Ram, Z. & Shahar, T. (2017) 'Regression of intracranial meningioma following treatment with nivolumab: Case report and review of the literature'. *J Clin Neurosci*, 37 pp. 51-53.

Germano, I. M., Edwards, M. S., Davis, R. L. & Schiffer, D. (1994) 'Intracranial meningiomas of the first two decades of life'. *J Neurosurg*, 80 (3), pp. 447-453.

Geurts van Kessel, A. (2010) 'The 'omics' of cancer'. *Cancer Genet Cytogenet*, 203 (1), pp. 37-42.

Giampietro, C., Disanza, A., Bravi, L., Barrios-Rodiles, M., Corada, M., Frittoli, E., Savorani, C., Lampugnani, M. G., Boggetti, B., Niessen, C., Wrana, J. L., Scita, G. & Dejana, E. (2015) 'The actin-binding protein EPS8 binds VE-cadherin and modulates YAP localization and signaling'. *J Cell Biol*, 211 (6), pp. 1177-1192.

Giansanti, P., Tsiatsiani, L., Low, T. Y. & Heck, A. J. (2016) 'Six alternative proteases for mass spectrometry-based proteomics beyond trypsin'. *Nat Protoc*, 11 (5), pp. 993-1006.

Goodwin, J. W., Crowley, J., Eyre, H. J., Stafford, B., Jaeckle, K. A. & Townsend, J. J. (1993) 'A phase II evaluation of tamoxifen in unresectable or refractory meningiomas: a Southwest Oncology Group study'. *J Neurooncol*, 15 (1), pp. 75-77.

Goutagny, S., Nault, J. C., Mallet, M., Henin, D., Rossi, J. Z. & Kalamarides, M. (2014) 'High incidence of activating TERT promoter mutations in meningiomas undergoing malignant progression'. *Brain Pathol*, 24 (2), pp. 184-189.

Graffeo, C. S., Leeper, H. E., Perry, A., Uhm, J. H., Lachance, D. J., Brown, P. D., Ma, D. J., Van Gompel, J. J., Giannini, C., Johnson, D. R. & Raghunathan, A. (2017) 'Revisiting Adjuvant Radiotherapy After Gross Total Resection of World Health Organization Grade II Meningioma'. *World Neurosurg*, 103 pp. 655-663.

Graillon, T., Defilles, C., Mohamed, A., Lisbonis, C., Germanetti, A. L., Chinot, O., Figarella-Branger, D., Roche, P. H., Adetchessi, T., Fuentes, S., Metellus, P., Dufour, H., Enjalbert, A. & Barlier, A. (2015) 'Combined treatment by octreotide and everolimus:

Octreotide enhances inhibitory effect of everolimus in aggressive meningiomas'. *J Neurooncol*, 124 (1), pp. 33-43.

Graves, P. R. & Haystead, T. A. (2002) 'Molecular biologist's guide to proteomics'. *Microbiol Mol Biol Rev*, 66 (1), pp. 39-63; table of contents.

Gusella, J. F., Ramesh, V., MacCollin, M. & Jacoby, L. B. (1999) 'Merlin: the neurofibromatosis 2 tumor suppressor'. *Biochim Biophys Acta*, 1423 (2), pp. M29-36.

Gustafson, E. A. & Wessel, G. M. (2010) 'DEAD-box helicases: posttranslational regulation and function'. *Biochem Biophys Res Commun*, 395 (1), pp. 1-6.

Hadfield, K. D., Smith, M. J., Trump, D., Newman, W. G. & Evans, D. G. (2010) 'SMARCB1 mutations are not a common cause of multiple meningiomas'. *J Med Genet*, 47 (8), pp. 567-568.

Hallinan, J. T., Hegde, A. N. & Lim, W. E. (2013) 'Dilemmas and diagnostic difficulties in meningioma'. *Clin Radiol*, 68 (8), pp. 837-844.

Han, K. K. & Martinage, A. (1992) 'Post-translational chemical modification(s) of proteins'. *Int J Biochem*, 24 (1), pp. 19-28.

Hanash, S. (2003) 'Disease proteomics'. *Nature*, 422 (6928), pp. 226-232.

Harmanci, A. S., Youngblood, M. W., Clark, V. E., Coskun, S., Henegariu, O., Duran, D., Erson-Omay, E. Z., Kaulen, L. D., Lee, T. I., Abraham, B. J., Simon, M., Krischek,

B., Timmer, M., Goldbrunner, R., Omay, S. B., Baranoski, J., Baran, B., Carrion-Grant, G., Bai, H., Mishra-Gorur, K., Schramm, J., Moliterno, J., Vortmeyer, A. O., Bilguvar, K., Yasuno, K., Young, R. A. & Gunel, M. (2017) 'Integrated genomic analyses of de novo pathways underlying atypical meningiomas'. *Nat Commun*, 8 pp. 14433.

Harsha, H. C. & Pandey, A. (2010) 'Phosphoproteomics in cancer'. *Mol Oncol*, 4 (6), pp. 482-495.

He, C., Holme, J. & Anthony, J. (2014) 'SNP genotyping: the KASP assay'. *Methods Mol Biol*, 1145 pp. 75-86.

He, Y., Wu, X., Luo, C., Wang, L. & Lin, J. (2010) 'Functional significance of the hepaCAM gene in bladder cancer'. *BMC Cancer*, 10 pp. 83.

Heerma van Voss, M. R., van Diest, P. J. & Raman, V. (2017) 'Targeting RNA helicases in cancer: The translation trap'. *Biochim Biophys Acta*, 1868 (2), pp. 510-520.

Hilton, D. A., Shivane, A., Kirk, L., Bassiri, K., Enki, D. G. & Hanemann, C. O. (2016) 'Activation of multiple growth factor signalling pathways is frequent in meningiomas'. *Neuropathology*, 36 (3), pp. 250-261.

Hodroj, D., Recolin, B., Serhal, K., Martinez, S., Tsanov, N., Abou Merhi, R. & Maiorano, D. (2017) 'An ATR-dependent function for the Ddx19 RNA helicase in nuclear R-loop metabolism'. *EMBO J*, 36 (9), pp. 1182-1198.

Hoffenberg, S., Liu, X., Nikolova, L., Hall, H. S., Dai, W., Baughn, R. E., Dickey, B. F., Barbieri, M. A., Aballay, A., Stahl, P. D. & Knoll, B. J. (2000) 'A novel membrane-anchored Rab5 interacting protein required for homotypic endosome fusion'. *J Biol Chem*, 275 (32), pp. 24661-24669.

Hood, L., Balling, R. & Auffray, C. (2012) 'Revolutionizing medicine in the 21st century through systems approaches'. *Biotechnol J*, 7 (8), pp. 992-1001.

Hood, L. & Friend, S. H. (2011) 'Predictive, personalized, preventive, participatory (P4) cancer medicine'. *Nat Rev Clin Oncol*, 8 (3), pp. 184-187.

Huang da, W., Sherman, B. T. & Lempicki, R. A. (2009) 'Systematic and integrative analysis of large gene lists using DAVID bioinformatics resources'. *Nat Protoc*, 4 (1), pp. 44-57.

Jalal, C., Uhlmann-Schiffler, H. & Stahl, H. (2007) 'Redundant role of DEAD box proteins p68 (Ddx5) and p72/p82 (Ddx17) in ribosome biogenesis and cell proliferation'. *Nucleic Acids Res*, 35 (11), pp. 3590-3601.

Jarmoskaite, I. & Russell, R. (2011) 'DEAD-box proteins as RNA helicases and chaperones'. *Wiley Interdiscip Rev RNA*, 2 (1), pp. 135-152.

Jensen, S. S. & Larsen, M. R. (2007) 'Evaluation of the impact of some experimental procedures on different phosphopeptide enrichment techniques'. *Rapid Commun Mass Spectrom*, 21 (22), pp. 3635-3645.

Ji, Y., Rankin, C., Grunberg, S., Sherrod, A. E., Ahmadi, J., Townsend, J. J., Feun, L. G., Fredericks, R. K., Russell, C. A., Kabbinavar, F. F., Stelzer, K. J., Schott, A. & Verschraegen, C. (2015) 'Double-Blind Phase III Randomized Trial of the Antiprogestin Agent Mifepristone in the Treatment of Unresectable Meningioma: SWOG S9005'. *J Clin Oncol*, 33 (34), pp. 4093-4098.

Johnson, M. D., Horiba, M., Winnier, A. R. & Arteaga, C. L. (1994) 'The epidermal growth factor receptor is associated with phospholipase C-gamma 1 in meningiomas'. *Hum Pathol*, 25 (2), pp. 146-153.

Johnson, M. D., Okedli, E., Woodard, A., Toms, S. A. & Allen, G. S. (2002) 'Evidence for phosphatidylinositol 3-kinase-Akt-p7S6K pathway activation and transduction of mitogenic signals by platelet-derived growth factor in meningioma cells'. *J Neurosurg*, 97 (3), pp. 668-675.

Johnson, M. D., Woodard, A., Kim, P. & Frexes-Steed, M. (2001) 'Evidence for mitogen-associated protein kinase activation and transduction of mitogenic signals by platelet-derived growth factor in human meningioma cells'. *J Neurosurg*, 94 (2), pp. 293-300.

Jones, D. T., Jager, N., Kool, M., Zichner, T., Hutter, B., Sultan, M., Cho, Y. J., Pugh, T. J., Hovestadt, V., Stutz, A. M., Rausch, T., Warnatz, H. J., Ryzhova, M., Bender, S., Sturm, D., Pleier, S., Cin, H., Pfaff, E., Sieber, L., Wittmann, A., Remke, M., Witt, H., Hutter, S., Tzaridis, T., Weischenfeldt, J., Raeder, B., Avci, M., Amstislavskiy, V., Zapatka, M., Weber, U. D., Wang, Q., Lasitschka, B., Bartholomae, C. C., Schmidt, M., von Kalle, C., Ast, V., Lawerenz, C., Eils, J., Kabbe, R., Benes, V., van Sluis, P., Koster, J., Volckmann, R., Shih, D., Betts, M. J., Russell, R. B., Coco, S., Tonini, G. P., Schuller,

U., Hans, V., Graf, N., Kim, Y. J., Monoranu, C., Roggendorf, W., Unterberg, A., Herold-Mende, C., Milde, T., Kulozik, A. E., von Deimling, A., Witt, O., Maass, E., Rossler, J., Ebinger, M., Schuhmann, M. U., Fruhwald, M. C., Hasselblatt, M., Jabado, N., Rutkowski, S., von Bueren, A. O., Williamson, D., Clifford, S. C., McCabe, M. G., Collins, V. P., Wolf, S., Wiemann, S., Lehrach, H., Brors, B., Scheurlen, W., Felsberg, J., Reifenberger, G., Northcott, P. A., Taylor, M. D., Meyerson, M., Pomeroy, S. L., Yaspo, M. L., Korbel, J. O., Korshunov, A., Eils, R., Pfister, S. M. & Lichter, P. (2012) 'Dissecting the genomic complexity underlying medulloblastoma'. *Nature*, 488 (7409), pp. 100-105.

Kaley, T. J., Wen, P., Schiff, D., Ligon, K., Haidar, S., Karimi, S., Lassman, A. B., Nolan, C. P., DeAngelis, L. M., Gavrilovic, I., Norden, A., Drappatz, J., Lee, E. Q., Purow, B., Plotkin, S. R., Batchelor, T., Abrey, L. E. & Omuro, A. (2015) 'Phase II trial of sunitinib for recurrent and progressive atypical and anaplastic meningioma'. *Neuro Oncol*, 17 (1), pp. 116-121.

Kandenwein, J. A., Park-Simon, T. W., Schramm, J. & Simon, M. (2011) 'uPA/PAI-1 expression and uPA promoter methylation in meningiomas'. *J Neurooncol*, 103 (3), pp. 533-539.

Karni, R., de Stanchina, E., Lowe, S. W., Sinha, R., Mu, D. & Krainer, A. R. (2007) 'The gene encoding the splicing factor SF2/ASF is a proto-oncogene'. *Nat Struct Mol Biol*, 14 (3), pp. 185-193.

Katz, L. M., Hielscher, T., Liechty, B., Silverman, J., Zagzag, D., Sen, R., Wu, P., Golfinos, J. G., Reuss, D., Neidert, M. C., Wirsching, H. G., Baumgarten, P., Herold-

Mende, C., Wick, W., Harter, P. N., Weller, M., von Deimling, A., Snuderl, M., Sen, C. & Sahm, F. (2018) 'Loss of histone H3K27me3 identifies a subset of meningiomas with increased risk of recurrence'. *Acta Neuropathol*, 135 (6), pp. 955-963.

Kavallaris, M. & Marshall, G. M. (2005) 'Proteomics and disease: opportunities and challenges'. *Med J Aust*, 182 (11), pp. 575-579.

Ketter, R., Rahnenfuhrer, J., Henn, W., Kim, Y. J., Feiden, W., Steudel, W. I., Zang, K. D. & Urbschat, S. (2008) 'Correspondence of tumor localization with tumor recurrence and cytogenetic progression in meningiomas'. *Neurosurgery*, 62 (1), pp. 61-69; discussion 69-70.

Kimura, H., Fumoto, K., Shojima, K., Nojima, S., Osugi, Y., Tomihara, H., Eguchi, H., Shintani, Y., Endo, H., Inoue, M., Doki, Y., Okumura, M., Morii, E. & Kikuchi, A. (2016) 'CKAP4 is a Dickkopf1 receptor and is involved in tumor progression'. *J Clin Invest*, 126 (7), pp. 2689-2705.

Knudson, A. G., Jr. (1971) 'Mutation and cancer: statistical study of retinoblastoma'. *Proc Natl Acad Sci U S A*, 68 (4), pp. 820-823.

Kondo, Y., Shen, L., Cheng, A. S., Ahmed, S., Boumber, Y., Charo, C., Yamochi, T., Urano, T., Furukawa, K., Kwabi-Addo, B., Gold, D. L., Sekido, Y., Huang, T. H. & Issa, J. P. (2008) 'Gene silencing in cancer by histone H3 lysine 27 trimethylation independent of promoter DNA methylation'. *Nat Genet*, 40 (6), pp. 741-750.

Kotake, Y., Sagane, K., Owa, T., Mimori-Kiyosue, Y., Shimizu, H., Uesugi, M., Ishihama, Y., Iwata, M. & Mizui, Y. (2007) 'Splicing factor SF3b as a target of the antitumor natural product pladienolide'. *Nat Chem Biol*, 3 (9), pp. 570-575.

Kros, J., de Greve, K., van Tilborg, A., Hop, W., Pieterman, H., Avezaat, C., Lekanne Dit Deprez, R. & Zwarthoff, E. (2001) 'NF2 status of meningiomas is associated with tumour localization and histology'. *J Pathol*, 194 (3), pp. 367-372.

Kuratsu, J., Kochi, M. & Ushio, Y. (2000) 'Incidence and clinical features of asymptomatic meningiomas'. *J Neurosurg*, 92 (5), pp. 766-770.

Lamszus, K., Lengler, U., Schmidt, N. O., Stavrou, D., Ergun, S. & Westphal, M. (2000) 'Vascular endothelial growth factor, hepatocyte growth factor/scatter factor, basic fibroblast growth factor, and placenta growth factor in human meningiomas and their relation to angiogenesis and malignancy'. *Neurosurgery*, 46 (4), pp. 938-947; discussion 947-938.

Lang, D. A., Neil-Dwyer, G. & Garfield, J. (1999) 'Outcome after complex neurosurgery: the caregiver's burden is forgotten'. *J Neurosurg*, 91 (3), pp. 359-363.

Lanzetti, L., Rybin, V., Malabarba, M. G., Christoforidis, S., Scita, G., Zerial, M. & Di Fiore, P. P. (2000) 'The Eps8 protein coordinates EGF receptor signalling through Rac and trafficking through Rab5'. *Nature*, 408 (6810), pp. 374-377.

Lasonder, E., Green, J. L., Camarda, G., Talabani, H., Holder, A. A., Langsley, G. & Alano, P. (2012) 'The Plasmodium falciparum schizont phosphoproteome reveals

extensive phosphatidylinositol and cAMP-protein kinase A signaling'. *J Proteome Res*, 11 (11), pp. 5323-5337.

Lee, J. H., Sade, B., Choi, E., Golubic, M. & Prayson, R. (2006) 'Meningothelioma as the predominant histological subtype of midline skull base and spinal meningioma'. *J Neurosurg*, 105 (1), pp. 60-64.

Lee, S. C. & Abdel-Wahab, O. (2016) 'Therapeutic targeting of splicing in cancer'. *Nat Med*, 22 (9), pp. 976-986.

Li, S. X., Liu, L. J., Dong, L. W., Shi, H. G., Pan, Y. F., Tan, Y. X., Zhang, J., Zhang, B., Ding, Z. W., Jiang, T. Y., Hu, H. P. & Wang, H. Y. (2014a) 'CKAP4 inhibited growth and metastasis of hepatocellular carcinoma through regulating EGFR signaling'. *Tumour Biol*, 35 (8), pp. 7999-8005.

Li, W., Wu, C., Yao, Y., Dong, B., Wei, Z., Lv, X., Zhang, J. & Xu, Y. (2014b) 'MUC4 modulates human glioblastoma cell proliferation and invasion by upregulating EGFR expression'. *Neurosci Lett*, 566 pp. 82-87.

Lifeinharmony (2018) 'Anatomy of Head Skin'. [Online]. Available at: http://www.lifeinharmony.me/anatomy-of-head-skin.

Lin, H., Zeng, J., Xie, R., Schulz, M. J., Tedesco, R., Qu, J., Erhard, K. F., Mack, J. F., Raha, K., Rendina, A. R., Szewczuk, L. M., Kratz, P. M., Jurewicz, A. J., Cecconie, T., Martens, S., McDevitt, P. J., Martin, J. D., Chen, S. B., Jiang, Y., Nickels, L., Schwartz, B. J., Smallwood, A., Zhao, B., Campobasso, N., Qian, Y., Briand, J., Rominger, C. M.,

Oleykowski, C., Hardwicke, M. A. & Luengo, J. I. (2016) 'Discovery of a Novel 2,6-Disubstituted Glucosamine Series of Potent and Selective Hexokinase 2 Inhibitors'. *ACS Med Chem Lett*, 7 (3), pp. 217-222.

Lis, P., Dylag, M., Niedzwiecka, K., Ko, Y. H., Pedersen, P. L., Goffeau, A. & Ulaszewski, S. (2016) 'The HK2 Dependent "Warburg Effect" and Mitochondrial Oxidative Phosphorylation in Cancer: Targets for Effective Therapy with 3-Bromopyruvate'. *Molecules*, 21 (12),

Lomas, J., Bello, M. J., Arjona, D., Alonso, M. E., Martinez-Glez, V., Lopez-Marin, I., Aminoso, C., de Campos, J. M., Isla, A., Vaquero, J. & Rey, J. A. (2005) 'Genetic and epigenetic alteration of the NF2 gene in sporadic meningiomas'. *Genes Chromosomes Cancer*, 42 (3), pp. 314-319.

Longstreth, W. T., Jr., Dennis, L. K., McGuire, V. M., Drangsholt, M. T. & Koepsell, T. D. (1993) 'Epidemiology of intracranial meningioma'. *Cancer*, 72 (3), pp. 639-648.

Lou, E., Sumrall, A. L., Turner, S., Peters, K. B., Desjardins, A., Vredenburgh, J. J., McLendon, R. E., Herndon, J. E., 2nd, McSherry, F., Norfleet, J., Friedman, H. S. & Reardon, D. A. (2012) 'Bevacizumab therapy for adults with recurrent/progressive meningioma: a retrospective series'. *J Neurooncol*, 109 (1), pp. 63-70.

Louis, D. N. (2016) *WHO classification of tumours of the central nervous system.* Lyon: International Agency For Research On Cancer.

Loven, D., Hardoff, R., Sever, Z. B., Steinmetz, A. P., Gornish, M., Rappaport, Z. H., Fenig, E., Ram, Z. & Sulkes, A. (2004) 'Non-resectable slow-growing meningiomas treated by hydroxyurea'. *J Neurooncol*, 67 (1-2), pp. 221-226.

Maira, S. M., Pecchi, S., Huang, A., Burger, M., Knapp, M., Sterker, D., Schnell, C., Guthy, D., Nagel, T., Wiesmann, M., Brachmann, S., Fritsch, C., Dorsch, M., Chene, P., Shoemaker, K., De Pover, A., Menezes, D., Martiny-Baron, G., Fabbro, D., Wilson, C. J., Schlegel, R., Hofmann, F., Garcia-Echeverria, C., Sellers, W. R. & Voliva, C. F. (2012) 'Identification and characterization of NVP-BKM120, an orally available pan-class I PI3-kinase inhibitor'. *Mol Cancer Ther*, 11 (2), pp. 317-328.

Maitra, S., Kulikauskas, R. M., Gavilan, H. & Fehon, R. G. (2006) 'The tumor suppressors Merlin and Expanded function cooperatively to modulate receptor endocytosis and signaling'. *Curr Biol*, 16 (7), pp. 702-709.

Makrantoni, V., Antrobus, R., Botting, C. H. & Coote, P. J. (2005) 'Rapid enrichment and analysis of yeast phosphoproteins using affinity chromatography, 2D-PAGE and peptide mass fingerprinting'. *Yeast*, 22 (5), pp. 401-414.

Mann, M., Ong, S. E., Gronborg, M., Steen, H., Jensen, O. N. & Pandey, A. (2002) 'Analysis of protein phosphorylation using mass spectrometry: deciphering the phosphoproteome'. *Trends Biotechnol*, 20 (6), pp. 261-268.

Manning, B. D. & Toker, A. (2017) 'AKT/PKB Signaling: Navigating the Network'. *Cell*, 169 (3), pp. 381-405.

Mariotti, A., Perotti, A., Sessa, C. & Ruegg, C. (2007) 'N-cadherin as a therapeutic target in cancer'. *Expert Opin Investig Drugs*, 16 (4), pp. 451-465.

Marosi, C., Hassler, M., Roessler, K., Reni, M., Sant, M., Mazza, E. & Vecht, C. (2008) 'Meningioma'. *Crit Rev Oncol Hematol*, 67 (2), pp. 153-171.

Matika, C. A., Wasilewski, M., Arnott, J. A. & Planey, S. L. (2012) 'Antiproliferative factor regulates connective tissue growth factor (CTGF/CCN2) expression in T24 bladder carcinoma cells'. *Mol Biol Cell*, 23 (10), pp. 1976-1985.

Mawrin, C., Chung, C. & Preusser, M. (2015) 'Biology and clinical management challenges in meningioma'. *Am Soc Clin Oncol Educ Book*, pp. e106-115.

Maxwell, M., Galanopoulos, T., Hedley-Whyte, E. T., Black, P. M. & Antoniades, H. N. (1990) 'Human meningiomas co-express platelet-derived growth factor (PDGF) and PDGF-receptor genes and their protein products'. *Int J Cancer*, 46 (1), pp. 16-21.

Meimoun, P., Ambard-Bretteville, F., Colas-des Francs-Small, C., Valot, B. & Vidal, J. (2007) 'Analysis of plant phosphoproteins'. *Anal Biochem*, 371 (2), pp. 238-246.

Mercado-Pimentel, M. E., Igarashi, S., Dunn, A. M., Behbahani, M., Miller, C., Read, C. M. & Jacob, A. (2016) 'The Novel Small Molecule Inhibitor, OSU-T315, Suppresses Vestibular Schwannoma and Meningioma Growth by Inhibiting PDK2 Function in the AKT Pathway Activation'. *Austin J Med Oncol*, 3 (1),

Merico, D., Isserlin, R. & Bader, G. D. (2011) 'Visualizing gene-set enrichment results using the Cytoscape plug-in enrichment map'. *Methods Mol Biol*, 781 pp. 257-277.

Metodiev, M. V., Timanova, A. & Stone, D. E. (2004) 'Differential phosphoproteome profiling by affinity capture and tandem matrix-assisted laser desorption/ionization mass spectrometry'. *Proteomics*, 4 (5), pp. 1433-1438.

Miller, R., Jr., DeCandio, M. L., Dixon-Mah, Y., Giglio, P., Vandergrift, W. A., 3rd, Banik, N. L., Patel, S. J., Varma, A. K. & Das, A. (2014) 'Molecular Targets and Treatment of Meningioma'. *J Neurol Neurosurg*, 1 (1),

Moazzam, A. A., Wagle, N. & Zada, G. (2013) 'Recent developments in chemotherapy for meningiomas: a review'. *Neurosurg Focus*, 35 (6), pp. E18.

Mukhopadhyay, A., Tabanor, K., Chaguturu, R. & Aldrich, J. V. (2013) 'Targeting inhibitor 2 of protein phosphatase 2A as a therapeutic strategy for prostate cancer treatment'. *Cancer Biol Ther*, 14 (10), pp. 962-972.

Murray, E. R. & Cameron, A. J. M. (2017) 'Towards specific inhibition of mTORC2'. *Aging (Albany NY)*, 9 (12), pp. 2461-2462.

Nagashima, G., Asai, J., Suzuki, R. & Fujimoto, T. (2001) 'Different distribution of c-myc and MIB-1 positive cells in malignant meningiomas with reference to TGFs, PDGF, and PgR expression'. *Brain Tumor Pathol*, 18 (1), pp. 1-5.

Nakada, M., Anderson, E. M., Demuth, T., Nakada, S., Reavie, L. B., Drake, K. L., Hoelzinger, D. B. & Berens, M. E. (2010) 'The phosphorylation of ephrin-B2 ligand promotes glioma cell migration and invasion'. *Int J Cancer*, 126 (5), pp. 1155-1165.

Nayak, L., Iwamoto, F. M., Rudnick, J. D., Norden, A. D., Lee, E. Q., Drappatz, J., Omuro, A. & Kaley, T. J. (2012) 'Atypical and anaplastic meningiomas treated with bevacizumab'. *J Neurooncol*, 109 (1), pp. 187-193.

Niapour, M., Farr, C., Minden, M. & Berger, S. A. (2012) 'Elevated calpain activity in acute myelogenous leukemia correlates with decreased calpastatin expression'. *Blood Cancer J*, 2 (1), pp. e51.

Norden, A. D., Drappatz, J. & Wen, P. Y. (2007) 'Targeted drug therapy for meningiomas'. *Neurosurg Focus*, 23 (4), pp. E12.

Norden, A. D., Raizer, J. J., Abrey, L. E., Lamborn, K. R., Lassman, A. B., Chang, S. M., Yung, W. K., Gilbert, M. R., Fine, H. A., Mehta, M., Deangelis, L. M., Cloughesy, T. F., Robins, H. I., Aldape, K., Dancey, J., Prados, M. D., Lieberman, F. & Wen, P. Y. (2010) 'Phase II trials of erlotinib or gefitinib in patients with recurrent meningioma'. *J Neurooncol*, 96 (2), pp. 211-217.

Nunes, F. P., Merker, V. L., Jennings, D., Caruso, P. A., di Tomaso, E., Muzikansky, A., Barker, F. G., 2nd, Stemmer-Rachamimov, A. & Plotkin, S. R. (2013) 'Bevacizumab treatment for meningiomas in NF2: a retrospective analysis of 15 patients'. *PLoS One*, 8 (3), pp. e59941.

Offenhauser, N., Borgonovo, A., Disanza, A., Romano, P., Ponzanelli, I., Iannolo, G., Di Fiore, P. P. & Scita, G. (2004) 'The eps8 family of proteins links growth factor stimulation to actin reorganization generating functional redundancy in the Ras/Rac pathway'. *Mol Biol Cell*, 15 (1), pp. 91-98.

Okamoto, H., Li, J., Vortmeyer, A. O., Jaffe, H., Lee, Y. S., Glasker, S., Sohn, T. S., Zeng, W., Ikejiri, B., Proescholdt, M. A., Mayer, C., Weil, R. J., Oldfield, E. H. & Zhuang, Z. (2006) 'Comparative proteomic profiles of meningioma subtypes'. *Cancer Res*, 66 (20), pp. 10199-10204.

Okamoto, M., Hirata, S., Sato, S., Koga, S., Fujii, M., Qi, G., Ogawa, I., Takata, T., Shimamoto, F. & Tatsuka, M. (2012) 'Frequent increased gene copy number and high protein expression of tRNA (cytosine-5-)-methyltransferase (NSUN2) in human cancers'. *DNA Cell Biol*, 31 (5), pp. 660-671.

Okudela, K., Woo, T., Mitsui, H., Suzuki, T., Tajiri, M., Sakuma, Y., Miyagi, Y., Tateishi, Y., Umeda, S., Masuda, M. & Ohashi, K. (2013) 'Downregulation of ALDH1A1 expression in non-small cell lung carcinomas--its clinicopathologic and biological significance'. *Int J Clin Exp Pathol*, 6 (1), pp. 1-12.

Okuzumi, T., Fiedler, D., Zhang, C., Gray, D. C., Aizenstein, B., Hoffman, R. & Shokat, K. M. (2009) 'Inhibitor hijacking of Akt activation'. *Nat Chem Biol*, 5 (7), pp. 484-493.

Ostrom, Q. T., Gittleman, H., Fulop, J., Liu, M., Blanda, R., Kromer, C., Wolinsky, Y., Kruchko, C. & Barnholtz-Sloan, J. S. (2015) 'CBTRUS Statistical Report: Primary Brain

and Central Nervous System Tumors Diagnosed in the United States in 2008-2012'. *Neuro Oncol*, 17 Suppl 4 pp. iv1-iv62.

Pachow, D., Andrae, N., Kliese, N., Angenstein, F., Stork, O., Wilisch-Neumann, A., Kirches, E. & Mawrin, C. (2013) 'mTORC1 inhibitors suppress meningioma growth in mouse models'. *Clin Cancer Res*, 19 (5), pp. 1180-1189.

Padma, V. V. (2015) 'An overview of targeted cancer therapy'. *Biomedicine (Taipei)*, 5 (4), pp. 19.

Parada, C. A., Osbun, J., Kaur, S., Yakkioui, Y., Shi, M., Pan, C., Busald, T., Karasozen, Y., Gonzalez-Cuyar, L. F., Rostomily, R., Zhang, J. & Ferreira, M., Jr. (2018) 'Kinome and phosphoproteome of high-grade meningiomas reveal AKAP12 as a central regulator of aggressiveness and its possible role in progression'. *Sci Rep*, 8 (1), pp. 2098.

Park, H. J., Kang, H. C., Kim, I. H., Park, S. H., Kim, D. G., Park, C. K., Paek, S. H. & Jung, H. W. (2013) 'The role of adjuvant radiotherapy in atypical meningioma'. *J Neurooncol*, 115 (2), pp. 241-247.

Pasquale, E. B. (2010) 'Eph receptors and ephrins in cancer: bidirectional signalling and beyond'. *Nat Rev Cancer*, 10 (3), pp. 165-180.

Paz, H., Pathak, N. & Yang, J. (2014) 'Invading one step at a time: the role of invadopodia in tumor metastasis'. *Oncogene*, 33 (33), pp. 4193-4202.

Perez-Magan, E., Campos-Martin, Y., Mur, P., Fiano, C., Ribalta, T., Garcia, J. F., Rey, J. A., Rodriguez de Lope, A., Mollejo, M. & Melendez, B. (2012) 'Genetic alterations associated with progression and recurrence in meningiomas'. *J Neuropathol Exp Neurol*, 71 (10), pp. 882-893.

Perry, A., Gutmann, D. H. & Reifenberger, G. (2004) 'Molecular pathogenesis of meningiomas'. *J Neurooncol*, 70 (2), pp. 183-202.

Perry, A., Stafford, S. L., Scheithauer, B. W., Suman, V. J. & Lohse, C. M. (1997) 'Meningioma grading: an analysis of histologic parameters'. *Am J Surg Pathol*, 21 (12), pp. 1455-1465.

Petrilli, A. M. & Fernandez-Valle, C. (2016) 'Role of Merlin/NF2 inactivation in tumor biology'. *Oncogene*, 35 (5), pp. 537-548.

Pettiford, S. M. & Herbst, R. (2000) 'The MAP-kinase ERK2 is a specific substrate of the protein tyrosine phosphatase HePTP'. *Oncogene*, 19 (7), pp. 858-869.

Pfister, C., Pfrommer, H., Tatagiba, M. S. & Roser, F. (2012) 'Vascular endothelial growth factor signals through platelet-derived growth factor receptor beta in meningiomas in vitro'. *Br J Cancer*, 107 (10), pp. 1702-1713.

Phillips, L. E., Koepsell, T. D., van Belle, G., Kukull, W. A., Gehrels, J. A. & Longstreth, W. T., Jr. (2002) 'History of head trauma and risk of intracranial meningioma: population-based case-control study'. *Neurology*, 58 (12), pp. 1849-1852.

Piao, S., Inglehart, R. C., Scanlon, C. S., Russo, N., Banerjee, R. & D'Silva, N. J. (2017) 'CDH11 inhibits proliferation and invasion in head and neck cancer'. *J Oral Pathol Med*, 46 (2), pp. 89-97.

Pinkse, M. W., Uitto, P. M., Hilhorst, M. J., Ooms, B. & Heck, A. J. (2004) 'Selective isolation at the femtomole level of phosphopeptides from proteolytic digests using 2D-NanoLC-ESI-MS/MS and titanium oxide precolumns'. *Anal Chem*, 76 (14), pp. 3935-3943.

Pistolesi, S., Boldrini, L., Gisfredi, S., De Ieso, K., Camacci, T., Caniglia, M., Lupi, G., Leocata, P., Basolo, F., Pingitore, R., Parenti, G. & Fontanini, G. (2004) 'Angiogenesis in intracranial meningiomas: immunohistochemical and molecular study'. *Neuropathol Appl Neurobiol*, 30 (2), pp. 118-125.

Preusser, M., Brastianos, P. K. & Mawrin, C. (2018) 'Advances in meningioma genetics: novel therapeutic opportunities'. *Nat Rev Neurol*, 14 (2), pp. 106-115.

Puttmann, S., Senner, V., Braune, S., Hillmann, B., Exeler, R., Rickert, C. H. & Paulus, W. (2005) 'Establishment of a benign meningioma cell line by hTERT-mediated immortalization'. *Lab Invest*, 85 (9), pp. 1163-1171.

Qi, J., Wang, J., Romanyuk, O. & Siu, C. H. (2006) 'Involvement of Src family kinases in N-cadherin phosphorylation and beta-catenin dissociation during transendothelial migration of melanoma cells'. *Mol Biol Cell*, 17 (3), pp. 1261-1272.

Quang, C. T., Leboucher, S., Passaro, D., Fuhrmann, L., Nourieh, M., Vincent-Salomon, A. & Ghysdael, J. (2015) 'The calcineurin/NFAT pathway is activated in diagnostic breast cancer cases and is essential to survival and metastasis of mammary cancer cells'. *Cell Death Dis*, 6 pp. e1658.

Rappsilber, J., Ishihama, Y. & Mann, M. (2003) 'Stop and go extraction tips for matrix-assisted laser desorption/ionization, nanoelectrospray, and LC/MS sample pretreatment in proteomics'. *Anal Chem*, 75 (3), pp. 663-670.

Reardon, D. A., Norden, A. D., Desjardins, A., Vredenburgh, J. J., Herndon, J. E., 2nd, Coan, A., Sampson, J. H., Gururangan, S., Peters, K. B., McLendon, R. E., Norfleet, J. A., Lipp, E. S., Drappatz, J., Wen, P. Y. & Friedman, H. S. (2012) 'Phase II study of Gleevec(R) plus hydroxyurea (HU) in adults with progressive or recurrent meningioma'. *J Neurooncol*, 106 (2), pp. 409-415.

Reifenberger, J., Wolter, M., Weber, R. G., Megahed, M., Ruzicka, T., Lichter, P. & Reifenberger, G. (1998) 'Missense mutations in SMOH in sporadic basal cell carcinomas of the skin and primitive neuroectodermal tumors of the central nervous system'. *Cancer Res*, 58 (9), pp. 1798-1803.

Reuss, D. E., Piro, R. M., Jones, D. T., Simon, M., Ketter, R., Kool, M., Becker, A., Sahm, F., Pusch, S., Meyer, J., Hagenlocher, C., Schweizer, L., Capper, D., Kickingereder, P., Mucha, J., Koelsche, C., Jager, N., Santarius, T., Tarpey, P. S., Stephens, P. J., Andrew Futreal, P., Wellenreuther, R., Kraus, J., Lenartz, D., Herold-Mende, C., Hartmann, C., Mawrin, C., Giese, N., Eils, R., Collins, V. P., Konig, R., Wiestler, O. D., Pfister, S. M.

& von Deimling, A. (2013) 'Secretory meningiomas are defined by combined KLF4 K409Q and TRAF7 mutations'. *Acta Neuropathol*, 125 (3), pp. 351-358.

Riemenschneider, M. J., Perry, A. & Reifenberger, G. (2006) 'Histological classification and molecular genetics of meningiomas'. *Lancet Neurol*, 5 (12), pp. 1045-1054.

Roig, J., Mikhailov, A., Belham, C. & Avruch, J. (2002) 'Nercc1, a mammalian NIMA-family kinase, binds the Ran GTPase and regulates mitotic progression'. *Genes Dev*, 16 (13), pp. 1640-1658.

Rong, R., Surace, E. I., Haipek, C. A., Gutmann, D. H. & Ye, K. (2004a) 'Serine 518 phosphorylation modulates merlin intramolecular association and binding to critical effectors important for NF2 growth suppression'. *Oncogene*, 23 (52), pp. 8447-8454.

Rong, R., Tang, X., Gutmann, D. H. & Ye, K. (2004b) 'Neurofibromatosis 2 (NF2) tumor suppressor merlin inhibits phosphatidylinositol 3-kinase through binding to PIKE-L'. *Proc Natl Acad Sci U S A*, 101 (52), pp. 18200-18205.

Rouleau, G. A., Merel, P., Lutchman, M., Sanson, M., Zucman, J., Marineau, C., Hoang-Xuan, K., Demczuk, S., Desmaze, C., Plougastel, B. & et al. (1993) 'Alteration in a new gene encoding a putative membrane-organizing protein causes neuro-fibromatosis type 2'. *Nature*, 363 (6429), pp. 515-521.

Ruttledge, M. H., Andermann, A. A., Phelan, C. M., Claudio, J. O., Han, F. Y., Chretien, N., Rangaratnam, S., MacCollin, M., Short, P., Parry, D., Michels, V., Riccardi, V. M., Weksberg, R., Kitamura, K., Bradburn, J. M., Hall, B. D., Propping, P. & Rouleau, G. A.

(1996) 'Type of mutation in the neurofibromatosis type 2 gene (NF2) frequently determines severity of disease'. *Am J Hum Genet*, 59 (2), pp. 331-342.

Ruttledge, M. H., Xie, Y. G., Han, F. Y., Peyrard, M., Collins, V. P., Nordenskjold, M. & Dumanski, J. P. (1994) 'Deletions on chromosome 22 in sporadic meningioma'. *Genes Chromosomes Cancer*, 10 (2), pp. 122-130.

Sadetzki, S., Flint-Richter, P., Ben-Tal, T. & Nass, D. (2002) 'Radiation-induced meningioma: a descriptive study of 253 cases'. *J Neurosurg*, 97 (5), pp. 1078-1082.

Sahm, F., Bissel, J., Koelsche, C., Schweizer, L., Capper, D., Reuss, D., Bohmer, K., Lass, U., Gock, T., Kalis, K., Meyer, J., Habel, A., Brehmer, S., Mittelbronn, M., Jones, D. T., Schittenhelm, J., Urbschat, S., Ketter, R., Heim, S., Mawrin, C., Hainfellner, J. A., Berghoff, A. S., Preusser, M., Becker, A., Herold-Mende, C., Unterberg, A., Hartmann, C., Kickingereder, P., Collins, V. P., Pfister, S. M. & von Deimling, A. (2013) 'AKT1E17K mutations cluster with meningothelial and transitional meningiomas and can be detected by SFRP1 immunohistochemistry'. *Acta Neuropathol*, 126 (5), pp. 757-762.

Sahm, F., Schrimpf, D., Olar, A., Koelsche, C., Reuss, D., Bissel, J., Kratz, A., Capper, D., Schefzyk, S., Hielscher, T., Wang, Q., Sulman, E. P., Adeberg, S., Koch, A., Okuducu, A. F., Brehmer, S., Schittenhelm, J., Becker, A., Brokinkel, B., Schmidt, M., Ull, T., Gousias, K., Kessler, A. F., Lamszus, K., Debus, J., Mawrin, C., Kim, Y. J., Simon, M., Ketter, R., Paulus, W., Aldape, K. D., Herold-Mende, C. & von Deimling, A. (2016) 'TERT Promoter Mutations and Risk of Recurrence in Meningioma'. *J Natl Cancer Inst*, 108 (5),

Sahm, F., Schrimpf, D., Stichel, D., Jones, D. T. W., Hielscher, T., Schefzyk, S., Okonechnikov, K., Koelsche, C., Reuss, D. E., Capper, D., Sturm, D., Wirsching, H. G., Berghoff, A. S., Baumgarten, P., Kratz, A., Huang, K., Wefers, A. K., Hovestadt, V., Sill, M., Ellis, H. P., Kurian, K. M., Okuducu, A. F., Jungk, C., Drueschler, K., Schick, M., Bewerunge-Hudler, M., Mawrin, C., Seiz-Rosenhagen, M., Ketter, R., Simon, M., Westphal, M., Lamszus, K., Becker, A., Koch, A., Schittenhelm, J., Rushing, E. J., Collins, V. P., Brehmer, S., Chavez, L., Platten, M., Hanggi, D., Unterberg, A., Paulus, W., Wick, W., Pfister, S. M., Mittelbronn, M., Preusser, M., Herold-Mende, C., Weller, M. & von Deimling, A. (2017) 'DNA methylation-based classification and grading system for meningioma: a multicentre, retrospective analysis'. *Lancet Oncol*, 18 (5), pp. 682-694.

Salvati, M., Cervoni, L., Puzzilli, F., Bristot, R., Delfini, R. & Gagliardi, F. M. (1997) 'High-dose radiation-induced meningiomas'. *Surg Neurol*, 47 (5), pp. 435-441; discussion 441-432.

Sandoval, J. & Esteller, M. (2012) 'Cancer epigenomics: beyond genomics'. *Curr Opin Genet Dev*, 22 (1), pp. 50-55.

Sano, A. & Nakamura, H. (2004) 'Chemo-affinity of titania for the column-switching HPLC analysis of phosphopeptides'. *Anal Sci*, 20 (3), pp. 565-566.

Santamaria, E., Sanchez-Quiles, V., Fernandez-Irigoyen, J. & Corrales, F. J. (2012) 'A combination of affinity chromatography, 2D DIGE, and mass spectrometry to analyze the phosphoproteome of liver progenitor cells'. *Methods Mol Biol*, 909 pp. 165-180.

Sarbassov, D. D., Guertin, D. A., Ali, S. M. & Sabatini, D. M. (2005) 'Phosphorylation and regulation of Akt/PKB by the rictor-mTOR complex'. *Science*, 307 (5712), pp. 1098-1101.

Sasaki, T., Hankins, G. R. & Helm, G. A. (2003) 'Comparison of gene expression profiles between frozen original meningiomas and primary cultures of the meningiomas by GeneChip'. *Neurosurgery*, 52 (4), pp. 892-898; discussion 898-899.

Saydam, O., Senol, O., Schaaij-Visser, T. B., Pham, T. V., Piersma, S. R., Stemmer-Rachamimov, A. O., Wurdinger, T., Peerdeman, S. M. & Jimenez, C. R. (2010) 'Comparative protein profiling reveals minichromosome maintenance (MCM) proteins as novel potential tumor markers for meningiomas'. *J Proteome Res*, 9 (1), pp. 485-494.

Saydam, O., Shen, Y., Wurdinger, T., Senol, O., Boke, E., James, M. F., Tannous, B. A., Stemmer-Rachamimov, A. O., Yi, M., Stephens, R. M., Fraefel, C., Gusella, J. F., Krichevsky, A. M. & Breakefield, X. O. (2009) 'Downregulated microRNA-200a in meningiomas promotes tumor growth by reducing E-cadherin and activating the Wnt/beta-catenin signaling pathway'. *Mol Cell Biol*, 29 (21), pp. 5923-5940.

Schmidt, M., Mock, A., Jungk, C., Sahm, F., Ull, A. T., Warta, R., Lamszus, K., Gousias, K., Ketter, R., Roesch, S., Rapp, C., Schefzyk, S., Urbschat, S., Lahrmann, B., Kessler, A. F., Lohr, M., Senft, C., Grabe, N., Reuss, D., Beckhove, P., Westphal, M., von Deimling, A., Unterberg, A., Simon, M. & Herold-Mende, C. (2016) 'Transcriptomic analysis of aggressive meningiomas identifies PTTG1 and LEPR as prognostic biomarkers independent of WHO grade'. *Oncotarget*, 7 (12), pp. 14551-14568.

Schneider, B., Pulhorn, H., Rohrig, B. & Rainov, N. G. (2005) 'Predisposing conditions and risk factors for development of symptomatic meningioma in adults'. *Cancer Detect Prev*, 29 (5), pp. 440-447.

Schrell, U. M., Rittig, M. G., Anders, M., Kiesewetter, F., Marschalek, R., Koch, U. H. & Fahlbusch, R. (1997) 'Hydroxyurea for treatment of unresectable and recurrent meningiomas. I. Inhibition of primary human meningioma cells in culture and in meningioma transplants by induction of the apoptotic pathway'. *J Neurosurg*, 86 (5), pp. 845-852.

Seo, S. B., McNamara, P., Heo, S., Turner, A., Lane, W. S. & Chakravarti, D. (2001) 'Regulation of histone acetylation and transcription by INHAT, a human cellular complex containing the set oncoprotein'. *Cell*, 104 (1), pp. 119-130.

Seshacharyulu, P., Ponnusamy, M. P., Rachagani, S., Lakshmanan, I., Haridas, D., Yan, Y., Ganti, A. K. & Batra, S. K. (2015) 'Targeting EGF-receptor(s) - STAT1 axis attenuates tumor growth and metastasis through downregulation of MUC4 mucin in human pancreatic cancer'. *Oncotarget*, 6 (7), pp. 5164-5181.

Shankar, G. M., Abedalthagafi, M., Vaubel, R. A., Merrill, P. H., Nayyar, N., Gill, C. M., Brewster, R., Bi, W. L., Agarwalla, P. K., Thorner, A. R., Reardon, D. A., Al-Mefty, O., Wen, P. Y., Alexander, B. M., van Hummelen, P., Batchelor, T. T., Ligon, K. L., Ligon, A. H., Meyerson, M., Dunn, I. F., Beroukhim, R., Louis, D. N., Perry, A., Carter, S. L., Giannini, C., Curry, W. T., Jr., Cahill, D. P., Barker, F. G., 2nd, Brastianos, P. K. & Santagata, S. (2017) 'Germline and somatic BAP1 mutations in high-grade rhabdoid meningiomas'. *Neuro Oncol*, 19 (4), pp. 535-545.

Sharma, S., Ray, S., Moiyadi, A., Sridhar, E. & Srivastava, S. (2014) 'Quantitative proteomic analysis of meningiomas for the identification of surrogate protein markers'. *Sci Rep*, 4 pp. 7140.

Sharma, S., Ray, S., Mukherjee, S., Moiyadi, A., Sridhar, E. & Srivastava, S. (2015) 'Multipronged quantitative proteomic analyses indicate modulation of various signal transduction pathways in human meningiomas'. *Proteomics*, 15 (2-3), pp. 394-407.

Sher, I., Hanemann, C. O., Karplus, P. A. & Bretscher, A. (2012) 'The tumor suppressor merlin controls growth in its open state, and phosphorylation converts it to a less-active more-closed state'. *Dev Cell*, 22 (4), pp. 703-705.

Sherman, W. J. & Raizer, J. J. (2012) 'Chemotherapy: What is its role in meningioma?'. *Expert Rev Neurother*, 12 (10), pp. 1189-1195; quiz 1196.

Shevchenko, A., Tomas, H., Havlis, J., Olsen, J. V. & Mann, M. (2006) 'In-gel digestion for mass spectrometric characterization of proteins and proteomes'. *Nat Protoc*, 1 (6), pp. 2856-2860.

Shih, K. C., Chowdhary, S., Rosenblatt, P., Weir, A. B., 3rd, Shepard, G. C., Williams, J. T., Shastry, M., Burris, H. A., 3rd & Hainsworth, J. D. (2016) 'A phase II trial of bevacizumab and everolimus as treatment for patients with refractory, progressive intracranial meningioma'. *J Neurooncol*, 129 (2), pp. 281-288.

Shin, S., Rossow, K. L., Grande, J. P. & Janknecht, R. (2007) 'Involvement of RNA helicases p68 and p72 in colon cancer'. *Cancer Res*, 67 (16), pp. 7572-7578.

Shinno, N., Kimura, H., Sada, R., Takiguchi, S., Mori, M., Fumoto, K., Doki, Y. & Kikuchi, A. (2018) 'Activation of the Dickkopf1-CKAP4 pathway is associated with poor prognosis of esophageal cancer and anti-CKAP4 antibody may be a new therapeutic drug'. *Oncogene*, 37 (26), pp. 3471-3484.

Singh, A. P., Chaturvedi, P. & Batra, S. K. (2007) 'Emerging roles of MUC4 in cancer: a novel target for diagnosis and therapy'. *Cancer Res*, 67 (2), pp. 433-436.

Smith, M. J. (2015) 'Germline and somatic mutations in meningiomas'. *Cancer Genet*, 208 (4), pp. 107-114.

Smith, M. J., Ahn, S., Lee, J. I., Bulman, M., Plessis, D. D. & Suh, Y. L. (2017) 'SMARCE1 mutation screening in classification of clear cell meningiomas'. *Histopathology*, 70 (5), pp. 814-820.

Smith, M. J., Higgs, J. E., Bowers, N. L., Halliday, D., Paterson, J., Gillespie, J., Huson, S. M., Freeman, S. R., Lloyd, S., Rutherford, S. A., King, A. T., Wallace, A. J., Ramsden, R. T. & Evans, D. G. (2011) 'Cranial meningiomas in 411 neurofibromatosis type 2 (NF2) patients with proven gene mutations: clear positional effect of mutations, but absence of female severity effect on age at onset'. *J Med Genet*, 48 (4), pp. 261-265.

Smith, M. J., O'Sullivan, J., Bhaskar, S. S., Hadfield, K. D., Poke, G., Caird, J., Sharif, S., Eccles, D., Fitzpatrick, D., Rawluk, D., du Plessis, D., Newman, W. G. & Evans, D.

G. (2013) 'Loss-of-function mutations in SMARCE1 cause an inherited disorder of multiple spinal meningiomas'. *Nat Genet*, 45 (3), pp. 295-298.

Smith, M. J., Wallace, A. J., Bennett, C., Hasselblatt, M., Elert-Dobkowska, E., Evans, L. T., Hickey, W. F., van Hoff, J., Bauer, D., Lee, A., Hevner, R. F., Beetz, C., du Plessis, D., Kilday, J. P., Newman, W. G. & Evans, D. G. (2014) 'Germline SMARCE1 mutations predispose to both spinal and cranial clear cell meningiomas'. *J Pathol*, 234 (4), pp. 436-440.

Soyuer, S., Chang, E. L., Selek, U., Shi, W., Maor, M. H. & DeMonte, F. (2004) 'Radiotherapy after surgery for benign cerebral meningioma'. *Radiother Oncol*, 71 (1), pp. 85-90.

Spinelli, L., Carpentier, S., Montanana Sanchis, F., Dalod, M. & Vu Manh, T. P. (2015) 'BubbleGUM: automatic extraction of phenotype molecular signatures and comprehensive visualization of multiple Gene Set Enrichment Analyses'. *BMC Genomics*, 16 pp. 814.

Stoletov, K. & Lewis, J. D. (2015) 'Invadopodia: a new therapeutic target to block cancer metastasis'. *Expert Rev Anticancer Ther*, 15 (7), pp. 733-735.

Striedinger, K., VandenBerg, S. R., Baia, G. S., McDermott, M. W., Gutmann, D. H. & Lal, A. (2008) 'The neurofibromatosis 2 tumor suppressor gene product, merlin, regulates human meningioma cell growth by signaling through YAP'. *Neoplasia*, 10 (11), pp. 1204-1212.

Szklarczyk, D., Morris, J. H., Cook, H., Kuhn, M., Wyder, S., Simonovic, M., Santos, A., Doncheva, N. T., Roth, A., Bork, P., Jensen, L. J. & von Mering, C. (2017) 'The STRING database in 2017: quality-controlled protein-protein association networks, made broadly accessible'. *Nucleic Acids Res*, 45 (D1), pp. D362-D368.

Takahashi, K., Tanabe, K., Ohnuki, M., Narita, M., Ichisaka, T., Tomoda, K. & Yamanaka, S. (2007) 'Induction of pluripotent stem cells from adult human fibroblasts by defined factors'. *Cell*, 131 (5), pp. 861-872.

Tan, B. C. & Lee, S. C. (2004) 'Nek9, a novel FACT-associated protein, modulates interphase progression'. *J Biol Chem*, 279 (10), pp. 9321-9330.

Tanaka, K., Sato, C., Maeda, Y., Koike, M., Matsutani, M., Yamada, K. & Miyaki, M. (1989) 'Establishment of a human malignant meningioma cell line with amplified c-myc oncogene'. *Cancer*, 64 (11), pp. 2243-2249.

Tauziede-Espariat, A., Parfait, B., Besnard, A., Lacombe, J., Pallud, J., Tazi, S., Puget, S., Lot, G., Terris, B., Cohen, J., Vidaud, M., Figarella-Branger, D., Monnien, F., Polivka, M., Adle-Biassette, H. & Varlet, P. (2018) 'Loss of SMARCE1 expression is a specific diagnostic marker of clear cell meningioma: a comprehensive immunophenotypical and molecular analysis'. *Brain Pathol*, 28 (4), pp. 466-474.

Tebani, A., Afonso, C., Marret, S. & Bekri, S. (2016) 'Omics-Based Strategies in Precision Medicine: Toward a Paradigm Shift in Inborn Errors of Metabolism Investigations'. *Int J Mol Sci*, 17 (9),

Tian, X., Han, Y., Yu, L., Luo, B., Hu, Z., Li, X., Yang, Z., Wang, X., Huang, W., Wang, H., Zhang, Q. & Ma, D. (2017) 'Decreased expression of ALDH5A1 predicts prognosis in patients with ovarian cancer'. *Cancer Biol Ther*, 18 (4), pp. 245-251.

Trofatter, J. A., MacCollin, M. M., Rutter, J. L., Murrell, J. R., Duyao, M. P., Parry, D. M., Eldridge, R., Kley, N., Menon, A. G., Pulaski, K. & et al. (1993) 'A novel moesin-, ezrin-, radixin-like gene is a candidate for the neurofibromatosis 2 tumor suppressor'. *Cell*, 72 (5), pp. 791-800.

Trotta, R., Ciarlariello, D., Dal Col, J., Mao, H., Chen, L., Briercheck, E., Yu, J., Zhang, J., Perrotti, D. & Caligiuri, M. A. (2011) 'The PP2A inhibitor SET regulates granzyme B expression in human natural killer cells'. *Blood*, 117 (8), pp. 2378-2384.

Tuchen, M., Wilisch-Neumann, A., Daniel, E. A., Baldauf, L., Pachow, D., Scholz, J., Angenstein, F., Stork, O., Kirches, E. & Mawrin, C. (2017) 'Receptor tyrosine kinase inhibition by regorafenib/sorafenib inhibits growth and invasion of meningioma cells'. *Eur J Cancer*, 73 pp. 9-21.

Tufan, K., Dogulu, F., Kurt, G., Emmez, H., Ceviker, N. & Baykaner, M. K. (2005) 'Intracranial meningiomas of childhood and adolescence'. *Pediatr Neurosurg*, 41 (1), pp. 1-7.

Tyanova, S., Temu, T., Sinitcyn, P., Carlson, A., Hein, M. Y., Geiger, T., Mann, M. & Cox, J. (2016) 'The Perseus computational platform for comprehensive analysis of (prote)omics data'. *Nat Methods*, 13 (9), pp. 731-740.

Uhlmann-Schiffler, H., Rossler, O. G. & Stahl, H. (2002) 'The mRNA of DEAD box protein p72 is alternatively translated into an 82-kDa RNA helicase'. *J Biol Chem*, 277 (2), pp. 1066-1075.

Upadhyay, G., Goessling, W., North, T. E., Xavier, R., Zon, L. I. & Yajnik, V. (2008) 'Molecular association between beta-catenin degradation complex and Rac guanine exchange factor DOCK4 is essential for Wnt/beta-catenin signaling'. *Oncogene*, 27 (44), pp. 5845-5855.

Vasudevan, H. N., Braunstein, S. E., Phillips, J. J., Pekmezci, M., Tomlin, B. A., Wu, A., Reis, G. F., Magill, S. T., Zhang, J., Feng, F. Y., Nicholaides, T., Chang, S. M., Sneed, P. K., McDermott, M. W., Berger, M. S., Perry, A. & Raleigh, D. R. (2018) 'Comprehensive Molecular Profiling Identifies FOXM1 as a Key Transcription Factor for Meningioma Proliferation'. *Cell Rep*, 22 (13), pp. 3672-3683.

Vedrenne, C., Klopfenstein, D. R. & Hauri, H. P. (2005) 'Phosphorylation controls CLIMP-63-mediated anchoring of the endoplasmic reticulum to microtubules'. *Mol Biol Cell*, 16 (4), pp. 1928-1937.

Villen, J., Beausoleil, S. A., Gerber, S. A. & Gygi, S. P. (2007) 'Large-scale phosphorylation analysis of mouse liver'. *Proc Natl Acad Sci U S A*, 104 (5), pp. 1488-1493.

Vizcaino, J. A., Csordas, A., del-Toro, N., Dianes, J. A., Griss, J., Lavidas, I., Mayer, G., Perez-Riverol, Y., Reisinger, F., Ternent, T., Xu, Q. W., Wang, R. & Hermjakob, H.

(2016) '2016 update of the PRIDE database and its related tools'. *Nucleic Acids Res*, 44 (D1), pp. D447-456.

Wang, D., Wang, M., Jiang, N., Zhang, Y., Bian, X., Wang, X., Roberts, T. M., Zhao, J. J., Liu, P. & Cheng, H. (2016) 'Effective use of PI3K inhibitor BKM120 and PARP inhibitor Olaparib to treat PIK3CA mutant ovarian cancer'. *Oncotarget*, 7 (11), pp. 13153-13166.

Wang, H., Zhang, Q., Wen, Q., Zheng, Y., Lazarovici, P., Jiang, H., Lin, J. & Zheng, W. (2012) 'Proline-rich Akt substrate of 40kDa (PRAS40): a novel downstream target of PI3k/Akt signaling pathway'. *Cell Signal*, 24 (1), pp. 17-24.

Wang, J. L., Nister, M., Hermansson, M., Westermark, B. & Ponten, J. (1990) 'Expression of PDGF beta-receptors in human meningioma cells'. *Int J Cancer*, 46 (5), pp. 772-778.

Watson, M. A., Gutmann, D. H., Peterson, K., Chicoine, M. R., Kleinschmidt-DeMasters, B. K., Brown, H. G. & Perry, A. (2002) 'Molecular characterization of human meningiomas by gene expression profiling using high-density oligonucleotide microarrays'. *Am J Pathol*, 161 (2), pp. 665-672.

Wechsler-Reya, R. J., Elliott, K. J. & Prendergast, G. C. (1998) 'A role for the putative tumor suppressor Bin1 in muscle cell differentiation'. *Mol Cell Biol*, 18 (1), pp. 566-575.

Weisman, A. S., Raguet, S. S. & Kelly, P. A. (1987) 'Characterization of the epidermal growth factor receptor in human meningioma'. *Cancer Res*, 47 (8), pp. 2172-2176.

Weller, M., Roth, P., Sahm, F., Burghardt, I., Schuknecht, B., Rushing, E. J., Regli, L., Lindemann, J. P. & von Deimling, A. (2017) 'Durable Control of Metastatic AKT1-Mutant WHO Grade 1 Meningothelial Meningioma by the AKT Inhibitor, AZD5363'. *J Natl Cancer Inst*, 109 (3), pp. 1-4.

Wen, P. Y., Quant, E., Drappatz, J., Beroukhim, R. & Norden, A. D. (2010) 'Medical therapies for meningiomas'. *J Neurooncol*, 99 (3), pp. 365-378.

Wen, P. Y., Yung, W. K., Lamborn, K. R., Norden, A. D., Cloughesy, T. F., Abrey, L. E., Fine, H. A., Chang, S. M., Robins, H. I., Fink, K., Deangelis, L. M., Mehta, M., Di Tomaso, E., Drappatz, J., Kesari, S., Ligon, K. L., Aldape, K., Jain, R. K., Stiles, C. D., Egorin, M. J. & Prados, M. D. (2009) 'Phase II study of imatinib mesylate for recurrent meningiomas (North American Brain Tumor Consortium study 01-08)'. *Neuro Oncol*, 11 (6), pp. 853-860.

Wernicke, A. G., Dicker, A. P., Whiton, M., Ivanidze, J., Hyslop, T., Hammond, E. H., Perry, A., Andrews, D. W. & Kenyon, L. (2010) 'Assessment of Epidermal Growth Factor Receptor (EGFR) expression in human meningioma'. *Radiat Oncol*, 5 pp. 46.

Whittle, I. R., Smith, C., Navoo, P. & Collie, D. (2004) 'Meningiomas'. *Lancet*, 363 (9420), pp. 1535-1543.

Wibom, C., Moren, L., Aarhus, M., Knappskog, P. M., Lund-Johansen, M., Antti, H. & Bergenheim, A. T. (2009) 'Proteomic profiles differ between bone invasive and noninvasive benign meningiomas of fibrous and meningothelial subtype'. *J Neurooncol*, 94 (3), pp. 321-331.

Wiemels, J., Wrensch, M. & Claus, E. B. (2010) 'Epidemiology and etiology of meningioma'. *J Neurooncol*, 99 (3), pp. 307-314.

Wisniewski, J. R., Nagaraj, N., Zougman, A., Gnad, F. & Mann, M. (2010) 'Brain phosphoproteome obtained by a FASP-based method reveals plasma membrane protein topology'. *J Proteome Res*, 9 (6), pp. 3280-3289.

Wolf, A., Agnihotri, S., Micallef, J., Mukherjee, J., Sabha, N., Cairns, R., Hawkins, C. & Guha, A. (2011) 'Hexokinase 2 is a key mediator of aerobic glycolysis and promotes tumor growth in human glioblastoma multiforme'. *J Exp Med*, 208 (2), pp. 313-326.

Wrobel, G., Roerig, P., Kokocinski, F., Neben, K., Hahn, M., Reifenberger, G. & Lichter, P. (2005) 'Microarray-based gene expression profiling of benign, atypical and anaplastic meningiomas identifies novel genes associated with meningioma progression'. *Int J Cancer*, 114 (2), pp. 249-256.

Wu, Q. W. (2016) 'Serpine2, a potential novel target for combating melanoma metastasis'. *Am J Transl Res*, 8 (5), pp. 1985-1997.

Wu, X., Nguyen, B. C., Dziunycz, P., Chang, S., Brooks, Y., Lefort, K., Hofbauer, G. F. & Dotto, G. P. (2010) 'Opposing roles for calcineurin and ATF3 in squamous skin cancer'. *Nature*, 465 (7296), pp. 368-372.

Xiang, T., Li, L., Yin, X., Zhong, L., Peng, W., Qiu, Z., Ren, G. & Tao, Q. (2013) 'Epigenetic silencing of the WNT antagonist Dickkopf 3 disrupts normal Wnt/beta-

catenin signalling and apoptosis regulation in breast cancer cells'. *J Cell Mol Med*, 17 (10), pp. 1236-1246.

Xu, S., Catapang, A., Braas, D., Stiles, L., Doh, H. M., Lee, J. T., Graeber, T. G., Damoiseaux, R., Shirihai, O. & Herschman, H. R. (2018) 'A precision therapeutic strategy for hexokinase 1-null, hexokinase 2-positive cancers'. *Cancer Metab*, 6 pp. 7.

Yamanaka, R., Hayano, A. & Kanayama, T. (2017) 'Radiation-Induced Meningiomas: An Exhaustive Review of the Literature'. *World Neurosurg*, 97 pp. 635-644 e638.

Yang, H. W., Kim, T. M., Song, S. S., Shrinath, N., Park, R., Kalamarides, M., Park, P. J., Black, P. M., Carroll, R. S. & Johnson, M. D. (2012) 'Alternative splicing of CHEK2 and codeletion with NF2 promote chromosomal instability in meningioma'. *Neoplasia*, 14 (1), pp. 20-28.

Yang, S. Y. & Xu, G. M. (2001) 'Expression of PDGF and its receptor as well as their relationship to proliferating activity and apoptosis of meningiomas in human meningiomas'. *J Clin Neurosci*, 8 Suppl 1 pp. 49-53.

Yi, J., Gao, R., Chen, Y., Yang, Z., Han, P., Zhang, H., Dou, Y., Liu, W., Wang, W., Du, G., Xu, Y. & Wang, J. (2017) 'Overexpression of NSUN2 by DNA hypomethylation is associated with metastatic progression in human breast cancer'. *Oncotarget*, 8 (13), pp. 20751-20765.

Yin, D. T., Wu, W., Li, M., Wang, Q. E., Li, H., Wang, Y., Tang, Y. & Xing, M. (2013) 'DKK3 is a potential tumor suppressor gene in papillary thyroid carcinoma'. *Endocr Relat Cancer*, 20 (4), pp. 507-514.

Yuzawa, S., Nishihara, H. & Tanaka, S. (2016) 'Genetic landscape of meningioma'. *Brain Tumor Pathol*, 33 (4), pp. 237-247.

Zhang, H., Berel, D., Wang, Y., Li, P., Bhowmick, N. A., Figlin, R. A. & Kim, H. L. (2013) 'A comparison of Ku0063794, a dual mTORC1 and mTORC2 inhibitor, and temsirolimus in preclinical renal cell carcinoma models'. *PLoS One*, 8 (1), pp. e54918.

Zhao, B., Wei, X., Li, W., Udan, R. S., Yang, Q., Kim, J., Xie, J., Ikenoue, T., Yu, J., Li, L., Zheng, P., Ye, K., Chinnaiyan, A., Halder, G., Lai, Z. C. & Guan, K. L. (2007) 'Inactivation of YAP oncoprotein by the Hippo pathway is involved in cell contact inhibition and tissue growth control'. *Genes Dev*, 21 (21), pp. 2747-2761.

Zhao, P., Hall, J., Durston, M., Voydanoff, A., VanSickle, E., Kelly, S., Nagulapally, A. B., Bond, J. & Saulnier Sholler, G. (2017) 'BKM120 induces apoptosis and inhibits tumor growth in medulloblastoma'. *PLoS One*, 12 (6), pp. e0179948.

Zhou, H., Di Palma, S., Preisinger, C., Peng, M., Polat, A. N., Heck, A. J. & Mohammed, S. (2013) 'Toward a comprehensive characterization of a human cancer cell phosphoproteome'. *J Proteome Res*, 12 (1), pp. 260-271.